Genome structure and pathogenicity of the fungal wheat pathogen *Mycosphaerella graminicola*

Sarrah Ben M'Barek-Ben Romdhane

Thesis committee

Thesis supervisor

Prof. dr. ir. P.J.G.M. de Wit
Professor of Phytopathology
Wageningen University

Thesis co-supervisor

Dr. ir. G.H.J. Kema
Senior Scientist
Plant Research International

Other members

Prof. dr. J.H.S.G.M. de Jong, Wageningen University

Prof. dr. S. Kamoun, The Sainsbury laboratory, Norwich,
United Kingdom

Dr. M. Rep, University of Amsterdam

Dr. ir. A.J.M. Debets, Wageningen University

This thesis was conducted under the auspices of the Graduate school of "Experimental Plant Sciences "

Sarrah Ben M'Barek-Ben Romdhane

Genome structure and pathogenicity of the fungal wheat pathogen *Mycosphaerella graminicola*

Thesis

Submitted in fulfillment of the requirements
for the degree of doctor at Wageningen University
by the authority of the Rector Magnificus
Prof. dr. M.J. Kropff,
in the presence of the
Thesis Committee appointed by the Academic Board
to be defended in public
on Monday 17 October 2011
at 4 pm in the Aula.

Sarrah Ben M'Barek-Ben Romdhane

Genome structure and pathogenicity of the fungal wheat pathogen *Mycosphaerella graminicola*

PhD Thesis, Wageningen University, Wageningen, The Netherlands, NL (2011)
With summaries in English, Dutch and French

ISBN 978-90-8585-997-0

This research was partially funded by the Sixth EU Framework Program (BioExploit-EU FP6) Food Quality and Safety priority (contract No. 513959), the Dutch Ministry of Economic Affairs, Agriculture and Innovation and the "Fonds de Soutien à l'Obtention Végétale (FSOV)".
Sarrah Ben M'Barek-Ben Romdhane acknowledges partial financial support from "la bourse d'alternance du ministère de l'Enseignement Supérieur et de la Recherche Scientifique-Tunisie and from the UNESCO-L'Oréal Fellowship for Women in Science.

If one day, people desire to live,
then fate will answer their call
and their night will then begin to fade,
and their chains break and fall.

A tunisian poet, Abou El Kacem Chebbi

A mes très chers parents et à ma sœur,

A mon époux,

Contents

Chapter 1

General introduction & outline of the thesis

“You give but little when you give of your possessions. It is when you give of yourself that you truly give”
— Khalil Gibran

Plant-fungal pathogen interactions

Plant pathogenic fungi developed different lifestyles and infection strategies on their host plants. These modes of nutrition are known as biotrophy, necrotrophy and hemibiotrophy. Biotrophic fungi colonize living host cells and necrotrophic fungi kill host tissue to obtain nutrients for growth and development. Hemibiotrophs have a mixed lifestyle with an initial biotrophic and symptomless phase that is followed by a necrotrophic growth phase (Horbach et al., 2011). Obviously, plants defend themselves in various ways to such versatile biotic threats and as a result successful pathogens are constantly perturbing host cell signaling or suppressing plant innate immunity. In turn, plants have to defend themselves through mechanisms that perceive and respond to pathogen attacks resulting in an arms race that is currently framed in the so-called zig-zag model (Jones and Dangl, 2006). Upon pathogen attack, the first line of plant defence is formed by pattern recognition receptors (PRRs) that recognize pathogen-associated molecular patterns (PAMPs) activating the so-called PAMP-triggered immunity (PTI) that prevents further colonization of potential pathogens. In order to suppress PTI, plant pathogens secrete effectors leading to host susceptibility known as effector-triggered susceptibility (ETS). In turn, plants have responded by evolving R proteins that recognize directly or indirectly effectors that trigger effector-triggered immunity (ETI), which is often associated with the hypersensitive response (HR). HR is initiated by the activation of various protein kinase cascades, oxidative burst responses and increased expression of numerous defense related genes eventually leading to host cell death. Pathogens evade the selection pressure by modulating recognition by numerical or structural effector changes to suppress ETI, leading again to susceptibility (Thomma et al., 2011). In biotrophic and hemibiotrophic fungi, numerous effectors (avirulence factors or elicitors) and associated resistance (R) genes have been cloned, characterized and proven to comply with the gene-for-gene (GFG) model (Flor, 1971; Bent and Mackey, 2007; Dodds et al., 2009) (Fig.1). For example, in the strictly biotrophic fungus *C. fulvum*, four avirulence effectors (Avrs) and six extracellular proteins (Ecps) were characterized that invoke an HR – but also have virulence functions – in tomato lines carrying cognate resistance traits (Stergiopoulos and de Wit, 2009).

In necrotrophic fungi, predominantly present in the order of Pleosporales, effectors have an alternative role by functioning directly as host selective toxins (HSTs) that induce plant cell death in the presence of HST-sensitivity genes. Thus, unlike the classical GFG interaction, resistance is controlled by the absence of HST-sensitivity genes.

Therefore, these interactions are described as inverse GFG (iGFG) systems (Fig.1) (Wolpert et al., 2002; Friesen et al., 2008).

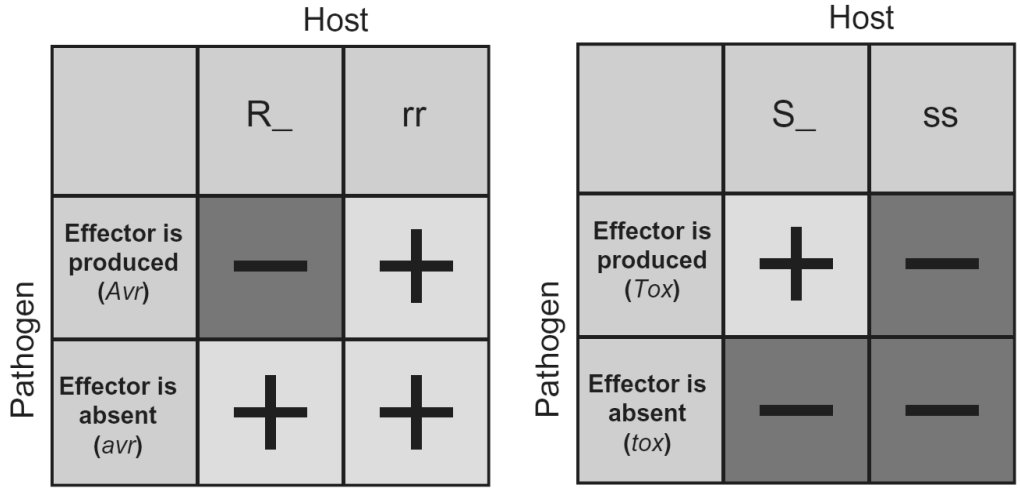

Fig. 1. Left: GFG models (effector-triggered immunity) frequently determine biotrophic plant–pathogen interactions. Fungal Avrs and plant resistance proteins directly or indirectly interact and this leads to disease resistance often involving an HR. Right: iGFG models (effector-triggered susceptibility) frequently determine necrotrophic plant–pathogen interactions. HSTs and host sensitivity genes interact and this leads to disease susceptibility. Plus signs (+) represent compatible (susceptible) interactions, minus signs (−) represent incompatible (resistant) interactions (Friesen and Faris, 2010).

However, effectors produced by both classes of pathogens operate in a species- and cultivar-specific manner. Currently, HSTs are known to be produced by about 20 fungal species, several of which produce multiple toxins. These fungal genera mostly belong to the large class of Dothideomycetes and include species from genera such as *Alternaria*, *Cochliobolus*, *Leptosphaeria*, *Venturia*, *Ascochyta*, *Pyrenophora* and *Stagonospora*. The devastating wheat tan spot pathogen *P. tritici repentis* (Ptr) produces several proteinaceous and nonproteinaceous HSTs (Ballance et al., 1989; Effertz et al., 2002). ToxA is the first isolated and best-studied proteinaceous HST. Its recent lateral transfer from the wheat glume blotch pathogen *S. nodorum* to *Ptr* turned tan spot from a negligible component of the cereal disease complex into a major global wheat disease (Friesen et al., 2006). In *S. nodorum* five HSTs and their corresponding HST-sensitivity genes have been identified (Liu et al., 2009). At this stage three sensitivity genes have been cloned; *LOV1* from Arabidopsis (Lorang et al., 2007), *Pc* from Sorghum (Nagy and Bennetzen, 2008) and *Tsn1* from wheat that all have disease resistance gene-like features, including S/TPK and NBS-LRR domains (Faris et al., 2010).

Mycosphaerella graminicola is a member of the Dothideomycetes

The genus *Mycosphaerella* together with its associated anamorph genera contains over 10,000 names (Crous et al., 2009), causing disease on a wide array of major food, fiber or fuel crops, including cereals, banana, soybeans and tree crops (Farr et al. 1995). Taxonomically, *Mycosphaerella* belongs to the class of the Dothideomycetes, formerly known as the loculoascomycetes (Eriksson and Winka, 1997), which is the largest and most diverse class of ascomycete fungi that comprises over 20,000 species, which infect almost every crop and are found on every continent including major plant pathogens such as the aforementioned *S. nodorum* and *Ptr* as well as the *Mycosphaerella fijiensis*, the banana black sigatoka pathogen, the Southern corn leaf blight pathogen *Cochliobolus heterostrophus* and the pine needle blight pathogen *Dothistroma septosporum* (Hane et al., 2007), as well as saprobes and a few lichen-forming and rock-inhabiting fungi (Ruibal et al., 2009).

The subject of this thesis, the heterothallic ascomycete *Mycosphaerella graminicola* (Fuckel) J. Schröt. in *Cohn* (anamorph *Zymoseptoria tritici* (Desm.) Quaedvlieg & Crous) (Quaedvlieg et al., 2011) is another major Dothideomycete plant pathogen. It causes septoria tritici blotch (STB), which is one of the most important global wheat diseases that defoliates plants and consequently diminishes yields (Eyal, 1981; Eyal, 1987; Eyal, 1999; Ponomarenko et al., 2011). The host range of *M. graminicola* includes both bread and durum wheat (*Triticum aestivum* L. and *T. turgidum* ssp. *durum* L.) and their graminaceous ancestors, but isolates show clear pathogenicity differences on these species, known as host specificity (Kema et al., 1996d; Kema et al., 1996b; Ware, 2006). Stukenbrock et al. (2007, 2010) provided evidence that *M. graminicola* emerged as a wheat pathogen from ancestral *Mycosphaerella* populations on wild grasses during wheat domestication around 10,500 years ago. Indeed, *Z. tritici* also infects grasses (Brokenshire, 1975; Suffert et al., 2010; Quaedvlieg et al., 2011), but their function as alternative hosts in natural habitats is not well understood (Suffert et al., 2010) as many of these species may actually be different *Mycosphaerella* species (Quaedvlieg et al., 2011).

The wheat-*M. graminicola* pathosystem

M. graminicola is a hemibiotroph characterized by a biotrophic and a necrotrophic phases during pathogenesis that have been extensively studied (Cohen and Eyal, 1993; Kema et al., 1996a; Duncan and Howard, 2000; Rohel et al., 2001; Shetty et al., 2003). The infection

process is completed within 12-24 hrs and commences when deposited spores germinate under conditions of high humidity and germ tubes penetrate the foliage, mainly through the stomata, without differentiation of infection structures and irrespective of host resistance (Kema et al., 1996a; Mehrabi et al., 2006).

Macroscopic symptoms vary greatly in the incompatible interaction from none detectable to substantial leaf chlorosis or necrosis, but without fungal proliferation (Ware, 2006; Rudd et al., 2008) and with the absence of an HR that is characteristic of many other pathosystems (Greenberg, 1997; Heath, 2000). The exact mechanism of resistance is still unknown (Shetty et al., 2003; Rudd et al., 2008; Shetty et al., 2009). Shetty et al. (2003, 2007) showed that the inhibition of pathogen development is correlated with H_2O_2 accumulation. However, H_2O_2 scavenging in a resistant cultivar did not render it fully susceptible and therefore, other factors are also considered to contribute to host resistance (Shetty et al., 2007). Recent reports showed an accumulation of β-1,3-glucanase and chitinase in the apoplast as well as callose deposition in incompatible interactions. Furthermore, it was shown that β-1,3-glucans in the fungal cell wall trigger the expression of the PR-2 protein β-1,3-glucanase, which is essential for cleaving elicitors from fungal cell walls and hence can act as PAMPs (Shetty et al., 2009).

Compatibility is characterized by a long apoplastic biotrophic phase with absence of macroscopic symptoms until approximately 10 days after inoculation, depending on environmental/experimental conditions, -without noticeable increase of fungal biomass (Kema et al., 1996a; Ware, 2006; Rudd et al., 2008). Marshall et al. (2011) suggested that *M. graminicola* could be considered as a necrotroph rather than a hemibiotroph since not much is known about the fungus' survival and nutrition during the long symptomless initial phase. Recently, three LysM effectors, *M. graminicola* homologues of Ecp6 from *C. fulvum*, were identified that were shown to mediate virulence through perturbation of chitin-triggered host immunity (de Jonge et al., 2010). These were up-regulated during the biotrophic phase, but only one played a role in virulence, suggesting that they may have different functions during plant infection (Marshall et al., 2011). The transition between the biotrophic and necrotrophic phases is associated with the induction of host defense processes that characterize HR associated with programmed cell death (PCD) as well as differential regulation of wheat mitogen-activated protein kinase (MAPK) pathways, and other markers that are typically associated with ETI, or occasionally with PTI (Keon et al., 2007; Rudd et al., 2008). They all affect cell permeability resulting in nutrient leakage from dying plant cells that facilitates fungal proliferation in the apoplast. Keon et al. (2007) identified a plethora of sugars and

amino acids in the apoplastic fluids released from wheat cells just before the onset of host cell death and thus STB lesion formation. Indeed, the massive mesophyll cell collapse during the biotrophic-necrotrophic switch is reminiscent of active cell-wall-degradation (Douaiher et al., 2007; Kema et al., 2008; Siah et al., 2010), but could also be due to toxic compounds that act as virulence factors (Kema et al., 1996a; Perrone, 2000; Shetty et al., 2009). This would significantly differ from the related pathogens *S. nodorum* and *P. tritici* that secrete proteinaceous toxins during host penetration, which are subsequently internalized in the wheat host cells (Ciuffetti et al., 2010; Faris et al., 2010). However, early chloroplast condensation in wheat mesophyll cells without proximate *M. graminicola* hyphae also suggests that apoplastic fungal compounds affect cell and organelle integrity (Kema et al., 1996a). Eventually, fungal proliferation during the necrotrophic phase culminates in the formation of numerous asexual and sexual fructifications (Kema et al., 1996a; Kema et al., 1996c) (Fig.2).
Under field conditions, *M. graminicola* has a compounded reproduction system of asexually produced splash-borne pycnidiospores and sexually produced air-borne ascospores. The epidemiological importance of plant tissues (wheat seeds, stubble and debris; wheat volunteers; other grasses) and the various fungal propagules for inoculum build-up and overseasoning (ascospores, pycnidiospores, mycelium) has been reviewed recently by Suffert et al. (2010). Ascospores are produced year-round, but their release from wheat debris during the fall is the most important source of primary inoculum. After symptom development, this is followed by secondary waves of pycnidiospores that drive STB epidemics during the growing season (Eyal, 1987; Shaw and Royle, 1989, 1993; Eyal, 1999; Hunter et al., 1999; McDonald and Linde, 2002; Zhan et al., 2007; Suffert et al., 2010; Ponamorenko et al., 2011).

Finally, specificity in the *M. graminicola*-wheat pathosystem has been frequently observed (Kema et al., 1996d; Kema et al., 1996b; Kema and van Silfhout, 1997; Kema et al., 2000; Brading et al., 2002; Ware, 2006; Ware et al., 2006). Since the elucidation of the *M. graminicola* mating system, the host-pathogen interaction was shown to comply with the GFG model (Brading et al., 2002) and the genetic control of host and cultivar specificity was studied in several mapping populations resulting in the identification of multiple quantitative trait loci involved in induction of necrosis and formation of pycnidia (Kema et al., 1996c; Kema et al., 2000; Ware, 2006). So far, 18 *Stb* genes have been reported in bread wheat cultivars (Arraiano et al., 2007; Goodwin, 2007; Chartrain et al., 2009; Tabib Ghaffary et al., 2011a; Tabib Ghaffary et al., 2011b).

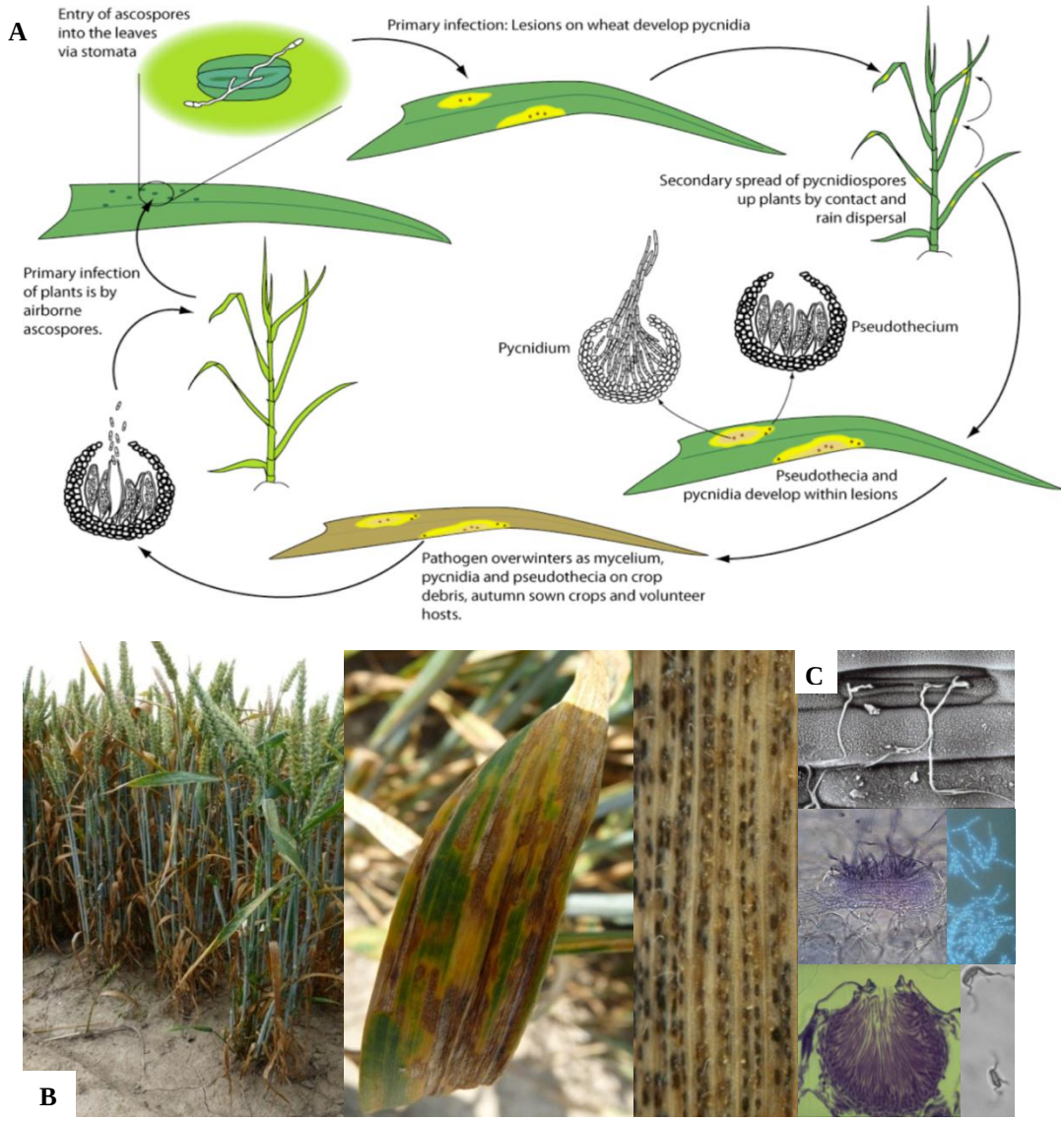

Fig. 2. A. Life cycle of the fungal wheat pathogen *Mycosphaerella graminicola* (after Ponomarenko et al., 2011); **B.** From left to right: septoria tritici blotch lesions on wheat leaves; **C.** From top to bottom: asexual spores called pycnidiospores germinate, form a germ tube, and enter a substomatal chamber by penetrating the leaf through a stomatum. Pycnidium exuding a cyrrhus containing pycnidiospores through the stomatal opening. Individual pycnidiospores are multicellular and uninucleate (stained with DAPI and observed with UV epifluorescent microscopy). Sexual reproduction occurs when two strains of opposite mating type meet and form a pseudothecium in which ascospores develop. Ascospores are two-celled, uninucleate, hyaline and elliptical with one cell slightly larger than the other (Kema et al., 1996a; Mehrabi et al., 2006).

Sexual recombination in *M. graminicola*

Meiosis shuffles linkage groups (chromosomes) and alleles within individual chromosomes generating therefore genetic diversity (Wahls, 1997). Recombination originates from crossing-overs between homologous chromosomes that result in physical structures, the chiasmata, enabling the proper segregation of recombinants during the meiotic stage (Roeder, 1997; Page and Hawley, 2003; Nishant and Rao, 2006). In most organisms, chiasmata are

positioned preferentially at hotspots along chromosomes and are important for the segregation of homologous chromosomes and sister chromatids during meiosis I and II, respectively (Roeder, 1997; Wahls et al., 2008) (Fig. 3).

M. graminicola has a bipolar heterothallic mating system and sexual development requires two mating partners - carrying different mating type alleles (*mat1-1* or *mat 1-2*) (Kema et al., 1996c; Waalwijk et al., 2004). From closely related species, it has been shown that spermagonia produce the male spermatia, and ascogonia produce the female trichogynes (Crous, 1998). When the cytoplasm of the two parent mycelia fuse, a spermatium fertilizes a trichogyne after which the nuclei undergo mitosis. A dikaryotic cell with two haploid nuclei will develop and undergoes mitosis leading to the formation of ascogenous hyphae containing nuclei from each parent. Ascus mother cells will form, and genetically distinct nuclei fuse into a zygote during karyogamy. The zygote divides meiotically and produces four haploid nuclei. Each of these nuclei undergoes mitosis yielding four twin pairs of daughter cells, the ascospores, in bitunicate asci in the pseudothecia.

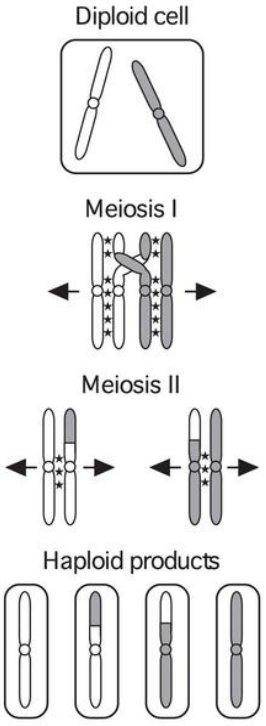

Fig. 3. Hallmarks of meiosis.
After DNA replication, homologues chromosomes (light and dark) pair and undergo a high rate of recombination (Wahls et al., 2008).

This sexual reproduction plays a major role in the genetic structure of *M. graminicola* populations that exhibit a high level of genetic diversity even within the same lesion (Chen and McDonald, 1996; Linde et al., 2002; Zhan et al., 2002). Understanding the genetic structure of a population is indicative for the epidemiology and evolutionary potential of a pathogen (McDonald and Linde, 2002). Molecular markers are commonly used to characterize pathogen populations and can also be used in segregating populations derived from a specific cross between two parents to generate genetic linkage maps that visualize genome organization and structure, and specific gene positions (Xu et al., 2009). Several methods, including PCR-based techniques such as Random Amplification of Polymorphic DNA (RAPD), Restriction Fragment Length Polymorphism (RFLP), Amplified Fragment Length Polymorphism (AFLP), microsatellites or simple sequence repeats (SSRs), have been used to construct genetic linkage maps in *Ascomycetes* (Cozijnsen et al., 2000; Jurgenson et al., 2002; Kema et

al., 2002; Pedersen et al., 2002; Zhong et al., 2002; De Vos et al., 2007; Manzo-Sanchez et al., 2008), *Basidiomycetes* (Larraya et al., 2000; Muraguchi et al., 2003; Marra et al., 2004; Lind et al., 2005), and *Oomycetes* (van der Lee et al., 1997; May et al., 2002; Sicard et al., 2003). Another recent technique is the Diversity Arrays Technology (DArT), which is a cost effective hybridization-based marker technology that offers a high multiplexing level while being independent of sequence information. This technique has been applied successfully in several crops including barley (Tinker et al., 2009), wheat (Akbari et al., 2006) and rice (Xie and Nevo, 2008). In this thesis its application in fungal genomes is described.

Dothideomycete genomics

Because of their relative small genome size, fungi are particularly amenable to genome studies (Dyer, 2008). High-throughput DNA sequencing provides a new window to study the structure and function of genomes and enable the rapid identification of genes that are important for plant infection and colonization, obviating the need for time consuming and laborious cloning (Desjardins et al., 2003). The first fungal genome ever published was the 12 Mb *Saccharomyces cerevisiae* genome in 1996 (Goffeau et al., 1996) followed by *Schizosaccharomyces pombe* six years later (Wood et al., 2002). Recent technical advances in DNA sequencing resulted in an explosion of genome projects with over 100 that are at least in the draft assembly phase (genomeprj) (Ma and Fedorova, 2010). So far, twelve Dothideomycete genomes have been sequenced by the Joint Genome Institute of the United States Department of Energy (DOE-JGI, http://www.jgi.doe.gov, see MycoCosm at http://genome.jgi-psf.org/programs/fungi/index.jsf) and other sequencing centers (Ohm et al., 2011). The availability of these genome sequences not only enabled advanced comparative genomic studies addressing the extreme phenotypic diversity in the fungal kingdom and showing the existence of mesosynteny between relatively distantly related *Ascomycetes* (Hane et al., 2007; Hane et al., 2011), but also enabled comparative transcriptomics (Ohm et al., 2011).

Recently, homologues of the *C. fulvum* Avr4 and Ecp2 effector proteins were identified in the related Dothideomycete banana pathogen *M. fijiensis* that evoked HR responses in tomato lines carrying cognate R genes (Stergiopoulos et al., 2010), illustrating the power of genome sequences for discovery research. Due to its genetic tractability and high economic significance, *M. graminicola* was the first filamentous fungal species that was sequenced in the Community Sequence Program of the DOE-JGI and currently represents the

first completed fungal genome which is presented in this thesis.

SCOPE OF THIS THESIS

The experiments and results described in this thesis provide insight into the genome structure and pathogenicity of *M. graminicola.*

Chapter 1 provides a brief overview of the biology and pathogenicity of *M. graminicola* and also briefly touches on the impact of improved and novel technologies for genetic and genome research that revolutionize the speed, scope and scale of comparative genomics.

Chapter 2 describes the detailed analyses of two *M. graminicola* mapping populations that were generated using the *in planta* crossing protocol. Chromosome length and number polymorphisms, CLPs and CNPs, respectively, were frequently discovered in progeny isolates, but had no apparent effect on sexual and pathogenic fitness. The observed genomic diversity in progeny isolates suggests that meiosis is an important driver of genome plasticity. The generated linkage map was instrumental for the finishing strategy of the *M. graminicola* genome.

Chapter 3 provides a summary of a complex research program in which the *M. graminicola* genome was unraveled. It provides highlights on genome structure and organization, including the identification of eight dispensable chromosomes and their plasticity as shown in comparative genome hybridizations. The dispensable chromosomes are distinct in structure, gene and repeat content but also contain parts from each core chromosome. Finally, this chapter describes various functional characteristics of the genome content in relation to *M. graminicola'*s lifestyle.

Chapter 4 presents a global analysis of fungal proteins that are mostly secreted during the compatible interaction with wheat. For this purpose, various proteome analytical tools were used and the generated data were blasted to the finished *M. graminicola* genome data to subtract all host proteins. The known and proposed role of the *in planta M. graminicola* proteome is discussed within the context of fungal virulence.

Chapter 5 further details on the initial identification and characterization of necrosis-inducing proteins from *M. graminicola*. Their activity in wheat seedlings strongly depends on

light intensity, which resembles characteristics of the iGFG model of other Dothideomycete-wheat pathosystems where susceptibility is driven by the interaction between fungal HSTs and HST-sensitivity genes in the host.

Chapter 6 is a summarizing discussion where the experimental data of the previous chapters are placed in a broader context, highlighting the importance of the discovered mechanisms for genome structure and function. The identification of necrosis-inducing proteins in *M. graminicola* and the implications of this finding are discussed in the context of its hemi-biotrophic lifestyle and its interaction with wheat.

LITERATURE CITED

Akbari, M., Wenzl, P., Caig, V., Carling, J., Xia, L., Yang, S., Uszynski, G., Mohler, V., Lehmensiek, A., and Kuchel, H. 2006. Diversity arrays technology (DArT) for high-throughput profiling of the hexaploid wheat genome. TAG Theoretical and Applied Genetics 113:1409-1420.

Arraiano, L.S., Chartrain, L., Bossolini, E., Slatter, H.N., Keller, B., and Brown, J.K.M. 2007. A gene in European wheat cultivars for resistance to an African isolate of *Mycosphaerella graminicola*. Plant Pathology 56:73-78.

Ballance, G., Lamari, L., and Bernier, C. 1989. Purification and characterization of a host-selective necrosis toxin from *Pyrenophora tritici-repentis.* Physiological and Molecular Plant Pathology 35:203-213.

Bent, A.F., and Mackey, D. 2007. Elicitors, Effectors, and R Genes: The New Paradigm and a Lifetime Supply of Questions. Annual Review of Phytopathology 45:399-436.

Brading, P.A., Verstappen, E.C.P., Kema, G.H.J., and Brown, J.K.M. 2002. A gene-for-gene relationship between wheat and *Mycosphaerella graminicola*, the Septoria tritici blotch pathogen. Phytopathology 92:439-445.

Brokenshire, T. 1975. The Role of Graminaceous Species in the Epidemiology of *Septoria tritici* on Wheat. Plant Pathology 24:33-38.

Chartrain, L., Sourdille, P., Bernard, M., and Brown, J.K.M. 2009. Identification and location of Stb9, a gene for resistance to septoria tritici blotch in wheat cultivars Courtot and Tonic. Plant Pathology 58:547-555.

Chen, R.S., and McDonald, B.A. 1996. Sexual reproduction plays a major role in the genetic structure of populations of the fungus *Mycosphaerella graminicola*. Genetics 142:1119-1127.

Ciuffetti, L.M., Manning, V.A., Pandelova, I., Betts, M.F., and Martinez, J.P. 2010. Research review: Host-selective toxins, Ptr ToxA and Ptr ToxB, as necrotrophic effectors in the *Pyrenophora tritici-repentis*–wheat interaction. New Phytologist 187:911-919.

Cohen, L., and Eyal, Z. 1993. The histology of processes associated with the infection of resistant and susceptible wheat cultivars with *Septoria tritici*. Plant Pathology 42:737-743.

Cozijnsen, A., Popa, K., Purwantara, A., Rolls, B., and Howlett, B. 2000. Genome analysis of the plant pathogenic ascomycete *Leptosphaeria maculans;* mapping mating type and host specificity loci. Molecular Plant Pathology 1:293-302.

Crous, P. 1998. Mycosphaerella spp. and their anamorphs: associated with leaf spot diseases of Eucalyptus. APS Press.

Crous, P.W., Summerell, B., Carnegie, A., Wingfield, M.J., Hunter, G.C., Burgess, T.I., Andjic, V., Barber, P., and Groenewald, J. 2009. Unravelling Mycosphaerella: do you believe in genera? Persoonia 23:99.

de Jonge, R., Peter van Esse, H., Kombrink, A., Shinya, T., Desaki, Y., Bours, R., van der Krol, S., Shibuya, N., Joosten, M.H.A.J., and Thomma, B.P.H.J. 2010. Conserved Fungal LysM Effector Ecp6 Prevents Chitin-Triggered Immunity in Plants. Science 329:953-955.

De Vos, L., Myburg, A., Wingfield, M., Desjardins, A., Gordon, T., and Wingfield, B. 2007. Complete genetic linkage maps from an interspecific cross between *Fusarium circinatum* and *Fusarium subglutinans*. Fungal Genetics and Biology 44:701-714.

Desjardins, A.E., Bhatnagar, D.2003. Fungal Genomics: An Overview. Pages 1-13 in: Applied Mycology and Biotechnology 3:1-13.

Dodds, P.N., Rafiqi, M., Gan, P.H.P., Hardham, A.R., Jones, D.A., and Ellis, J.G. 2009. Effectors of biotrophic fungi and oomycetes: pathogenicity factors and triggers of host resistance. New Phytologist 183:993-1000.

Douaiher, M., Nowak, E., Durand, R., Halama, P., and Reignault, P. 2007. Correlative analysis of *Mycosphaerella graminicola* pathogenicity and cell wall-degrading enzymes produced in vitro: the importance of xylanase and polygalacturonase. Plant Pathology 56:79-86.

Duncan, K., and Howard, R. 2000. Cytological analysis of wheat infection by the leaf blotch pathogen *Mycosphaerella graminicola*. Mycological Research 104:1074-1082.

Dyer, P.S. 2008. Fungal genomics. Mycological Research 112:1007-1008.

Effertz, R., Meinhardt, S., Anderson, J., Jordahl, J., and Francl, L. 2002. Identification of a chlorosis-inducing toxin from *Pyrenophora tritici-repentis* and the chromosomal location of an insensitivity locus in wheat. Phytopathology 92:527-533.

Eriksson, O., and Winka, K. 1997. Supraordinal taxa of Ascomycota. Myconet.

Eyal, Z. 1981. Integrated Control of Septoria Diseases of Wheat. Plant Disease 65:763-768.

Eyal, Z. 1987. The Septoria diseases of wheat: Concepts and methods of disease management. Agribookstore.

Eyal, Z. 1999. The *Septoria tritici* and *Stagonospora nodorum* blotch diseases of wheat. European Journal of Plant Pathology 105:629-641.

Faris, J.D., Zhang, Z., Lu, H., Lu, S., Reddy, L., Cloutier, S., Fellers, J.P., Meinhardt, S.W., Rasmussen, J.B., Xu, S.S., Oliver, R.P., Simons, K.J., and Friesen, T.L. 2010. A unique wheat disease resistance-like gene governs effector-triggered susceptibility to necrotrophic pathogens. Proceedings of the National Academy of Sciences 107:13544-13549.

Farr D.F., Bills G.F., Chamuris, G.P., Rossman, A.Y. 1995. Fungi on plants and plant products in the United States APS Press, St Paul, MN, USA.

Flor, H.H. 1971. Current status of the gene-for-gene concept. Annual Review of Phytopathology 9:275-296.

Friesen, T., Faris, J., Solomon, P., and Oliver, R. 2008. Host-specific toxins: effectors of necrotrophic pathogenicity. Cellular Microbiology 10:1421-1428.

Friesen, T.L., and Faris, J.D. 2010. Characterization of the wheat-*Stagonospora nodorum* disease system: what is the molecular basis of this quantitative necrotrophic disease interaction?. Canadian Journal of Plant Pathology 32:20-28.

Friesen, T.L., Stukenbrock, E.H., Liu, Z.H., Meinhardt, S., Ling, H., Faris, J.D., Rasmussen, J.B., Solomon, P.S., McDonald, B.A., and Oliver, R.P. 2006. Emergence of a new disease as a result of interspecific virulence gene transfer. Nature Genetics 38:953-956.

Genomeprj. 2011. www.ncbi.nlm.nih.gov/genomeprj

Goffeau, A., Barrell, B.G., Bussey, H., Davis, R.W., Dujon, B., Feldmann, H., Galibert, F., Hoheisel, J.D., Jacq, C., Johnston, M., Louis, E.J., Mewes, H.W., Murakami, Y., Philippsen, P., Tettelin, H., and Oliver, S.G. 1996. Life with 6000 Genes. Science 274:546-567.

Goodwin, S.B. 2007. Back to basics and beyond: increasing the level of resistance to Septoria tritici blotch in wheat. Australasian Plant Pathology 36:532-538.

Greenberg, J.T. 1997. Programmed cell death in plant-pathogen interactions. Annual Review of Plant Biology 48:525-545.

Hane, J., Lowe, R., Solomon, P., Tan, K., Schoch, C., Spatafora, J., Crous, P., Kodira, C., Birren, B., and Galagan, J. 2007. Dothideomycete plant interactions illuminated by genome sequencing and EST analysis of the wheat pathogen *Stagonospora nodorum.* The Plant Cell Online 19:3347-3368.

Hane, J.K., Rouxel, T., Howlett, B.J., Kema, G.H.J., Goodwin, S.B., and Oliver, R.P. 2011. A novel mode of chromosomal evolution peculiar to filamentous Ascomycete fungi. Genome Biology 12:R45.

Heath, M.C. 2000. Hypersensitive response-related death. Plant Molecular Biology 44:321-334.

Horbach, R., Navarro-Quesada, A., Knogge, W., and Deising, H. 2011. When and how to kill a plant cell: Infection strategies of plant pathogenic fungi. Journal of Plant Physiology 168: 51-62.

Hunter, T., Coker, R., and Royle, D. 1999. The teleomorph stage, *Mycosphaerella graminicola*, in epidemics of septoria tritici blotch on winter wheat in the UK. Plant Pathology 48:51-57.

Jones, J., and Dangl, J. 2006. The plant immune system. Nature 444:323-329.

Jurgenson, J., Bowden, R., Zeller, K., Leslie, J., Alexander, N., and Plattner, R. 2002. A genetic map of *Gibberella zeae* (*Fusarium graminearum*). Genetics 160:1451.

Kema, G.H.J., Verstappen, E.C.P., and Waalwijk, G. 2000. Avirulence in the wheat septoria tritici leaf blotch fungus *Mycosphaerella graminicola* is controlled by a single locus. Molecular Plant-Microbe Interactions 13:1375-1379.

Kema, G.H.J., and van Silfhout, C. 1997. Genetic variation for virulence and resistance in the wheat-*Mycosphaerella graminicola* pathosystem III. Comparative seedling and adult plant experiments. Phytopathology 87:266-272.

Kema, G.H.J., Yu, D., Rijkenberg Frits, H.J., Shaw Michael, W., and Baayen Robert, P. 1996a. Histology of the pathogenesis of *Mycosphaerella graminicola* in wheat. Phytopathology 86:777-786.

Kema, G.H.J., Sayoud, R., Annone, J.G., and Van Silfhout, C.H. 1996b. Genetic variation for virulence and resistance in the wheat-*Mycosphaerella graminicola* pathosystem: II. Analysis of interaction between pathogen isolates and host cultivars. Phytopathology 86:213-220.

Kema, G.H.J., Verstappen, E.C.P., Todorova, M., and Waalwijk, C. 1996c. Successful crosses and molecular tetrad and progeny analyses demonstrate heterothallism in *Mycosphaerella graminicola*. Current Genetics 30:251-258.

Kema, G.H.J., Annone, J., G, Sayoud, R., Van Silfhout, C.H., Van Ginkel, M., and De Bree, J. 1996d. Genetic variation for virulence and resistance in the wheat-*Mycosphaerella graminicola* pathosystem: I. Interactions between pathogen isolates and host cultivars. Phytopathology 86:200-212.

Kema, G.H.J., Goodwin, S.B., Hamza, S., Verstappen, E.C.P., Cavaletto, J.R., Van der Lee, T.A.J., De Waard, M., Bonants, P.J.M., and Waalwijk, C. 2002. A combined amplified fragment length polymorphism and randomly amplified polymorphism DNA genetic linkage map of *Mycosphaerella graminicola*, the Septoria tritici leaf blotch pathogen of wheat. Genetics 161:1497-1505.

Kema, G.H.J., van der Lee, T.A.J., Mendes, O., Verstappen, E.C.P., Lankhorst, R.K., Sandbrink, H., van der Burgt, A., Zwiers, L.-H., Csukai, M., and Waalwijk, C. 2008. Large-Scale Gene Discovery in the Septoria Tritici Blotch Fungus *Mycosphaerella graminicola* with a Focus on In Planta Expression. Molecular Plant-Microbe Interactions 21:1249-1260.

Keon, J., Antoniw, J., Carzaniga, R., Deller, S., Ward, J., Baker, J., Beale, M., Hammond-Kosack, K., and Rudd, J. 2007. Transcriptional adaptation of *Mycosphaerella graminicola* to programmed cell death (PCD) of its susceptible wheat host. Molecular Plant-Microbe Interactions 20:178-193.

Larraya, L., Perez, G., Ritter, E., Pisabarro, A., and Ramirez, L. 2000. Genetic linkage map of the edible basidiomycete *Pleurotus ostreatus*. Applied and Environmental microbiology 66:5290.

Lind, M., Olson, Å., and Stenlid, J. 2005. An AFLP-markers based genetic linkage map of *Heterobasidion annosum* locating intersterility genes. Fungal Genetics and Biology 42:519-527.

Linde, C., Zhan, J., and McDonald, B. 2002. Population structure of *Mycosphaerella graminicola*: from lesions to continents. Phytopathology 92:946-955.

Liu, Z.H., Faris, J.D., Oliver, R.P., Tan, K.C., Solomon, P.S., McDonald, M.C., McDonald, B.A., Nunez, A., Lu, S.W., Rasmussen, J.B., and Friesen, T.L. 2009. SnTox3 Acts in Effector Triggered Susceptibility to Induce Disease on Wheat Carrying the Snn3 Gene. PLoS Pathog 5(9): e1000581. doi:10.1371/journal.ppat.1000581.

Lorang, J.M., Sweat, T.A., and Wolpert, T.J. 2007. Plant disease susceptibility conferred by a "resistance" gene. Proceedings of the National Academy of Sciences 104:14861-14866.

Ma, L.J., and Fedorova, N.D. 2010. A practical guide to fungal genome projects: strategy, technology, cost and completion. Mycology 1:9-24.

Manzo-Sanchez, G., Zapater, M., Luna-Martinez, F., Conde-Ferraez, L., Carlier, J., James-Kay, A., and Simpson, J. 2008. Construction of a genetic linkage map of the fungal pathogen of banana *Mycosphaerella fijiensis*, causal agent of black leaf streak disease. Current Genetics 53:299-311.

Marra, R., Huang, J., Fung, E., Nielsen, K., Heitman, J., Vilgalys, R., and Mitchell, T. 2004. A genetic linkage map of *Cryptococcus neoformans* variety neoformans serotype D (*Filobasidiella neoformans*). Genetics 167:619-631.

Marshall, R., Kombrink, A., Motteram, J., Loza-Reyes, E., Lucas, J., Hammond-Kosack, K., Thomma, B., and Rudd, J. 2011. Analysis of two *in planta* expressed LysM effector homologues from the fungus *Mycosphaerella graminicola* reveals novel functional properties and varying contributions to virulence on wheat. Plant physiology 156:756-769.

May, K., Whisson, S., Zwart, R., Searle, I., Irwin, J., Maclean, D., Carroll, B., and Drenth, A. 2002. Inheritance and mapping of 11 avirulence genes in *Phytophthora sojae*. Fungal Genetics and Biology 37:1-12.

McDonald, B.A., and Linde, C. 2002. Pathogen population genetics, evolutionary potential, and durable resistance. Annual Review of Phytopathology 40:349-379.

Mehrabi, R., Zwiers, L.-H., de Waard, M.A., and Kema, G.H.J. 2006. MgHog1 Regulates Dimorphism and Pathogenicity in the Fungal Wheat Pathogen *Mycosphaerella graminicola*. Molecular Plant-Microbe Interactions 19:1262-1269.

Muraguchi, H., Ito, Y., Kamada, T., and Yanagi, S. 2003. A linkage map of the basidiomycete *Coprinus cinereus* based on random amplified polymorphic DNAs and restriction fragment length polymorphisms. Fungal Genetics and Biology 40:93-102.

MycoCosm. 2011. http://genome.jgi-psf.org/programs/fungi/tools.jsf

Nagy, E.D., and Bennetzen, J.L. 2008. Pathogen corruption and site-directed recombination at a plant disease resistance gene cluster. Genome research 18:1918-1923.

Nishant, K., and Rao, M. 2006. Molecular features of meiotic recombination hot spots. Bioessays 28:45-56.

Ohm, R., Aerts, A., Salamov, A., Goodwin, S.B., and Grigoriev, I. (2011). Comparative analysis of twelve Dothideomycete plant pathogens (Ernest Orlando Lawrence Berkeley National Laboratory, Berkeley, CA (US).

Page, S.L., and Hawley, R.S. 2003. Chromosome Choreography: The Meiotic Ballet. Science 301:785-789.

Pedersen, C., Rasmussen, S., and Giese, H. 2002. A genetic map of *Blumeria graminis* based on functional genes, avirulence genes, and molecular markers. Fungal Genetics and Biology 35:235-246.

Perrone, G., Logrieco, A., Kema, G.H.J., Ritieni, A., Bottalico, A. 2000. Phytotoxic activity of *Mycosphaerella graminicola* culture filtrates. Developments in Plant Genetics and Breeding 6:195-201.

Ponomarenko, A., Goodwin, S.B., and Kema, G.H.J. 2011. Septoria tritici blotch lesson. APS.

Quaedvlieg, W., Kema, G.H.J., Groenewald, J.Z., Verkley, G.J.M., Seifbarghi, S., Razavi, M., Mirzadi Gohari, A., Mehrabi, R., and Crous, P.W., 2011. *Zymoseptoria* gen. nov.: a new genus to accommodate Septoria-like species occurring on graminicolous hosts. Persoonia 26:57-69.

Roeder, G.S. 1997. Meiotic chromosomes: it takes two to tango. Genes & Development 11:2600-2621.

Rohel, E.A., Cavelier, N., and Hollomon, D.W. 2001. Microscopic analysis of the effect of azoxystrobin treatments on *Mycosphaerella graminicola* infection using green fluorescent protein (GFP)-expressing transformants. Pest Management Science 57:1017-1022.

Rudd, J., Keon, J., and Hammond-Kosack, K. 2008. The wheat mitogen-activated protein kinases TaMPK3 and TaMPK6 are differentially regulated at multiple levels during compatible disease interactions with *Mycosphaerella graminicola*. Plant Physiology 147:802-815.

Ruibal, C., Gueidan, C., Selbmann, L., Gorbushina, A.A., Crous, P.W., Groenewald, J.Z., Muggia, L., Grube, M., Isola, D., Schoch, C.L., Staley, J.T., Lutzoni, F., and de Hoog, G.S. 2009. Phylogeny of rock-inhabiting fungi related to Dothideomycetes 64:123-133.

Shaw, M.W., and Royle, D.J. 1989. Airborne Inoculum as a Major Source of *Septoria tritici* (*Mycosphaerella graminicola*) Infections in Winter-Wheat Crops in the Uk. Plant Pathology 38:35-43.

Shaw, M.W., and Royle, D.J. 1993. Factors Determining the Severity of Epidemics of *Mycosphaerella graminicola* (*Septoria tritici*) on Winter-Wheat in the Uk. Plant Pathology 42:882-899.

Shetty, N., Mehrabi, R., Lutken, H., Haldrup, A., Kema, G., Collinge, D., and Jorgensen, H. 2007. Role of hydrogen peroxide during the interaction between the hemibiotrophic fungal pathogen *Septoria tritici* and wheat. New Phytologist 174:637-647.

Shetty, N.P., Kristensen, B.K., Newman, M.A., Moller, K., Gregersen, P.L., and Jorgensen, H.J.L. 2003. Association of hydrogen peroxide with restriction of *Septoria tritici* in resistant wheat. Physiological and Molecular Plant Pathology 62:333-346.

Shetty, N.P., Jensen, J.D., Knudsen, A., Finnie, C., Geshi, N., Blennow, A., Collinge, D.B., and Jorgensen, H.J.L. 2009. Effects of b-1,3-glucan from *Septoria tritici* on structural defence responses in wheat. The Journal of Experimental Botany. 60:4287-4300.

Siah, A., Deweer, C., Duyme, F., Sanssené, J., Durand, R., Halama, P., and Reignault, P. 2010. Correlation of in planta endo-beta-1, 4-xylanase activity with the necrotrophic phase of the hemibiotrophic fungus *Mycosphaerella graminicola*. Plant Pathology 59:661–670.

Sicard, D., Legg, E., Brown, S., Babu, N., Ochoa, O., Sudarshana, P., and Michelmore, R. 2003. A genetic map of the lettuce downy mildew pathogen, Bremia lactucae, constructed from molecular markers and avirulence genes. Fungal Genetics and Biology 39:16-30.

Stergiopoulos, I., and de Wit, P. 2009. Fungal effector proteins. Annual Review of Phytopathology 47: 233-263.

Stergiopoulos, I., van den Burg, H.A., Okmen, B., Beenen, H.G., van Liere, S., Kema, G.H.J., and de Wit, P.J.G.M. 2010. Tomato Cf resistance proteins mediate recognition of cognate homologous effectors from fungi pathogenic on dicots and monocots. Proceedings of the National Academy of Sciences 107:7610-7615.

Stukenbrock, E.H., Banke, S., Javan-Nikkhah, M., and McDonald, B.A. 2007. Origin and domestication of the fungal wheat pathogen *Mycosphaerella graminicola* via sympatric speciation. Molecular Biology and Evolution 24:398-411.

Stukenbrock, E.H., Jørgensen, F.G., Zala, M., Hansen, T.T., McDonald, B.A., Schierup, M.H., and Malik, H.S. 2010. Whole-Genome and Chromosome Evolution Associated with Host Adaptation and Speciation of the Wheat Pathogen *Mycosphaerella graminicola*. PLoS Genetics 6:279-308.

Suffert, F., Sache, I., and Lannou, C. 2010. Early stages of septoria tritici blotch epidemics of winter wheat: build- up, overseasoning, and release of primary inoculum. Plant Pathology: 60:166–177.

Tabib Ghaffary, S.M., Robert, O., Laurent, V., Lonnet, P., Margalé, E., van der Lee, T.A.J., Visser, R.G.F., and Kema, G.H.J. 2011a. Genetic analysis of resistance to septoria tritici blotch in the French winter wheat cultivars Balance and Apache. TAG Theoretical and Applied Genetics:1-14.

Tabib Ghaffary , S.M., Faris, J.D., Friesen, T.L., Visser, R.G.F., van der Lee, T.A.J., Robert, O., Kema,G.H.J. 2011b. New broad- spectrum resistance to septoria tritici blotch derived from synthetic hexaploid wheat. Submitted to TAG.

Thomma, B.P.H.J., Nürnberger, T., and Joosten, M.H.A.J. 2011. Of PAMPs and Effectors: The Blurred PTI-ETI Dichotomy. The Plant Cell 23: 4-15.

Tinker, N.A., Kilian, A., Wight, C.P., Heller-Uszynska, K., Wenzl, P., Rines, H.W., Bjørnstad, Å., Howarth, C.J., Jannink, J.L., and Anderson, J.M. 2009. New DArT markers for oat provide enhanced map coverage and global germplasm characterization. BMC Genomics 10:39.

van der Lee, T., De Witte, I., Drenth, A., Alfonso, C., and Govers, F. 1997. AFLP Linkage Map of the Oomycete *Phytophthora infestans*. Fungal Genetics and Biology 21:278-291.

Waalwijk, C., van der Lee, T., de Vries, I., Hesselink, T., Arts, J., and Kema, G.H.J. 2004. Synteny in toxigenic Fusarium species: The fumonisin gene cluster and the mating type region as examples. European Journal of Plant Pathology 110:533-544.

Wahls, W.P. 1997. Meiotic Recombination Hotspots: Shaping the Genome and Insights into Hypervariable Minisatellite DNA Change. Pages 37-75 in: Current Topics in Developmental Biology.

Wahls, W.P., Siegel, E.R., and Davidson, M.K. 2008. Meiotic Recombination Hotspots of Fission Yeast Are Directed to Loci that Express Non-Coding RNA. PLoS One 3:e2887.

Ware, S.B. 2006. Aspects of sexual reproduction in Mycosphaerella species on wheat and barley: genetic studies on specificity, mapping, and fungicide resistance. Wageningen University, The Netherlands: Ph.D. thesis.

Ware, S.B, Wittenberg, A., Verstappen, E., van der Lee, T., Schouten, H., and Kema, G. 2006. Quantitative trait loci determine specificity to bread and durum wheat cultivars in the fungal wheat pathogen *Mycosphaerella graminicola*. Aspects of sexual reproduction in Mycosphaerella species on wheat and barley:75.

Wolpert, T., Dunkle, L., and Ciuffetti, L. 2002. Host-selective toxins and a virulence determinants: What's in a name? Annual Review of Phytopathology 40:251-285.

Wood, V., Gwilliam, R., Rajandream, M., Lyne, M., Lyne, R., Stewart, A., Sgouros, J., Peat, N., Hayles, J., and Baker, S. 2002. The genome sequence of *Schizosaccharomyces pombe*. Nature 415:871-880.

Xie, W.L., and Nevo, E. 2008. Wild emmer: genetic resources, gene mapping and potential for wheat improvement. Euphytica 164:603-614.

Xu, X., Roberts, T., Barbara, D., Harvey, N., Gao, L., and Sargent, D. 2009. A genetic linkage map of *Venturia inaequalis*, the causal agent of apple scab. BMC Research Notes 2:163.

Zhan, J., Mundt, C., and McDonald, B. 2007. Sexual reproduction facilitates the adaptation of parasites to antagonistic host environments: evidence from empirical study in the wheat-*Mycosphaerella graminicola* system. International journal for parasitology 37:861-870.

Zhan, J., Kema, G.H.J., Waalwijk, C., and McDonald, B.A. 2002. Distribution of mating type alleles in the wheat pathogen *Mycosphaerella graminicola* over spatial scales from lesions to continents. Fungal Genetics and Biology. 2002; 36:128-136.

Zhong, S., Steffenson, B.J., Martinez, J.P., and Ciuffetti, L.M. 2002. A molecular genetic map and electrophoretic karyotype of the plant pathogenic fungus *Cochliobolus sativus*. Molecular Plant Microbe Interactions 15:481-492.

Chapter 2

Meiosis drives extraordinary genome plasticity in the haploid fungal plant pathogen *Mycosphaerella graminicola*

Alexander H.J. Wittenberg[*], Theo A.J. van der Lee[*], **Sarrah Ben M'Barek**[*], Sarah B. Ware Stephen B. Goodwin, Andrzej Kilian, Richard G.F. Visser, Gert H.J. Kema, Henk J. Schouten.

Published in: PLoS One (2009) 4 (6): e5863

[*]These authors contributed equally to this research.

ABSTRACT

Meiosis in the haploid plant-pathogenic fungus *Mycosphaerella graminicola* results in eight ascospores due to a mitotic division following the two meiotic divisions. The transient diploid phase allows for recombination among homologous chromosomes. However, some chromosomes of *M. graminicola* lack homologs and do not pair during meiosis. Because these chromosomes are not present universally in the genome of the organism they can be considered to be dispensable. To analyze the meiotic transmission of unequal chromosome numbers, two segregating populations were generated by crossing genetically unrelated parent isolates originating from Algeria and The Netherlands that had pathogenicity towards durum or bread wheat, respectively. Detailed genetic analyses of these progenies using high-density mapping (1793 DArT, 258 AFLP and 25 SSR markers) and graphical genotyping revealed that *M. graminicola* has up to eight dispensable chromosomes, the highest number reported in filamentous fungi. These chromosomes vary from 0.39 to 0.77 Mb in size, and represent up to 38% of the chromosomal complement. Chromosome numbers among progeny isolates varied widely, with some progeny missing up to three chromosomes, while other strains were disomic for one or more chromosomes. Between 15-20% of the progeny isolates lacked one or more chromosomes that were present in both parents. The two high-density maps showed no recombination of dispensable chromosomes and hence, their meiotic processing may require distributive disjunction, a phenomenon that is rarely observed in fungi. The maps also enabled the identification of individual twin isolates from a single ascus that shared the same missing or doubled chromosomes indicating that the chromosomal polymorphisms were mitotically stable and originated from nondisjunction during the second division and, less frequently, during the first division of fungal meiosis. High genome plasticity could be among the strategies enabling this versatile pathogen to quickly overcome adverse biotic and abiotic conditions in wheat fields.

INTRODUCTION

Fungi provide attractive model systems to analyze processes that occur during meiosis. Many fungi are haploid, which greatly simplifies genetic studies. Furthermore, complete recovery of the meiotic products, or tetrads, is possible in ascomycete fungi, and these tetrads can be analyzed for the segregation of genetic markers. Tetrad analyses of *Aspergillus nidulans* and *Neurospora crassa* have been instrumental in answering fundamental questions concerning meiosis (Raju, 1980; Geiser et al., 1996; Davis and Perkins, 2002). Here we describe genetic studies in another filamentous ascomycete, *Mycosphaerella graminicola* (asexual stage: *Septoria tritici*). This fungus causes septoria tritici blotch (STB) of wheat, a disease characterized by necrotic blotches on the foliage. These blotches contain asexual (pycnidia) and sexual (pseudothecia) fructifications. *M. graminicola* represents an intriguing model for fundamental genetic studies of plant-pathogenic fungi. Field isolates of this pathogen usually have 18-21 chromosomes, the highest number reported among ascomycetes. Furthermore, these chromosomes have an extraordinary size range, varying from 0.39 to 6.09 Mb (Mehrabi et al., 2007). Genome plasticity - comprising processes such as inversions, deletions, insertions and translocations that translate into chromosome length polymorphisms (CLPs) as well as chromosome number polymorphisms (CNPs) - results in a genome size that varies between 32 and 40 Mb, similar to other filamentous ascomycetes (McDonald and Martinez, 1991; Kema et al., 1999; Dean et al., 2005; Cuomo et al., 2007; Hane et al., 2007; Mehrabi et al., 2007). *M. graminicola* has an active sexual cycle under natural conditions, which is an important driver of STB epidemics and results in high genetic diversity of populations in the field (Kema et al., 1996c; Kema et al., 1996a; Zhan et al., 2003).

Analyses of a cross between two *M. graminicola* strains that originated from bread wheat fields in The Netherlands resulted in the first genetic linkage map of a *Mycosphaerella* species (Kema et al., 2002; Goodwin et al., 2004). Although this map was a major milestone, the anonymous AFLP and RAPD markers complicated integration of genetic data sets. In addition, the number of markers was limited and the map resolution was too low to assess the complications anticipated during meiosis due to the CLPs and CNPs commonly observed among *M. graminicola* isolates (McDonald and Martinez, 1991).

The exact origin and maintenance of CNPs and CLPs are not known. A likely hypothesis is that they can be generated or lost during meiosis. Recombination between chromosomes that differ in length could give rise to derivatives with CLPs (Zolan, 1995). Nondisjunction during meiosis I or II would generate CNPs. To test these hypotheses, we

used the recently developed Diversity Arrays Technology (DArT) for the first time on a haploid fungal genome (Jaccoud et al., 2001; Wenzl et al., 2004; Wittenberg et al., 2005; Akbari et al., 2006; Semagn et al., 2006). The parallel genotyping of progeny isolates using several thousands of DNA fragments spotted on a microarray and subsequent analysis resulted in one of the most dense genetic linkage maps currently available for a fungus. This enabled high-resolution genetic linkage analyses to study the meiotic processing of CNPs and CLPs as well as the generation of new genome plasticity in *M. graminicola*. We frequently observed the loss of one or more chromosomes, disomy and translocations. This extraordinary genome plasticity helps to explain the high genetic diversity observed within natural populations of this fungus and most likely facilitates rapid adaptation to changing environments.

RESULTS

Marker selection and quality

Among the 68 progeny isolates from the *M. graminicola* IPO323 x IPO94269 cross, 1042 new DArT markers were obtained. The DArT markers were added to the first genetic linkage map of *M. graminicola* (Kema et al., 2002), consisting of 271 AFLP markers, 57 RAPD markers and two markers for the biological traits avirulence (*Avr*) and mating type (*mat*). Twenty-five SSR markers also were added to the combined linkage map (Table S7) (Goodwin et al., 2007). For the 148 progeny isolates of the *M. graminicola* IPO323 x IPO95052 cross, 1154 DArT markers were obtained that were combined with six SSR markers and the markers for the two biological traits (Table S8). After analysis of the marker data, 31 twins were detected in the *M. graminicola* progenies (Table S9). These twins result from the mitotic division that follows meiosis II in the ascus. The twin data enabled the dissection of mitotic or meiotic events that drive the generation of CLPs and CNPs. Eventually, the merged scoring tables comprised 60 individuals for the IPO323 x IPO94269 cross and 125 individuals for the IPO323 x IPO95052 cross (Table S10). Because twins can be regarded as biological replicates, they also were used to evaluate the reproducibility of the marker scores for the different marker technologies. In our study, DArT and AFLP markers appeared to be more reproducible than the RAPD markers. Therefore, RAPD markers were excluded to improve the quality of the maps. Although the reproducibility for both DArT and AFLP was very high, the frequency of double crossovers in the final maps was much lower for DArT than for AFLP markers (0.24% compared to 0.96%), indicating the superior

reliability of the DArT markers.

Construction and comparison of the linkage maps

The combined genetic linkage maps contain 2078 markers comprising 1793 DArT, 258 AFLP, and 25 SSR DNA markers, plus the two markers that co-segregate with the biological traits *Mat* and *Avr* (Table S11). The grouping and the order of the markers in the *M. graminicola* IPO323 x IPO94269 cross were highly similar to those in the previous maps (Kema et al., 2002; Goodwin et al., 2007). Compared to the previous map both new maps span a considerably larger part of the genome. In both crosses close to 99 % of the segregating markers were reliably positioned, indicating that the current genetic linkage maps cover the complete genome.

The new genetic linkage map of the IPO323 x IPO94269 cross is 638 cM longer than the first linkage map, and spans 1854 cM with 1317 markers on 451 unique map positions, with an average distance of 4.1 cM between the markers (Table S12). Nearly all markers (98.2%) were positioned on 24 LGs. Some of the smaller LGs that were observed in the first map merged with other LGs (Kema et al., 2002): 10 LGs in the first map merged into five larger LGs, while six small new LGs were formed. For example, LGs 3 and 4 in the first map merged with LGs 22 and 17, respectively, in the new map. The order of the AFLP markers in the first and new map remained similar, although more AFLP markers were positioned in the latter (223 vs. 258 out of 271, representing 82.3% and 95.2%, respectively). The genetic linkage map of the *M. graminicola* isolate IPO323 x IPO95052 cross spans 1946 cM and contains 1144 markers on 486 unique map positions on 23 LGs (comprising 98.5% of the generated markers), with an average distance of 4.0 cM between the markers (Table S12).

We also constructed a bridge map to compare the individual linkage maps using markers that segregated in both mapping populations. The resulting integrated map spans 1435 cM (~75% of both individual maps) and contains 372 markers on 251 unique map positions. A total of 22 LGs from each of the individual crosses was aligned with the bridge map, and the marker order was similar to those on the two individual genetic maps (Fig. 1 and Fig. S1). The 21 LGs in the bridge map is close to the estimated number of chromosomes based on electrophoretic and cytological karyotyping (Kema et al., 2002; Mehrabi et al., 2007) and is identical to the number of chromosomes of the finished genome sequence (http://genome.jgi-psf.org/Mycgr3/Mycgr3.home.html) (Table S13).

Translocations

We identified eight DArT markers that were positioned very differently in the two maps, which is indicative of translocations. They represented five translocations between isolate IPO323 and either IPO94269 or IPO95052 and involved four inter-LG and one intra-LG translocations (CBBMR_14G17 in LG 6) (Table S11). Another translocation between IPO323 and IPO94269 involved an SSR locus (Goodwin et al., 2007) that segregated in a diploid fashion in the isolate IPO323 x IPO94269 cross (1:1:1:1 ratio, $\chi^2 = 1.25$, $0.25 < P < 0.75$) and was mapped on LG 21 in IPO323 and on LG 4+17 in IPO94269. In addition, we obtained indications for a possible larger translocation involving LG F (Fig. S1).

Meiosis drives extraordinary genome plasticity

Parental CNPs. LGs 21 and C in the *M. graminicola* IPO323 x IPO94269 cross span less than 2 cM and contain 21 and 36 markers (AFLP, SSR and DArT), respectively. Interestingly, all of these markers are inherited from isolate IPO323. This suggests that these two LGs are present in IPO323 but absent in isolate IPO94269. In the progeny of the IPO323 x IPO95052 cross these linkage groups do show recombination, which resulted in much larger genetic distances of 21 cM and 24 cM, respectively. These results indicate that both linkage groups are present in isolates IPO323 and IPO95052, but are absent in IPO94269. An example of the difference in recombination frequency is shown for LG 21 in Fig. S2.

Meiotic transmission of CNPs. Graphical genotyping allows the tracing of the genetic make up of progeny isolates. Among the progeny of the *M. graminicola* IPO323 x IPO95052 cross, LGs that were regularly absent either individually or in combination included LGs 8, 12, 13, 15, 21, A, B and C. LGs 21 and C are absent in IPO94269, and frequently were missing in the *M. graminicola* IPO323 x IPO94269 progeny along with LGs 8, 12, 13 and A that were also often missing in this progeny (Table S4). In these cases LGs present in both parents were absent in one or more progeny isolates (Fig. 2). We also observed a progeny isolate (#40) from the *M. graminicola* IPO323 x IPO94269 cross that contained all markers from both parents on LG 13, indicating that this isolate was disomic for this relatively small chromosome (577 kb). In the same progeny set we identified another isolate (#51) that was disomic for LG 1, which represents one of the largest chromosomes (3.26 Mb) in the genome of *M. graminicola* isolate IPO323.

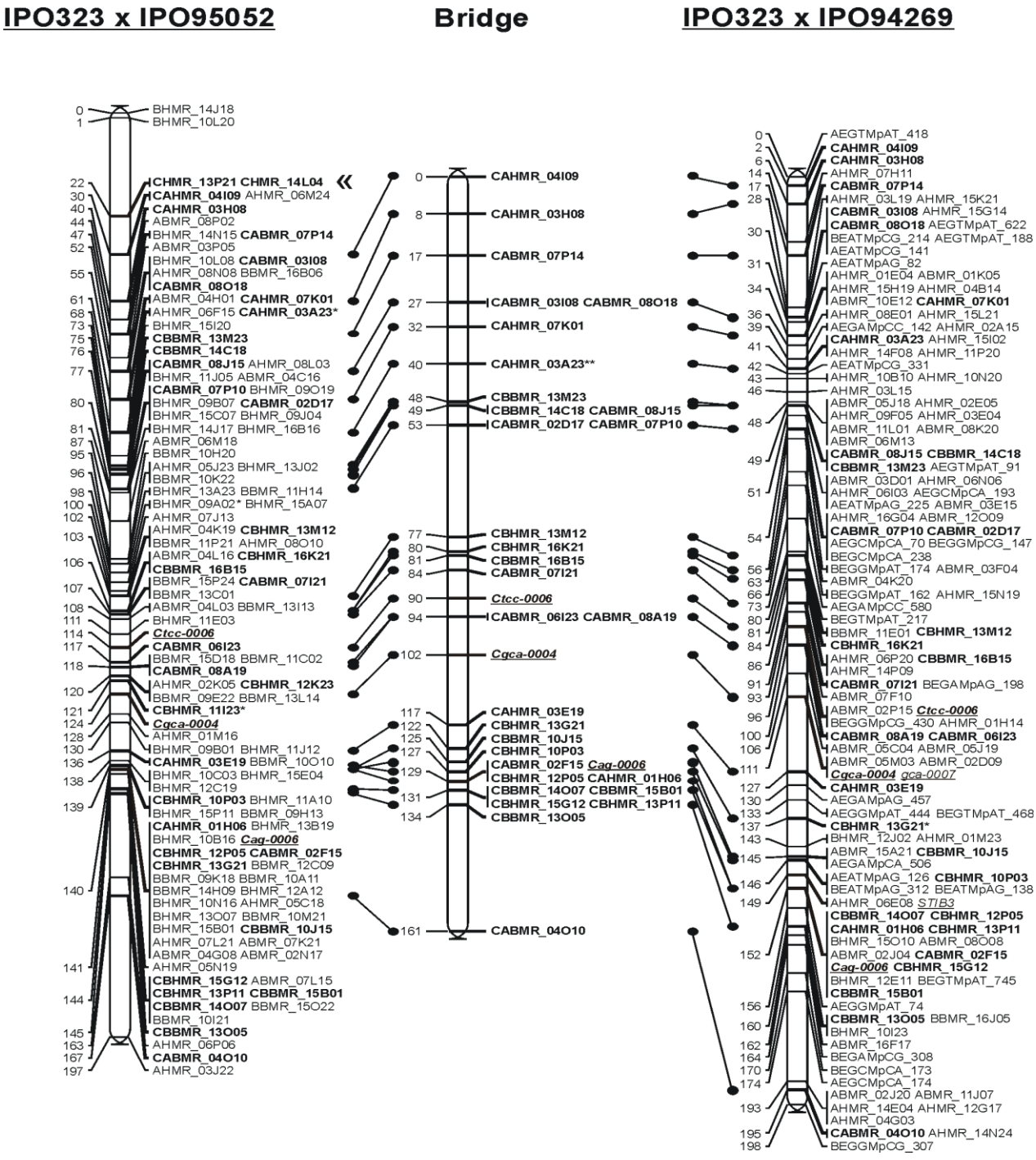

Fig. 1. Co-linearity of genetic linkage maps for *Mycosphaerella graminicola* crosses IPO323×IPO95052 (left) and IPO323×IPO94269 (right) with a bridge map (middle) generated with markers that segregated in both crosses.

Common markers are shown in bold and start with the prefix C, SSR markers are shown in blue and markers that are translocated in red. DArT markers were named according to phase of the marker (A = IPO323, B = IPO95052 or IPO94269), complexity reduction method used (BMR or HMR), and location in the spotting plate (e.g. BBMR_15L11). LG and AFLP nomenclature is according to Kema et al., 2002. Segregation distortion of the markers is indicated with * (P<0.05), ** (P<0.01), *** (P<0.005) or **** (P<0.001).

If nondisjunction occurs during meiosis I, two paired chromosomes are pulled to one cell leading to loss of that chromosome in the other cell (Fig. 2B). In this case, one haploid *M. graminicola* isolate would become heterozygous disomic for that chromosome. If nondisjunction occurs during meiosis II, two sister chromatids are not divided between the two cells but are both pulled to the same cell (Fig. 2C). This evidently leads to two identical copies of the chromosome in that cell, and hence to homozygous disomy in one cell and to absence in the other cell. Unfortunately, homozygous disomy could not be detected with the techniques used for our analysis.

Twins do not show CNPs. The large number of markers permitted easy identification of identical progeny and allowed determination of the stage at which CNPs were generated. In total, we detected 31 twins in the *M. graminicola* progenies, whose identity was visualized by graphical genotyping (Table S12). In four cases we could demonstrate that LGs that were present in both parents were absent in both isolates of a twin pair (Table S15). This is illustrated for twin pair 2137-2139 in Fig. 2D.

PCR confirmation. The observed aberrations and graphical genotyping analyses were confirmed by PCR assays (Fig. 2D, E). Additional SSR and PCR assays confirmed the graphical genotyping results for six out of eight LGs. The absence of two LGs was confirmed by scoring of co-dominant SSR markers that are located on LG 8 (*ac-0007*) and LG 12 (*gga-0001*). In all progeny isolates that lacked these LGs, none of the parental alleles was amplified (Fig. S3A). The absence of LGs 8, 12, 13, 15, A and C was further confirmed by diagnostic PCR analysis (Table S4a) for the mapped DArT markers. Indeed, none of these markers was amplified in the progeny isolates that, according to the graphical genotyping, lacked these particular LGs (Fig. S3B and S3C). However, amplicons of the expected size were always generated from the relevant checks, i.e., parental isolates, two progeny isolates that inherited the LG normally and a PCR amplification control.

To confirm the disomy for LG 1 in progeny isolate #51, we performed PCR assays based on deletion polymorphisms (Fig. 2E, Table S6) identified by comparative analyses of IPO94269 BAC-end sequences with the draft genome sequence (v.2.5) of IPO323. These PCRs confirmed the graphical genotyping results indicating that a series of progeny isolates lost one or more complete chromosomes, while other isolates received an extra copy of a particular chromosome.

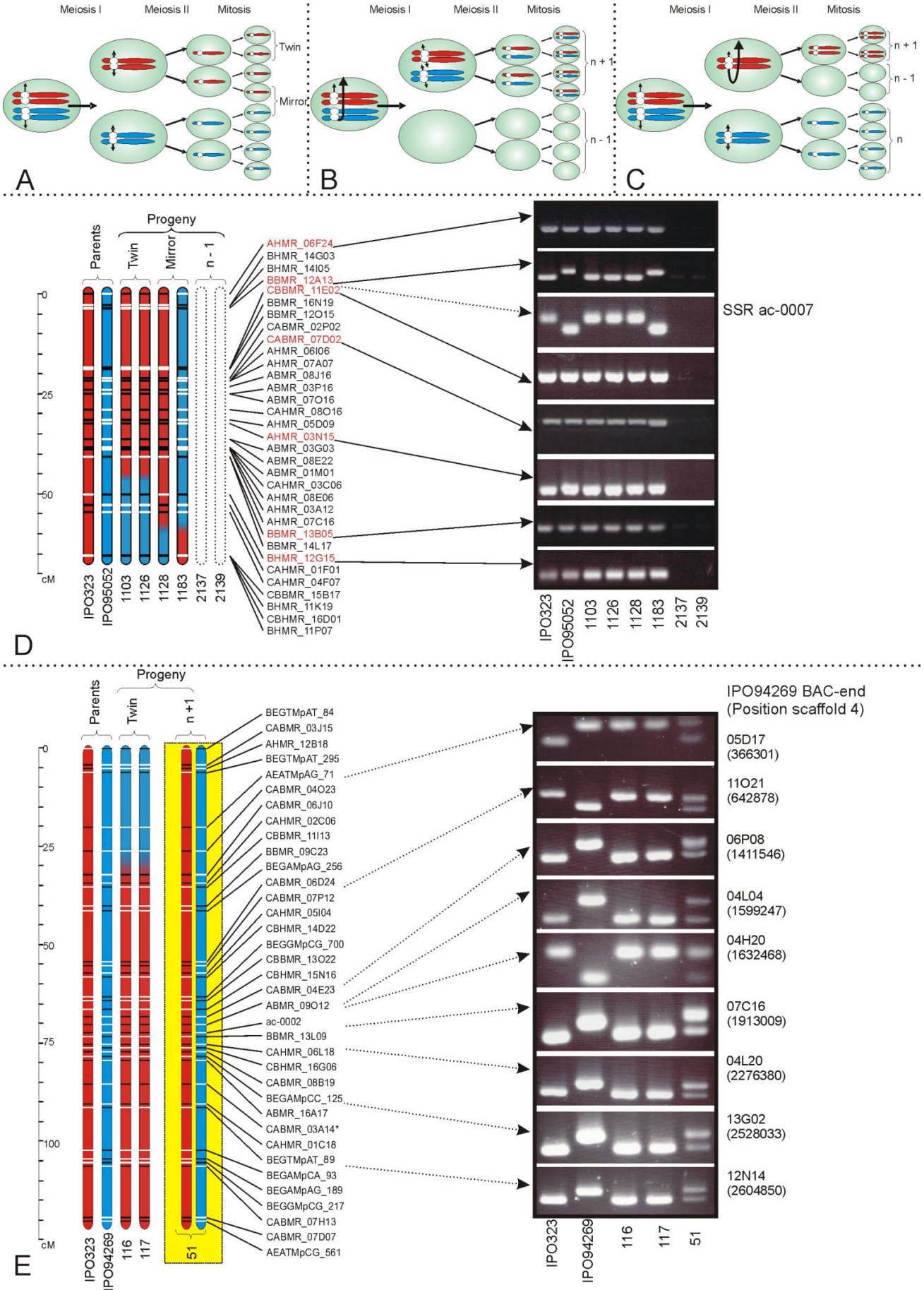
Meiosis I
Meiosis II
Mitosis
Twin
Mirror
A
n + 1
n - 1
B
n
C
Progeny
Parents
Twin
Mirror
n - 1
0
25
50
cM
IPO323
IPO95052
1103
1126
1128
1183
2137
2139
AHMR_06F24
BHMR_14G03
BHMR_14I05
BBMR_12A13
CBBMR_11E02
BBMR_16N19
BBMR_12O15
CABMR_02P02
CABMR_07D02
AHMR_06I06
AHMR_07A07
ABMR_08J16
ABMR_03P16
ABMR_07O16
CAHMR_08O16
AHMR_05D09
AHMR_03N15
ABMR_03G03
ABMR_08E22
ABMR_01M01
CAHMR_03C06
AHMR_08E06
AHMR_03A12
AHMR_07C16
BBMR_13B05
BBMR_14L17
BHMR_12G15
CAHMR_01F01
CAHMR_04F07
CBBMR_15B17
BHMR_11K19
CBHMR_16D01
BHMR_11P07
SSR ac-0007
D
Progeny
Parents
Twin
n +1
0
25
50
75
100
cM
IPO323
IPO94269
116
117
51
BEGTMpAT_84
CABMR_03J15
AHMR_12B18
BEGTMpAT_295
AEATMpAG_71
CABMR_04O23
CABMR_06J10
CAHMR_02C06
CBBMR_11I13
BBMR_09C23
BEGAMpAG_256
CABMR_06D24
CABMR_07P12
CAHMR_05I04
CBHMR_14D22
BEGGMpCG_700
CBBMR_13O22
CBHMR_15N16
CABMR_04E23
ABMR_09O12
ac-0002
BBMR_13L09
CAHMR_06L18
CBHMR_16G06
CABMR_08B19
BEGAMpCC_125
ABMR_16A17
CABMR_03A14*
CAHMR_01C18
BEGTMpAT_89
BEGAMpCA_93
BEGAMpAG_189
BEGGMpCG_217
CABMR_07H13
CABMR_07D07
AEATMpCG_561
IPO94269 BAC-end
(Position scaffold 4)
05D17
(366301)
11O21
(642878)
06P08
(1411546)
04L04
(1599247)
04H20
(1632468)
07C16
(1913009)
04L20
(2276380)
13G02
(2528033)
12N14
(2604850)
E

Fig. 2. Nondisjunction during meiosis in the haploid fungus *Mycosphaerella graminicola* results in chromosome number polymorphisms due to the loss or gain of specific chromosomes. **A.** Meiosis starts with the merging of nuclei from two different strains, leading to a transitory diploid cell. Karyogamy is followed immediately by meiosis I and II, resulting in four haploid cells. These four cells are duplicated during a subsequent mitotic step, leading to eight ascospores per ascus. Each ascospore is genetically identical to one other ascospore within the same ascus. Such pairs of identical ascospores are called twins. We identified several twins in progenies of *M. graminicola*. When a strain of a descendant lacked one or more chromosomes, the twins originating from the first mitotic cell division after meiosis always appeared to lack the same chromosomes. This indicates that chromosomes are stable during mitosis but can be lost during meiosis. **B.** Chromosome loss during meiosis can be a result of failure of separation of homologous chromosomes during meiosis I, or **C.** of the failure of separation of sister chromatids during meiosis II. **D.** Graphical genotyping of LG 8. The chromosomal segments descending from IPO323 are rendered in red, and the segments from IPO95052 in blue. Markers are scored as present (black) or absent (white). As the marker scores on all linkage groups were identical for these two isolates, we concluded that the descendants 2137 and 2139 are twins. However, both isolates lack all markers located on LG 8. This is a clear indication of absence of this linkage group in these isolates. Strikingly, this linkage group is present in both parents. For further verification, seven DArT markers spanning the length of LG 8 were converted into simple PCR markers. In addition, one SSR marker was used. All markers appeared to be absent in the twin isolates 2137 and 2139. This confirms the absence of LG 8 in these twins and indicates nondisjunction during meiosis as the cause. **E.** Nondisjunction not only results in loss of a chromosome in one twin but also to disomy for that chromosome in another twin from the same ascus. The graphical genotyping of isolate #51 illustrates heterozygous disomy for LG 1, which was confirmed by a PCR screen for deletion markers that unequivocally showed the presence of two copies of this chromosome in this haploid fungus.

In summary, the high-density mapping enabled the detection of meiotically driven and frequently occurring CNPs and CLPs in sexual progenies of the haploid plant pathogen *M. graminicola*. We identified 42 isolates that showed loss of a linkage group that was present in both parents compared to only two disomic isolates. Progenies showed 15 and 20% CNPs compared to the parents in the IPO323 x IPO94269 and IPO323 x IPO95052 crosses, respectively. Interestingly, the chromosomes lost were the same in both populations (Table S4). We performed 17 additional backcrosses and F_2 crosses between progeny isolates that showed substantial CNPs. All crosses except one were successful and resulted in viable progeny (Table S15).

DISCUSSION

The genome of *M. graminicola* is highly plastic, based on the detailed analyses provided by the high-density genetic linkage maps. Eight chromosomes were missing in one or more progeny and can be considered dispensable, while other chromosomes occasionally were disomic. As many as three chromosomes were missing from individual progeny isolates, with no apparent effect on fitness. As expected, much of the genome plasticity is generated during meiosis and this could help to explain the high adaptability observed in field populations of this pathogen.

Dispensable chromosomes have been found in other fungi but they usually occur at a

low frequency and typically represent single or a few chromosomes. For example the plant-pathogenic fungi *Alternaria alternata, Cochliobolus heterostrophus, Leptosphaeria maculans*, *Magnaporthe grisea* and *Nectria haematococca* as well as the insect pathogen *Metarhizium amisopliae* each had only a single chromosome that was dispensable (Tzeng et al., 1992; Leclair et al., 1996; Han et al., 2001; Hatta et al., 2002; Chuma et al., 2003; Wang et al., 2003). Dispensable chromosomes in these species usually contain genes involved in pathogenicity or virulence (Han et al., 2001; Hatta et al., 2002; Wang et al., 2003; Garmaroodi and Taga, 2007), whereas in others they don't (Orbach et al., 1996). In *M. graminicola*, genes involved in host plant perception did not map to any of the eight identified dispensable chromosomes (Ware, 2006). Hence, the function of genes on dispensable chromosomes in *M. graminicola* is yet unknown.

Genome instability is a major cause of disorders, and a range of genes has been identified that have a role in maintaining genome integrity (Aguilera and Gomez-Gonzalez, 2008). In addition, polyploidy and aneuploidy are considered evolutionary pathways to reproductive isolation and speciation (Koszul et al., 2004; Kohn, 2005). The mitotic and meiotic pairing and transmission of homologous chromosomes with length polymorphisms has been studied intensively in models such as the fungi *Saccharomyces cerevisiae*, *N. crassa* and *Coprinus cinereus* (Zolan, 1995; Perkins, 1997; Koszul et al., 2006). These model systems have substantially increased our knowledge of meiotic processes (Perkins and Davis, 2000), but they mostly involved cytogenetic studies and mutant strains (Cutter, 1951; Hardham and Mitchell, 1998). A high-density genetic linkage map provides a strong genome-wide alternative for precise analyses of meiosis. However, the number of high-density genetic maps for fungi is limited due to difficulties and costs of high-quality marker generation and scoring required for their generation (Hackett and Broadfoot, 2003). Here, we report the meiotic processing and generation of genomic plasticity using a high-density genetic linkage map for *M. graminicola*. This unusual approach enabled the detection of Mendelian and non-Mendelian inheritance patterns and elucidated the underlying meiotic principles that frequently resulted in progeny with CNPs.

It is very clear that meiosis not only maintains but also drives novel CNPs in *M. graminicola*, which most likely result from nondisjunction during the second meiotic division. We noticed that 15-20 % of progeny isolates were missing one or more chromosomes that were present in the two parents. Interestingly, the same chromosomes were dispensable in both crosses. PCR analyses confirmed most of the CNPs, including the disomic chromosomes. Despite graphical genotyping indications for the absence of LGs 21 and B in

the *M. graminicola* IPO323 x IPO95052 progeny, PCR amplifications with several primer combinations derived from the mapped DArT markers on these LGs were inconclusive, although BLAST analyses to the genome of IPO323 revealed that they are single copy. The cause is unknown but may be due to the high repetitive content of these LGs (not shown).

The high number of markers on the current linkage map enabled accurate identification of twin isolates. These originate from the mitotic division after meiosis and provided a unique opportunity to test the meiotic origin of CNPs. If CNPs resulted from aberrations during mitosis, twin isolates would show differences in chromosome number and could not have been identified. In *M. graminicola*, we repeatedly observed the loss of the same chromosome in both twin isolates, which demonstrates it was lost during meiosis and that CNPs are mitotically stable. We cannot exclude the possibility of occasional mitotic instability between isolates that otherwise would have been identified as twins, but if it occurs it appears to be very rare. Hence, we conclude that CNPs in *M. graminicola* are driven by meiosis. Nondisjunction during either meiotic division results in progeny with CNPs due to gains or losses of entire chromosomes. However, the number of CNPs is twice as high after nondisjunction during meiosis I compared to meiosis II. Moreover, besides chromosome loss, meiosis I results in heterozygous and meiosis II in homozygous disomy. Crossovers may result in heterozygozity for part of the chromosome only, but the dispensable chromosomes are small so crossovers occur less frequently. Our data revealed frequent loss of chromosomes, but we only rarely observed heterozygozity. This indicates that nondisjunction occurred preferentially during meiosis II. Unfortunately, our marker technology did not enable the quantitative determination of copy numbers to confirm homozygous disomy.

Meiotic processing of CNPs in other fungi varies. For the related ascomycete *Leptosphaeria maculans*, twin genotypes were also always identical in respect to the presence or absence of a dispensable chromosome (Leclair et al., 1996). This indicates that, similar to *M. graminicola*, the dispensable chromosome in *L. maculans* is mitotically stable. However, in the evolutionarily more distantly related ascomycete *Magnaporthe oryzae* (Chuma et al., 2003), presence of a dispensable chromosome varied in twin isolates, indicating that mitotic transmission of dispensable chromosomes may be unstable in some ascomycetes.

Apart from these differences and the fact that *M. graminicola* has up to eight dispensable chromosomes, a most striking aspect is that the widespread CNPs - involving multiple chromosomes - in *M. graminicola* do not hamper sexual reproduction. Interestingly, one of the factors inhibiting female fertility in *M. grisea* is present on a dispensable chromosome (Orbach et al., 1996). We do not have such evidence for *M. graminicola*. Recent

karyotyping experiments showed that isolate IPO323 has at least two additional chromosomes compared to IPO94269 (Mehrabi et al., 2007). Nevertheless, we were successful in crossing these two isolates and made 17 additional crosses between *M. graminicola* isolates that showed substantial CNPs. Chromosomes without a homologous partner cannot pair, will have zero recombination and might be expected to be lost during meiosis. However, our data indicate that in *M. graminicola* they are normally transmitted to progeny without distortion of the segregation ratio. For example, in the progeny of the IPO323 x IPO94269 cross, 34 and 35 out of 60 isolates contained the dispensable LGs 21 and C, respectively. This shows that the CNPs present between the parents are maintained during meiosis and are transmitted to approximately 50% of the progeny. Neither LG showed evidence of recombination as indicated by zero genetic distance between markers. The segregation of the unique IPO323 markers on these LGs confirmed the results of previous karyotyping experiments, that individual dispensable chromosomes are transmitted intact through meiosis (Mehrabi et al., 2007). This may well be among the first examples of distributive disjunction in fungi, a process that involves separation and distribution of non-recombining or non-homologous chromosomes during meiosis that is commonly observed in *Drosophila*. In fungi distributive disjunction was shown in *S. cerevisiae* by crossing strains that were monosomic for non-homologous chromosome I and III (Guacci and Kaback, 1991). In *M. graminicola* monosomic strains do not occur as the fungus is haploid, but the dispensable chromosomes were shown to segregate regularly. In *S. cerevisiae* distributive disjunction is considered to be extremely rare as monosomy does not frequently occur (Guacci and Kaback, 1991). In *M graminicola*, it might be essential as this study shows that CNPs occur frequently and are generated during meiosis. It is unknown whether distributive disjunction in *M. graminicola* also complies with the physical interactions between non-homologous chromosomes as was observed in *S. cerevisiae* (Loidl et al., 1994).

In contrast, all LGs in the entire progeny set of the IPO323 x IPO95052 cross contain markers from both parents, indicating that all parental chromosomes have homologous partners. Hence, in this respect the differences between the two Dutch bread wheat isolates (IPO323 and IPO94269) seem to be larger than were those between IPO323 and the Algerian durum wheat isolate IPO95052, underscoring the extraordinarily large genetic differences within local populations of *M. graminicola* (Zhan et al., 2003; Stukenbrock et al., 2007).

CLPs have been observed in at least 37 fungal species and hence seem to be a common feature of fungal genomes (Zolan, 1995). Clearly, recombination between homologous chromosomes of unequal length can result in new chromosome size variants.

Moreover, the pairing of repeated sequences, for instance resulting from transposons, on different chromosomes during meiosis may lead to translocations that may be an important cause of CLPs as opposed to CNPs (Perkins, 1997). Subtelomeric variable regions such as those in *M. grisea* are also a potential source of meiotically driven CLPs (Farman and Leong, 1995). The observed translocations in this study, as well as those in previous analyses (McDonald and Martinez, 1991; Chen and McDonald, 1996; Kema et al., 1999; Goodwin et al., 2001), most likely are responsible for the widespread CLPs in the genome of *M. graminicola* (McDonald and Martinez, 1991; Kema et al., 1999; Mehrabi et al., 2007).

Compared to CLPs, CNPs in other fungi are observed less frequently, have not been analyzed through a map-based approach, and are generally highly unstable. For instance, a minichromosome in *M. grisea* showed non-Mendelian inheritance, which was also observed in *L. maculans* whenever one parent missed such a chromosome (Leclair et al., 1996; Orbach et al., 1996). Crosses between *L. maculans* isolates that both carried this minichromosome resulted in CLPs (Leclair et al., 1996). Duplication of large chromosomal fragments in *S. cerevisiae* occasionally results in the formation of supernumerary chromosomes that are highly unstable during mitosis (Koszul et al., 2004; Koszul et al., 2006). In the usually haploid human pathogen *Cryptococcus neoformans*, CNPs occur frequently in diploid AD serotypes as a potential mechanism to overcome slow filamentous growth (Lengeler et al., 2001) and, more recently, CNPs were discovered resulting from the generation and subsequent breakage of a dicentric chromosome (Fraser et al., 2005). CNPs in haploid filamentous fungi such as *N. crassa* are generally either lethal or seriously impair the sexual phase (Perkins, 1997). Diploid and disomic isolates of *N. crassa*, originating from nondisjunction at meiosis I, are highly unstable and do not differ in rates and mechanisms of haploidization and mitotic crossing over (Smith, 1975). Similarly, disomic strains in *A. nidulans* that resulted from nondisjunction in meiotic metaphase I also were vegetatively unstable (Bainbridge and Roper, 1966; Swart et al., 2001).

In contrast to other species, CNPs in *M. graminicola* are vegetatively stable. We hypothesize that the extraordinarily high chromosome number of the *M. graminicola* genome (Mehrabi et al., 2007) may influence the frequency and fate of CNPs. The genome of *M. graminicola* (39.8 Mb) is in the same size range as those of *Magnaporthe oryzae* (41.6 Mb), *Fusarium graminearum* (36.5 Mb), *A. nidulans* (30.0 Mb) and *N. crassa* (39.2 Mb). However, the number of chromosomes in these fungi (N=8, 4, 7 and 7, for *A. nidulans*, *F. graminearum*, *M. oryzae*, and *N. crassa*, respectively) is much lower than in *M. graminicola* (N=21). Hence, loss of entire chromosomes in these organisms may be lethal due to the presence of essential

genes. *M. graminicola* has the highest chromosome number and the smallest autosomes in filamentous ascomycetes (Mehrabi et al., 2007). The present study has revealed that *M. graminicola* also has the highest number of dispensable chromosomes that vary from 0.39 to 0.77 Mb, representing up to 38% of the chromosomal complement and approximately 12% of its genome size. The frequent loss of chromosomes in *M. graminicola* without noticeable effect on fitness may be due to their small size. Dispensable chromosomes in many other fungi carry functional genes that play an important role in host-pathogen interactions (Miao et al., 1991; Tzeng et al., 1992; VanEtten et al., 1994; Han et al., 2001; Hatta et al., 2002; Garmaroodi and Taga, 2007). In *M. graminicola*, loci controlling host-pathogen interactions were not mapped on dispensable chromosomes and substantial CNPs in progeny isolates - up to three chromosomes per isolate covering as much as 1.59 Mb - neither reduced pathogenicity nor sexual compatibility (Kema et al., 2002; Ware, 2006). Therefore, pathogenicity in *M. graminicola* does not appear to be influenced by dispensable chromosomes.

In summary, our map-based approach is unique in analyses of genomic plasticity and demonstrates that CNPs in *M. graminicola* are meiotically generated and occur at much higher frequencies than reported previously for any ascomycete. These aberrations were observed in two crosses between field strains (Kema et al., 1996a). Since the sexual cycle occurs continuously under field conditions it is likely that meiotically driven CNPs play an important role in the high level of genetic diversity (Kema et al., 1996c; Kema et al., 1996b; Zhan et al., 2003) observed among isolates of *M. graminicola*. The total genome content of *M. graminicola* isolates varies between 32-40 Mb and each field isolate represents a unique karyotype (McDonald and Martinez, 1991; Mehrabi et al., 2007). In this study we showed that in addition to CLPs resulting from translocations, CNPs originate from aberrations during meiosis, mostly by nondisjunction during meiosis II. We hypothesize that the plasticity of the *M. graminicola* genome, as characterized by its large and flexible set of dispensable chromosomes, plays an important role in yet unknown processes of adaptation. This is currently being addressed in a *M. graminicola* crossing program aiming at individuals with a minimal genome size that is devoid of any dispensable chromosome. Backcrosses of such individuals with parental isolates will enable the selection of progeny with individual dispensable chromosome additions. Such a set will contribute significantly to understanding the role of dispensable chromosomes in the life strategy of *M. graminicola*.

MATERIALS AND METHODS

Fungal isolates and DNA extraction

We used three isolates of *M. graminicola*: IPO323 and IPO94269 were isolated from bread wheat in the Netherlands and IPO95052 was isolated from durum wheat in Algeria. Isolate IPO323 was crossed to both IPO94269 and IPO95052 using a previously developed *in planta* protocol (Kema et al., 1996a), resulting in 68 and 148 progeny, respectively. All progeny isolates were collected and analyzed individually. DNA of parents and progeny was isolated using the Wizard Genomic DNA purification kit (Promega Madison, WI), starting with approximately 10 mg of lyophilized spores. Tables S1 and 2 provide an overview of the progeny isolates used in this study.

DArT procedure

Generation of genomic representations, library construction, target preparation and image analysis were essentially performed as described previously (Jaccoud et al., 2001; Wenzl et al., 2004), with the modifications described by Wittenberg et al. (Wittenberg et al., 2005). The adapter and primer oligonucleotide sequences used in this study are listed in Table S3. For details see Text S1.

Nomenclature of markers

AFLP markers were designated by the primer combination used for the amplification and the approximate length of the generated fragment (Kema et al., 2002). For both AFLP and DArT markers the prefix A or B indicated the phase of the marker; those originating from parent IPO323 had the prefix A while markers from parent IPO95052 were indicated by the prefix B. DArT markers identified in cross IPO323 x IPO94269 originating from isolate IPO95052 could be assigned the prefix A or B, as IPO94269 was not used for the library construction. Markers segregating in both populations received the prefix C. In addition, DArT markers were designated by the enzyme combination used for complexity reduction (BamHI, MseI and RsaI: BMR or HindIII, MseI, RsaI: HMR), the 384-well plate number and the position of the fragment in that plate (i.e., AHMR_04I09). Recently, 23 SSR loci were identified in *M. graminicola*, 21 of which could be positioned on the existing linkage map along with two previously published SSR loci (Owen et al., 1998; Goodwin et al., 2007). The newly generated DArT markers were used to integrate the new IPO323 x IPO94269 map with

the existing map of that population (Kema et al., 2002). Moreover, six of these SSRs also differentiated the parents of the second mapping population. To enable the mapping of these SSRs in the IPO323 x IPO95052 progeny, amplification reactions were performed as described by Goodwin et al. (Goodwin et al., 2007).

Selection of unique segregation patterns and merging of twin isolates

The binary scores of polymorphic markers were converted to the correct allelic phase based on the scores of the parents. A Perl script was written that grouped loci with identical segregation patterns after disregarding unknown scores. The marker with the highest call rate (percentage of scored individuals) was selected as a representative for each group. The script also calculated the call rate for each individual genotype and the global call rate for the whole dataset. Individual genotypes were incorporated into the scoring table when at least 95% of the grouped markers could be scored. In *M. graminicola,* twin progeny isolates arise from the mitotic division that follows meiosis II in the ascus, resulting in four pairs of genetically identical ascospores. Although the random-ascospore progenies that resulted from the crossing protocol minimized the isolation of twin isolates, the large number of markers identified identical progeny efficiently. These were used to calculate the reproducibility of the different marker types and were merged before the mapping analyses.

Construction and comparison of the linkage maps

The genetic linkage maps of the individual crosses as well as the bridge map were constructed with the software package JoinMap 3.0 (Stam, 1993). A detailed description of the mapping process for the individual maps is given in Text S1. The use of IPO323 in both crosses enabled the efficient generation of an integrated bridge map of the *M. graminicola* genome. The bridge map was used to compare the order of the loci in the constructed IPO323 x IPO94269 and IPO323 x IPO95052 maps. We used MapChart 2.2 (Voorrips, 2002) for the graphical representation of the genetic linkage maps.

Evaluation of loss or gain of chromosomes

We used graphical genotyping to compare the marker scores (A or B) and the phase (A or B) of the markers, which enabled us to identify whether each marker was present or absent in a particular progeny isolate. In cases where a linkage group (LG) was constructed

from both marker types and a specific progeny isolate lacked all of these markers, we concluded that the isolate missed that LG. In cases where a LG was constructed from both marker types and a specific progeny isolate was scored present for all markers, we concluded that the isolate had an extra copy, derived from the other parent, of that particular LG. Hence, chromosome polymorphisms in progeny isolates were determined *in silico* if A and B markers that were assigned to a specific LG were always absent or present in a particular progeny.

PCR verification of loss and gain of chromosomes

DNA samples of the parental isolates (IPO323, IPO94269 and IPO95052), progeny isolates that showed absence of specific LGs by graphical genotyping (Table S4) and two control progeny without these aberrations were used as templates in the PCR reactions. PCR was performed using SSR markers and specific primer pairs developed from the sequenced DArT markers located on the missing linkage groups (Tables S5 and S6). To assure that absence of an amplicon was not caused by PCR failure, a positive PCR control was included that should be present in all parents and progeny that were tested. The SSR marker loci *ac-0007* (LG8) and *gga-0001* (LG12) were amplified in combination with the PCR control SSR locus *ag-0003* (LG2). For the amplicons derived from the DArT marker sequences, the DArT fragments CABMR_07D07 (129 bp; LG1) or AHMR_08O09 (728 bp; LG15) served as positive PCR controls.

PCR reactions were performed in a total volume of 20 µl containing 20 ng of genomic DNA, 1x PCR buffer (Roche), 1 µl of each of the forward and reverse primers used as a control (2 µM), 2 µl of each forward and reverse primer (2 µM), 0.8 µl of dNTPs (5 mM) and 0.2 µl of Taq DNA polymerase (5 U/ µl). Amplification conditions were as follows: 94°C for 2 min, 12 cycles of 94°C for 30 sec, 66°C for 30 sec minus 1°C per cycle, 72°C for 30 sec; 27 cycles of 94°C for 30 sec, 53°C for 30 sec, 72°C for 30 sec; 72°C for 7 min, followed by a cooling-down step to 10°C. The SSR amplicons were separated on 6 % non-denaturating acrylamide gels using a Mega-Gel Dual High-Throughput Vertical Electrophoresis Unit (CBS Scientific, Del Mar, California, USA). Amplicons based on the DArT sequences were separated on 2.5 % agarose gels.

ACKNOWLEDGMENTS

We thank Els C.P. Verstappen for generating the *M. graminicola* progenies and Ineke de Vries for helping with the DNA isolations. We gratefully acknowledge the support in DNA sequencing and analyses of Jim Bristow,

Len Pennacchio and Igor Grigoriev at the US Department of Energy – Joint Genome Institute and Jane Grimwood at the HudsonAlpha Institute for Biotechnology.

LITERATURE CITED

Aguilera, A., and Gomez-Gonzalez, B. 2008. Genome instability: a mechanistic view of its causes and consequences. Nat Rev Genet 9:204-217.

Akbari, M., Wenzl, P., Caig, V., Carling, J., Xia, L., Yang, S., Uszynski, G., Mohler, V., Lehmensiek, A., Kuchel, H., Hayden, M.J., Howes, N., Sharp, P., Vaughan, P., Rathmell, B., Huttner, E., and Kilian, A. 2006. Diversity arrays technology (DArT) for high-throughput profiling of the hexaploid wheat genome. Theor Appl Genet 113:1409-1420.

Bainbridge, B.W., and Roper, J.A. 1966. Observations on the effects of a chromosome duplication in *Aspergillus nidulans*. J. Gen. Microbiol. 42:417-424.

Chen, R.S., and McDonald, B.A. 1996. Sexual reproduction plays a major role in the genetic structure of populations of the fungus *Mycosphaerella graminicola*. Genetics 142:1119-1127.

Chuma, I., Tosa, Y., Taga, M., Nakayashiki, H., and Mayama, S. 2003. Meiotic behavior of a supernumerary chromosome in *Magnaporthe oryzae*. Current genetics 43:191-198.

Cuomo, C.A., Güldener, U., Xu, J-R., Trail, F., Turgeon, B.G., Di Pietro, A., Walton, J.D., Baker, S.E., Rep, M., Adam, G., Baldwin, T., Calvo, S., Chang, Y-L., DeCaprio, D., Gale, L., Gnerre, S., Goswami, R.S., Hammond-Kosack, K., Harris, L.J., Hilburn, K., Kennell, J., Kroken, S., Ma, L-J., Magnuson, J.K., Mannhaupt, G., Mauceli, E., Mewes, H-W., Mitterbauer, R., Muehlbauer, G., Münsterkotter, M., Nelson, D., O'Donnell, K., Ouellette, T., Qi, W., Quesneville, H., Roncero, M.T.G., Seong, K-Y., Tetko, I., Urban, M., Waalwijk, C., Ward, T., Yao, J., Birren, B.W., Kistler, H.C. 2006. The Fusarium genome reveals localized polymorphism and pathogen specialization. Science 317:1400-1402.

Cutter, V.M. 1951. The cytology of the fungi. Annu Rev Microbiol 5:17-34.

Davis, R.H., and Perkins, D.D. 2002. *Neurospora*: a model of model microbes. Nat Rev Genet 3:397-403.

Dean, R.A., Talbot, N.J., Ebbole, D.J., Farman, M.L., Mitchell, T.K., Orbach, M.J., Thon, M., Kulkarni, R., Xu, J.R., and Pan, H. 2005. The genome sequence of the rice blast fungus *Magnaporthe grisea*. Nature 434:980-986.

Farman, M.L., and Leong, S.A. 1995. Genetic and Physical Mapping of Telomeres in the Rice Blast Fungus, *Magnaporthe grisea*. Genetics 140:479-492.

Fraser, J.A., Huang, J.C., Pukkila-Worley, R., Alspaugh, J.A., Mitchell, T.G., and Heitman, J. 2005. Chromosomal translocation and segmental duplication in Cryptococcus neoformans. Eukaryot Cell 4:401-406.

Garmaroodi, H.S., and Taga, M. 2007. Duplication of a conditionally dispensable chromosome carrying pea pathogenicity (PEP) gene clusters in Nectria haematococca. Mol Plant Microbe Interact 20:1495-1504.

Geiser, D.M., Timberlake, W.E., and Arnold, M.L. 1996. Loss of meiosis in Aspergillus. Mol Biol Evol 13:809-817.

Goodwin, S.B., Waalwijk, C., and Kema, G.H.J. 2004. Genetics and Genomics of *Mycosphaerella graminicola*, a Model for the Dothideales Pages 315-330 in: Applied Mycology & Biotechnology.

Goodwin, S.B., Cavaletto, J.R., Waalwijk, C., and Kema, G.H.J. 2001. DNA fingerprint probe from *Mycosphaerella graminicola* identifies an active transposable element. Phytopathology 91:1181-1188.

Goodwin, S.B., van der Lee, T.A., Cavaletto, J.R., Te Lintel Hekkert, B., Crane, C.F., and Kema, G.H.J. 2007. Identification and genetic mapping of highly polymorphic microsatellite loci from an EST database of the septoria tritici blotch pathogen *Mycosphaerella graminicola*. Fungal Genet Biol 44:398-414.

Guacci, V., and Kaback, D.B. 1991. Distributive disjunction of authentic chromosomes in *Saccharomyces cerevisiae*. Genetics 127:475-488.

Hackett, C.A., and Broadfoot, L.B. 2003. Effects of genotyping errors, missing values and segregation distortion in molecular marker data on the construction of linkage maps. Heredity 90:33-38.

Han, Y., Liu, X., Benny, U., Kistler, H.C., and VanEtten, H.D. 2001. Genes determining pathogenicity to pea are clustered on a supernumerary chromosome in the fungal plant pathogen *Nectria haematococca*. The Plant Journal 25:305-314.

Hane, J.K., Lowe, R.G., Solomon, P.S., Tan, K.C., Schoch, C.L., Spatafora, J.W., Crous, P.W., Kodira, C., Birren, B.W., Galagan, J.E., F., T.S., McDonald, B.A., and Oliver, R.P. 2007. Dothideomycete Plant Interactions Illuminated by Genome Sequencing and EST Analysis of the Wheat Pathogen *Stagonospora nodorum*. Plant Cell 19:3347-3368.

Hardham, A.R., and Mitchell, H.J. 1998. Use of molecular cytology to study the structure and biology of phytopathogenic and mycorrhizal fungi. Fungal Genet Biol 24:252-284.

Hatta, R., Ito, K., Hosaki, Y., Tanaka, T., Tanaka, A., Yamamoto, M., Akimitsu, K., and Tsuge, T. 2002. A conditionally dispensable chromosome controls host-specific pathogenicity in the fungal plant pathogen *Alternaria alternata*. Genetics 161:59-70.

Jaccoud, D., Peng, K., Feinstein, D., and Kilian, A. 2001. Diversity arrays: a solid state technology for sequence information independent genotyping. Nucleic Acids Res 29:E25.

Kema, G.H.J., Verstappen, E.C.P., Todorova, M., and Waalwijk, C. 1996a. Successful crosses and molecular tetrad and progeny analyses demonstrate heterothallism in *Mycosphaerella graminicola*. Curr Genet 30:251-258.

Kema, G.H.J., Sayoud, R., Annone, J.G., and van Silfhout, C.H. 1996b. Genetic variation for virulence and resistance in the wheat-*Mycosphaerella graminicola* pathosystem. II. Analysis of interactions between pathogen isolates and host cultivars. Phytopathology 86:213-220.

Kema, G.H.J., Annone, J.G., Sayoud, R., van Silfhout, C.H., van Ginkel, M., and de Bree, J. 1996c. Genetic variation for virulence and resistance in the wheat-*Mycosphaerella graminicola* pathosystem. I. Interactions between pathogen isolates and host cultivars. Phytopathology 86:200-212.

Kema, G.H.J., Verstappen, E.C.P., Waalwijk, C., Bonants, P.J.M., de Koning, J.R.A., Hagenaar-de Weerdt, M., Hamza, S., Koeken, J.G.P., and van der Lee, T.A.J. 1999. Genetics of biological and molecular markers in *Mycosphaerella graminicola*, the cause of Septoria tritici leaf blotch of wheat. Pages 161-180 in: Septoria on Cereals: a Study of Pathosystems.

Kema, G.H.J., Goodwin, S.B., Hamza, S., Verstappen, E.C.P., Cavaletto, J.R., van der Lee, T.A.J., de Weerdt, M., Bonants, P.J.M., and Waalwijk, C. 2002. A combined amplified fragment length polymorphism and randomly amplified polymorphism DNA genetic kinkage map of *Mycosphaerella graminicola*, the septoria tritici leaf blotch pathogen of wheat. Genetics 161:1497-1505.

Kohn, L.M. 2005. Mechanisms of Fungal Speciation. Annual review of phytopathology 43:279-308.

Koszul, R., Dujon, B., and Fischer, G. 2006. Stability of large segmental duplications in the yeast genome. Genetics 172:2211-2222.

Koszul, R., Caburet, S., Dujon, B., and Fischer, G. 2004. Eucaryotic genome evolution through the spontaneous duplication of large chromosomal segments. Embo J 23:234-243.

Leclair, S., Ansan-Melayah, D., Rouxel, T., and Balesdent, M. 1996. Meiotic behaviour of the minichromosome in the phytopathogenic ascomycete *Leptosphaeria maculans*. Curr Genet 30:541-548.

Lengeler, K.B., Cox, G.M., and Heitman, J. 2001. Serotype AD strains of Cryptococcus neoformans are diploid or aneuploid and are heterozygous at the mating-type locus. Infect Immun 69:115-122.

Loidl, J., Scherthan, H., and Kaback, D.B. 1994. Physical association between nonhomologous chromosomes precedes distributive disjunction in yeast. Proceedings of the National Academy of Sciences of the United States of America 91: 331-334.

McDonald, B.A., and Martinez, J.P. 1991. Chromosome length polymorphisms in a *Septoria tritici* population. Curr Genet 19:265-271.

Mehrabi, R., Taga, M., and Kema, G.H.J. 2007. Electrophoretic and cytological karyotyping of the wheat pathogen *Mycosphaerella graminicola*. Mycologia 99:804-812.

Miao, V.P., Covert, S.F., and VanEtten, H.D. 1991. A fungal gene for antibiotic resistance on a dispensable ("B") chromosome. Science 254:1773-1776.

Orbach, M.J., Chumley, F.G., and Valent, B. 1996. Electrophoretic karyotypes of *Magnaporthe grisea* pathogens of diverse grasses. Mol Plant Microbe Interact 9:261-271.

Owen, P.G., Pei, M., Karp, A., Royle, D.J., and Edwards, K.J. 1998. Isolation and characterization of microsatellite loci in the wheat pathogen *Mycosphaerella graminicola*. Molecular ecology 7:1611-1612.

Perkins, D.D. 1997. Chromosome rearrangements in Neurospora and other filamentous fungi. Adv Genet 36:239-398.

Perkins, D.D., and Davis, R.H. 2000. Neurospora at the millennium. Fungal Genet Biol 31:153-167.

Raju, N.B. 1980. Meiosis and ascospore genesis in *Neurospora*. Eur J Cell Biol 23:208-223.

Semagn, K., Bjornstad, A., Skinnes, H., Maroy, A.G., Tarkegne, Y., and William, M. 2006. Distribution of DArT, AFLP, and SSR markers in a genetic linkage map of a doubled-haploid hexaploid wheat population. Genome 49:545-555.

Smith, D.A. 1975. A mutant affecting meiosis in Neurospora. Genetics 80:125-133.

Stam, P. 1993. Construction of integrated genetic linkage maps by means of a new computer package: JoinMap. Plant J 3:739-744.

Stukenbrock, E.H., Banke, S., Javan-Nikkhah, M., and McDonald, B.A. 2007. Origin and domestication of the fungal wheat pathogen *Mycosphaerella graminicola* via sympatric speciation. Mol Biol Evol 24:398-411.

Swart, K., van Heemst, D., Slakhorst, M., Debets, F., and Heyting, C. 2001. Isolation and characterization of sexual sporulation mutants of *Aspergillus nidulans*. Fungal Genet Biol 33:25-35.

Tzeng, T.H., Lyngholm, L.K., Ford, C.F., and Bronson, C.R. 1992. A restriction fragment length polymorphism

map and electrophoretic karyotype of the fungal maize pathogen *Cochliobolus heterostrophus*. Genetics 130:81-96.
VanEtten, H., Funnell-Baerg, D., Wasmann, C., and McCluskey, K. 1994. Location of pathogenicity genes on dispensable chromosomes in *Nectria haematococca* MPVI. Antonie Van Leeuwenhoek 65:263-267.
Voorrips, R.E. 2002. MapChart: software for the graphical presentation of linkage maps and QTLs. J Hered 93:77-78.
Wang, C., Skrobek, A., and Butt, T.M. 2003. Concurrence of losing a chromosome and the ability to produce destruxins in a mutant of *Metarhizium anisopliae*. FEMS Microbiology Letters 226:373-378.
Ware, S.B. 2006. Aspects of sexual reproduction in *Mycosphaerella* species on wheat and barley: genetic studies on specificity, mapping, and fungicide resistance. Pages 75-99 in: Aspects of sexual reproduction in *Mycosphaerella* species on wheat and barley: genetic studies on specificity, mapping, and fungicide resistance.Wageningen university. The Netherlands. PhD Thesis.
Wenzl, P., Carling, J., Kudrna, D., Jaccoud, D., Huttner, E., Kleinhofs, A., and Kilian, A. 2004. Diversity Arrays Technology (DArT) for whole-genome profiling of barley. Proc Natl Acad Sci USA 101:9915-9920.
Wittenberg, A.H.J., van der Lee, T., Cayla, C., Kilian, A., Visser, R.G.F., and Schouten, H.J. 2005. Validation of the high-throughput marker technology DArT using the model plant *Arabidopsis thaliana*. Mol Gen Genomics 274:30-39.
Zhan, J., Pettway, R.E., and McDonald, B.A. 2003. The global genetic structure of the wheat pathogen *Mycosphaerella graminicola* is characterized by high nuclear diversity, low mitochondrial diversity, regular recombination, and gene flow. Fungal Genet Biol 38:286-297.
Zolan, M.E. 1995. Chromosome-length polymorphism in fungi. Microbiological reviews 59:686-698.

SUPPLEMENTAL DATA

Text S1

Construction and comparison of the linkage maps

Segregation ratios of all markers were analyzed with JoinMap, version 3.0 [1]. Markers with segregation ratios significantly different from 1:1 ($P < 0.01$) were initially set aside, and linkage analysis using the Kosambi mapping function was performed on the remaining markers. Initial assignment to linkage groups (LGs) was based on the logarithm of the odds (LOD) ratio for each possible marker pair. We used LOD values in the range of 3–8; the final assembly of LGs was completed using a LOD value of 4 or higher. We used linkages with a recombination rate (REC) < 0.4, a map LOD value of 0.05 and a χ^2-jump threshold of 5 for inclusion into the map and for the calculation of the linear order of the markers within a LG. Finally, we tested whether the markers with distorted segregation ratios contributed to the map using an iterative addition process from markers with little to substantial segregation distortions. After each JoinMap run, the map was inspected for changes in marker order and distance. When these were not disturbed and when synteny between the two parallel crosses (IPO323 x IPO94269 and IPO323 x IPO95052) was observed, the addition of markers with distorted segregation ratios to the map was accepted. The individual maps were inspected either in Excel or with the graphical genotyping software package GGT [2,3], which allowed detection of singletons and visualized the recombination events in all progeny.

Marker data were grouped and merged using a Perl script. For the IPO323 x IPO94269 cross, merging of the marker data from the twins resulted in a scoring table with 60 individuals and 1341 markers. Grouping of the markers resulted in 473 unique segregation patterns containing 297 DArT, 165 AFLP and 11 SSR markers. The global call rate (percentage of scored individuals) we obtained for this dataset was 99.1%.

For the IPO323 x IPO95052 cross, merging of the marker data from the twins resulted in a scoring table

with 125 individuals. One isolate had a genotype call rate less than 95% and was therefore omitted from further analysis. This resulted in a scoring table of 124 individuals and 1162 markers. Grouping resulted in 496 unique segregation patterns containing 491 DArT markers, four SSR markers, and the marker that co-segregates with the (a)virulence locus *MgAvrStb6*. The global call rate for this dataset was 98.8%.
For the bridge map the scores for markers segregating in both populations were merged. This resulted in a dataset of 184 individuals with 389 markers yielding 263 unique segregation patterns. The global call rate for this dataset was 99.03 %.

Individual maps were constructed using Joinmap 3.0. In the IPO323 x IPO94269 cross, 29 of the 473 (6.1%) segregation patterns exhibited a significant distortion ($P < 0.01$; based on χ^2) from the expected (1:1) Mendelian ratio. These markers were therefore set aside during the first phase of the map construction. Using a LOD threshold of 4.0, 443 out of the 444 (99.8%) markers could be grouped into 24 LGs. One marker (AHMR_07I02) was not grouped while two AFLP markers (BEGGMpAT_439 and AEGAMpAC_114) exceeded the threshold for the χ^2 jump and therefore were not positioned. The order of the markers in all 24 LGs was determined in a single round of JoinMap, and different settings of the thresholds did not alter the marker order or distance. Subsequently, we tried to incorporate the 29 markers that showed segregation distortion, and 10 of them were positioned based on the criteria listed above.

In the IPO323 x IPO95052 cross, 38 of the 496 (7.7 %) segregation patterns exhibited a significant distortion ($P < 0.01$; based on χ^2) from the expected 1:1 Mendelian ratio and were initially omitted from the mapping. Using LOD thresholds of 4.0 (1 group), 5.0 (2 groups) and 5.5 (20 groups) all markers were grouped into 23 LGs. The order of the markers on the 23 LGs was determined in a single round of JoinMap, and again different settings of the thresholds did not alter the order or distance of the markers. Subsequently, we tried to incorporate the 38 markers that showed segregation distortion, and 28 of them could be positioned.

For the construction of the bridge map, loci with strong segregation distortion ($P < 0.005$) were removed and linkage analysis was performed on the remaining markers. Groups were selected at LOD ≥ 5.5 and the order of the markers within the LGs was determined using the same settings as for the construction of the individual maps.

DArT analysis

DNA of *M. graminicola* isolates IPO323 and IPO95052 was used to construct two genomic representations for each isolate essentially as described previously [4]. Genomic representations were generated by digesting 100 ng of genomic DNA with 2 units of either *Hin*dIII or *Bam*HI in combination with the 4-base cutters *Mse*I and *Rsa*I (New England Biolabs; NEB, USA). Cloning adapters (Table S9) were simultaneously ligated to the complementary overhangs with T4 DNA ligase (NEB). A 1-µl aliquot of the ligation product was used as a template in a 50-µl amplification reaction using primers complementary to the adapter sequences and cycling conditions as described [5].

A 3072-clone library for IPO323 and IPO95052 was prepared for each of the *Hind*III-*Mse*I-*Rsa*I and the *Bam*HI-*Mse*I-*Rsa*I complexity-reduction methods [6] with the modifications described by Wenzl et al. [5]. PCR products were dried, washed once with 70 % ETOH, and re-suspended in 25 µl of spotting buffer. The amplification products were spotted in duplicate on polylysine coated slides (Erie Scientific, Portsmouth, NH, USA) using a MicroGrid II arrayer (Biorobotics, Cambridge, UK). After printing, the slides were processed by

incubation in hot water (95°C) for 2 min., dipped in a 100 mM EDTA and 100 mM DTT solution and dried by centrifugation.

The genomic representations of individual progeny isolates to be hybridized as targets on the array were generated by applying the complexity-reduction methods [5,6], with the exception that genotyping adapters rather than cloning adapters were used (Table S9). The products of the 50-µl PCR reactions were concentrated 10 fold by precipitation with 1 volume of isopropanol and denatured at 95°C for 3 min. Each reaction was labeled with 0.1 µl of Cy3-dUTP using 1 µl of 500 µM random decamers (Amersham Biosciences, Castle Hill, NSW, Australia) and the exo$^-$ Klenow fragment of *Escherichia coli* DNA polymerase I (NEB). In experiments for which DNA was isolated twice, a replicate target labeled with Cy5-dUTP was co-hybridized with the Cy3-dUTP labeled target to the same array. The polylinker fragment of the plasmid was used as a reference [6] and labeled with 6-FAM. Labeled representations, called targets, were denaturated, hybridized to microarrays overnight at 65°C, and slides were washed according to Wenzl et al. [5].

Typically, each experiment was comprised of 96 bar-coded slides that were scanned using a Tecan LS 300 (Grödig, Austria) confocal laser scanner. Each image pair (cy3-FAM or cy5-FAM) was stored directly in the database and analyzed subsequently with DArTSoft (version 7.4.1), a software package developed at DArT P/L. DArTSoft was used to both identify and score the markers that were polymorphic within each experiment as described previously [5,7-12]. The program computes several quality parameters for each clone [7] and markers were selected by simultaneously applying thresholds for four of those: P-value, call rate, reproducibility and polymorphism information content (PIC). Clones with P values ≥ 77%, call rate ≥ 80%, reproducibility ≥ 95% and PIC ≥ 0.3 were selected for both libraries.

1. Stam P (1993) Construction of integrated genetic linkage maps by means of a new computer package: JoinMap. Plant J 3: 739-744.
2. Berloo RV (1999) GGT: Software for the display of graphical genotypes. Journal of Heredity 90: 328-329.
3. Berloo RV (2008) GGT 2.0: versaltile software for the visualization and analysis of genetic data. J Hered 99: 232-236.
4. Wittenberg AHJ, van der Lee T, Cayla C, Kilian A, Visser RGF, et al. (2005) Validation of the high-throughput marker technology DArT using the model plant *Arabidopsis thaliana*. Mol Gen Genomics 274: 30-39.
5. Wenzl P, Carling J, Kudrna D, Jaccoud D, Huttner E, et al. (2004) Diversity Arrays Technology (DArT) for whole-genome profiling of barley. Proc Natl Acad Sci USA 101: 9915-9920.
6. Jaccoud D, Peng K, Feinstein D, Kilian A (2001) Diversity arrays: a solid state technology for sequence information independent genotyping. Nucleic Acids Res 29: E25.
7. Akbari M, Wenzl P, Caig V, Carling J, Xia L, et al. (2006) Diversity arrays technology (DArT) for high-throughput profiling of the hexaploid wheat genome. Theor Appl Genet 113: 1409-1420.
8. Wenzl P, Li H, Carling J, Zhou M, Raman H, et al. (2006) A high-density consensus map of barley linking DArT markers to SSR, RFLP and STS loci and agricultural traits. BMC Genomics 7: 206.
9. Yang S, Pang W, Ash G, Harper J, Carling J, et al. (2006) Low level of genetic diversity in cultivated Pigeonpea compared to its wild relatives is revealed by diversity arrays technology. Theor Appl Genet 113: 585-595.
10. Wenzl P, Raman H, Wang J, Zhou M, Huttner E, et al. (2007) A DArT platform for quantitative bulked segregant analysis. BMC Genomics 8: 196.
11. James KE, Schneider H, Ansell SW, Evers M, Robba L, et al. (2008) Diversity Arrays Technology (DArT) for Pan-Genomic Evolutionary Studies of Non-Model Organisms. PLoS ONE 3: e1682.
12. Mace ES, Xia L, Jordan DR, Halloran K, Parh DK, et al. (2008) DArT markers: diversity analyses and mapping in Sorghum bicolor. BMC Genomics 9: 26.

Link: http://www.plosone.org/article/info:doi%2F10.1371%2Fjournal.pone.0005863#s5

Fig. S1. Co-linearity of genetic linkage maps for *Mycosphaerella graminicola* crosses IPO323×IPO95052 (left) and IPO323×IPO94269 (right) with a bridge map (middle) generated with markers that segregated in both crosses. Common markers are shown in bold and start with the prefix C, SSR markers are shown in blue and markers that are translocated in red. DArT markers were named according to phase of the marker (A = IPO323, B = IPO95052 or IPO94269), complexity reduction method used (BMR or HMR), and location in the spotting plate (e.g. BBMR_15L11). LG and AFLP nomenclature is according to Kema et al., 2002. Segregation distortion of the markers is indicated with * (P<0.05), ** (P<0.01), *** (P<0.005) or **** (P<0. 001).

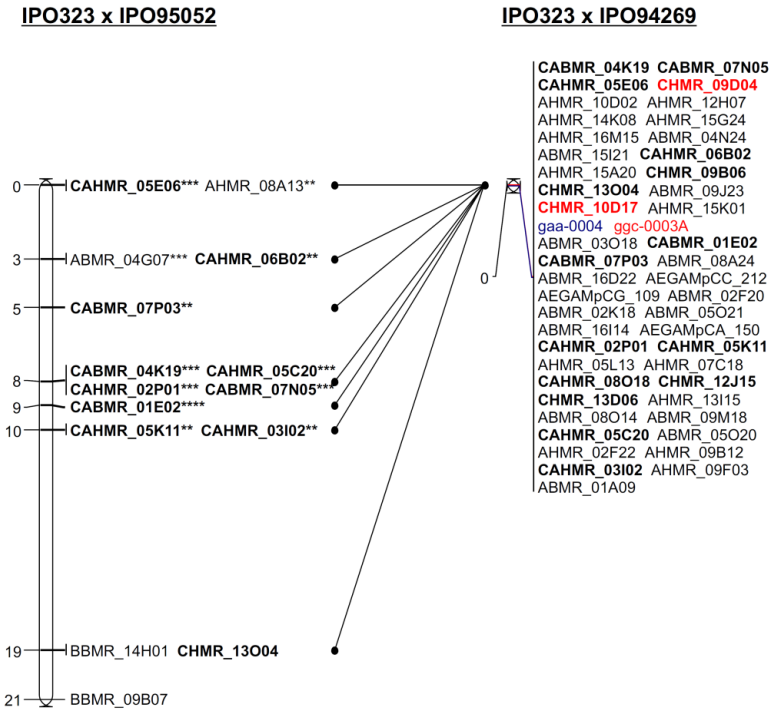

Fig. S2. Alignment of linkage group 21 between the IPO323×IPO95052 cross (left) and the IPO323×IPO94269 cross (right) shows recombination in the former but not in the latter. This indicates absence of this linkage group in isolate IPO94269. For IPO323×IPO94269, only markers from IPO323 could be mapped on this linkage group, and no markers from IPO94269, confirming that IPO94269 lacks this linkage group. Lines are drawn between markers that segregated in both populations. Stars next to the markers for the IPO323×IPO94269 cross indicate segregation distortion of the markers; * (P<0.05), ** (P<0.01), *** (P<0.005) or **** (P<0.001).

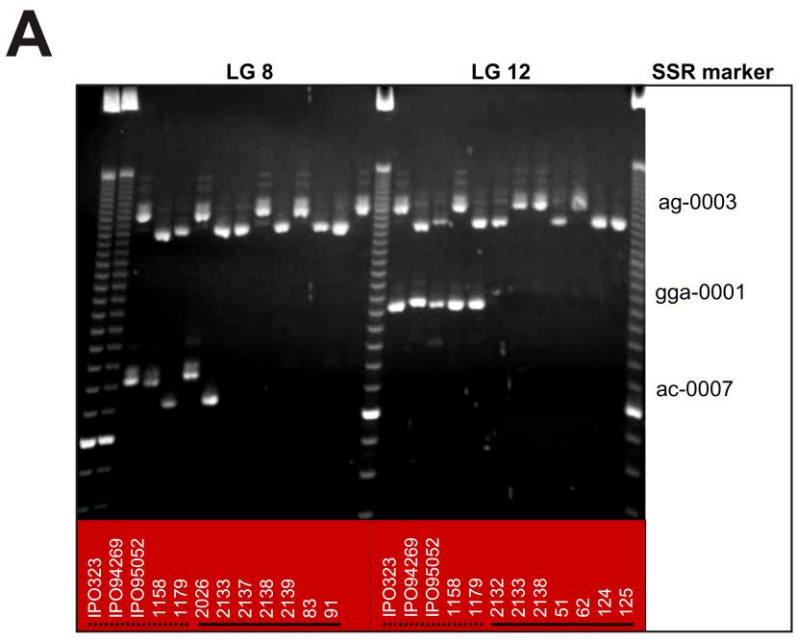

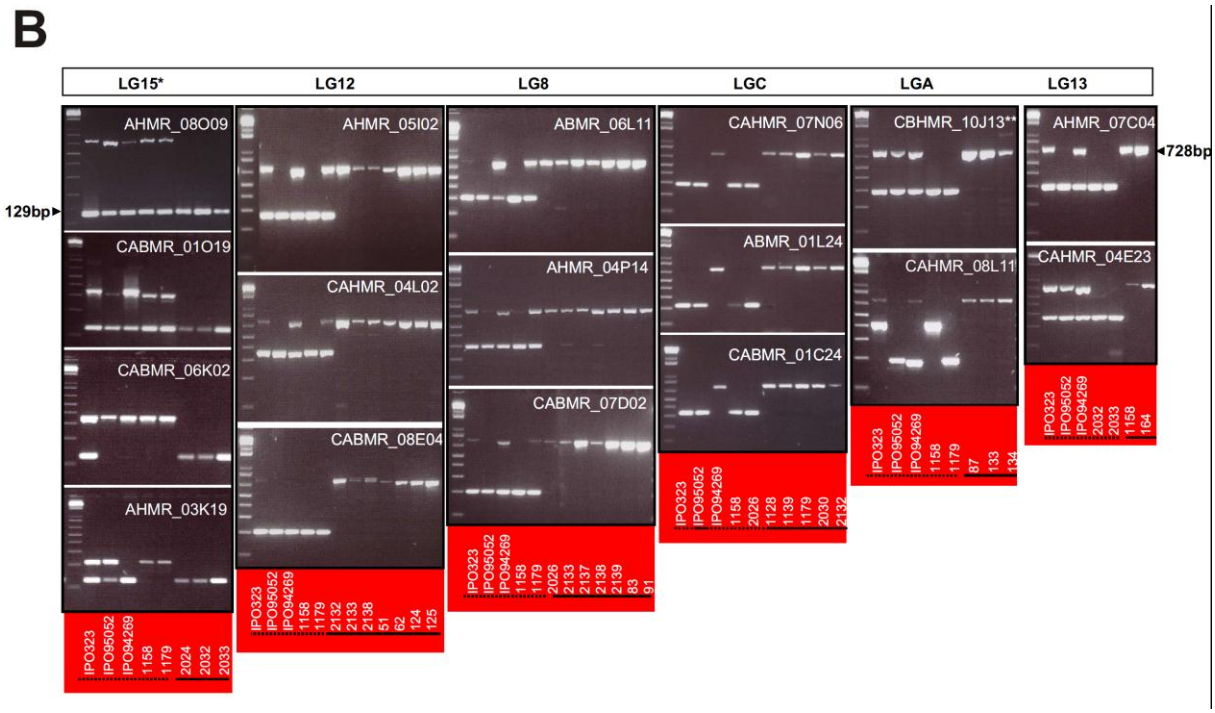
B
LG15*
LG12
LG8
LGC
LGA
LG13
129bp
728bp
AHMR_08O09
CABMR_01O19
CABMR_06K02
AHMR_03K19
AHMR_05I02
CAHMR_04L02
CABMR_08E04
ABMR_06L11
AHMR_04P14
CABMR_07D02
CAHMR_07N06
ABMR_01L24
CABMR_01C24
CBHMR_10J13**
CAHMR_08L11
AHMR_07C04
CAHMR_04E23
IPO323
IPO95052
IPO94269

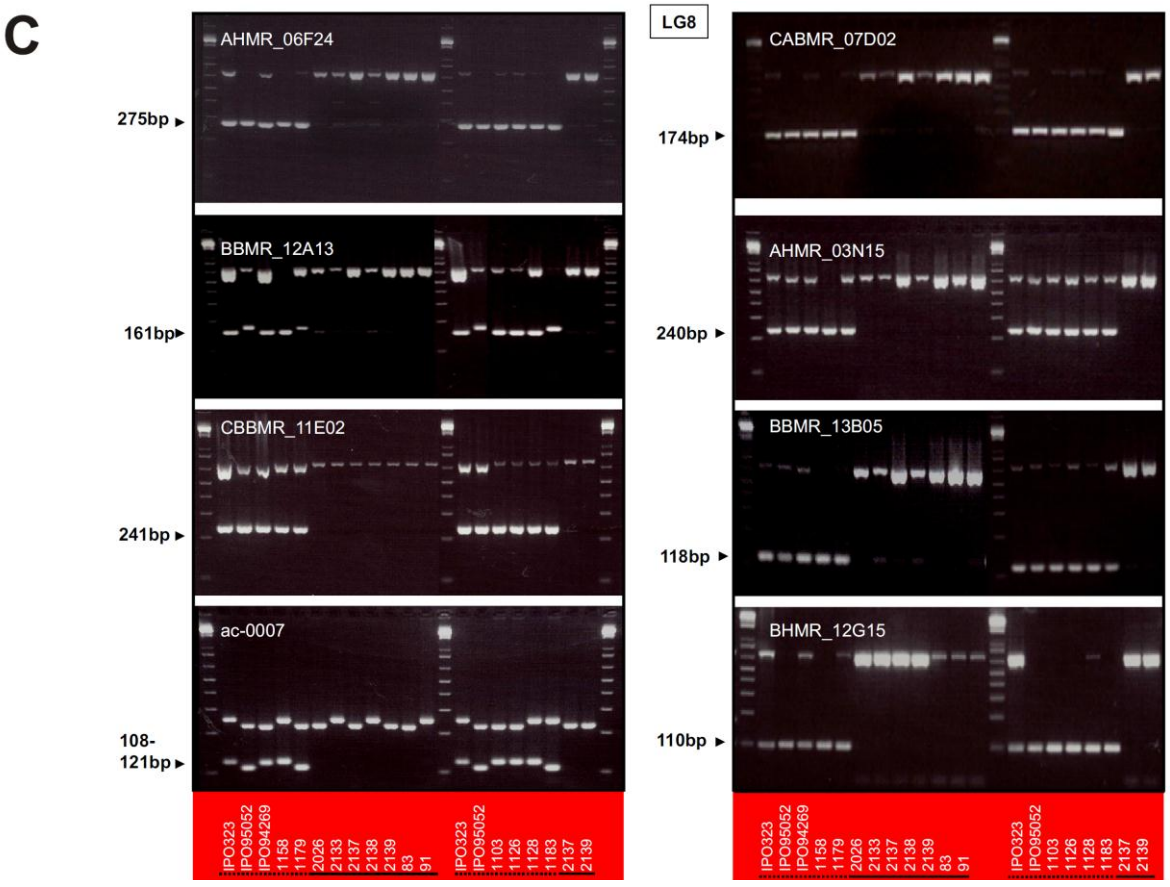
C
LG8
AHMR_06F24
275bp
BBMR_12A13
161bp
CBBMR_11E02
241bp
ac-0007
108-
121bp
CABMR_07D02
174bp
AHMR_03N15
240bp
BBMR_13B05
118bp
BHMR_12G15
110bp
IPO323
IPO95052
IPO94269

Fig. S3. Confirmation of chromosome loss by PCR amplification. A. Confirmation of loss of LG 8 and LG 12 by SSR amplification. Loci ac-0007 (LG 8) and gga-0001 (LG 12) confirm that these linkage groups are absent in the underlined progeny isolates from the crosses IPO323×IPO94269 and IPO323×IPO95052 as neither of the parental alleles are amplified. Isolates 1158 and 1179 are positive controls and SSR ag-0003 (LG 2) is a positive PCR control in all duplex reactions. B. Confirmation of loss of LGs 13, 15, A and C by PCR with primers developed from DArT marker sequence data in the underlined progeny isolates derived from crosses between *M. graminicola* IPO323×IPO94269 and IPO323×IPO95052. Isolates 1158 and 1179 are positive control isolates, except in LGs C and 13 that have isolates 1158/2026 and 2032/2033, respectively, as positive checks. For LG 15* the CABMR_07D07 DArT fragment (129 bp) was used as a positive PCR control, while for the other linkage groups DArT fragment AHMR_08O09 (728 bp) was used. C. Confirmation of loss of LG 8 by PCR with primers developed from DArT marker sequence data in underlined progeny isolates derived from crosses between *M. graminicola* IPO323×IPO94269 and IPO323×IPO95052. This figure is composed of eight panels that are individually divided by a central marker lane. The left part of each panel represents the three parental isolates of the mapping populations (IPO323, IPO94269 and IPO95052), two positive control isolates (1158/1179), and seven progeny isolates that lack LG 8. The right part of each panel links to Fig. 2D and represents the two parental isolates (IPO323 and IPO95052), two twin isolates (1103/1126), two mirror isolates (1128/1183) and two twin isolates that lack LG 8 (2137/2139). In all panels DArT fragment AHMR_08O09 is the positive control (top band in each panel, 728 bp, located on LG 15).

Table S1. *Mycosphaerella graminicola* progeny isolates (n=76) from the IPO323 x IPO94269 *in planta* cross, that was made on the susceptible bread wheat cultivar Obelisk, that were used for hybridization to the DArT arrays.

Isolate number	**Used for construction of genetic linkage map**	**Isolate number**	**Used for construction of genetic linkage map**
IPO323[1]	-	116	-
IPO94269[2]	-	117	Yes
1	Yes	118	Yes
10	Yes	119	Yes
11	-	124	Yes
12	Yes	125	Yes
14	Yes	126	Yes
16	-	131	Yes
18	-	132	Yes
22	-	134	Yes
23	Yes	136	Yes
24	Yes	137	Yes
25	-	139	-
27	Yes	140	-
29	Yes	142	Yes
30	-	144	Yes
36	-	147	Yes
40	Yes	148	-
46	-	150	-
47	Yes	157	Yes
50	Yes	158	Yes
51	Yes	160	Yes
58	-	164	Yes
62	Yes	167	Yes
68	Yes	173	Yes
70	-	174	Yes
73	Yes	176	Yes
83	Yes	179	Yes
84	Yes	180	Yes
87	Yes	182	Yes
88	Yes	183	Yes
90	Yes	184	Yes

91	Yes	192	Yes
94	Yes	193	Yes
95	Yes	197	Yes
100	Yes	198	Yes
109	Yes	200	Yes
110	-	202	Yes
111	Yes		
115	Yes		

[1] Parental isolate IPO323 was isolated from the bread wheat cultivar Arminda.
[2] Parental isolate IPO94269 was isolated from the bread wheat cultivar Vivant.

Table S2. *Mycosphaerella graminicola* progeny isolates (n=164) from the IPO323 x IPO95052 *in planta* crosses that were made on the bread wheat cultivar Obelisk and the durum wheat cultivar Inbar. Sixteen isolates (gray-shaded) were not used, leaving a total of 148 that were used in the construction of the genetic linkage map. The first two numbers indicate the year of isolation and the next three numbers the order of isolation.

Isolated from bread wheat cultivar Obelisk						**Isolated from durum wheat cultivar Inbar**			
IPO323[1]		01	135	01	171	IPO95052[2]		02	043
01	101	01	136	01	172	01	426	02	044
01	102	01	137	01	173	01	427	02	045
01	103	01	138	01	174	01	428	02	046
01	104	01	139	01	175	01	429	02	047
01	105	01	140	01	176	01	430	02	121
01	106	01	141	01	177	01	431	02	122
01	107	01	142	01	178	01	432	02	123
01	108	01	143	01	179	01	433	02	124
01	109	01	144	01	180	01	434	02	125
01	110	01	146	01	181	01	435	02	126
01	111	01	147	01	182	01	436	02	127
01	112	01	148	01	183	01	437	02	128
01	113	01	149	01	184	01	438	02	129
01	114	01	150	01	185	01	439	02	130
01	115	01	151	01	186	01	440	02	131
01	116	01	152	01	187	02	024	02	132
01	117	01	153	01	188	02	025	02	133
01	118	01	154	01	189	02	026	02	134
01	119	01	155	01	190	02	027	02	135
01	120	01	156	01	191	02	028	02	136
01	121	01	157	01	192	02	029	02	137
01	122	01	158	01	193	02	030	02	138
01	123	01	159	01	194	02	031	02	139
01	124	01	160	01	195	02	032	02	140
01	125	01	161	01	196	02	033	02	141
01	126	01	162	01	197	02	034		
01	127	01	163	01	198	02	035		
01	128	01	164	01	199	02	036		
01	129	01	165	01	200	02	037		
01	130	01	166	01	421	02	038		
01	131	01	167	01	422	02	039		
01	132	01	168	01	423	02	040		
01	133	01	169	01	424	02	041		
01	134	01	170	01	425	02	042		

[1] Parental isolate IPO323 was isolated from the bread wheat cultivar Arminda
[2] Parental isolate IPO95052 was isolated from an unknown durum wheat cultivar.

Table S3. The adapter and primer oligonucleotide sequences used for generation of the genomic representation (cloning) from *Mycosphaerella graminicola* isolates IPO323 and IPO95052 and for hybridization to the micro-arrays (genotyping) of parental and progeny isolates.

Endonuclease and recognition site	**Used for**	**Adapter sequences[a]**	**Primer sequences (5' to 3')**
*Hind*III 5'-A$^{\downarrow}$AGCTT-3' 3'-TTCGA$_{\uparrow}$A-5'	Cloning	5'-CTCGTAGACTGCGTCAC-3' 3'-ATCTGACGCAGTGTCGA -5'	TAGACTGCGTCACAGCTT
	Genotyping	5'-GTGCTACAGTCGCTGAG-3' 3'-ATGTCAGCGACTCTCGA-5'	TACAGTCGCTGAGAGCTT
*Bam*HI 5'-G$^{\downarrow}$GATCC-3' 3'-CCTAG$_{\uparrow}$G-5'	Cloning	5'-CTCGTAGACTGCGATCA-3' 3'-CATCTGACGCTAGTCTAG-5'	GTAGACTGCGATCAGATCC
	Genotyping	5'-GTGCTACAGTCGCTAGA-3' 3'-GATGTCAGCGATCTCTAG-5'	CTACAGTCGCTAGAGATCC
*Mse*I 5'-T$^{\downarrow}$TAA-3' 3'-AAT$_{\uparrow}$T-5'	Cloning	5'-ACTCGATCCTCACACGTA AAGTATAGATCCCA-3' 3'- NH_2-TTCATATCTAGGGTAT-5'	ACTCGATCCTCACACGTA
	Genotyping	5'-AGTGCATGGTGAGAGCTA AACTATACATGGGA-3' 3'- NH_2-TTGATATGTACCCTAT-5'	AGTGCATGGTGAGAGCTA
*Rsa*I 5'-GT$^{\downarrow}$AC-3' 3'-CA$_{\uparrow}$TG-5'	Co-digestion	-	-

[a] Adapter sequences were formed by annealing the strands whose sequences are listed. Complementary sequences are underlined.

Table S4. Overview of *Mycosphaerella graminicola* F_1 isolates that lack one or more linkage groups compared to the parental isolates IPO323, IPO94269 and IPO95052.

Missing linkage group	**Isolates in cross IPO323 x IPO95052**	**Isolates in cross IPO323 x IPO94269[a]**
8	2026, 2133, 2138, 2137, 2139[b]	83, 91
12	2132, 2133, 2138	51, 62, 124, 125
13	1158	164
15	2024, 2032, 2033	-
21	1114, 1121, 1122, 1127, 1151, 1159, 1170, 1176, 1186, 1200, 2133, 2138, 2137, 2139	[c]
A	-	87, 134 and 133
B	1108, 1169, 1179, 1425, 1438, 2134, 2141	[c]
C	1128, 1139, 1179, 2030, 2132	[c]

[a] In the IPO323 x IPO94269 progeny, isolate #40 is disomic for LG 13 and isolate #51 is disomic for LG 1.
[b] Underlined isolates are identified twins
[c] Not assessed, as the LGs only contained IPO323-derived markers.

Table S5. Primer sequences used to verify the absence of several linkage groups in some progeny isolates of the two crosses. The primers were developed using the sequences of the DArT markers located on these linkage groups.

Linkage Group	DArT markers	Forward primer (5'-3')	Reverse primer (5'-3')
LG 8			
	AHMR_04P14	GCTTAAGTGACTACGAGTGC	CGCAAAGCTTCGATCCATTC
	CABMR_07D02	GATATTGCTTGGTGGATCCG	ATGTACCGTTCGGCAGAGTC
	ABMR_06L11	GGATCCCATGTTGTTCAGAG	CCTCGAACGAGTCGGTTTAA
	AHMR_06F24	GGTAGGGCGAATATTGCTGA	AGTGTCGAGCGGTATCGAGT
	BBMR_12 A13	ATTCGGATGAGCAGAGCAAG	CTCATCGCCATCATCACATC
	CBBMR_11E02	CTAGGCAAGGAGATCGAACG	GATGAGCGCCTTGTTTTCTC
	AHMR_03N15	TGAAGGGAAGTGGATTCTGG	AAGCTTCCAGGGGAAATTGT
	BBMR_13B05	TCCGAACCCTTCTTGCTCTA	CCAGATACTCCATCGGCATT
	BHMR_12G15	ACGACTAGACTTTCGCTTCTTG	TTAAGAGCTCGGAAATCGTG
LG 12			
	CABMR_08E04	TTAAGGACATGGTCAAGCCA	TCTCATCTGTGTGAGGATCC
	CAHMR_04L02	CGGTTAATAGCTAGAGTCAA	GATCAAGACAGGAAGCTTCG
	AHMR_05I02	CGTCTACCACTATCCGAGAT	CAGAAAGCTTCGGTCCTGCT
LG 13			
	AHMR_07C04	GACGCAGGCCAGTCATTTAT	GTTCCAGCTCGCAAAAGCTT
	CAHMR_04E23	CCGCCTTAATCAGACTATCG	CATTCACTGTGACGAAGCTT
LG 15			
	CABMR_01O19	GTCACTATCCTCGCCGCATT	CCGGAATAAATGGAGGATCC
	AHMR_08O09	GTGTAGATTCGCGAGACTGG	GCTTCTTGGAAGCTTTGGTC
	CABMR_06K02	GGATCCACGAGTAAGCACAA	CGAGCATTAAAGCCTTCACG
	AHMR_03K19	TTAAACAACCCTCATCTGCC	CGCTTGAAGCTTCACATCAC
LG A			
	CBHMR_10J13**	GAGGCAGGAAGATCGTTAAA	ATGTAGCGGTACCAATCGAC
	CAHMR_08L11	GCATTTCCTTAGGTTGGACC	CTTGCCTGTGGACTTTCTAG
LG B			
	CAHMR_02A19	AAGCTTAGCAGCAGAACCCT	CAGGTTGCGATAGGAGTACG
	ABMR_04L19	ATACAAGACGACGCTTGATG	GGTCTCCAAGGGACATATCT
	ABMR_08E05	GCAGTAACGACACCGATACA	TATAGAGCTAGCAGGACTGG
LG C			
	CABMR_01C24	GTCCCTATGCAGAGGATCCT	TTCAACATTAAGGAGGGCGG
	CAHMR_07N06	CAGTTAAAACTCCATCTCGG	GTAGCTGTAACAAAGCTTGC
	ABMR_01L24	CTCACGGAACGGATCCAAAG	CATATCGATTCCAACCAGCG
LG 21	CAHMR_05C20	GGTAGTGTTGTGCCTTCGTT	GTAGTGAAGCTTGCTGATGG
	CABMR_07P03	GAATCGGCGTGTGCGCTATC	TTCTCAAAATCCGAGGATCC
	CAHMR_05E06	CGAATATCGGATGTTAAAAG	AGAGAAGCTTCAAGATATCG
	CHMR_09B06	TGGTAGCATGGTCGATGGAA	AACGTACCGCATCGATAGAG
Controls			
LG 1	CABMR_07D07 [a]	GGATCCGAAACGTCCGAAGA	ACATCCAGAGGAAAGAACGC
LG 15	AHMR_08O09 [b]	GTGTAGATTCGCGAGACTGG	GCTTCTTGGAAGCTTTGGTC

[a] Primer control used in duplex PCR for LG15.
[b] Primer control used in duplex PCR for LGs 8, 12, 13, A, B, C and 21.

Table S6. Primer sequences used to verify the disomy for linkage group 1, isolate #51. The primers were developed around InDels obtained by comparison of BAC-end sequences from parental isolate IPO94269 with the genome sequence of isolate IPO323.

BAC-end IPO94269	Scaffold 4 position (bp)*	InDel size (bp)	Forward primer (5'-3')	Reverse primer (5'-3')
05D17	366301	6	TGCAGGACATCGATCTTCAC	TATGCTCAAATGGGGCAAAG
11O21	642878	9	TCCACCTCTCTGGGCTGATT	CATTTCCTGCTTCTGGAGGT
06P08	1411546	9	CCATCCACCGCGTAACTAAT	ATGCTGCTGGCCATGAGGA
04L04	1599247	10	GAATACACGGGATCCATTCG	GGCACCGTCAAAGCTTACAT
07C16	1913009	7	GACCTGGGAAATGAGCTGAC	CTCAGGGACACATGTTGGTG
04L20	2276380	7	GCGAATTGTTGAGAAGTCCA	TCTCGAAGGATCAGCGACAT
13G02	2528033	7	CTTCCTTCGTCTCCTTCGTG	ACATGGGAACAGACCGGATA
12N14	2604850	7	TGTTGAGGAGGGTGAGATGA	ATCATGACTGGGGTTTGTCG

* Derived from genome assembly IPO323 v 2.5.

Table S7. Overview of type and number of molecular markers that were scored in the progeny of the cross between *Mycosphaerella graminicola* isolates IPO323 and IPO94269 before and after grouping.

Marker type	Isolate	Complexity reduction method	Number of markers	Unique segregation patterns	Percentage of total no. of unique segregation patterns
AFLP	IPO323	[1]	151	93	19.66
AFLP	IPO94269	[1]	120	72	15.22
DArT	IPO323	BMR	375	156	32.98
	IPO95052[2]	BMR	183	33	6.98
DArT	IPO323	HMR	383	80	16.91
	IPO95052	HMR	101	28	5.92
SSR	-	-	25+1[3]	11	2.33
Mat and *Avr*	-	-	2	0	-
Sum			1341	473	100%

[1]AFLP markers were generated using 11 *Eco*RI-*Msp*I primer combinations
[2] DArT fragment was derived from isolate IPO95052, but segregated in IPO323 x IPO94269
[3]One SSR marker segregated in a diploid fashion and therefore could be positioned on two locations.

Table S8. Overview of type and number of molecular markers that were scored in the progeny of the cross between *Mycosphaerella graminicola* isolates IPO323 and IPO95052 before and after grouping.

Marker type	Isolate	Complexity reduction method	Number of markers	Unique segregation patterns	Percentage of total no. of unique segregation patterns
DArT	IPO323	BMR	265	137	27.62
	IPO95052	BMR	258	113	22.78
DArT	IPO323	HMR	296	121	24.40
	IPO95052	HMR	335	120	24.19
SSR	-	-	6	4	0.81
Mat and *Avr*	-	-	2	1	0.20
Sum			1162	496	100 %

Table S9. Identified twin isolates in the two progenies derived from crosses between either *Mycosphaerella graminicola* isolates IPO323 and IPO94269 or IPO323 and IPO95052.

IPO323 x IPO94269		IPO323 x IPO95052	
9	10	01101	01102
22	27	01103	01126
109	110	01105	01106
111	112	01109	01112
116	117	01115	01119
133	134	01132	01133
148	150	01142	01143
156	158	01154	01162
159	160	01177	01184
174	175	01196	01197
176	178	01426	01433
		01429	01430
		01434	01437
		01435	01439
		02034	02047
		02035	02043
		02037	02046
		02041	02042
		02128	02131
		02130	02136
		02133	02138
		02137	02139
		02134	02141

Table S10. Scoring tables

http://www.plosone.org/article/info:doi%2F10.1371%2Fjournal.pone.0005863#s5

Table S11. Overview of the number of markers for both crosses. Mapping was performed using the software package JoinMap 3.0.

Genetic map	Total number of markers selected	Unique segregation patterns	Segregation distortion removed (P ≤ 0.01)	Grouped	Mapped excluding segregation distortion	Mapped including segregation distortion	Total number of markers positioned on map
IPO323 x IPO94269	1341	473 35.3 %	444	443	441	451	1317 98.21 %
IPO323 x IPO95052	1162	496 42.7 %	458	457	457	486	1144 98.45 %
Bridge	389	263 67.6 %	243	241	236	251	372[a] 95.63 %

[a] To construct the bridge map, eight markers that showed translocations were removed and three common markers were placed on the individual linkage maps but not on the bridge map. This resulted in a total of 2078 genetic markers, which are comprised of 1793 DArT markers, 258 AFLP markers, 25 SSR markers and the PCR markers for mating type (*Mat*) and avirulence (*Avr*).

Table S12. Graphical genotyping

See link: http://www.plosone.org/article/info:doi%2F10.1371%2Fjournal.pone.0005863#s5

Table S13. Alignment of the identified linkage groups in the *Mycosphaerella graminicola* IPO323 x IPO94269 and IPO323 x IPO95052 mapping populations with the identified chromosomes in the *Mycosphaerella graminicola* genome sequence.

		IPO323 x IPO94269	**IPO323 x IPO95052**
LGs	**Chromosomes**	**cM**	**cM**
5+10	1	198.2	197.3
6	2	160.1	150.1
2	3	163.7	154.3
1	4	120.0	112.6
3+22	5	125.5	126.4
7	6	117.6	136.0
4+17	7	133.3	117.0
11+20	8	80.3	93.3
18+19	9	141.1	130.0
9	10	93.2	118.1
14	11	92.6	63.8
23	12	105.3	92.6
16	13	31.7	100.0
B	14	23.2	46.0
8	15	61.1	65.7
15	16	53.3	63.1
13	17	43.8	25.0
21	18	1.7	21.0
A	19	20.0	60.4
C	20	1.7	14.5
12	21	58.4	40.6
E	-	6.7	8.5
F	-	20.1	9.9
D		1.8	
Sum		1854.1	1946.4

Table S14. DArT and SSR markers that showed translocations between two genetic linkage maps derived from crosses between either *Mycosphaerella graminicola* isolates IPO323 and IPO94269 or IPO95052.

Markers	**Position in one parent**	**Position in other parent**
CHMR_09D04, CHMR10D17	IPO323; LG 21	IPO95052; LG 18+19
CHMR_14L04, CHMR_13P21	IPO323; LG 3+22	IPO95052; LG 5+10
CBBMR_15H01	IPO94269; LG 1	IPO95052; LG 3+22
CBBMR_14G17, CBMR_14D07	IPO94269; LG 6 (7cM)	IPO95052; LG 6 (79cM)
CBBMR_11N22	IPO94269; LG 7	IPO95052; LG 9
ggc-0003A/B	IPO323; LG21	IPO94269; LG 4+17

Table S15. Back crosses and intercrosses of *M. graminicola* IPO323 X IPO94269 progeny isolates with isolates that either lost or gained specific chromosomes.

Type of cross	Isolates	Chromosome number polymorphisms	LG	Scaffold*	Size (Mbp)	Success
Back crosses	323*40	P /disomic LG13	13	16	0.58	Yes
	323*62	P /-LG12	12	21	0.39	Yes
	323*87	P/-LGA	A	17	0.55	Yes
	323*124	P/-LG12	12	21	0.39	Yes
	94269*51	P/-LG12+ disomic LG1	1	4	2.88	Yes
	94269*83	P/-LG8	8	14	0.64	Yes
	94269*91	P/-LG8	8	14	0.64	Yes
	94269*125	P/-LG12	12	21	0.39	Yes
	94269*133	P/-LGA	A	17	0.55	Yes
	94269*134	P/-LGA	A	17	0.55	Yes
	94269*164	P/-LG13	13	16	0.58	Yes
Inter crosses of F1 progeny isolates	2133x2137	-LG8,12,21/-LG8,21	8, 12 and 21	14, 21 and 20	0.64, 0.39, 0.56	Yes
	2133x2132	-LG8,12,21/-LG12,C	8, 12, 21 and C	14, 21, 20 and 18	0.64, 0.39, 0.56, 0.47	Yes
	2132x2024	-LG21,C/-LG15	21, C and 15	20, 18 and 15	0.56, 0.47, 0.6	Yes
	2133x1179	-LG8,12,21/-LGB,C	8, 12, 21, B and C	14, 21, 20, 13 and 18	0.64, 0.39, 0.56, 0.77, 0.47	Yes
	2133x1158	-LG8,12,21/-LG13	8, 12, 21 and 13	14, 21, 20 and 16	0.64, 0.39, 0.56, 0.58	Yes
	51x124	-LG12 + disomic LG1/-LG12	12 and 1	21 and 4	0.39, 2.88	No
Control	323x94269	P/-LG21, -LGC	21 and C	-	-	Yes

* Derived from genome assembly IPO323 v 2.5.

Chapter 3

Finished genome of the fungal wheat pathogen *Mycosphaerella graminicola* reveals dispensome structure, chromosome plasticity and stealth pathogenesis

Stephen B. Goodwin, **Sarrah Ben M'Barek**, Braham Dhillon, Alexander H. J. Wittenberg, Charles F. Crane, et al.,

Published in: PLoS Genetics (2011) 7 (6): e1002070.

ABSTRACT

The plant-pathogenic fungus *Mycosphaerella graminicola* (asexual stage: *Septoria tritici*) causes septoria tritici blotch, a disease that greatly reduces the yield and quality of wheat. This disease is economically important in most wheat-growing areas worldwide and threatens global food production. Control of the disease has been hampered by a limited understanding of the genetic and biochemical bases of pathogenicity, including mechanisms of infection and of resistance in the host. Unlike most other plant pathogens, *M. graminicola* has a long latent period during which it evades host defenses. Although this type of stealth pathogenicity occurs commonly in Mycosphaerella and other Dothideomycetes, the largest class of plant-pathogenic fungi, its genetic basis is not known. To address this problem, the genome of *M. graminicola* was sequenced completely. The finished genome contains 21 chromosomes, eight of which could be lost with no visible effect on the fungus and thus are dispensable. This eight-chromosome dispensome is dynamic in field and progeny isolates, is different from the core genome in gene and repeat content, and appears to have originated by ancient horizontal transfer from an unknown donor. Synteny plots of the *M. graminicola* chromosomes versus those of the only other sequenced Dothideomycete, *Stagonospora nodorum*, revealed conservation of gene content but not order or orientation, suggesting a high rate of intra-chromosomal rearrangement in one or both species. This observed "mesosynteny" is very different from synteny seen between other organisms. A surprising feature of the *M. graminicola* genome compared to other sequenced plant pathogens was that it contained very few genes for enzymes that break down plant cell walls, which was more similar to endophytes than to pathogens. The stealth pathogenesis of *M. graminicola* probably involves degradation of proteins rather than carbohydrates to evade host defenses during the biotrophic stage of infection and may have evolved from endophytic ancestors.

INTRODUCTION

The ascomycete fungus *Mycosphaerella graminicola* (Fig. S1) causes septoria tritici blotch (STB), a foliar disease of wheat that poses a significant threat to global food production. Losses to STB can reduce yields of wheat by 30 to 50% with a huge economic impact (Eyal et al., 1987); global expenditures for fungicides to manage STB total hundreds of millions of dollars each year (Hardwick et al., 2001; McDougall, 2006). This fungus is difficult to control because populations contain extremely high levels of genetic variability (Linde et al., 2002) and it has very unusual biology for a pathogen. Unlike most other plant pathogens (Kema et al., 1996b; Duncan and Howard, 2000; Jing et al., 2008), *M. graminicola* infects through stomata rather than by direct penetration and there is a long latent period of up to two weeks following infection before symptoms develop. The fungus evades host defenses (Adhikari et al., 2007) during the latent phase, followed by a rapid switch to necrotrophy immediately prior to symptom expression 12-20 days after penetration (Kema et al., 1996b; Keon et al., 2007; Kema et al., 2008). Such a switch from biotrophic to necrotrophic growth at the end of a long latent period is an unusual characteristic shared by most fungi in the genus Mycosphaerella. Very little is known about the cause or mechanism of this lifestyle switch (Keon et al., 2007; Kema et al., 2008) even though Mycosphaerella is one of the largest and most economically important genera of plant-pathogenic fungi.

A striking aspect of *M. graminicola* genetics is the presence of many dispensable chromosomes (Wittenberg et al., 2009). These can be lost readily in sexual progeny with no apparent effect on fitness. However, the structure and function of dispensable chromosomes are not known. Here we report the first genome of a filamentous fungus to be finished according to current standards (Chain et al., 2009). The 21-chromosome, 39.7-Mb genome of *M. graminicola* revealed an apparently novel origin for dispensable chromosomes by horizontal transfer followed by extensive recombination, a possible mechanism of stealth pathogenicity and exciting new aspects of genome structure. The genome provides a finished reference for the Dothideomycetes, the largest class of ascomycete fungi, which also includes the apple scab pathogen *Venturia inaequalis*, the southern corn leaf blight pathogen *Cochliobolus heterostrophus*, the black Sigatoka pathogen of banana, *M. fijiensis*, and numerous other pathogens of almost every crop.

RESULTS

Features of the finished genome

The finished genome of *M. graminicola* isolate IPO323 consists of 21 complete chromosomes, telomere to telomere (Fig. S2), with the exceptions of one telomere of chromosome 21 and two internal gaps of unclonable DNA that are missing from chromosome 18 (Table 1). Alignments between the 21 chromosomes and two genetic linkage maps yielded an excellent correspondence (Figs. 1 and S3), representing the most complete and the first finished sequence of a filamentous fungus. The next most complete genome of a filamentous fungus is that of *Aspergillus fumigatus*, which did not include centromere sequences and contained 11 gaps in total (Nierman et al., 2005). The complete 43,960-bp mitochondrial genome also was obtained and has been described elsewhere (Torriani et al., 2008).

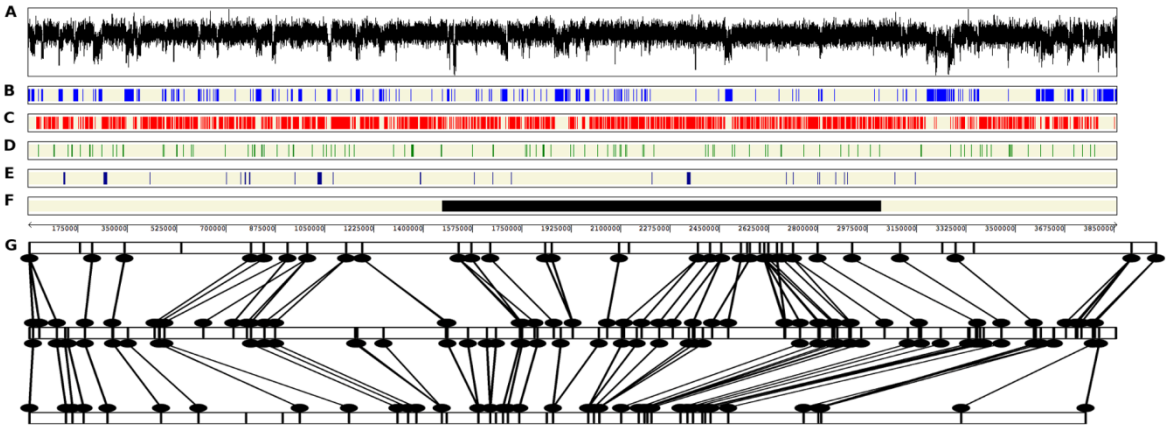

Fig. 1. Features of chromosome 2 of *Mycosphaerella graminicola* and alignment to genetic linkage maps.
A. Plot of GC content. Areas of low GC usually correspond to regions of repetitive DNA. **B.** Repetitive regions of the *M. graminicola* genome. **C.** Single-copy (red) regions of the *M. graminicola* genome. **D.** Locations of genes for proteins containing signal peptides. **E.** Locations of homologs involved in pathogenicity or virulence that have been experimentally verified in species pathogenic to plant, animal or human hosts. **F.** Approximate locations of quantitative trait loci (QTL) for pathogenicity to wheat. **G.** Alignments between the genomic sequence and two genetic linkage maps of crosses involving isolate IPO323. Top half, Genetic linkage map of the cross between IPO323 and the Algerian durum wheat isolate IPO95052. Bottom half, Genetic linkage map of the cross between bread wheat isolates IPO323 and IPO94269. The physical map represented by the genomic sequence is in the center. Lines connect mapped genetic markers in each linkage map to their corresponding locations on the physical map based on the sequences of the marker loci. Exceptions to the almost perfect alignment between the three maps are indicated by crossed lines, most likely due to occasional incorrect scorings of the marker alleles. Chromosome 2 was used for this illustration because no QTL mapped to chromosome 1.

Table 1. Sizes and gene contents of the 21 chromosomes of *Mycosphaerella graminicola* isolate IPO323.

Chromosome		All genes		Unique genes[a]		Signal	Average gene	Genes/	Percent	Percent	milRNAs/
Number	Size	Number	Annotated	Number	Annotated	Peptides	size (bp)	Mb DNA	G+C	repetitive	Mb DNA[b]
1	6,088,797	1,980	1,258	1,067	497	208	1338.6	325	53.1	9.5	9.7
2	3,860,111	1,136	650	607	238	108	1402.7	294	52.4	15.7	9.6
3	3,505,381	1,071	630	583	246	122	1337.1	306	52.6	14.2	6.3
4	2,880,011	821	498	421	182	81	1388.6	285	52.2	16.1	13.2
5	2,861,803	778	489	389	180	91	1352.6	272	52.0	19.1	18.9
6	2,674,951	692	427	328	152	66	1353.0	259	51.4	22.2	12.3
7	2,665,280	766	357	462	131	96	1202.7	287	52.6	14.0	16.1
8	2,443,572	689	397	384	159	62	1311.2	282	51.7	17.6	13.5
9	2,142,475	604	353	305	134	69	1345.1	282	51.5	20.8	18.7
10	1,682,575	516	298	266	110	46	1418.7	307	52.5	14.1	9.5
11	1,624,292	488	279	270	115	65	1352.5	300	52.8	10.5	5.5
12	1,462,624	408	227	232	96	59	1254.3	279	52.3	14.5	10.9
13	1,185,774	330	183	165	68	47	1195.7	278	52.0	17.8	17.7
14	773,098	114	25	48	5	3	920.1	147	48.5	36.7	23.3
15	639,501	86	6	44	1	2	773.7	134	51.0	34.4	25.0
16	607,044	88	5	40	1	5	898.5	145	51.5	25.6	31.3
17	584,099	78	6	36	1	1	777.9	134	52.0	26.4	18.8
18[c]	573,698	64	7	28	4	0	965.1	112	48.6	40.3	33.1
19	549,847	87	8	53	3	4	658.3	158	51.3	25.1	23.6
20	472,105	79	4	41	2	4	863.1	167	51.5	21.1	25.4
21[d]	409,213	58	4	21	1	2	921.6	142	51.9	30.1	14.7
Total	39,686,251	10,933	6,111	5,790	2,326	1,141					13.5

[a] At a BLAST cutoff value of $1 \times e^{-20}$.
[b] Predicted numbers of loci for pre-microRNA-like small RNAs.
[c] This chromosome contains two internal gaps of unclonable DNA marked by gaps of 1.4 and 4.5 kb; all other chromosomes are complete.
[d] The sequence of one telomere is missing from this chromosome; all other telomeres are complete.

Sexual activation of chromosome plasticity and repeat-induced point mutation

Comparative genome hybridizations using a whole-genome tiling array made from the genome sequence of IPO323 demonstrated striking sexually activated chromosomal plasticity in progeny isolates (Fig. 2) and chromosome number polymorphisms in field isolates. For example, isolate IPO94269, a field strain from bread wheat in the Netherlands, was missing two chromosomes that were present in IPO323 (Fig. 2A).

Sexual-driven genome plasticity was particularly evident among progeny isolates in the two mapping populations, including losses of chromosomes that were present in both parents and disomy for others (Wittenberg et al., 2009). For example, progeny isolate #51 of the cross between IPO323 and IPO94269 lost chromosomes 14 and 21 (Fig. 2B) even though they were present in both parents. This isolate also was missing chromosome 20, which was polymorphic for presence between the parents of the cross. More surprisingly, this isolate was disomic for chromosomes 4 and 18 (Fig. 2B), indicating that chromosomes can be both gained and lost during meiosis. For chromosome 18, both copies must have originated from IPO323 because no homolog was present in IPO94269. Molecular markers for chromosome 4 appeared to be heterozygous indicating that both parents contributed a copy to progeny isolate #51 (data not shown). Progeny isolate #2133 of the cross between isolates IPO323 and IPO95052 showed loss of three dispensable chromosomes (15, 18 and 21) that were present in both parents (Fig. 2C), most likely due to non-disjunction during meiosis. Thus, extreme genome plasticity was manifested as chromosome number and size polymorphisms (Wittenberg et al., 2009) that were generated during meiosis and extended to core as well as dispensable chromosomes.

The whole-genome hybridizations also indicated that the core and dispensable chromosomes can be remarkably uniform for gene content, given the high capacity of the latter for change. Comparative genome hybridizations between IPO323 and IPO95052, an isolate from a field of durum wheat in Algeria, showed that they had the same complement of core and dispensable chromosomes (Fig. 2D). This was surprising, because populations of the pathogen from durum wheat (a tetraploid) usually are adapted to that host and not to hexaploid bread wheat, yet the chromosomal complements of isolates from these hosts on different continents were the same.

Evidence for repeat-induced point mutation (RIP), a mechanism in fungi that inactivates transposons by introducing C to T transitions in repeated sequences (Cambareri et al., 1989; Selker, 2002), was seen in genome-wide analyses of transition:transversion ratios in

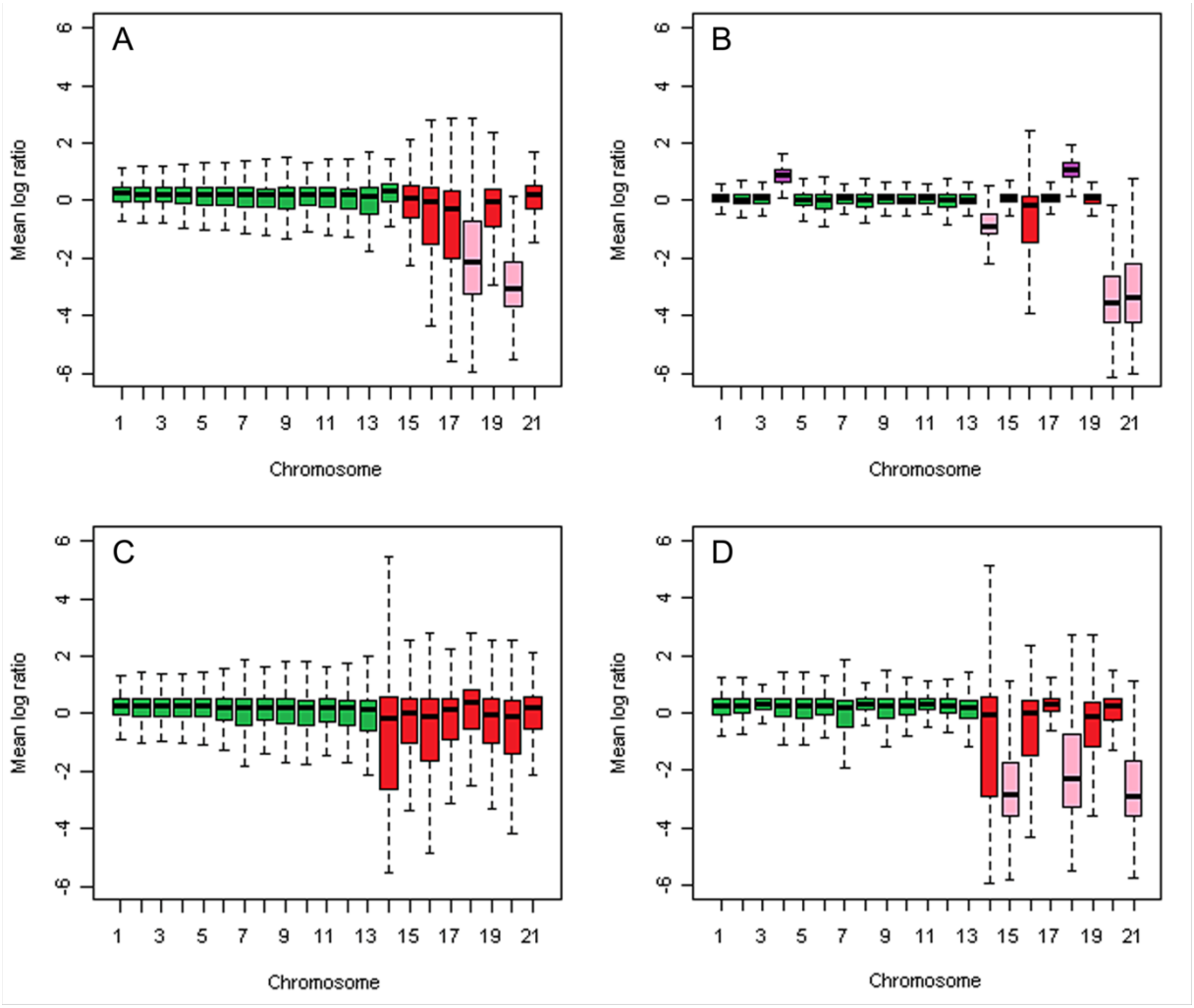

Fig. 2. Box plots of comparative genome hybridizations (CGH) of DNA from five isolates of *Mycosphaerella graminicola* to a whole-genome tiling array made from the finished sequence of isolate IPO323. **A.** CGH between IPO323 and the Dutch field isolate IPO94269. **B.** CGH between IPO323 and progeny isolate #51 from the cross between IPO323 and IPO94269. **C.** CGH between IPO323 and progeny isolate #2133 of the cross between IPO323 and IPO95052. **D.** CGH between IPO323 and Algerian field isolate IPO95052, which was isolated from and is adapted to durum (tetraploid) wheat. The genomic difference between the strains for each CGH is shown by 21 box plots, one for each chromosome of *M. graminicola*. The horizontal line in each box is the median log ratio of hybridization signals of the two strains; the upper and lower ends of a box represent the 25% and 75% quartiles. The whiskers extending from each box indicate 1.5 times the interquartile range, the distance between the 25% and 75% quartiles. The larger the deviation from 0, the greater the difference between the strains for a particular chromosome. Pink boxes that are significantly less than the zero line indicate missing chromosomes. The purple boxes in panel B (4 and 18) that are significantly higher than the zero line indicate chromosomes that are disomic.

long terminal repeat (LTR) pairs from 20 retrotransposon insertions which had 255 transitions and 6 transversions for a ratio of 42.5:1. Similarly high transition:transversion ratios were found in all repetitive sequences analyzed and extended to the coding regions in addition to the LTRs (Dhillon et al., 2010). The reverse transcriptase coding regions from transposon families RT11 and RT15 had transition:transversion ratios of 27.8:1 and 25.3:1, respectively, instead of the 1:1 ratio expected among 6,939 mutations analyzed. This high incidence of

transitions most likely reflects changes caused by RIP. The coding regions of all transposons with more than 10 copies included stop codons that prevent proper translation, indicating that they were inactivated.

Core and dispensable chromosomes are highly divergent

There were significant differences in structure and gene content between the 13 core and eight dispensable chromosomes (Tables 1 and 2); the latter are referred to collectively as the dispensome. The dispensome constituted about 12% of the genomic DNA but contained only 6% of the genes. In contrast, the 13 core chromosomes had twice as many genes per Mb of DNA, about half as much repetitive DNA, a significantly higher G+C content, and much higher numbers of unique genes (Tables 1 and 2). Genes in the dispensome were significantly shorter, usually were truncated relative to those on the core chromosomes (Table 2) and had dramatic differences in codon usage (Fig. S4).

About 59% of the genes on core chromosomes could be annotated compared to only 10% of those on the dispensome (Table 2). Some unique genes in the dispensome with intact, presumably functional reading frames, had possible paralogs on the core chromosomes (Fig. S5) that appeared to be inactivated by mutations (Fig. S6). A majority of the annotated dispensome genes coded for putative transcription factors or otherwise may function in gene regulation or signal transduction (Table S1). Most of the redundant genes on the dispensome were copies of genes present on core chromosomes, yet no syntenic relationships could be identified. Instead, each dispensable chromosome contained genes and repetitive sequences from all or most of the core chromosomes (Figs. 3 and S7) with additional unique genes of unknown origin. Sharing of genetic material applied to core chromosomes as well as the dispensome, consistent with a high level of recombination (Fig. S8). Whether the primary direction of transfer is from core to dispensable chromosomes or vice versa is not known.

The dispensome contained fewer genes encoding secreted proteins such as effectors and other possible pathogenicity factors compared to the core set. Signal peptides showed no enrichment on the dispensome (Table S1) except for a few clusters overlapping with transposon-related repeats. Although mature microRNAs have not been demonstrated in fungi, they may be important regulatory molecules. In the *M. graminicola* genome, 418 non-overlapping loci potentially encoding pre-microRNA-like small RNA (pre-milRNA) were predicted computationally based on the RFAM database (Gardner et al., 2009). This number was similar to the 434 loci predicted in the 41-Mb genome of *Neurospora crassa* using the

Table 2. Differences between essential and dispensable chromosomes in the genome of *Mycosphaerella graminicola* isolate IPO323.

	Chromosomes		
Statistic	**Core (1-13)**	**Dispensable (14-21)**	**Combined (1-21)**
Size in bp			
Total	35,077,646	4,608,605	39,686,251
Mean	2,698,280	576,076***	1,889,821
Percent	88.4	11.6	100.0
All genes			
Total	10,279	654	10,933
Mean	790.7	81.8***	521
Percent of total	94.0	6.0	100.0
Unique genes[a]			
Total	5,479	311	5,790
Mean	421.5	38.9***	276
Percent of all	53.3	47.6	53.0
Annotated genes			
Total	6,046	65	6,111
Mean	465.1	8.1***	291.0
Percent of all	58.8	9.9	55.9
Unique total	2,308	18	2,326
Unique mean	177.5	2.3***	110.8
Transcript size, mean in bp	1327.1	847.3***	1144.3
Gene density, Mb^{-1}	288.9	142.4***	233.1
Repetitive DNA, mean	15.9%	30.0%***	21.2%
G+C, mean	52.3%	50.9%**	51.7%

[a] At a BLAST cutoff value of $1 \times e^{-20}$.

*** The mean for the dispensable chromosomes is significantly different from that for the essential chromosomes at $P < 0.001$ by one-tailed t test.

** The mean for the dispensable chromosomes is significantly different from that for the essential chromosomes at $P = 0.012$ by one-tailed t test.

same approach. Of the 418 putative pre-milRNA loci predicted in the genome of *M. graminicola*, 88 (21%) are located on the 11% of the genome present as dispensome. This is about twice as much as is expected on the basis of a random distribution. Therefore, the dispensome is enriched for pre-milRNA loci.

The 418 pre-milRNA loci code for 385 non-redundant pre-milRNA sequences that can give rise to distinguishable mature milRNAs. The occurrence of mature milRNAs derived from the predicted set was analyzed in a small-RNA data consisting of almost 6 million reads (Illumina platform) generated from germinated spores of *M. graminicola* isolate IPO323 (Table S2).

Many of the non-redundant predicted milRNA sequences were represented in the RNA reads, at widely different amounts per sequence. In total, 65 of the 385 non-redundant sequences were observed 10 times or more. Two predicted sequences occurred more than a thousand times each, experimentally confirming the presence of putatively mature milRNAs derived from computationally predicted pre-milRNA sequences. In *N. crassa*,

computationally predicted putative milRNA sequences also were confirmed experimentally (Lee et al., 2010), supporting the likelihood of their existence in *M. graminicola*.

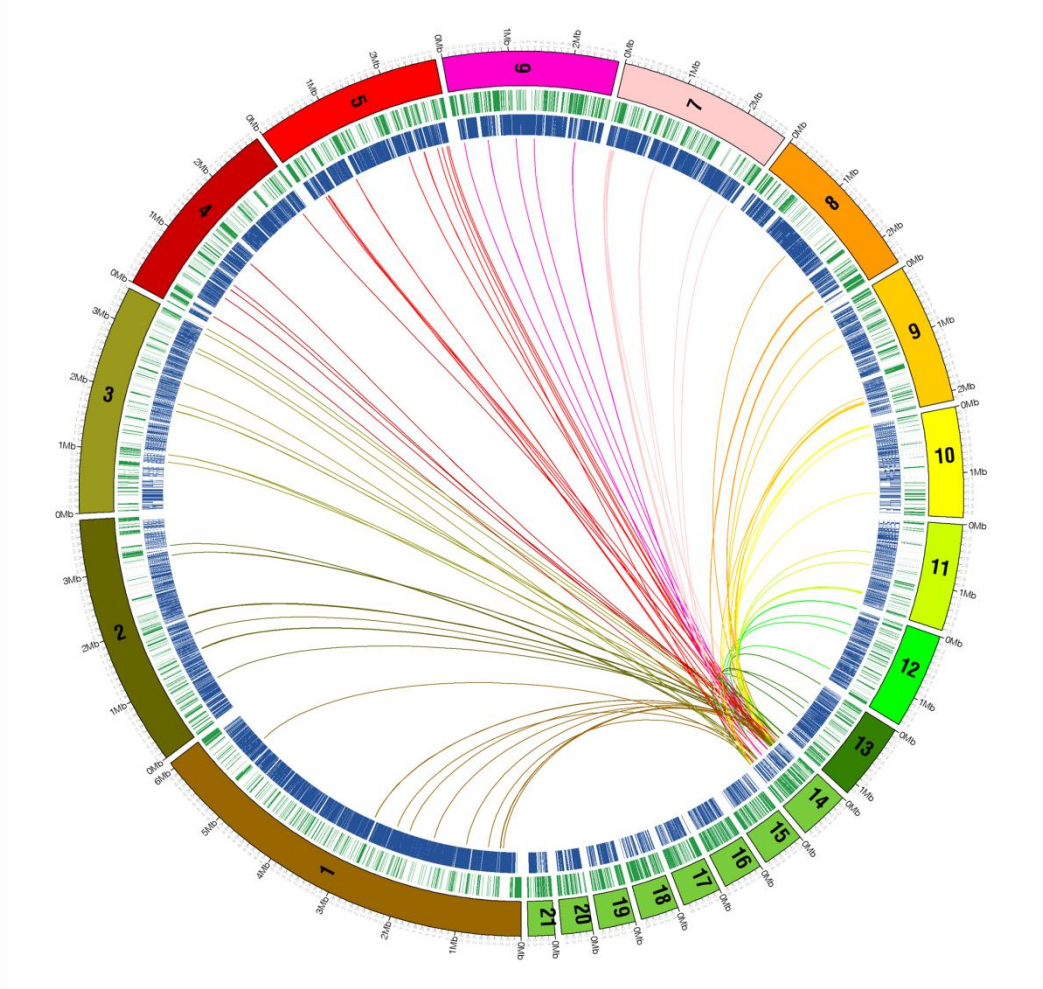

Fig. 3. Analysis of genes that are shared between dispensable chromosome 14 and the 13 core chromosomes of *Mycosphaerella graminicola* isolate IPO323. Each chromosome is drawn to scale as a numbered bar around the outer edge of the circle, and the sequence was masked for repetitive DNA prior to analysis. Lines connect regions of 100 bp or larger that are similar between each core chromosome and the corresponding region on chromosome 14 at $1 \times e^{-5}$ or lower. Chromosome 14 is an amalgamation of genes from all of the core chromosomes but they are mixed together with no synteny. Genes on the other dispensable chromosomes were not included in this analysis.

The origin of the dispensome of *M. graminicola* is not clear. The two most likely origins would be degeneration of copies of the core chromosomes or by horizontal transfer. Disomy for core chromosomes, as seen in one of the progeny isolates, could provide the origin for a dispensable chromosome. If one of the two chromosome copies became preferentially subject to RIP followed by breakage or interstitial deletions this could result in a degenerated copy of that core chromosome. However, in that case we would expect the dispensome to share large regions of synteny with specific core chromosomes, and this was not observed, which renders this explanation less likely.

The large differences in codon usage between core and dispensable chromosomes could be explained by horizontal transfer or possibly by RIP. To discriminate between these hypotheses, RIP was simulated on the genes of the core chromosomes. Principal components analysis (PCA) of the simulated data set did not reduce the differences in codon bias (Fig. S9A); if anything, it made them farther apart. This result was consistent whether it included only putative functional, truncated copies or entire pseudogenes after RIPping (data not shown). DeRIPping of genes on the dispensable chromosomes also did not affect the results (Fig. S9B), so RIP could not explain the observed differences in codon usage between core and dispensable chromosomes. PCA of a sample of genes shared between core and dispensable chromosomes showed few differences in codon bias (Fig. S9C) or amino acid composition (Fig. S9D), consistent with an origin by duplication and exchange among chromosomes. This conclusion was supported when the analysis was expanded to include all genes with putative homologs on core and dispensable chromosomes (Fig. S9E) even though these genes had a very different codon usage compared to the entire sets of genes on the core chromosomes (Fig. S9F).

To test the horizontal transfer hypothesis, additional PCAs were performed on simulated horizontal transfer data sets made by combining the genome of *M. graminicola* with those of two other fungi. Best non-self BLAST hits for genes on the *M. graminicola* dispensome most often were to fungi in the Pleosporales or Eurotiales (Table S3), so published genomes from species representing those orders were chosen for analysis. PCA of the combined genomes of *M. graminicola* and *Stagonospora nodorum* (representing the Pleosporales) gave separate, tight clusters for the core chromosomes of *M. graminicola* versus most of those from *S. nodorum* (Fig. S10A). Dispensable chromosomes of *M. graminicola* formed a looser, distinct cluster, and a fourth cluster was comprised of *M. graminicola* chromosome 14 plus scaffolds 44 and 45 of *S. nodorum* (Fig. S10A); this may indicate the existence of dispensable chromosomes in the latter species. Analysis of the combined genomes of *M. graminicola* plus *Aspergillus fumigatus* (Eurotiales) gave a similar result (Fig. S10B). The separate clustering by PCA of the *M. graminicola* dispensome and core chromosomes is consistent with an origin by horizontal transfer, but not from either of the two species tested. PCA on the frequencies of repetitive elements also indicated a separation between core and dispensable chromosomes (Fig. S11), consistent with the horizontal transfer hypothesis.

A more refined test of the RIP hypothesis was performed by using the observed rates of all mutations in families of transposons with 10 or more elements to simulate mutational

changes on replicated samples drawn from the core chromosomes. Observed mutation rates were calculated from aligned sequences; multicopy transposons were chosen for this analysis because they are the most likely to have been processed through the RIP machinery so will reflect the actual biases that occur in *M. graminicola*. Codon bias and other parameters in the mutated samples were then compared to those in the dispensome and in the original, non-mutated samples. Application of the mutational changes moved the samples drawn from the core chromosomes closer to the value observed for the dispensome, but the dispensome remained distinct except for a few of the analyses that are least likely to be affected by selection (Fig. 4). This confirmed that the dispensome has been subject to RIP but that this alone was not sufficient to explain the observed pattern of codon usage.

A new type of synteny

Pairwise sequence comparisons between the chromosomes of *M. graminicola* and scaffolds of *Stagonospora nodorum*, another wheat pathogen in the Dothideomycetes but in a different order from Mycosphaerella, revealed multiple regions with approximately 70-90% similarity (Fig. 5). However, the similarity did not extend to the dispensome, which generally was different from all of the *S. nodorum* scaffolds. Detailed examination showed that each region of similarity generally represents only one or a few genes in both organisms. Comparisons between the initial draft genome (version 1.0) of *M. graminicola* (Fig. 5A) and the finished sequence (Fig. 5B) revealed some misassemblies and also indicated scaffolds that ultimately were joined in the final assembly.

A surprising result was that the dot-plot patterns were very different from those that characterize the macro- or microsynteny seen in other organisms when viewed at a whole-scaffold/chromosome scale. Instead of the expected diagonal lines indicating chromosomal regions with content in the same order and orientation, the dots are scattered quasi-randomly within 'blocks' defined by scaffold/chromosome boundaries (Fig. 5). For many *S. nodorum* scaffolds the vast majority of dots related are shared exclusively with one or a small number of *M. graminicola* chromosomes. For example, there are predominant one-to-one relationships between *M. graminicola* version 3 chromosomes 11 and 12 with *S. nodorum* scaffolds 21 and 7 (Fig. 5B, circle V), respectively. Similarly, *M. graminicola* chromosomes 5-10 each had strong relationships with 2 to 4 scaffolds of *S. nodorum*. We refer to this conservation of gene content but not order or orientation among chromosomes as 'mesosynteny'. Analyses of additional genomes has shown that mesosynteny as defined here

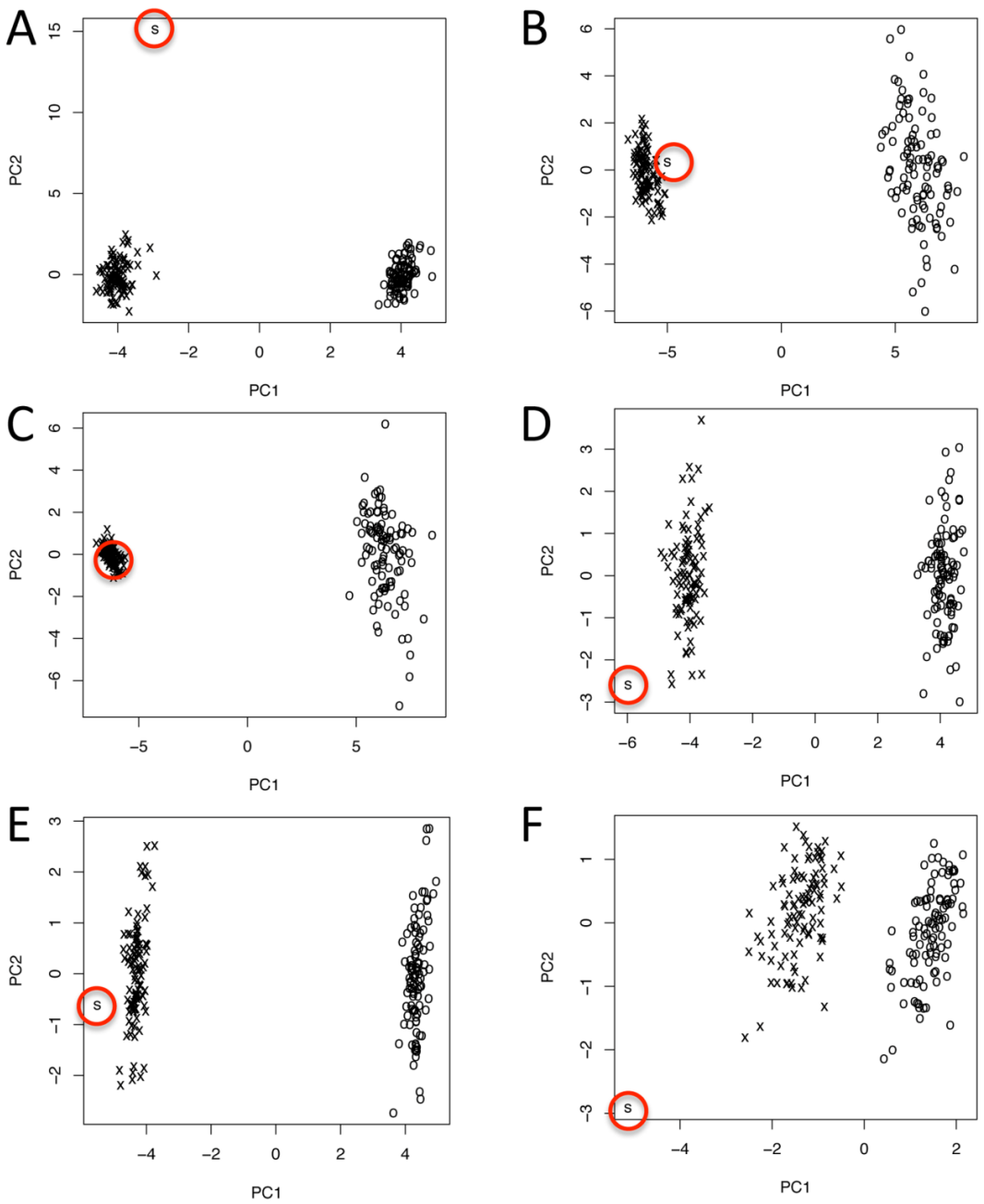

Fig. 4. Principal Component Analysis of: S, observed genes on the dispensome; O, observed samples of genes on the core chromosomes before mutation; and x, samples of genes from the core chromosomes after mutation. Mutation was simulated using observed frequencies of all mutations in families of transposable elements with ten or more copies, and included mutations from RIP and other processes. Mutating the samples of genes from the core chromosomes always made them more similar to the observed value for the dispensome but only rarely included the dispensome value (see panel **C**). This occurred primarily with codon preference and GC content by amino acid, which are the quantities that are least subject to natural selection for protein function. **A.** amino acid frequency using the values for the aligned sequence with the highest GC content to build the table of mutation frequencies; **B.** codon preference using the consensus of the aligned sequences to make the table of mutation frequencies covering only the 5' portion of each gene; **C.** codon preference using the values for the aligned sequence with the highest GC content to build the table of mutation frequencies covering only the 5' portion of each gene; **D.** codon usage using the values for the aligned sequence with the highest GC content to build the table of mutation frequencies but with all mutation frequencies cut in half; **E.** codon usage using the values for the aligned sequence with the highest GC content to build the table of mutation frequencies; and **F.** GC skew using the consensus of the aligned sequences to make the table of mutation frequencies. The first principal component always separated out the pre- and post-mutated chromosome samples. The locations of the observed values for the dispensome (S) are circled.

occurs among all Dothideomycetes tested and may be unique to that class of fungi (data not presented).

Mesosynteny as a tool to assist genome assembly

Macrosyntenic relationships are used commonly to assist the assembly and finishing of fragmented genome sequences (Giles et al., 1991; Kay et al., 2007; Fedorova et al., 2008; Ma et al., 2010), particularly in prokaryotes. Sequences that are macrosyntenic to a long segment of a closely related genome are highly likely to be joined physically. If mesosynteny between a new genome assembly and a reference genome also may be used to suggest scaffolds that should be juxtaposed it could significantly reduce the cost and complexity of assembling and finishing genomes. To test whether mesosynteny could be used to predict scaffold or contig joins in a genomic sequence, versions 1 and 2 of the *M. graminicola* genome assembly were analyzed to determine whether any of the improvements in the finished genome could have been predicted bioinformatically by mesosynteny (Supplementary Information S1).

The first version of the *M. graminicola* genome consisted of 129 scaffolds (http://genome.jgi-psf.org/Mycgr1/Mycgr1.home.html). Comparison of *M. graminicola* version 1 scaffolds with those of the *P. nodorum* genome predicted all scaffold joins made in version 2 (Fig. 5, Supplementary Information S1). Version 1 scaffolds 10 and 14 (Fig. 5: group I), 7 and 17 (groups II, VII and IX), and 12 and 22 (groups III and VIII) were joined into chromosomes 7, 5 and 10, respectively. Mesosynteny also indicated both instances where version 1 scaffolds were assembled incorrectly and subsequently were split in version 2. Compared to the scaffolds of *P. nodorum*, *M. graminicola* version 1 scaffold 4 exhibited regions of meso- synteny adjacent to regions of no synteny. Corrections to the assembly made in version 2 separated these two distinct regions into separate chromosomes. Version 1 scaffolds 4 and 9 (Fig. 5: groups IV/VI and V) were corrected to version 2 chromosomes 6 and 16 (Fig. 5: group IV/VI) and chromosomes 12 and 21 (Fig. 5: group V) respectively. Mesosynteny was remarkably successful and has great potential to assist the assembly and finishing of fungal genomes.

A mechanism of stealth pathogenesis

Generally, gene families involved in cell wall degradation are expanded in fungal

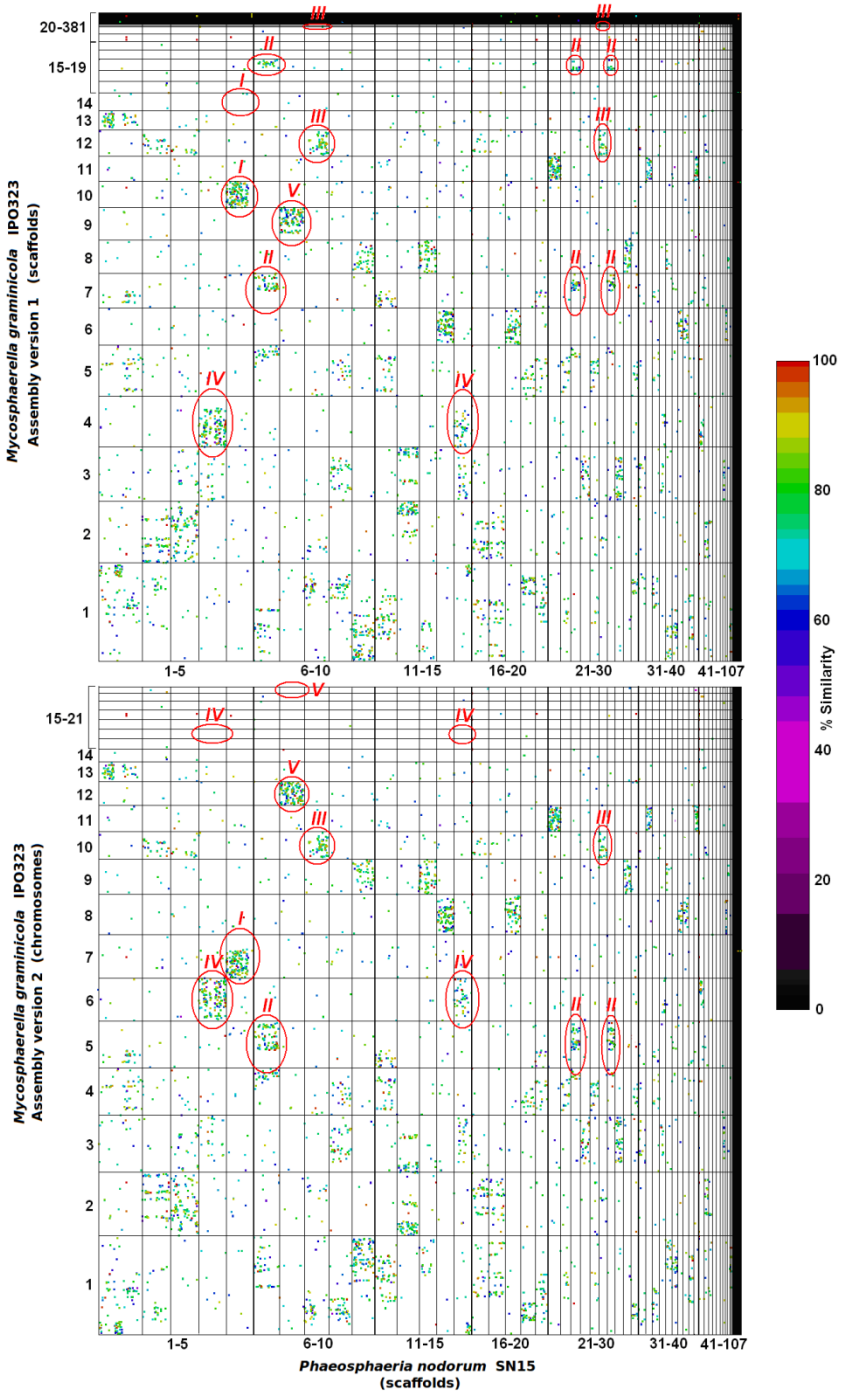

Fig. 5. Comparisons of *Mycosphaerella graminicola* genome assembly versions 1 (A) and 2 (B) against that of *Stagonospora nodorum* isolate SN15. Scaffolds/chromosomes are ordered along their respective axes according to both decreasing length and increasing number. The 6-frame translations of both genomes were compared via MUMMER 3.0 (Kurtz et al., 2004). Homologous regions are plotted as dots, which are color coded for percent similarity as per the bar on the right. Amendments made in the version 2 assembly and their corresponding regions in assembly version 1 are circled in red. Version 2 chromosomes 5 (**B**, circle II), 7 (**B**, circle I) and 10 (**B**, circle III) were derived from joined version 1 scaffolds 7 and 17 (**A**, circle II), 10 and 14 (**A**, circle I) and 12 and 22 (**A**, circle III), respectively, validating the method. Observation of the mesosyntenic pattern also could be used to identify inappropriately joined scaffolds. For example, *M. graminicola* v2 chromosomes 6 and 16 (**B**, circle IV) and 12 and 21 (**B**, circle V) were derived from split version 1 scaffolds 4 (**A**, circle IV) and 9 (**A**, circle V), respectively. These scaffolds are characterized by an abrupt termination of the mesosyntenic block at the split point as indicated by red lines (**A**, circles IV and V). A total of 21 predictions was made and 14 were validated.

plant pathogens (Yun et al., 2000; Martin et al., 2010). However, in *M. graminicola*, gene families characterized by the Carbohydrate-Active Enzyme database (CAZy) (Dean et al., 2005) as plant cell wall polysaccharidases were severely reduced in size (Fig. 6). According to the CAZy analysis, the genome of *M. graminicola* contains fewer genes for cellulose degradation than those of six other fungi with sequenced genomes including both grass pathogens and saprophytes (Table 3), and only about one-third as many genes for cell wall degradation in total compared to the other plant pathogens (Table S4). This reduction in CAZymes in *M. graminicola* was very visible when the putative genes were divided based on polysaccharide substrate (Table S4). In addition, genes involved in appressorium formation, which are required for pathogenesis of many plant pathogens including *Magnaporthe oryzae* (Cuomo et al., 2007), were absent or reduced in the *Mycosphaerella graminicola* genome, reflecting its alternative host-penetration strategy.

To further analyze the mechanism of stealth pathogenesis, we profiled the growth on polysaccharides of *M. graminicola* compared to *Stagonospora nodorum* and *Magnaporthe oryzae*, two pathogens of the cereals wheat and rice, respectively, with sequenced genomes (Fig. S12). Growth of *M. graminicola* corresponded with the CAZy annotation for a strongly reduced number of genes encoding putative xylan-degrading enzymes. Furthermore, the CAZy annotation demonstrated that *M. graminicola* contains a much smaller set of glycoside hydrolases, carbohydrate esterases, and carbohydrate binding modules (CBMs) compared to the other two cereal pathogens (Table S5). The strong reduction of CBMs in *M. graminicola* suggests a different strategy in the degradation of plant cell walls compared to the other two species. The *M. graminicola* genome is particularly depauperate for enzymes degrading cellulose, xylan and xyloglucan compared to the other two species, so is very atypical for a cereal pathogen.

A possible mechanism of stealth pathogenesis was indicated by gene families that were expanded in the genome of *M. graminicola*. In comparative analyses of gene families and PFAM domains with several other fungi, the most striking expansions were observed for peptidases (M3, S28, pro-kuma, M24, metalloendopeptidase, metalloproteinase) and alpha amylases (glycoside hydrolase family 13) (Tables S6 and S7). This suggests that alternative nutrition sources during the biotrophic phase of infection may be proteins which are available in the apoplast, or possibly starch from chloroplasts that are released early in the infection process (Kema et al., 1996a). Overall, these analyses revealed that the genome of *M. graminicola* differs significantly from those of other cereal pathogens with respect to genes

involved in plant penetration as well as polysaccharide and protein degradation (Fig. 6, Table 3), which most likely reflects its stealthy mode of pathogenesis.

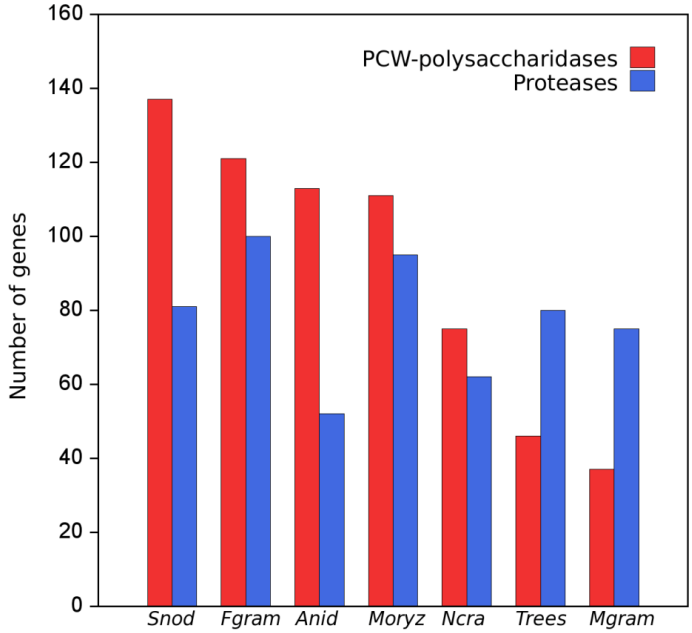

Fig. 6. Numbers of genes for proteases and plant cell wall (PCW) degrading polysaccharidases in the genomes of seven fungi with sequenced genomes. Genes for PCW-polysaccharidases were severely reduced in the genome of *Mycosphaerella graminicola* but proteases were about the same. The overall profile of the enzymes in *M. graminicola* was most similar to that of *T. reesei* than to any of the other plant pathogens. Species analyzed included the saprophytes *Aspergillus nidulans* (Anid), *Neurospora crassa* (Ncra), and *Trichoderma reesei* (Trees), and the plant pathogens *Fusarium graminearum* (Fgram), *Mycosphaerella graminicola* (Mgram), *Magnaporthe oryzae* (Moryz), and *Stagonospora nodorum* (Snod).

Table 3. Numbers of predicted enzymes degrading cellulose across seven ascomycete species with sequenced genomes.

	Saprophytes[a]			**Pathogens**[a]			
CAZy family[b]	**Anid**	**Ncra**	**Trees**	**Fgram**	**Mgram**	**Moryz**	**Snod**
GH5 cellulases[c]	3	1	2	2	0	2	3
GH6	2	3	1	1	0	3	4
GH7	3	5	2	2	1	6	5
GH12	1	1	2	4	1	3	4
GH45	1	1	1	1	1	1	3
GH61	9	14	3	15	2	17	30
GH74	2	1	1	1	0	1	0
CBM1	8	19	15	12	0	22	13
Total cellulases	29	45	27	38	5	55	62

[a] Species analyzed included the saprophytes *Aspergillus nidulans* (Anid), *Neurospora crassa* (Ncra), and *Trichoderma reesii* (Trees), and the plant pathogens *Fusarium graminearum* (Fgram), *Mycosphaerella graminicola* (Mgram), *Magnaporthe oryzae* (Moryz), and *Stagonospora nodorum* (Snod).
[b] Families defined in the Carbohydrate-active enzymes database (www.cazy.org).
[c] GH5 is a family containing many different enzyme activities; only those targeting cellulose are included.

Differences in gene expression during the different stages of infection were evident from an analysis of EST sequences (Kema et al., 2008) from wheat leaves 5, 10 and 16 days after inoculation (DAI) with *M. graminicola*. Most genes were present at only one sampling time with little overlap, particularly between the library from the biotrophic stage of infection (5 DAI) compared to the other two (Fig. S13A). Lack of overlap extended to a library from minimal medium minus nitrogen to simulate the nitrogen starvation thought to occur during infection (Fig. S13B). Expression of genes for cell wall-degrading enzymes also was reduced during the biotrophic stage of infection (Kema et al., 2008), consistent with the stealth-pathogenicity hypothesis.

DISCUSSION

The dispensome as defined here includes all parts of the genome that can be missing in field or progeny isolates with no obvious effects on fitness in axenic culture, on a susceptible host or during mating. For *M. graminicola*, this includes the eight known dispensable chromosomes in isolate IPO323 plus any others that may be discovered in the future. The core genome consists of all chromosomes that are always present in field and progeny isolates, presumably because they contain genes that are vital for survival so cannot be lost. Both core and dispensable chromosomes may be present in two or possibly more copies, but core chromosomes are never absent.

The dispensome of *M. graminicola* is very different from the supernumerary or B chromosomes in plants and some animals. The B chromosomes of plants contain few if any genes and are composed mostly of repetitive elements assembled from the A chromosomes. They may have a negative effect on fitness (Cantarel et al., 2009) and appear to be maintained primarily by meiotic drive (Caracuel-Rios and Talbot, 2007). In contrast, the dispensome of *M. graminicola* contains many unique and redundant genes and is not maintained by meiotic drive, as individual chromosomes are lost readily during meiosis (Wittenberg et al., 2009).

Dispensable chromosomes have been reported in other fungi but they are significantly fewer and larger (from 0.7 to 4.9 Mb with an average of about 1.5 to 2.0 Mb) than those in *M. graminicola* (from 0.42 to 0.77 Mb) and mostly are composed of repetitive DNA with few known genes (Jones et al., 2008). Unlike the dispensome of *M. graminicola*, the few genes on dispensable chromosomes in other fungi often are pathogenicity factors (Miao et al., 1991; Covert, 1998; Jones et al., 2008) and whole chromosomes may be transferred asexually (Hatta et al., 2002). Dispensable chromosomes in other fungi are different from the dispensome of

M. graminicola except for the conditionally dispensable or lineage-specific chromosomes reported recently in *Nectria haematococca* (asexual stage: *Fusarium solani*) and other species of Fusarium (Masel et al., 1996; Wang et al., 2003), which also were different from core chromosomes in structure and gene content and contained numerous unique genes. However, unlike those in *M. graminicola*, dispensable chromosomes of Fusarium species had clear functions in ecological adaptation, were transferred more or less intact among closely related species (Wang et al., 2003) and did not show extensive recombination with core chromosomes.

The high instability of the *M. graminicola* dispensome during meiosis and mitosis would cause it to be eliminated unless it provided a selective advantage to the pathogen at least under some conditions. The unique genes with annotations indicated possible functions in transcription or signal transduction. There also was an enrichment for predicted pre-milRNAs, which may indicate that parts of the dispensome are involved in gene regulation. Based on dispensable chromosomes in other plant pathogens, genes on the dispensome were expected to be involved with host adaptation or pathogenicity, yet so far no genes for pathogenicity or fitness of *M. graminicola* have been mapped to the dispensome (Coleman et al., 2009). A more interesting possibility is that the dispensome facilitates high recombination among chromosomes and could provide a repository of genes that may be advantageous under certain environmental conditions. This hypothesis should be tested by additional experimentation.

A recent comparison of the *M. graminicola* genome with that of its closest known relative, the unnamed species S1 from wild grasses in Iran, identified probable homologs for all of the dispensome chromosomes in the sibling species except for chromosome 18 (Ware, 2006). These putative homologs presumably are dispensable also in species S1, but this has not been proven and only one isolate has been sequenced. Species S1 and *M. graminicola* are thought to have diverged approximately 10,500 years ago (Stukenbrock et al., 2010), concomitant with the domestication of wheat as a crop. Therefore, unlike dispensable chromosomes in other fungi, the dispensome of *M. graminicola* appears to be relatively ancient and has survived at least one speciation event. Analyses of two recently sequenced Dothideomycetes with Mycosphaerella sexual stages, *M. pini* (asexual stage: *Dothistroma septosporum*) and *M. populorum* (asexual stage: *Septoria musiva*), showed that they contained clear homologs of all of the core chromosomes of *M. graminicola*, but none of their chromosomes corresponded to the dispensome (B. Dhillon and S. B. Goodwin, unpublished). Taken together, these observations indicate that the dispensome of *M. graminicola* most likely

was acquired prior to its divergence from a common ancestor with species S1 more than 10,000 years ago, but after the split of the *M.graminicola*-S1 lineage from that which gave rise to *M. pini* and *M. populorum*. The mechanism for the longevity of this dispensome with no obvious effects on fitness is not known.

More than half of the genes on the dispensome and almost all of the transposons also were present on core chromosomes. Moreover, there was no increase in gene numbers so a simple transfer of chromosomes from another species does not explain all of the observations. Instead, we propose a new model for the origin of dispensable chromosomes in *M. graminicola* by horizontal transfer followed by degeneration and extensive recombination with core chromosomes. The tight clustering of the dispensable chromosomes in the PCAs, with the possible exception of chromosome 14, indicates that they probably came from the same donor species. However, it is difficult to explain why they are so numerous. The most likely mechanism of horizontal transfer is via a sexual or somatic fusion with another species that had eight or more chromosomes, in which only a few genes were maintained on each donated chromosome. Chromosome segments that were redundant with the core set could be eliminated, leaving only those that are unique or that could confer some sort of selective advantage to the individual or to the dispensome. The fitness advantage could be transitory or occur only under certain conditions to allow those chromosomes to be dispensable, at least on an individual or population basis. Another possibility is that the numerous dispensable chromosomes are fragments from one or two larger chromosomes that were broken, acquired additional telomeres and lost content to result in their current, reduced complements of genes. High recombination within chromosomes and transfer of content between the donor and host chromosomes must have occurred to explain the observed pattern of shared genes.

The recombination hypothesis is supported by degenerated copies of some unique genes that were found on core chromosomes. These most likely represent genes that were copied from core to dispensable chromosomes, after which the copy on the core chromosome became inactivated, probably by RIP. Duplication, diversification and differential gene loss were proposed recently as the origin of lineage-specific gene islands in *Aspergillus fumigatus* (Stukenbrock et al., 2007), but that process seems to be very different from what occurred in *M. graminicola.* In *A. fumigatus*, large blocks of genes with synteny to other chromosomes were found, the opposite of what was seen for *M. graminicola*. The origin and evolution of the dispensome in *M. graminicola* seems to be very different from those reported for dispensable chromosomes in other fungi (Wang et al., 2003). Unlike other fungi in which single chromosomes seem to have been transferred recently, the dispensome of *M.*

graminicola most likely originated by ancient horizontal transfer of many chromosomes thousands of years ago. So far it is not known to be conditionally dispensable, unlike dispensable chromosomes in other fungi, which have clear roles in ecological adaptation.

The mesosyntenic analyses provided a new approach that complements the use of genetic linkage maps to support whole-genome assembly. Gene content was highly conserved on syntenic chromosomes in the two distantly related species, but there was little or no conservation of gene order or orientation. The comparison of the version 1 assembly of *M. graminicola* with the related *S. nodorum* genome sequence indicated scaffolds that should be merged and others that were erroneously assembled into one scaffold. Hence, mesosynteny validated the high-density genetic analyses and may provide an additional tool for whole-genome assembly for fungi where linkage maps do not exist or cannot be generated. Groups of genes in *S. nodorum* that corresponded to more than one group in *M. graminicola* may indicate scaffolds that should be joined in *S. nodorum* or, more likely, may reflect chromosomal rearrangements that have occurred since the divergence of *S. nodorum* and *M. graminicola* from an ancient common ancestor.

Considering their early divergence (James et al., 2006) relative to species within the same genus, the degree of mesosyntenic conservation between *M. graminicola* and *S. nodorum* is striking. However, it is very surprising that the synteny only applied to gene content but not order or orientation. In comparisons between other organisms, synteny plots usually yield diagonal lines even between unrelated species such as humans and cats (Housworth and Postlethwait, 2002). The lack of diagonal lines in the comparisons of *S. nodorum* with *M. graminicola* indicate a high rate of shuffling of genes on chromosomal blocks that have remained constant over long periods of evolutionary time. The mechanism by which these small chromosomal rearrangements occur is not known.

The greatly reduced number of cell wall-degrading enzymes (CWDEs) in the genome of *M. graminicola* compared with other sequenced fungal genomes might be an evolutionary adaptation to avoid detection by the host during its extended, biotrophic latent phase and thus evade plant defenses long enough to cause disease. Similar loss of CWDEs in the ectomycorrhizal fungus *Laccaria bicolor* was thought to represent an adaptation to a symbiotic lifestyle (Martin et al., 2008). Based on these results we propose a novel, biphasic mechanism of stealth pathogenesis. During penetration and early colonization, *M. graminicola* produces a reduced set of proteins that facilitate pathogenicity and function as effectors in other fungi. Instead of the usual carbohydrate metabolism, nutrition during the extended biotrophic phase may be by degradation of proteins rather than carbohydrates in the

apoplastic fluid and intercellular spaces. The large number of proteases expressed during the early stages of the infection process supports this hypothesis. The biotrophic phase terminates by a switch to necrotrophic growth, production of specific cell wall-degrading enzymes and possibly by triggering programmed cell death (Kema et al., 1996b; Keon et al., 2007; Kema et al., 2008).

Stealth biotrophy raises the intriguing possibility that *M. graminicola* and possibly other Dothideomycetes may have evolved originally as endophytes or could be evolving towards an endophytic lifestyle. The finished genome of *M. graminicola* provides a gold standard (Chain et al., 2009) for this class of fungi, which is the largest and most ecologically diverse group of Ascomycetes with approximately 20,000 species, classified in 11 orders and 90 families, and provides a huge advantage for comparative genomics to identify the genetic basis of highly divergent lifestyles.

MATERIALS AND METHODS

Biological material

Mycosphaerella graminicola isolates IPO323 and IPO94269 are Dutch field strains that were isolated in 1984 and 1994 from the wheat cultivar Arminda and an unknown cultivar, respectively. Isolate IPO95052 was isolated from a durum (tetraploid) wheat sample from Algeria. All isolates are maintained at the CBS-KNAW Fungal Biodiversity Centre of the Royal Netherlands Academy of Arts and Sciences (Utrecht, the Netherlands) under accession numbers CBS 115943 (IPO323), CBS 115941 (IPO94269) and CBS 115942 (IPO95052). Mycelia of each isolate were used to inoculate 200 mL of YG broth (10 g of yeast extract and 30 g of glucose per L) and were cultured until cloudy by shaking at 120 rpm at 18°C, after which the spores were lyophilized, 50 mg of lyophilised spores were placed in a 2-mL tube and ground with a Hybaid Ribolyser (model n° FP120HY-230) for 10 s at 2500 rpm with a tungsten carbide bead. DNA was extracted using the Promega Wizard Magnetic DNA Purification system for food according to instructions provided by the manufacturer.

Initial sequencing and assembly

Whole-genome shotgun (WGS) sequencing of the genome of *M. graminicola* used three libraries with insert sizes of 2-3, 6-8, and 35-40 kb. The sequenced reads were screened for vector using cross_match, trimmed for vector and quality, and filtered to remove reads

shorter than 100 bases. WGS assembly was done using Jazz, a tool developed at the JGI (Aparicio et al., 2002). After excluding redundant and short scaffolds, the assembly v1.0 contained 41.2 Mb of sequence in 129 scaffolds, of which 4.0 Mb (7.5%) was in gaps (Table S8). The sequence depth derived from the assembly was 8.88 ± 0.04.

Gap closure and finishing

To perform finishing, the *M. graminicola* WGS assembly was broken down into scaffold-size pieces and each piece was reassembled with phrap. These scaffold pieces were then finished using a Phred/Phrap/Consed pipeline. Initially, all low-quality regions and gaps were targeted with computationally selected sequencing reactions completed with 4:1 BigDye terminator: dGTP chemistry (Applied Biosystems). These automated rounds included resequencing plasmid subclones and walking on plasmid subclones or fosmids using custom primers. Following completion of the automated rounds, a trained finisher manually inspected each assembly. Further reactions were then manually selected to complete the genome. These included additional resequencing reactions and custom primer walks on plasmid subclones or fosmids as described above guided by a genetic map of more than 2,031 sequenced markers plus paired-end reads from a library of Bacterial Artificial Chromosome clones. Smaller repeats in the sequence were resolved by transposon-hopping 8-kb plasmid clones. Fosmid and BAC clones were shotgun sequenced and finished to fill large gaps, resolve larger repeats and to extend into the telomere regions. Each assembly was then validated by an independent quality assessment. This included a visual examination of subclone paired ends using Orchid (http://www-hagsc.org), and visual inspection of high-quality discrepancies and all remaining low-quality areas. All available EST resources were also placed on the assembly to ensure completeness. The finished genome consists of 39,686,251 base pairs of finished sequence with an estimated error rate of less than 1 in 100,000 base pairs. Genome contiguity is very high with a total of 21 chromosomes represented, 19 of which are complete and 20 of which are sequenced from telomere to telomere.

Genome annotation

Both draft (v1.0) and finished (v2.0) assemblies of *M. graminicola* were processed using the JGI annotation pipeline, which combines several gene predictors:1) putative full-length genes from EST cluster consensus sequences; 2) homology-based gene models were predicted using FGENESH+ (Salamov and Solovyev, 2000) and Genewise (Birney and

Durbin, 2000) seeded by Blastx alignments against sequences from the NCBI non-redundant protein set; 3) *ab initio* gene predictor FGENESH (Salamov and Solovyev, 2000) was trained on the set of putative full-length genes and reliable homology-based models. Genewise models were completed using scaffold data to find start and stop codons. ESTs were used to extend, verify, and complete the predicted gene models. Because multiple gene models per locus were often generated, a single representative gene model for each locus was chosen based on homology and EST support and used for further analysis. Those comprised a filtered set of gene models supported by different lines of evidence. These were further curated manually during community annotation and used for analysis.

All predicted gene models were annotated using InterProScan (Zdobnov and Apweiler, 2001) and hardware-accelerated double-affine Smith-Waterman alignments (www.timelogic.com) against the SwissProt (www.expasy.org/sprot) and other specialized databases such as KEGG (Kanehisa et al., 2004). Finally, KEGG hits were used to map EC numbers (http://www.expasy.org/enzyme/), and Interpro hits were used to map GO terms (Ashburner et al., 2000). Predicted proteins also were annotated according to KOG (Tatusov et al., 2003; Koonin et al., 2004) classification.

Following the machine annotation, manual validation and correction of selected gene sets was performed by more than 30 annotators through a jamboree held at the JGI facilities in Walnut Creek, California, USA. Annotators were trained by JGI staff and continue to make modifications as necessary.

Potential microRNA-like small RNA (milRNAs) loci were annotated using the INFERNAL software tool and based on 454 microRNA families (covarion models) from the RFAM database version 9.1 (Griffiths-Jones et al., 2005). milRNAs were predicted if their scores were higher than thresholds, defined individually for each family, in the same way as PFAM domains are predicted.

Experimental validation of the predicted milRNAs was done by sequencing of an RNA library Total RNA was isolated from spores germinated on water agar of *M. graminicola* isolate IPO323. A small RNA library was prepared according to the protocol for Illumina sequencing; small RNAs from 16-~50 nt were isolated from gels, sequenced with an Illumina/Solexa single read DNA 50 cycles Genome Analyzer II, and compared by BLAST search against the list of 535 predicted pre-milRNAs from the genome sequence.

Assembly and annotations of the *M. graminicola* finished genome are available from the JGI Genome Portal at http://www.jgi.doe.gov/Mgraminicola and were deposited at DDBJ/EMBL/GenBank under the project accession ACPE00000000.

Microarray analyses

Whole-genome tiling microarrays were designed by choosing one 50-mer primer every 100 bases spanning the entire finished genome. The arrays were manufactured and hybridized by the Nimblegen Corporation with total DNA extracted from each field isolate.

Principal component analyses of core and dispensable chromosomes

The CodonW package (http://codonw.sourceforge.net/) was used for correspondence analysis of codon usage, which mathematically is identical to principal component analysis. CodonW requires as an input a set of coding sequences, usually of individual genes. For chromosome-level analyses coding sequences from the frozen gene catalog models for each chromosomes were concatenated, forming 21 'superORFs', one for each chromosome. Because partial models may introduce some potential frameshifts with internal stop codons they were removed from the analysis; this did not affect the results as their total number is low. CodonW has no graphical outputs, so they were used as inputs for scatter plots in R (http://www.r-project.org/).

For *M. graminicola* only a similar analysis was done for repeats. RepeatScout was run on the genome to produce a set of *ab initio*-identified repeat sequences. From that set 81 distinct repeat sequences, each with an occurrence exceeding 20 times in the genome, were extracted. For each chromosome a vector of length 81 was calculated with the relative frequency of each repeat. A PC analysis was run on the resulting vectors using the standard principal component function pcomp in R. Separation at the repeat level means that these chromosomes have distinct evolutionary profiles not only on the protein-coding level, but also on other parts of the chromosomes, suggesting that entire chromosomes may be transferred horizontally.

Mesosynteny

Dot plots were generated via MUMMER 3.0 (Kurtz et al., 2004) with data derived from default PROmer comparisons between the *M. graminicola* genome assembly versions 1 and 2 (http://genome.jgi-psf.org/Mycgr3/Mycgr3.home.html) and *S. nodorum* SN15 assembly version 2 (Hane et al., 2007), available under GenBank accessions CH445325-CH445384, CH445386-CH445394 and CH959328-CH959365, or AAGI00000000. Additional comparisons and statistical analyses were made with custom-designed perl scripts.

Data from the *M. graminicola* version 2 comparison with *S. nodorum* were used to test the efficacy of mesosyntenic comparisons to assist the completion of fungal genomes. The mesosynteny-based prediction of scaffold joining involved 3 stages: determining the percent coverage of scaffolds/chromosomes for each scaffold/chromosome pair (i.e., a function of the number of 'dots' per 'block'); determining which scaffold/chromosome pairs were significantly related and forming groups of joined scaffolds; and filtering out background levels of similarity due to sequence redundancy and incomplete genome assemblies.

Coordinates of homologous regions were obtained from PROmer coordinate outputs (MUMMER 3.0) and used to determine the percent of sequence covered by matches to a sequence from the alternate genome for each sequence pair. Where match coordinates overlapped on the sequence of interest, those matches were merged into a single feature to avoid redundancy. A perl script for conversion of PROmer coordinate outputs to a table of percent coverage is available on request.

Coverage values for each *M. graminicola-S. nodorum* sequence pair were subject to a binomial test for significance. The threshold for significance (*Psig*) ≥ 0.95 was:

$$P_{sig} = F(x, p, n) = \sum_{i=0}^{x} \binom{n}{i} (p)^{i} (1-p)^{n-1}$$

where x is the percent coverage, n equals 100, and p is the probability of chromosome homology.

The probability of chromosome homology (p) was equal to 1/(21 x 19), which was derived from the number of *M. graminicola* chromosomes (21) and the approximate PFGE estimate of *S. nodorum* chromosomes (19) (Cooley and Caten, 1991). This is the likelihood that a given sequence pair represents related chromosomes. This model assumes that no whole-genome/chromosome duplication events have occurred previously between either fungal genome since divergence from their last common ancestor.

The significance of percent coverage (*Psig*) was tested bidirectionally for each sequence pair (i.e., for sequence pair A-B, both coverage of sequence A by B and coverage of sequence B by A were tested). Sequence pairs were significantly related if a test in either direction was successful. A minimum length threshold of 1 kb was also imposed for both sequences. Where multiple scaffolds of *M. graminicola* were significantly related to the same *S. nodorum* scaffold, those *M. graminicola* scaffolds formed a 'joined group' of candidates for representation of the same chromosome.

All possible paired combinations of *M. graminicola* scaffolds present within predicted joined groups were subject to filtering for high levels of background similarity as follows:

$$retention = \frac{\#\text{ joined groups (scaffolds joined)}}{\#\text{ joined groups (either scaffold present)}}$$

The retention score is a measure of the reliability of scaffold join relationships. Joins between *M. graminicola* scaffold pairs with retention scores < 0.25 were discarded.

CAZy annotation and growth profiling

Annotation of carbohydrate-related enzymes was performed using the Carbohydrate-Active Enzyme database (CAZy) annotation pipeline (Dean et al., 2005). BLAST was used to compare the predicted proteins of *M. graminicola* to a collection of catalytic and carbohydrate-binding modules derived from CAZy. Significant hits were compared individually by BLAST to assign them to one or more CAZy families. Ambiguous family attributions were processed manually along with all identified models that presented defects (deletions, insertions, splicing issues, etc.).

Growth profiling of *S. nodorum* and *M. graminicola* was on *Aspergillus niger* minimal medium (de Vries et al., 2005). Cultures were grown at 25 degrees for seven days after which pictures were taken for growth comparison. Carbon sources used were: glucose (Sigma); soluble starch (Difco); alpha-cellulose (Sigma); Guar Gum (Sigma, galactomannan); Oat spelt xylan (Sigma); and Apple Pectin (Sigma).

Genome structure analyses

Comparisons of sequence content between core and dispensable chromosomes was with Circos (Krzywinski et al., 2009). This tool draws ribbons connecting sequences that align in different data sets.

ACKNOWLEDGEMENTS

We thank Els C.P. Verstappen, Jessica R. Cavaletto, Ineke De Vries and Odette Mendes for excellent technical support.

LITERATURE CITED

Adhikari, T.B., Balaji, B., Breeden, J., and Goodwin, S.B. 2007. Resistance of wheat to *Mycosphaerella graminicola* involves early and late peaks of gene expression. Physiological and Molecular Plant Pathology 71:55-68.

Aparicio, S., Chapman, J., Stupka, E., Putnam, N., Chia, J.M., Dehal, P., Christoffels, A., Rash, S., Hoon, S., Smit, A., Sollewijn Gelpke, M.D., Roach, J., Oh, T., Ho, I.Y., Wong, M., Detter, C., Verhoef, F., Predki, P., Tay, A., Lucas, S., Richardson, P., Smith, S.F., Clark, M.S., Edwards, Y.J.K., Doggett, N., Zharkikh, A., Tavtigian, S.V., Pruss, D., Barnstead, M., Evans, C., Baden, H., Powell, J., Glusman, G.,

Rowen, L., Hood, L., Tan, Y.H., Elgar, G., Hawkins, T., Venkatesh, B., Rokhsar, D., and Brenner, S. 2002. Whole-genome shotgun assembly and analysis of the genome of *Fugu rubripes.* Science 297:1301-1310.

Ashburner, M., Ball, C.A., Blake, J.A., Botstein, D., Butler, H., Cherry, J.M., Davis, A.P., Dolinski, K., Dwight, S.S., Eppig, J.T., Harris, M.A., Hill, D.P., Issel-Tarver, L., Kasarskis, A., Lewis, S., Matese, J.C., Richardson, J.E., Ringwald, M., Rubin, G.M., and Sherlock, G. 2000. Gene ontology: Tool for the unification of biology. Nature Genetics 25:25-29.

Birney, E., and Durbin, R. 2000. Using GeneWise in the Drosophila annotation experiment. Genome Research 10:547-548.

Cambareri, E.B., Jensen, B.C., Schabtach, E., and Selker, E.U. 1989. Repeat-induced G-C to A-T mutations in Neurospora. Science 244:1571-1575.

Cantarel, B.I., Coutinho, P.M., Rancurel, C., Bernard, T., Lombard, V., and Henrissat, B. 2009. The Carbohydrate-Active EnZymes database (CAZy): An expert resource for glycogenomics. Nucleic Acids Research 37:D233-D238.

Caracuel-Rios, Z., and Talbot, N.J. 2007. Cellular differentiation and host invasion by the rice blast fungus *Magnaporthe grisea*. Current Opinion in Microbiology 10:339-345.

Chain, P.S., Grafham, D.V., Fulton, R.S., Fitzgerald, M.G., Hostetler, J., Muzny, D., Ali, J., Birren, B., Bruce, D.C., Buhay, C., Cole, J.R., Ding, Y., Dugan, S., Field, D., Garrity, G.M., Gibbs, R., Graves, T., Han, C.S., Harrison, S.H., Highlander, S., Hugenholtz, P., Khouri, H.M., Kodira, C.D., Kolker, E., Kyrpides, N.C., Lang, D., Lapidus, A., Malfatti, S.A., Markowitz, V., Metha, T., Nelson, K.E., Parkhill, J., Pitluck, S., Qin, X., Read, T.D., Schmutz, J., Sozhamannan, S., Sterk, P., Strausberg, R.L., Sutton, G., Thomson, N.R., Tiedje, J.M., Weinstock, G., Wollam, A., and Detter, J.C. 2009. Genomics. Genome project standards in a new era of sequencing. Science 326:236-237.

Coleman, J.J., Rounsley, S.D., Rodriguez-Carres, M., Kuo, A., Wasmann, C.C., Grimwood, J., Schmutz, J., Taga, M., White, G.J., Zhou, S., Schwartz, D.C., Freitag, M., Ma, L.J., Danchin, E.G.J., Henrissat, B., Coutinho, P.M., Nelson, D.R., Straney, D., Napoli, C.A., Barker, B.M., Gribskov, M., Rep, M., Kroken, S., MolnÃ¡r, I., Rensing, C., Kennell, J.C., Zamora, J., Farman, M.L., Selker, E.U., Salamov, A., Shapiro, H., Pangilinan, J., Lindquist, E., Lamers, C., Grigoriev, I.V., Geiser, D.M., Covert, S.F., Temporini, E., and Vanetten, H.D. 2009. The genome of *Nectria haematococca*: Contribution of supernumerary chromosomes to gene expansion. PLoS Genetics 5: e1000618.

Cooley, R.N., and Caten, C.E. 1991. Variation in electrophoretic karyotype between strains of *Septoria nodorum*. Molecular and General Genetics 228:17-23.

Covert, S.F. 1998. Supernumerary chromosomes in filamentous fungi. Current Genetics 33:311-319.

Cuomo, C.A., Güldener, U., Xu, J-R., Trail, F., Turgeon, B.G., Di Pietro, A., Walton, J.D., Baker, S.E., Rep, M., Adam, G., Baldwin, T., Calvo, S., Chang, Y-L., DeCaprio, D., Gale, L., Gnerre, S., Goswami, R.S., Hammond-Kosack, K., Harris, L.J., Hilburn, K., Kennell, J., Kroken, S., Ma, L-J., Magnuson, J.K., Mannhaupt, G., Mauceli, E., Mewes, H-W., Mitterbauer, R., Muehlbauer, G., Münsterkotter, M., Nelson, D., O'Donnell, K., Ouellette, T., Qi, W., Quesneville, H., Roncero, M.T.G., Seong, K-Y., Tetko, I., Urban, M., Waalwijk, C., Ward, T., Yao, J., Birren, B.W., Kistler, H.C. 2006. The Fusarium genome reveals localized polymorphism and pathogen specialization. Science 317:1400-1402.

de Vries, R.P., Frisvad, J.C., van de Vondervoort, P.J.I., Burgers, K., Kuijpers, A.F.A., Samson, R.A., and Visser, J. 2005. *Aspergillus vadensis*, a new species of the group of black Aspergilli. Antonie van Leeuwenhoek, International Journal of General and Molecular Microbiology 87:195-203.

Dean, R.A., Talbot, N.J., Ebbole, D.J., Farman, M.L., Mitchell, T.K., Orbach, M.J., Thon, M., Kulkarni, R., Xu, J.R., Pan, H., Read, N.D., Lee, Y.I., Carbone, I., Brown, D., Yeon, Y.O., Donofrio, N., Jun, S.J., Soanes, D.M., Djonovic, S., Kolomlots, E., Rehmeyer, C., Li, W., Harding, M., Kim, S., Lebrun, M.H., Bohnert, H., Coughlan, S., Butler, J., Calvo, S., Ma, L.J., Nicol, R., Purcell, S., Nusbaum, C., Galagan, J.E., and Dirren, B.W. 2005. The genome sequence of the rice blast fungus *Magnaporthe grisea*. Nature 434:980-986.

Dhillon, B., Cavaletto, J.R., Wood, K.V., and Goodwin, S.B. 2010. Accidental amplification and inactivation of a methyltransferase gene eliminates cytosine methylation in *Mycosphaerella graminicola*. Genetics 186:67-77.

Duncan, K.E., and Howard, R.J. 2000. Cytological analysis of wheat infection by the leaf blotch pathogen *Mycosphaerella graminicola*. Mycology Research 104:1074-1082.

Eyal, Z., Scharen, A.L., Prescott, J.M., and van Ginkel, M. 1987. The Septoria Diseases of Wheat: Concepts and Methods of Disease Management. CIMMYT, Mexico.

Fedorova, N.D., Khaldi, N., Joardar, V.S., Maiti, R., Amedeo, P., Anderson, M.J., Crabtree, J., Silva, J.C., Badger, J.H., Albarraq, A., Angiuoli, S., Bussey, H., Bowyer, P., Cotty, P.J., Dyer, P.S., Egan, A., Galens, K., Fraser-Liggett, C.M., Haas, B.J., Inman, J.M., Kent, R., Lemieux, S., Malavazi, I., Orvis, J., Roemer, T., Ronning, C.M., Sundaram, J.P., Sutton, G., Turner, G., Venter, J.C., White, O.R., Whitty,

B.R., Youngman, P., Wolfe, K.H., Goldman, G.H., Wortman, J.R., Jiang, B., Denning, D.W., and Nierman, W.C. 2008. Genomic islands in the pathogenic filamentous fungus *Aspergillus fumigatus*. PLoS Genetics 4: e1000046.

Gardner, P.P., Daub, J., Tate, J.G., Nawrocki, E.P., Kolbe, D.L., Lindgreen, S., Wilkinson, A.C., Finn, R.D., Griffiths-Jones, S., Eddy, S.R., and Bateman, A. 2009. Rfam: Updates to the RNA families database. Nucleic Acids Research 37:D136-D140.

Giles, N.H., Geever, R.F., Asch, D.K., Avalos, J., and Case, M.E. 1991. The Wilhelmine E. Key 1989 invitational lecture. Organization and regulation of the qa (quinic acid) genes in *Neurospora crassa* and other fungi. Journal of Heredity 82:1-7.

Griffiths-Jones, S., Moxon, S., Marshall, M., Khanna, A., Eddy, S.R., and Bateman, A. 2005. Rfam: Annotating non-coding RNAs in complete genomes. Nucleic Acids Research 33:D121-D124.

Hane, J.K., Lowe, R.G.T., Solomon, P.S., Tan, K.C., Schoch, C.L., Spatafora, J.W., Crous, P.W., Kodira, C., Birren, B.W., Galagan, J.E., Torriani, S.F.F., McDonald, B.A., and Oliver, R.P. 2007. Dothideomycete-plant interactions illuminated by genome sequencing and EST analysis of the wheat pathogen *Stagonospora nodorum*. Plant Cell 19:3347-3368.

Hardwick, N.V., Jones, D.R., and Slough, J.E. 2001. Factors affecting diseases of winter wheat in England and Wales, 1989-98. Plant Pathology 50:453-462.

Hatta, R., Ito, K., Hosaki, Y., Tanaka, T., Tanaka, A., Yamamoto, M., Akimitsu, K., and Tsuge, T. 2002. A conditionally dispensable chromosome controls host-specific pathogenicity in the fungal plant pathogen *Alternaria alternata*. Genetics 161:59-70.

Housworth, E.A., and Postlethwait, J. 2002. Measures of synteny conservation between species pairs. Genetics 162:441-448.

James, T.Y., Kauff, F., Schoch, C.L., Matheny, P.B., Hofstetter, V., Cox, C.J., Celio, G., Gueidan, C., Fraker, E., Miadlikowska, J., Lumbsch, H.T., Rauhut, A., Reeb, V., Arnold, A.E., Amtoft, A., Stajich, J.E., Hosaka, K., Sung, G.H., Johnson, D., O'Rourke, B., Crockett, M., Binder, M., Curtis, J.M., Slot, J.C., Wang, Z., Wilson, A.W., Schüßler, A., Longcore, J.E., O'Donnell, K., Mozley-Standridge, S., Porter, D., Letcher, P.M., Powell, M.J., Taylor, J.W., White, M.M., Griffith, G.W., Davies, D.R., Humber, R.A., Morton, J.B., Sugiyama, J., Rossman, A.Y., Rogers, J.D., Pfister, D.H., Hewitt, D., Hansen, K., Hambleton, S., Shoemaker, R.A., Kohlmeyer, J., Volkmann-Kohlmeyer, B., Spotts, R.A., Serdani, M., Crous, P.W., Hughes, K.W., Matsuura, K., Langer, E., Langer, G., Untereiner, W.A., Lucking, R., Budel, B., Geiser, D.M., Aptroot, A., Diederich, P., Schmitt, I., Schultz, M., Yahr, R., Hibbett, D.S., Lutzoni, F., McLaughlin, D.J., Spatafora, J.W., and Vilgalys, R. 2006. Reconstructing the early evolution of Fungi using a six-gene phylogeny. Nature 443:818-822.

Jing, H.C., Lovell, D., Gutteridge, R., Jenk, D., Kornyukhin, D., Mitrofanova, O.P., Kema, G.H., and Hammond-Kosack, K.E. 2008. Phenotypic and genetic analysis of the Triticum monococcum-*Mycosphaerella graminicola* interaction. New Phytol 179:1121-1132.

Jones, R.N., Viegas, W., and Houben, A. 2008. A century of B chromosomes in plants: So what? Annals of Botany 101:767-775.

Kanehisa, M., Goto, S., Kawashima, S., Okuno, Y., and Hattori, M. 2004. The KEGG resource for deciphering the genome. Nucleic Acids Research 32:D277-D280.

Kay, S., Hahn, S., Marois, E., Hause, G., and Bonas, U. 2007. A bacterial effector acts as a plant transcription factor and induces a cell size regulator. Science 318:648-651.

Kema, G.H., van der Lee, T.A., Mendes, O., Verstappen, E.C., Lankhorst, R.K., Sandbrink, H., van der Burgt, A., Zwiers, L.H., Csukai, M., and Waalwijk, C. 2008. Large-scale gene discovery in the septoria tritici blotch fungus *Mycosphaerella graminicola* with a focus on *in planta* expression. Mol Plant Microbe Interact 21:1249-1260.

Kema, G.H.J., Yu, D., Rijkenberg, F.H.J., Shaw, M.W., and Baayen, R.P. 1996a. Histology of the pathogenesis of *Mycosphaerella graminicola* in wheat. Phytopathology 86:777-786.

Kema, G.H.J., Yu, D., Rijkenberg, F.H.J., Shaw, M.W., and Bayen, R.P. 1996b. Histology of the pathogenesis of *Mycosphaerella graminicola* in wheat. Phytopathology 86:777-786.

Keon, J., Antoniw, J., Carzaniga, R., Deller, S., Ward, J.L., Baker, J.M., Beale, M.H., Hammond-Kosack, K., and Rudd, J.J. 2007. Transcriptional adaptation of *Mycosphaerella graminicola* to programmed cell death (PCD) of its susceptible wheat host. Mol Plant Microbe Interact 20:178-193.

Koonin, E.V., Fedorova, N.D., Jackson, J.D., Jacobs, A.R., Krylov, D.M., Makarova, K.S., Mazumder, R., Mekhedov, S.L., Nikolskaya, A.N., Rao, B.S., Rogozin, I.B., Smirnov, S., Sorokin, A.V., Sverdlov, A.V., Vasudevan, S., Wolf, Y.I., Yin, J.J., and Natale, D.A. 2004. A comprehensive evolutionary classification of proteins encoded in complete eukaryotic genomes. Genome biology 5:R7.

Krzywinski, M., Schein, J., Birol, I., Connors, J., Gascoyne, R., Horsman, D., Jones, S.J., and Marra, M.A. 2009. Circos: An information aesthetic for comparative genomics. Genome Research 19:1639-1645.

Kurtz, S., Phillippy, A., Delcher, A.L., Smoot, M., Shumway, M., Antonescu, C., and Salzberg, S.L. 2004. Versatile and open software for comparing large genomes. Genome biology 5:R12.

Lee, H.C., Li, L., Gu, W., Xue, Z., Crosthwaite, S.K., Pertsemlidis, A., Lewis, Z.A., Freitag, M., Selker, E.U., Mello, C.C., and Liu, Y. 2010. Diverse pathways generate microRNA-like RNAs and Dicer-independent small interfering RNAs in fungi. Molecular cell 38:803-814.

Linde, C.C., Zhan, J., and McDonald, B.A. 2002. Population structure of *Mycosphaerella graminicola*: From lesions to continents. Phytopathology 92:946-955.

Ma, L.J., Van Der Does, H.C., Borkovich, K.A., Coleman, J.J., Daboussi, M.J., Di Pietro, A., Dufresne, M., Freitag, M., Grabherr, M., Henrissat, B., Houterman, P.M., Kang, S., Shim, W.B., Woloshuk, C., Xie, X., Xu, J.R., Antoniw, J., Baker, S.E., Bluhm, B.H., Breakspear, A., Brown, D.W., Butchko, R.A.E., Chapman, S., Coulson, R., Coutinho, P.M., Danchin, E.G.J., Diener, A., Gale, L.R., Gardiner, D.M., Goff, S., Hammond-Kosack, K.E., Hilburn, K., Hua-Van, A., Jonkers, W., Kazan, K., Kodira, C.D., Koehrsen, M., Kumar, L., Lee, Y.H., Li, L., Manners, J.M., Miranda-Saavedra, D., Mukherjee, M., Park, G., Park, J., Park, S.Y., Proctor, R.H., Regev, A., Ruiz-Roldan, M.C., Sain, D., Sakthikumar, S., Sykes, S., Schwartz, D.C., Turgeon, B.G., Wapinski, I., Yoder, O., Young, S., Zeng, Q., Zhou, S., Galagan, J., Cuomo, C.A., Kistler, H.C., and Rep, M. 2010. Comparative genomics reveals mobile pathogenicity chromosomes in Fusarium. Nature 464:367-373.

Martin, F., Kohler, A., Murat, C., Balestrini, R., Coutinho, P.M., Jaillon, O., Montanini, B., Morin, E., Noel, B., Percudani, R., Porcel, B., Rubini, A., Amicucci, A., Amselem, J., Anthouard, V., Arcioni, S., Artiguenave, F., Aury, J.M., Ballario, P., Bolchi, A., Brenna, A., Brun, A., Buée, M., Cantarel, B., Chevalier, G., Couloux, A., Da Silva, C., Denoeud, F., Duplessis, S., Ghignone, S., Hilselberger, B., Iotti, M., Marçais, B., Mello, A., Miranda, M., Pacioni, G., Quesneville, H., Riccioni, C., Ruotolo, R., Splivallo, R., Stocchi, V., Tisserant, E., Viscomi, A.R., Zambonelli, A., Zampieri, E., Henrissat, B., Lebrun, M.H., Paolocci, F., Bonfante, P., Ottonello, S., and Wincker, P. 2010. Perigord black truffle genome uncovers evolutionary origins and mechanisms of symbiosis. Nature 464:1033-1038.

Martin, F., Aerts, A., Ahrén ,D., Brun, A., Danchin, E.G.J., Duchaussoy, F., Gibon, J., Kohler, A., Lindquist, E., Pereda, V., Salamov, A., Shapiro, H.J., Wuyts, J., Blaudez, D., Buée, M., Brokstein, P., Canbäck, B., Cohen, D., Courty, P.E., Coutinho, P.M., Delaruelle, C., Detter, J.C., Deveau, A., DiFazio, S., Duplessis, S., Fraissinet-Tachet, L., Lucic, E., Frey-Klett, P., Fourrey, C., Feussner, I., Gay, G., Grimwood, J., Hoegger, P.J., Jain, P., Kilaru, S., Labbé, J., Lin, Y.C., Legué, V., Le Tacon, F., Marmeisse, R., Melayah, D., Montanini, B., Muratet, M., Nehls, U., Niculita-Hirzel, H., Secq, M.P.O.L., Peter, M., Quesneville, H., Rajashekar, B., Reich, M., Rouhier, N., Schmutz, J., Yin, T., Chalot, M., Henrissat, B., Kües, U., Lucas, S., Van De Peer, Y., Podila, G.K., Polle, A., Pukkila, P.J., Richardson, P.M., Rouzé, P., Sanders, I.R., Stajich, J.E., Tunlid, A., Tuskan, G., and Grigoriev, I.V. 2008. The genome of *Laccaria bicolor* provides insights into mycorrhizal symbiosis. Nature 452:88-92.

Masel, A.M., He, C., Poplawski, A.M., Irwin, J.A.G., and Manners, J.M. 1996. Molecular evidence for chromosome transfer between biotypes of *Colletotrichum gloeosporioides*. Molecular Plant-Microbe Interactions 9:339-348.

McDougall, P. 2006. Phillips McDougall Agriservice Report (Pathhead, Midlothian, Scotland, UK).

Miao, V.P., Covert, S.F., and VanEtten, H.D. 1991. A fungal gene for antibiotic resistance on a dispensable ('B') chromosome. Science 254:1773-1776.

Nierman, W.C., Pain, A., Anderson, M.J., Wortman, J.R., Kim, H.S., Arroyo, J., Berriman, M., Abe, K., Archer, D.B., Bermejo, C., Bennett, J., Bowyer, P., Chen, D., Collins, M., Coulsen, R., Davies, R., Dyer, P.S., Farman, M., Fedorova, N., Fedorova, N., Feldblyum, T.V., Fischer, R., Fosker, N., Fraser, A., García, J.L., García M.J., Goble, A., Goldman, G.H., Gomi, K., Griffith-Jones, S., Gwilliam, R., Haas, B., Haas, H., Harris, D., Horiuchi, H., Huang, J., Humphray, S., Jiménez, J., Keller, N., Khouri, H., Kitamoto, K., Kobayashi, T., Konzack, S., Kulkarni, R., Kumagai, T., Lafton, A., Latgé, J.P., Li, W., Lord, A., Lu, C., Majoros, W.H., May, G.S., Miller, B.L., Mohamoud, Y., Molina, M., Monod, M., Mouyna, I., Mulligan, S., Murphy, L., O'Neil, S., Paulsen, I., Peñalva, M.A., Pertea, M., Price, C., Pritchard, B.L., Quail, M.A., Rabbinowitsch, E., Rawlins, N., Rajandream, M.A., Reichard, U., Renauld, H., Robson, G.D., Rodriguez De Cordoba, S., Rodríguez-Peña, J.M., Ronning, C.M., Rutter, S., Salzberg, S.L., Sanchez, M., Sánchez-Ferrero, J.C., Saunders, D., Seeger, K., Squares, R., Squares, S., Takeuchi, M., Tekaia, F., Turner, G., Vazquez De Aldana, C.R., Weidman, J., White, O., Woodward, J., Yu, J.H., Fraser, C., Galagan, J.E., Asai, K., Machida, M., Hall, N., Barrell, B., and Denning, D.W. 2005. Genomic sequence of the pathogenic and allergenic filamentous fungus *Aspergillus fumigatus.* Nature 438:1151-1156.

Salamov, A.A., and Solovyev, V.V. 2000. Ab initio gene finding in Drosophila genomic DNA. Genome Research 10:516-522.

Selker, E.U. 2002. Repeat-induced gene silencing in fungi. Adv Genet 46:439-450.

Stukenbrock, E.H., Banke, S., Javan-Nikkhah, M., and McDonald, B.A. 2007. Origin and domestication of the fungal wheat pathogen *Mycosphaerella graminicola* via sympatric speciation. Molecular Biology and Evolution 24:398-411.

Stukenbrock, E.H., Jørgensen, F.G., Zala, M., Hansen, T.T., McDonald, B.A., and Schierup, M.H. 2010. Whole-genome and chromosome evolution associated with host adaptation and speciation of the wheat pathogen *Mycosphaerella graminicola.* PLoS genetics 6: e1001189.

Tatusov, R.L., Fedorova, N.D., Jackson, J.D., Jacobs, A.R., Kiryutin, B., Koonin, E.V., Krylov, D.M., Mazumder, R., Smirnov, S., Nikolskaya, A.N., Rao, B.S., Mekhedov, S.L., Sverlov, A.V., Vasudevan, S., Wolf, Y.I., Yin, J.J., and Natale, D.A. 2003. The COG database: An updated vesion includes eukaryotes. BMC Bioinformatics 4:41.

Torriani, S.F.F., Goodwin, S.B., Kema, G.H.J., Pangilinan, J.L., and McDonald, B.A. 2008. Intraspecific comparison and annotation of two complete mitochondrial genome sequences from the plant pathogenic fungus *Mycosphaerella graminicola*. Fungal Genetics and Biology 45:628-637.

Wang, C., Skrobek, A., and Butt, T.M. 2003. Concurrence of losing a chromosome and the ability to produce destruxins in a mutant of *Metarhizium anisopliae*. FEMS Microbiology Letters 226:373-378.

Ware, S.B. 2006. Aspects of sexual reproduction in Mycosphaerella species on wheat and barley: Genetic studies on specificity, mapping, and fungicide resistance: Genetic studies on specificity, mapping and fungicide resistance. Wageningen University, The Netherlands: Ph.D. thesis.

Wittenberg, A.H.J., van der Lee, T.A.J., M'Barek, S.B., Ware, S.B., Goodwin, S.B., Kilian, A., Visser, R.G.F., Kema, G.H.J., and Schouten, H.J. 2009. Meiosis drives extraordinary genome plasticity in the haploid fungal plant pathogen *Mycosphaerella graminicola*. PLoS ONE 4: e5863.

Yun, S.H., Arie, T., Kaneko, I., Yoder, O.C., and Turgeon, B.G. 2000. Molecular organization of mating type loci in heterothallic, homothallic, and asexual Gibberella/Fusarium species. Fungal Genetics and Biology 31:7-20.

Zdobnov, E.M., and Apweiler, R. 2001. InterProScan - An integration platform for the signature-recognition methods in InterPro. Bioinformatics 17:847-848.

SUPPLEMENTAL DATA

Supplementary Information S1. The method and calculations for using mesosynteny to predict scaffold joins from version 1 to version 2 of the *Mycosphaerella graminicola* genomic sequence.

Dataset S1.

http://www.plosgenetics.org/article/info%3Adoi%2F10.1371%2Fjournal.pgen.1002070#s5

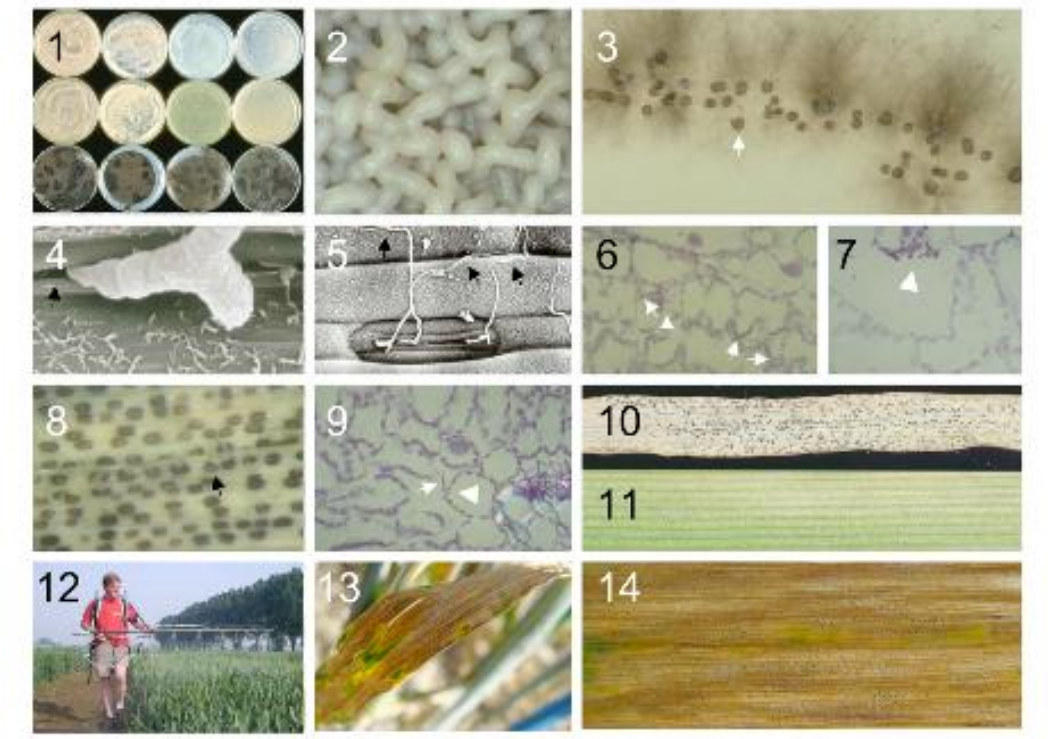

Fig. S1. Aspects of the *in vitro* and *in vivo* lifestyle of *Mycosphaerella graminicola*. **1**. Typical colony appearance of *M. graminicola* isolates grown under light (upper two rows) and dark (lower low) conditions. Light stimulates yeast-like growth whereas darkness induces filamentous growth. **2**. Close-up of yeast-like growth on V8 agar. **3**. *In vitro* production of asexual fructifications (pycnidia; arrow) on wheat leaf extract agar. **4**. Penetration of a wheat leaf stoma (arrow) by a pycnidiospore germ tube. **5**. Simultaneous penetration of a wheat leaf stoma by three germ tubes of sexual airborne ascospores (arrows) that are transported over vast distances. **6**. Colonization of the mesophyll tissue by an intercellular hypha (arrows) during the symptomless biotrophic phase of pathogenesis. **7**. Initiation (arrow head) of a pycnidium in the substomatal cavity of a wheat leaf. **8**. Ripe pycnidia in a primary leaf of a susceptible wheat seedling. High humidity stimulates the extrusion of cyrrhi, tendril-like mucilages containing asexual pycnidiospores that are rain-splash dispersed over short distances. **9**. Typical infection of the primary leaf of a resistant cultivar. Note the low fungal density in the apoplast (arrow) and the response of the mesophyll cells (arrow head), particularly the chloroplasts, to the presence of intercellular hyphae. **10**. Typical symptoms on a primary seedling leaf of a highly susceptible wheat cultivar. **11**. Typical response on a primary leaf of a highly resistant wheat cultivar. **12**. Adult-plant evaluation plots are inoculated at the adult plant stage with individual isolates using air-driven equipment. **13**. Symptoms on an adult plant flag leaf after field inoculations. **14**. Symptoms on a naturally infected adult plant flag leaf.

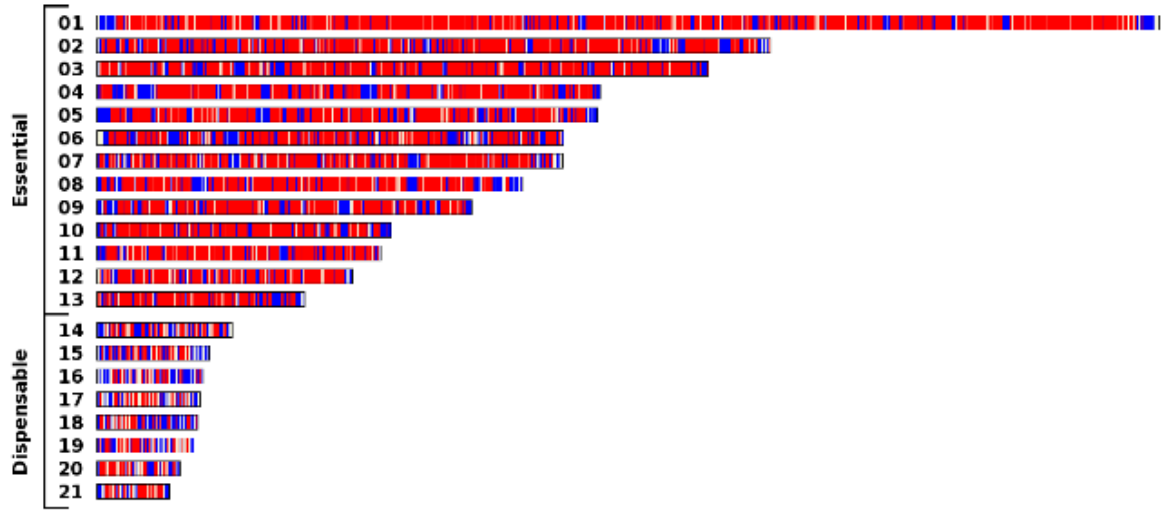

Fig. S2. The 21 chromosomes of the *Mycosphaerella graminicola* genome drawn to scale**.** Red indicates regions of single-copy sequence; repetitive sequences are in shown blue. Chromosome 1 is almost twice as long as any of the others. The core chromosomes 1-13 are the largest. Dispensable chromosomes 14-21 are smaller than the core chromosomes and have a higher proportion of repetitive DNA as indicated by the blue bands.

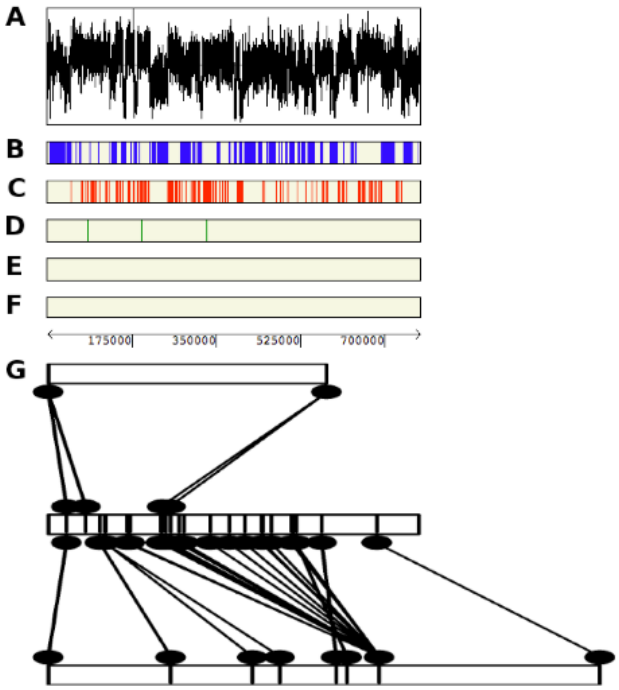

Fig. S3. Features of chromosome 14, the largest dispensable chromosome of *Mycosphaerella graminicola*, and alignment to genetic linkage maps. **A.** Plot of GC content. Areas of low GC usually correspond to regions of repetitive DNA. **B.**Repetitive regions of the *M. graminicola* genome. **C.** Single-copy (red) regions of the *M. graminicola* genome. **D.** Locations of genes for proteins containing signal peptides. **E.** Locations of homologs of pathogenicity or virulence genes that have been experimentally verified in species pathogenic to plant, animal or human hosts. **F.** Approximate locations of quantitative trait loci (QTL) for pathogenicity to wheat. **G.** Alignments between the genomic sequence and two genetic linkage maps of crosses involving isolate IPO323. Top half, Genetic linkage map of the cross between IPO323 and the Algerian durum wheat isolate IPO95052. Bottom half, Genetic linkage map of the cross between bread wheat isolates IPO323 and IPO94269. The physical map represented by the genomic sequence is in the center. Lines connect mapped genetic markers in each linkage map to their corresponding locations on the physical map based on the sequences of the marker loci. Very few secreted proteins (track **D**) or pathogenicity-related genes (**E**) and no pathogenicity QTL mapped to the dispensome.

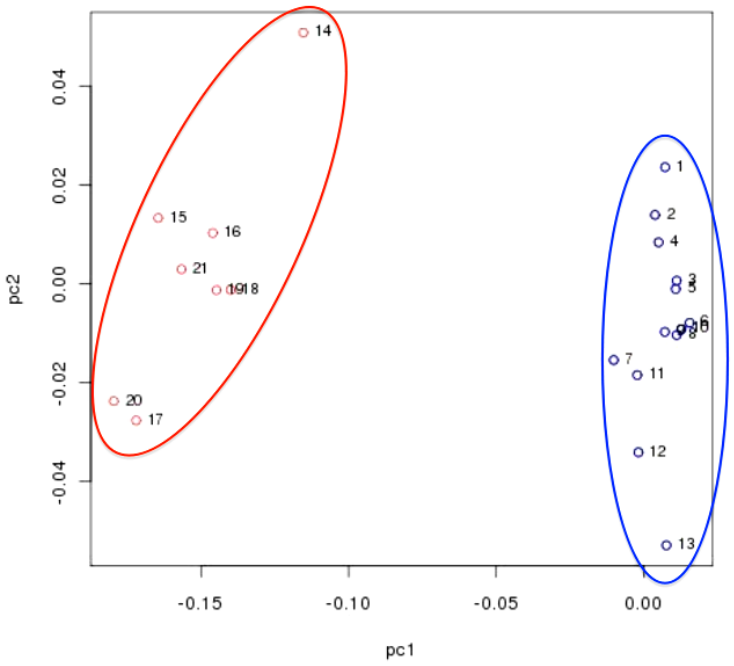

Fig. S4. Principal Component Analysis of codon usage in 21 chromosomes of the *Mycosphaerella graminicola* finished genome**.** Factor 1 gave good discrimination between core (blue circles) and dispensable (red) chromosomes.

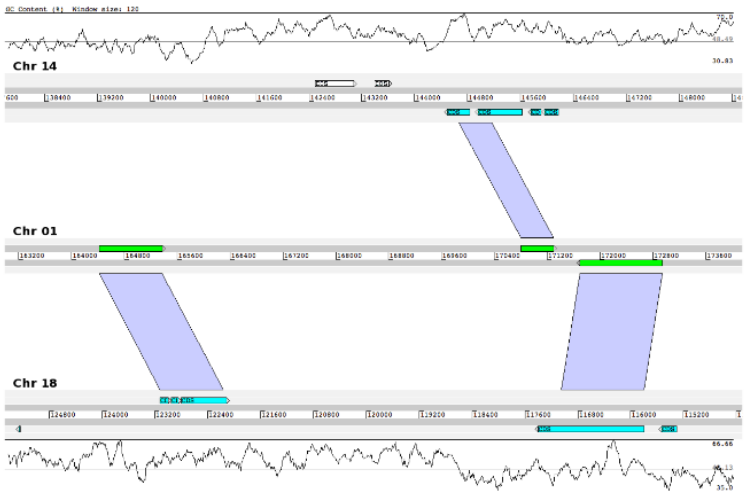

Fig. S5. Examples of unique genes on dispensable chromosomes with an inactivated copy on a core chromosome. A unique gene on chromosome 14 and two on chromosome 18 showed excellent alignments to footprints of genes on chromosome 1. The copies on chromosome 1 matched those on the dispensable chromosomes with an expected value of 1 x 10^{-5} or better, but contained numerous stop codons indicating that they were pseudogenes and possibly could have been the progenitor copies for the intact, unique genes on dispensable chromosomes 14 and 18. The graphs above chromosome 14 and below chromosome 18 indicate GC content.

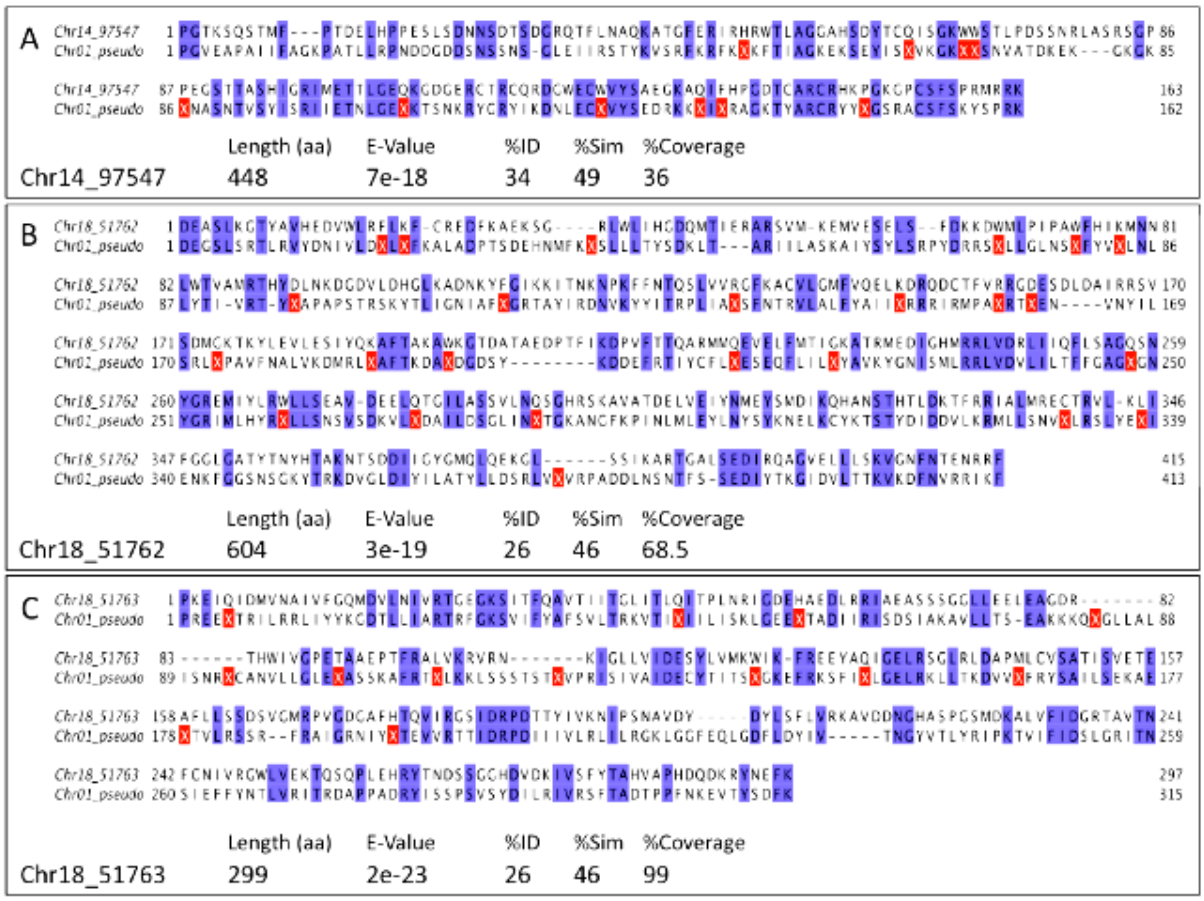

Fig. S6. Examples of amino acid alignments between protein sequences of unique genes on dispensable chromosomes to their inactivated putative homologs on core chromosomes. **A.** A unique gene on dispensable chromosome 14 aligned to a footprint of its homologous pseudogene on core chromosome 1. **B** and **C.** Alignments between two genes on dispensable chromosome 18 to homologous pseudogenes on core chromosome 1. Identical amino acids are shaded blue. Stop codons in pseudogenes are indicated by X and are shaded red. Details are provided beneath each alignment. Each unique gene is at least 26% identical and 46% similar to its putative homolog.

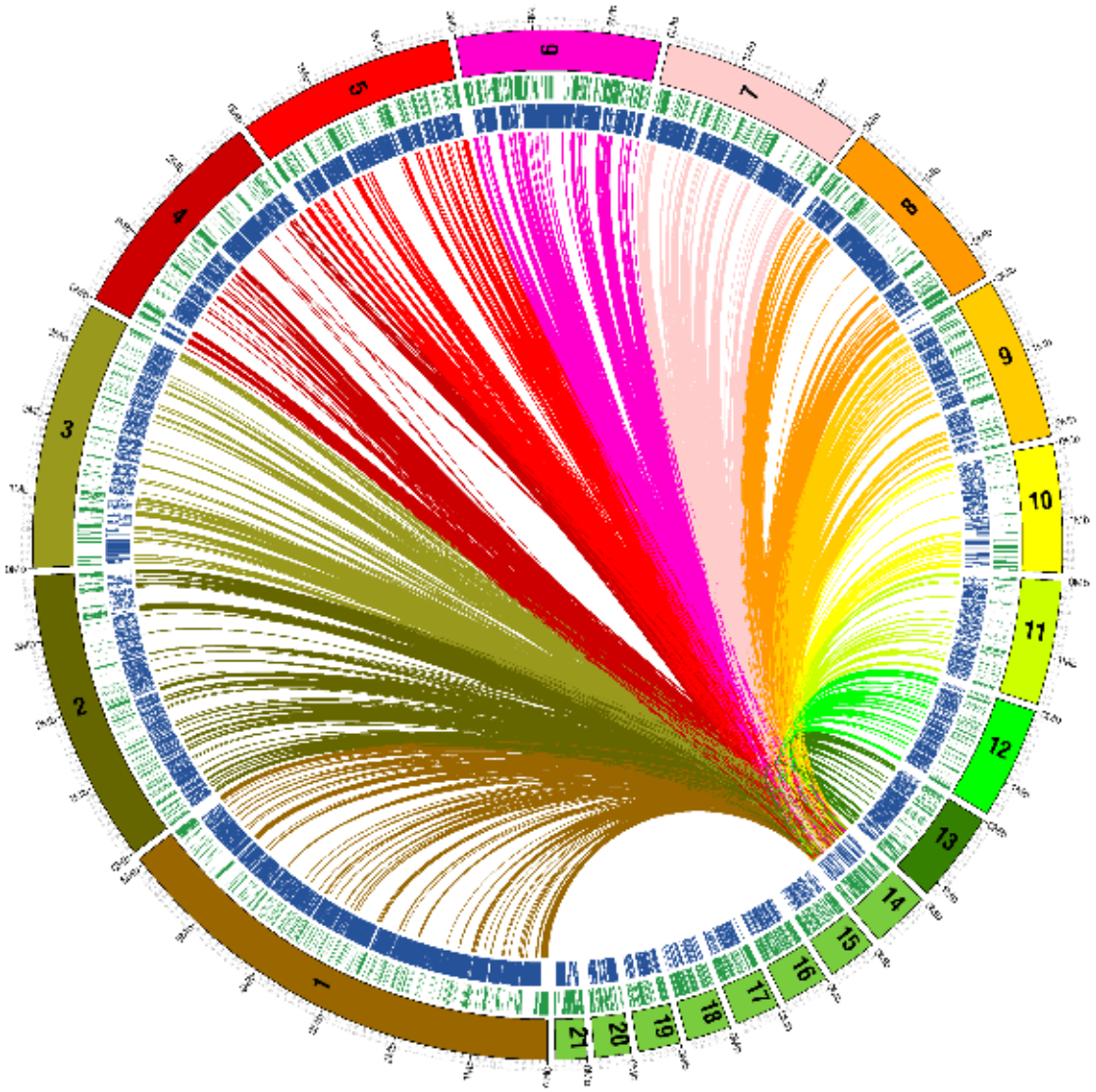

Fig. S7. Analysis of genes and repetitive DNAs that are shared between dispensable chromosome 14 and the 13 core chromosomes of *Mycosphaerella graminicola*. Each chromosome is drawn to scale as a numbered bar around the outer edge of the circle. Lines connect regions of 100 bp or larger that are similar between each core chromosome and the corresponding region on chromosome 14 at $1 \times e^{-5}$ or lower. Chromosome 14 contains parts of all of the core chromosomes that are mixed in together with no synteny. Genes on the other dispensable chromosomes were not included in this analysis.

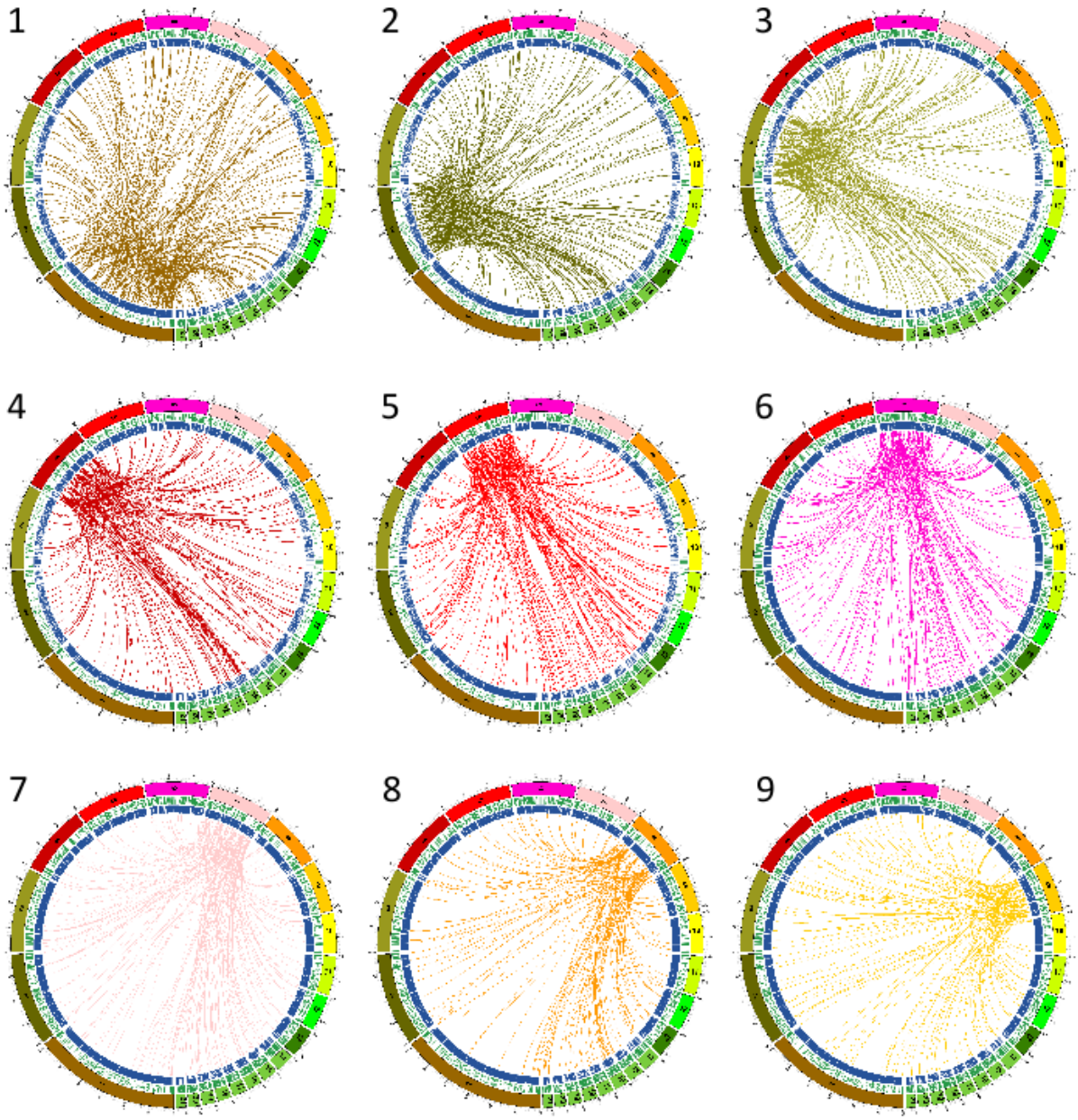

Fig. S8. Analysis of genes that are shared between each of the nine largest core chromosomes (1-9) and all other chromosomes of the *Mycosphaerella graminicola* genome**.** Each chromosome is drawn to scale as a numbered bar around the outer edge of the circle. Lines connect regions of 100 bp or larger that are similar between the indicated core chromosome and each of the remaining 20 chromosomes at $1 \times e^{-5}$ or lower. Each chromosome contains parts of all of the other chromosomes mixed in together with no synteny. Genes on the 12 smallest chromosomes were similar but are not shown.

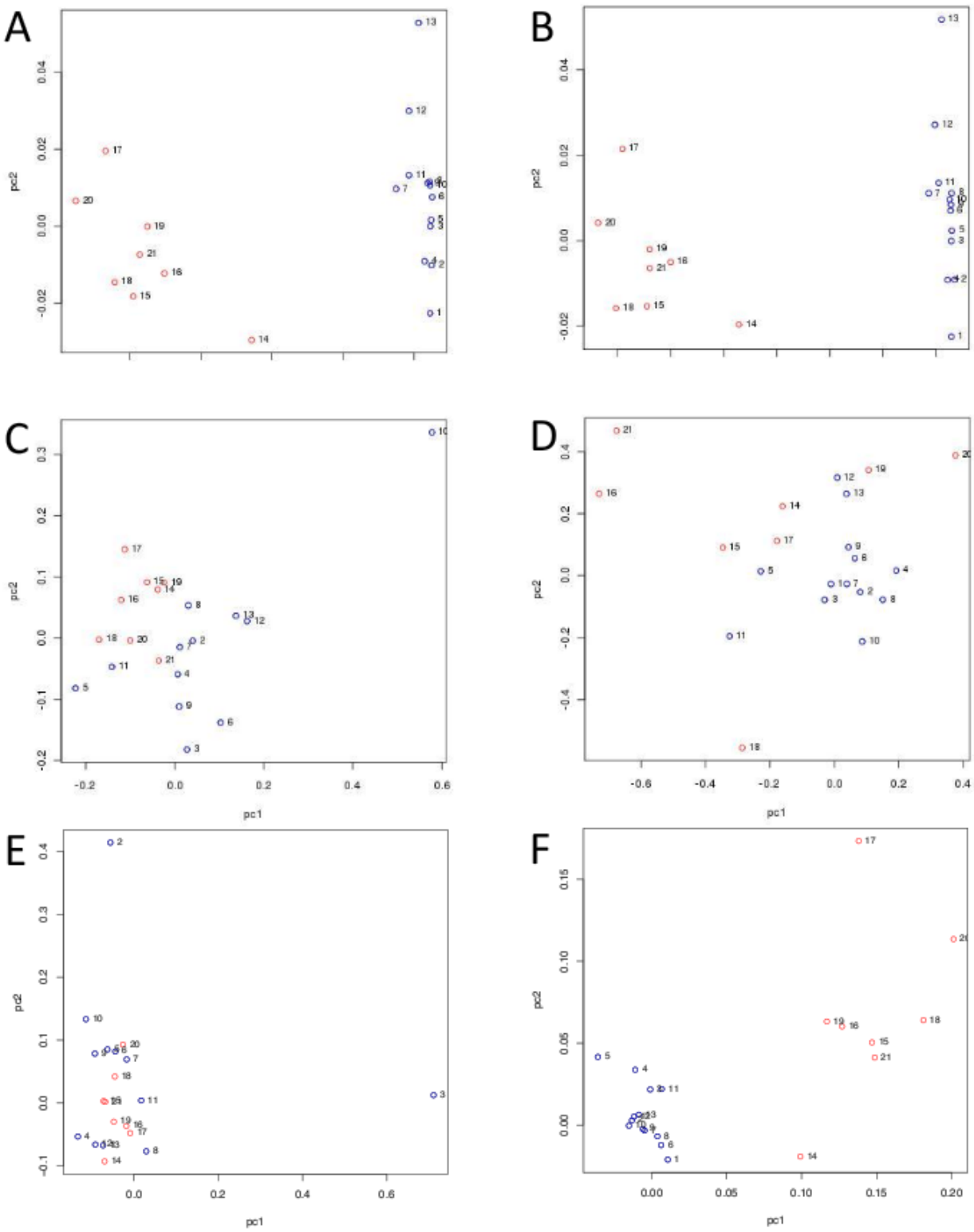

Fig. S9. Principal Component Analysis of codon usage. **A.** in 21 chromosomes of the *Mycosphaerella graminicola* finished genome after simulated RIPping. **B.** in 21 chromosomes of the *M. graminicola* finished genome after simulated deRIPping. **C.** of about 150 genes with shared putative homologs between the core and dispensable chromosomes of *M. graminicola*. **D.** of amino acid composition of about 150 genes with shared putative homologs between the core and dispensable chromosomes of *M. graminicola*. **E.** of all genes with shared putative homologs between the core and dispensable chromosomes of *M. graminicola*. **F.** of all genes on dispensable chromosomes with shared putative homologs on core chromosomes against all genes on the core chromosomes of *M. graminicola*.

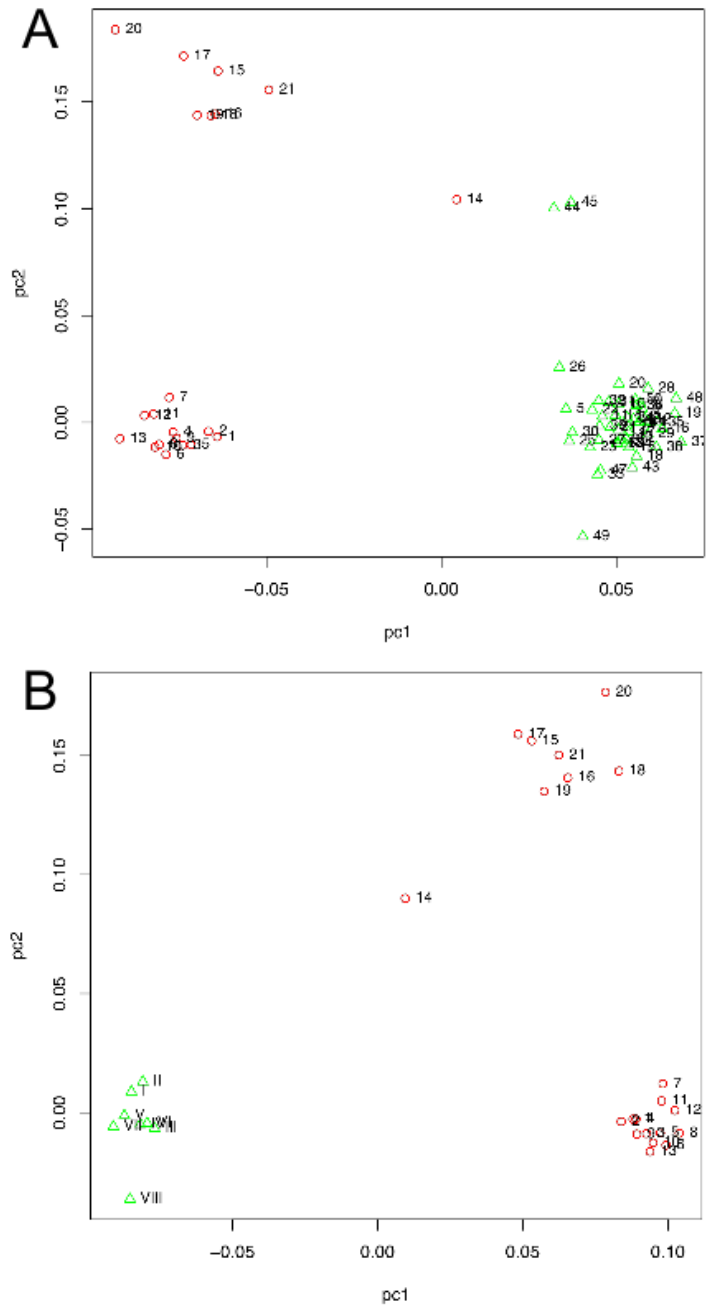

Fig. S10. Principal Component Analysis of codon usage. **A.** between the genomes of *M. graminicola* and *Stagonospora nodorum*. **B.** between the genomes of *M. graminicola* and *Aspergillus fumigatus*. Values for the chromosomes of *M. graminicola* are indicated by red circles, those for *S. nodorum* and *A. fumigatus* by green triangles.

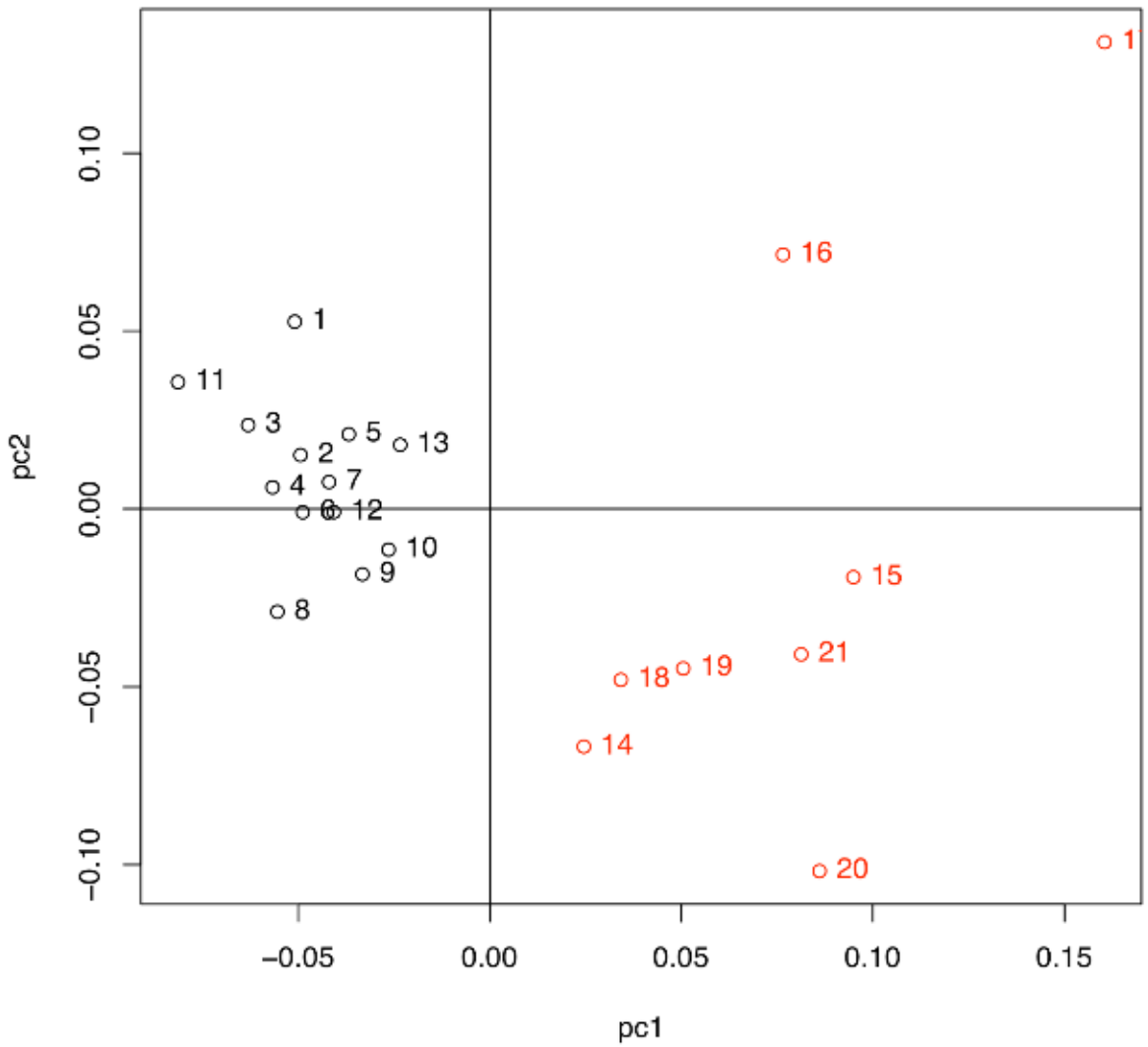

Fig. S11. Principal Component Analysis of repeats in 21 chromosomes of the *Mycosphaerella graminicola* finished genome. Core chromosomes (black circles) were clearly separated from the dispensome (red).

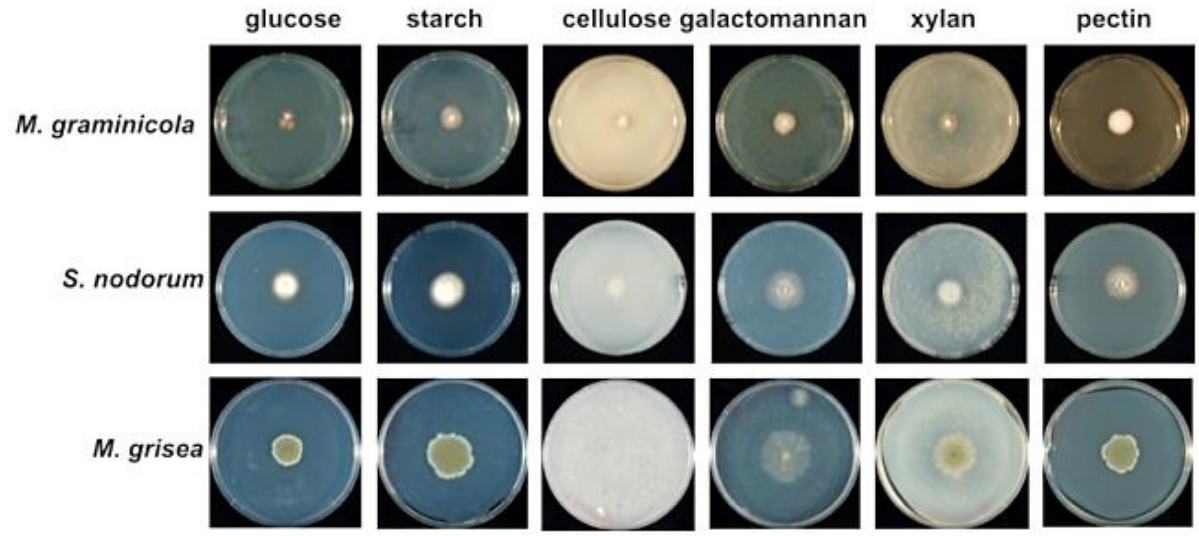

Fig. S12. Growth of *Mycosphaerella graminicola*, *Stagonospora nodorum* and *Magnaporthe oryzae* (*M. grisea*) on glucose and several plant polysaccharides. Growth of *M. graminicola* was decreased on xylan, consistent with the CAZy annotation for fewer genes involved in degradation of that substrate.

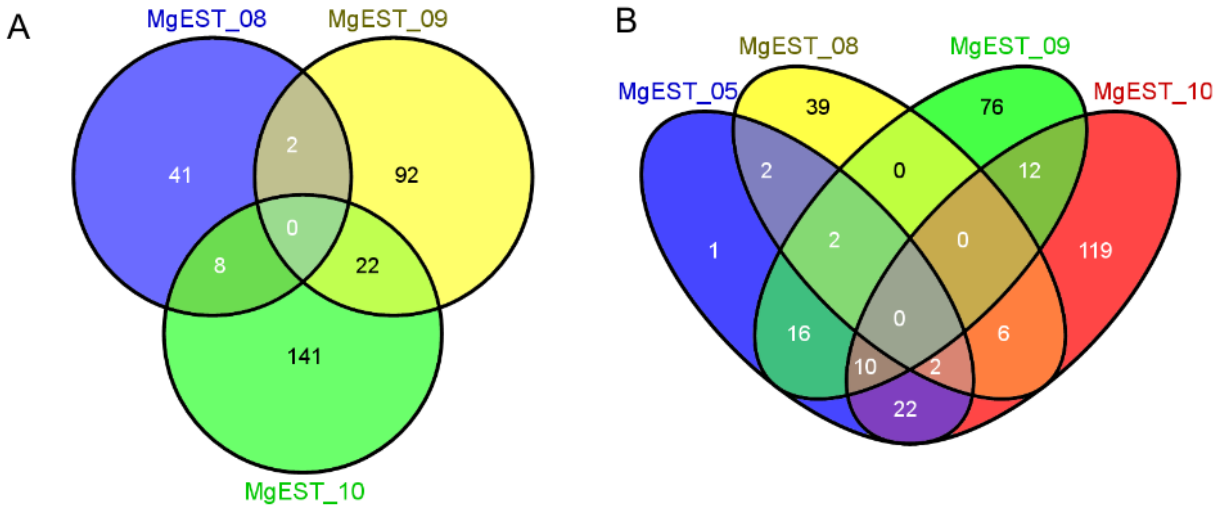

Fig. S13. Venn diagrams showing the expression of *Mycosphaerella graminicola* genes at different times during the infection process and with a sample grown *in vitro*. **A.** Libraries MgEST_08, MgEST_09, and MgEST_10 contain EST sequences from wheat leaf tissue collected at 5, 10 and 16 days after inoculation, respectively. **B.** four-way diagram with the same three in vitro-produced libraries plus *in vitro* library MgEST_05, grown on minimal medium minus nitrogen to mimic the early stages of the infection process.

Table S1. List of functional domains or other annotations for 65 genes on dispensable chromosomes 14-21 of the genome of *Mycosphaerella graminicola.*

Location	Protein ID number[a]	Annotation/domain information
Chromosome 14	30708	Protein kinase
	51580	Kinesin, motor region
	51592	Zn-finger, RING
	51612	Allergen V5/Tpx-1 related
	51613	BTB/POZ
	51638	Amidase
	51659 [b]	Tyrosine protein kinase, active site
	51681	3'-5' exonuclease
	78038	C4-dicarboxylate transporter/malic acid transport protein
	88520	Bile acid:sodium symporter
	88521	Rhodanese-like
	97533	Zn-finger, C2H2 type
	97547 [b]	ATP-dependent DNA ligase
	97549	BPD_TRANSP_INN_MEMBR
	97573 [b]	Transcription factor, MADS-box
	97575	Tyrosine protein kinase, active site
	97582	Cof protein
	97584 [b]	Cyclin-like F-box
	97585	Fungal transcriptional regulatory protein, N-terminal
	97592	Fungal transcriptional regulatory protein, N-terminal
	97613	Cytochrome c heme-binding site
	101931	Camphor resistance CrcB protein
	106589 [b]	Forkhead-associated
	111731	N-6 Adenine-specific DNA methylase
	111740	ATP-dependent helicase, DEAD-box
Chromosome 15	51695	Beta tubulin
	97626	Alpha tubulin
	97640	CRYSTALLIN_BETAGAMMA
	97646	Cupin region
	97668 [b]	Helix-turn-helix, Fis-type
	97675	Ferritin/ribonucleotide reductase-like
Chromosome 16	97702	Peptidase A4, scytalidopepsin B
	97707	R3H domain
	97717	Peptidase S8 and S53, subtilisin, kexin, sedolisin
	97741	dsRNA-binding domain-like
	106635 [b]	Homeobox
Chromosome 17	51731	Prefoldin
	51740	Heat shock protein Hsp20
	97780	Peptidase C48, SUMO/Sentrin/Ubl1
	97790 [b]	Glycoside hydrolase, family 11
	97837	Shugoshin, N terminal
	106639	Zn-finger, C2H2 type
Chromosome 18	19703	HAT dimerisation
	30482	Serine/threonine protein kinase
	51763 [b]	DEAD/DEAH box helicase, N-terminal
	97851 [b]	Ankyrin
	97867 [b]	TonB box, N-terminal
	97908	DHH phosphoesterase
	111781 [b]	Calcium-binding EF-hand
Chromosome 19	27948	BTB/POZ
	31017	Chaperonin Cpn60/TCP-1
	97915 [b]	Myb, DNA-binding
	97929	Carbonic anhydrase, prokaryotic and plant

	97931 [b]	Thaumatin, pathogenesis-related
	97943	H+-transporting two-sector ATPase, alpha/beta subunit, central region
	97953 [b]	Eukaryotic RNA polymerase II heptapeptide repeat
	111792	Arthropod hemocyanin/insect LSP
Chromosome 20	98020 [b]	TonB box, N-terminal
	98042	Helix-turn-helix, Fis-type
	98050 [b]	Inorganic pyrophosphatase
	111795	Cytochrome c heme-binding site
Chromosome 21	51798	Tubulin/FtsZ, GTPase
	98073	Asp/Glu racemase
	98102[b]	Regulator of chromosome condensation, RCC1
	98110	Kinesin, motor region

[a] Protein IDs are from the *M. graminicola* gene catalog in the database of the Joint Genome Institute. The genome sequence and annotations are available from the JGI web portal at http://www.jgi.doe.gov/Mgraminicola.
[b] These genes are unique to the dispensable chromosomes.

Table S2. Analysis of small RNA sequences (generated on the Illumina platform) for the presence of computationally predicted pre-microRNA-like (milRNA) sequences in germinated spores of *Mycosphaerella graminicola* isolate IPO323.

Small-RNA library[a]	Trimmed reads[b]	Average length (nt)	Number[c]			
			>1	>10	>100	>1000
Germinated spores	5.926.175	26.1	220	65	26	2[d]

[a] RNA was isolated with standard procedures and the small RNAs were isolated with the Illumina small RNA kit and sequenced using standard procedures.
[b] The number remaining after quality control and removal of adapter sequences.
[c] The total number of the 385 predicted non-redundant pre-milRNA sequences with the indicated number of perfect hits (i.e., no mismatches were allowed over the full length of the RNA read) in the RNA data set using Blast.
[d] The two predicted pre-milRNA sequences with more than a thousand perfect hits in the small-RNA data occurred 7342 and 4134 times.

Table S3. Best non-self BLAST hits for 654 called genes on dispensable chromosomes of *Mycosphaerella graminicola* queried with *tblastn* against a combined database containing the GenBank nt and EST datasets plus *M. graminicola* version 2.0 and *M. fijiensis* v1.0 from the Joint Genome Institute.

Genus or type	Class	Order	Number
No hits	Not applicable	Not applicable	225
M. graminicola GenBank	Dothideomycetes	Capnodiales	140
M. graminicola JGI D chromosome	Dothideomycetes	Capnodiales	136
M. graminicola JGI core chromosome	Dothideomycetes	Capnodiales	86
M. fijiensis	Dothideomycetes	Capnodiales	13
Animal	Not applicable	Not applicable	8
Ajellomyces	Eurotiomycetes	Onygenales	7
Aspergillus	Eurotiomycetes	Eurotiales	6
Penicillium	Eurotiomycetes	Eurotiales	5
Phaeosphaeria	Dothideomycetes	Pleosporales	5
Cercospora	Dothideomycetes	Capnodiales	3
Coccidioides	Eurotiomycetes	Onygenales	3
Geomyces	Eurotiomycetes	Onygenales	2
Pyrenophora	Dothideomycetes	Pleosporales	2
Botryotinia	Leotiomycetes	Helotiales	2
Talaromyces	Eurotiomycetes	Eurotiales	1

Trichoderma	Sordariomycetes	Hypocreales	1
Uncinocarpus	Eurotiomycetes	Onygenales	1
Grosmannia	Sordariomycetes	Ophiostomatales	1
Neurospora	Sordariomycetes	Sordariales	1
Cordyceps	Sordariomycetes	Hypocreales	1
Pichia	Saccharomycetes	Saccharomycetales	1
Claviceps	Sordariomycetes	Hypocreales	1
Neosartorya	Eurotiomycetes	Eurotiales	1
Podospora	Sordariomycetes	Sordariales	1
Candida	Saccharomycetes	Saccharomycetales	1
Sclerotinia	Leotiomycetes	Helotiales	1
Chaetomium	Sordariomycetes	Sordariales	1

Table S4. Numbers of predicted enzymes degrading hemicellulose, pectin and cutin across seven ascomycete species with sequenced genomes.

	Saprophytes[a]			Pathogens[a]				
CAZy family[b]	**An**	**Nc**	**Tr**	**Fg**	**Mg**	**Mo**	**Sn**	**Plant cell wall target**
GH5 mannosidases[c]	6	1	1	2	0	2	2	Hemicellulose
GH26	3	1	0	0	0	0	0	Hemicellulose
GH62	2	0	1	1	1	3	3	Hemicellulose
GH67	1	1	1	1	0	1	1	Hemicellulose
GH10	3	4	1	5	2	5	7	Hemicellulose
GH11	2	2	4	3	1	5	7	Hemicellulose
GH115	1	1	1	2	1	0	2	Hemicellulose
Total hemicellulases	18	10	9	14	5	16	22	Hemicellulose
GH28	9	2	4	6	2	3	4	Pectin
GH78	8	0	1	7	2	1	4	Pectin
GH88	2	0	0	1	0	1	1	Pectin
GH105	3	1	1	3	2	3	3	Pectin
PL1	8	1	0	9	2	2	4	Pectin
PL3	5	1	0	7	1	1	2	Pectin
PL4	4	1	0	3	0	1	4	Pectin
PL9	0	0	0	1	0	0	0	Pectin
PL11	1	0	0	0	0	0	0	Pectin
CE8	3	1	0	6	1	1	6	Pectin
CE12	2	1	0	3	0	2	3	Pectin
Total pectinases	45	8	6	46	10	15	31	Pectin
GH43	15	7	2	17	10	19	15	Pectin & hemicellulose
GH51	2	1	0	2	3	3	2	Pectin & hemicellulose
GH53	1	1	0	1	2	1	1	Pectin & hemicellulose
GH54	1	1	2	1	1	1	1	Pectin & hemicellulose
GH93	2	2	0	2	1	1	3	Pectin & hemicellulose
Total pectinases & hemicellulases	21	12	4	23	17	25	22	Pectin & hemicellulose
CE5	4	3	4	12	6	17	11	Cutin
Overall total including cellulases (Table 3)	117	78	50	133	43	128	148	All cell wall substrates

[a] Species analyzed included the saprophytes *Aspergillus nidulans* (An), *Neurospora crassa* (Nc), and *Trichoderma reesii* (Tr), and the plant pathogens *Fusarium graminearum* (Fg), *Mycosphaerella graminicola* (Mg), *Magnaporthe oryzae* (Mo), and *Stagonospora nodorum* (Sn).

[b] Families defined in the Carbohydrate-active enzymes database (www.cazy.org).

[c] GH5 is a family containing many different enzyme activities; only those targeting the stated substrate are included

Table S5. Total numbers of predicted CAZymes in *Mycosphaerella graminicola* and selected ascomycetes.

Species	GH	GT	PL	CE	CBM	EXPN
Mycosphaerella graminicola	184	97	3	20	20	3
Trichoderma reesei	192	93	6	17	48	4
Fusarium graminearum	247	102	21	44	67	4
Neurospora crassa	173	76	4	22	42	1
Magnaporthe grisea	232	92	5	47	65	1
Aspergillus nidulans	251	91	21	31	41	1
Stagonospora nodorum	284	92	10	57	74	4

GH = glycoside hydrolases; GT = glycosyl transferases; PL = polysaccharide lyases; CE =carbohydrate esterases; CBM = carbohydrate binding modules; EXPN = distantly related to plant expansins.
Predicted CAZymes were identified using the carbohydrate-active enzymes database tools (www.cazy.org).

Table S6. PFAM domains that are expanded in the genome of *Mycosphaerella graminicola* relative to those of five other Ascomycetes[a] and two plant-pathogenic Stramenopiles[b].

Name	Mgram	Snod	Fgram	Moryz	Trees	Ncra	Pram	Psoj	Domain function
PF01432	16	2	4	2	2	2	3	3	Peptidase_M3
PF00128	13	5	7	9	4	9	2	1	Alpha-amylase
PF01070	12	8	10	6	6	3	2	1	FMN_dh
PF05577	10	4	2	6	3	2	5	5	Peptidase_S28
PF09286	10	6	3	5	5	3	2	2	Pro-kuma_activ
PF00180	9	7	8	7	7	5	3	2	Iso_dh
PF03061	9	4	5	6	6	5	4	3	4HBT
PF04193	8	7	7	5	5	6	4	1	PQ-loop
PF00320	8	6	7	7	6	6	0	0	GATA
PF02714	7	6	4	4	5	5	2	3	DUF221
PF00682	6	4	4	5	4	4	3	3	HMGL-like
PF06747	6	5	3	3	3	4	4	2	CHCH
PF00250	6	4	4	3	4	3	0	0	Fork_head
PF01501	6	5	5	2	2	2	1	1	Glyco_transf_8
PF00206	5	4	3	3	3	3	3	3	Lyase_1
PF00130	5	2	3	2	2	2	2	2	C1_1
PF03476	4	2	3	2	2	2	2	2	MOSC_N
PF00686	4	3	2	3	1	2	0	0	CBM_20
PF03055	4	3	2	3	1	1	0	0	RPE65
PF05875	3	2	2	1	2	1	2	1	aPHC
PF04303	3	2	2	2	1	0	0	0	DUF453
PF01645	3	1	1	1	1	1	1	1	Glu_synthase
PF08760	3	2	0	2	1	2	0	0	DUF1793
PF06964	3	1	2	2	0	1	0	0	Alpha-L-AF_C
PF08323	3	0	0	1	0	2	0	0	Glyco_transf_5
PF09260	3	0	0	1	0	2	0	0	DUF1966
PF00692	2	1	1	1	1	1	1	1	dUTPase
PF01916	2	1	1	1	1	1	1	1	DS
PF01715	2	1	1	1	1	1	1	1	IPPT
PF08313	2	1	1	1	1	1	0	0	SCA7
PF03641	2	1	1	1	1	1	0	0	Lysine_decarbox
PF03600	2	1	1	1	1	1	0	0	CitMHS
PF02705	2	1	1	1	0	1	0	0	K_trans
PF07558	2	1	1	0	1	1	0	0	Shugoshin_N
PF09296	2	1	1	0	1	1	0	0	NUDIX-like
PF02982	2	1	1	1	0	1	0	0	Scytalone_dh
PF01422	2	0	1	0	1	1	0	0	zf-NF-X1
PF05390	2	1	0	0	0	0	0	0	KRE9

[a] Species abbreviations for Ascomycetes: Mgram, *M. graminicola*; Snod, *Stagonospora nodorum*; Fgram, *Fusarium graminearum*; Moryz, *Magnaporthe oryzae*; Trees, *Trichoderma reesei*; and Ncra, *Neurospora crassa*.
[b] Species abbreviations for Stramenopiles: Pram, *Phytophthora ramorum*; Psoj, *P. sojae*.

Table S7. PFAM domains that are expanded in the genome of *Mycosphaerella graminicola* relative to those of five other *Ascomycetes*[a] but not the two plant-pathogenic *Stramenopiles*[b].

Name	Mgram	Snod	Fgram	Moryz	Trees	Ncra	Pram	Psoj	Domain function
PF00560	16	14	14	12	14	15	84	100	LRR_1
PF07728	16	13	12	13	11	12	33	34	AAA_5
PF00043	14	10	7	4	9	4	12	19	GST_C
PF00450	13	10	9	6	5	4	14	16	Peptidase_S10
PF00230	10	8	5	6	7	1	29	32	MIP
PF00557	10	9	9	8	9	7	11	11	Peptidase_M24
PF04055	9	8	7	5	7	5	12	12	Radical_SAM
PF00782	8	7	6	5	6	5	17	23	DSPc
PF01553	8	6	5	6	5	5	12	10	Acyltransferase
PF01590	6	4	3	4	3	4	31	32	GAF
PF01757	6	2	1	2	1	2	10	14	Acyl_transf_3
PF00520	4	2	2	2	3	2	40	61	Ion_trans
PF03330	4	1	2	2	2	1	13	12	DPBB_1

[a] Species abbreviations for Ascomycetes: Mgram, *M. graminicola*; Snod, *Stagonospora nodorum*; Fgram, *Fusarium graminearum*; Moryz, *Magnaporthe oryzae*; Trees, *Trichoderma reesei*; and Ncra, *Neurospora crassa*.
[b] Species abbreviations for Stramenopiles: Pram, *Phytophthora ramorum*; Psoj, *P. sojae*.

Table S8. Assembly statistics for the *Mycosphaerella graminicola* version 1 (8.9× draft) and version 2 (finished) sequences compared to the 10× draft sequence of *Stagonospora nodorum.*

Category	*M. graminicola* v1.0 (draft)	*M. graminicola* v2.0 (finished)	*S .nodorum* draft
Sequence total, Mb	41.2	39.7	37.1
Number of scaffolds	129	21	107
Number of contigs	1,008	21	496
Scaffold N50/L50	6/2.4 Mb	Finished	13/1.1 Mb
Coverage	8.88×	Finished	> 10×
Gaps, Mbp	2.5 (7.5%)	0.006 (0.01%)	0.16 (0.43%)
Repeats, Mbp		7.17	2.62
Repeats, percent		18	7

Chapter 4

A global *in planta* proteome analysis of the fungal wheat pathogen *Mycosphaerella graminicola*

Sarrah Ben M'Barek, Jan H.G. Cordewener, Theo A.J. van der Lee, Antoine H.P. America, Sonia Hamza, Pierre J.G.M de Wit, Gert H.J. Kema

Submitted for publication

ABSTRACT

The ascomycete *Mycosphaerella graminicola* is economically one of the most important foliar pathogens of wheat that causes septoria tritici blotch. This disease threatens both bread wheat and durum wheat and results in significant yield losses. The molecular and physiological processes that are employed by this pathogen during pathogenesis are still poorly understood. Here, we exploited the recently completed genome sequence of *M. graminicola* strain IPO323 that enabled us to identify and globally analyse its *in planta* proteome. At four time points after inoculation apoplastic fluids (AFs) were isolated from compatible and incompatible interactions between strain IPO323 and cvs Obelisk and Shafir, respectively, to identify fungal secreted proteins. The proteome of *M. graminicola* expressed in the AFs was analyzed by sodium dodecyl sulphate polyacrylamide gel electrophoresis (SDS-PAGE) and data-independent acquisition liquid chromatography/mass spectrometry LC/MS^E combined with data-dependent acquisition LC-MS/MS analyses. The search for mapping mass spectrometry-derived peptide sequence data against the genome sequence of *M. graminicola* identified 665 peptides with the MS^E mode and 93 peptides with LC-MS/MS that matched to 85 proteins (65 proteins for MS^E, 55 proteins for LC-MS/MS of which 35 overlapped). Many of the annotated fungal secreted proteins have putative functions in pathogenicity, including cell-wall degrading enzymes and proteases, but the function of a significant number of identified proteins is unknown. The majority of the fungal secreted proteins accumulated at later stages of the compatible interaction at the onset of the necrotrophic phase, whereas most of the pathogenesis-related (PR) host proteins, such as PR-2, PR-3 and PR-9 accumulated at an early stage and at a higher level in the incompatible interaction.This global *in planta* proteome survey of *M. graminicola* provides an excellent basis for future detailed studies on fungal genes and their encoded proteins inducing susceptibility or resistance in wheat.

INTRODUCTION

Pathogenic fungi and plants communicate and interact in a sophisticated way which leads to a cascade of responses that eventually result in either healthy or diseased plants depending of their genetic make-up. Plant pathogens can manipulate host defences by effector proteins that allow the pathogen to evade pathogen-associated molecular pattern (PAMP) - triggered immunity (PTI) resulting in effector-triggered susceptibility (ETS). However, in the course of evolution plants have evolved surveillance systems to recognize effectors by corresponding plant disease resistance proteins in a cultivar-specific manner and activate effector-triggered immunity (ETI) that blocks pathogen infection (Jones and Dangl, 2006; Dodds and Rathjen, 2010). Fungal pathogens have different lifestyles that vary from obligate biotrophy for obligate pathogens that can only proliferate on living host tissues to necrotrophy for necrotrophic pathogens that prepare to kill host tissue before extensive proliferation on dead host tissue takes place. Many fungal plant pathogens, however, are hemibiotrophs that initially behave as a biotroph colonizing the intercellular space of plant tissues- the apoplast -, and subsequently switch to a necrotrophic lifestyle at later stages of infection (Horbach et al., 2011). The apoplast is therefore an important interface between host and pathogen, where both manipulation of the host by the pathogen, and recognition of the pathogen by the host and initiation defence responses take place during the course of infection of susceptible and resistant plants, respectively. Hence, it is an important resource for the discovery of key determinants of both virulence and avirulence (Joosten and de Wit, 1999; Rep, 2005; Thomma et al., 2005; Kamoun, 2006; Houterman et al., 2007; Bolton et al., 2008; Stergiopoulos and de Wit, 2009; de Jonge et al., 2010). An example of a biotroph is the tomato pathogen *Cladosporium fulvum* that colonizes the apoplast and by analyses of apoplastic fluids (AFs) several effector proteins, such as Avr2, Avr4, Avr4E, Avr9, Ecp1, Ecp2, Ecp5-Ecp7 that play crucial roles in both virulence and avirulence were identified (Joosten and de Wit, 1988; Ackerveken et al., 1992; Laugé et al., 2000; Bolton et al., 2008). Similarly, secretome analysis of the vascular tomato pathogen *Fusarium oxysporum* f.sp. *lycopersici* resulted in the identification of the small secreted in xylem (six) proteins. In total 11 (candidate) effector proteins have been identified including Six1-Six7, an arabinanase, an oxidoreductase and a serine protease (Lievens et al., 2009; Takken and Rep, 2009).

The ascomycete *Mycosphaerella graminicola* (anamorph *Zymoseptoria tritici* (Desm.) Quaedvlieg & Crous) (Quaedvlieg et al., 2011) is the causal agent of Septoria tritici leaf blotch (STB), which is currently the major wheat disease in Europe and the Mediterranean

region (Eyal, 1999; Bearchell et al., 2005) and the primary target for the breeding and agrochemical industry (McDougall, 2003; Russell, 2005). *M. graminicola* has a hemibiotrophic lifestyle with a relatively long latent period and a necrotrophic phase that is characterized by massive host killing and fungal proliferation culminating in production of pycnidia producing massive amounts of asexual pycnidiospores. Genetic studies have shown that the wheat–*M. graminicola* pathosystem complies with the gene-for-gene model (Kema et al., 2000; Brading et al., 2002). Upon germination of the conidia or ascospores (both are infectious) the fungus penetrates wheat plants through stomata within 12-24 hrs in both compatible and incompatible interactions without differentiating infection structures like appressoria or haustoria (Kema et al., 1996; Mehrabi, 2006). Subsequent fungal development is biotrophic, strictly apoplastic and the host stays symptomless for at least 10 days in which substomatal cavities and the surrounding mesophyll tissue is gradually but moderately colonized. The transition between the biotrophic and necrotrophic phases is reminiscent of the hypersensitive response (HR) and is accompanied by the differential regulation of wheat mitogen-activated protein kinase cascades (Keon et al., 2007; Rudd et al., 2008). As a result, the contents of killed plant cells leak into the apoplast, boosting rapid fungal proliferation in necrotic tissue that starts around 10-14 days post-inoculation (dpi), which is associated with appearance of macroscopically visible chlorosic and necrosic foliage. During the onset of lesion formation, Keon et al. (2007) identified the accumulation of glucose and fructose and amino acids in wheat AFs. The increase of fungal biomass is subsequently accompanied by the formation of pycnidia, the asexual fructifications that occupy the necrotic lesions at full symptom development at 21 dpi (Kema et al., 1996; Duncan and Howard, 2000).

Very little is known about the cause(s) and mechanism(s) of this lifestyle switch (Keon et al., 2007; Kema et al., 2008), but several reports speculated on or showed the toxicity of specific metabolites or proteins that might act as virulence factors (Kema et al., 1996; Perrone, 2000; Shetty et al., 2003; Shetty et al., 2007; Hammond-Kosack and Rudd, 2008; Rudd et al., 2008; Shetty et al., 2009). Douaiher et al. (2007) suggested a causal relationship between the production of cell wall-degrading enzymes (CWDEs) and *M. graminicola* pathogenicity. Indeed, Kema et al. (2008) identified many CWDEs in interaction libraries with a majority being expressed during the later phases of infection, which was later confirmed by Siah et al. (2010).

In the incompatible interaction, macroscopic symptoms vary greatly from none detectable to leaf chlorosis, but without significant fungal proliferation (Kema et al., 1996; Ware, 2006; Rudd et al., 2008). Studies on the molecular mechanisms of resistance of wheat

against *M. graminicola* have only recently begun (Shetty et al., 2003; Shetty et al., 2007; Rudd et al., 2008). Despite the lack of an HR (Kema et al., 1996; Ware, 2006; Rudd et al., 2008) which is a hallmark of resistance in biotrophic host-pathogen interactions (Greenberg, 1997; Heath, 2000), H_2O_2 accumulation, also often used as a marker of HR, was reported to negatively affect *M. graminicola* at a late stage of infection, but it seems to be able to tolerate it (Shetty et al., 2003; Shetty et al., 2007). More recently, Shetty et al. (2009) demonstrated that β-1,3-glucan components of the fungal cell wall trigger the expression of the PR-2 protein β-1,3-glucanase accompanied with callose depositions that provide complete disease protection. Hence, β-1,3-Glucans can be considered as fungal PAMPs as they also trigger the expression of the same PR proteins in susceptible wheat plants after exogenous addition.

Detailed histological studies showed that the apoplast is the major battlefield in the *M. graminicola*-wheat pathosystem (Kema et al., 1996; Rudd et al., 2008). Here, we capitalized on the recently finished genome sequence of *M. graminicola* strain IPO323 (Goodwin et al., 2011) and present a global *in planta* proteome survey of *M. graminicola* in both compatible and incompatible interactions with two wheat cultivars that provides an excellent basis for future detailed studies on fungal genes and their encoded proteins inducing susceptibility or resistance in wheat.

RESULTS

Differential symptom development induced by *Mycosphaerella graminicola* strain IPO323 on susceptible and resistant wheat cultivars

We followed symptom development induced by strain IPO323 on cvs Obelisk (susceptible) and Shafir (resistant) until 21 days post-inoculation (dpi; Fig. 1). Until seven dpi, resistant and susceptible plants did not show any visible disease symptoms. In the resistant plant, patchy chlorosis developed at 14 dpi that maintained until 21 dpi without any formation of pycnidia. In the susceptible plant, the first macroscopical symptoms appeared at 10 dpi as greyish sunken necrotic lesions that coalesced into larger ones that eventually covered the entire leaf and gradually showed increasing numbers of pycnidia at 14 dpi until full symptom development at 21 dpi. AFs isolated from strain IPO323-inoculated susceptible and resistant cultivar yielded similar volumes from the susceptible and resistant cultivars (0.5-0.6 ml/gr fresh weight) until 7 dpi, but from 14 dpi onwards volumes in the susceptible cultivar increased to 2.3 ml/gr fresh weight *vs* 0.8 ml/gr fresh weight for the resistant cultivar

probably reflecting increased leakage of soluble wheat proteins during the onset of the necrotic phase.

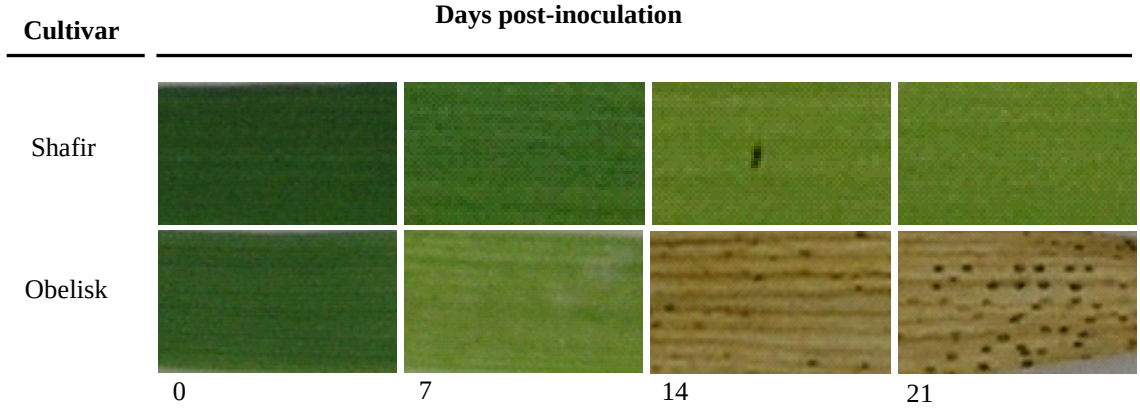

Fig. 1. Symptom development of septoria tritici blotch on resistant cv. Shafir and susceptible cv. Obelisk after inoculation with *Mycosphaerella graminicola* strain IPO323. Note that leaf tissue of cv. Obelisk has become necrotic at 14 and 21 days post-inoculation which is associated with fungal proliferation and the development of increasing numbers of pycnidia (black structures on the leaves). Leaves of resistant cv. Shafir show only some slight chlorosis.

Analysis of the apoplastic proteome

SDS-PAGE. Major changes were observed in the protein profiles of AFs isolated at different time points after inoculation and between the susceptible and resistant cultivars Obelisk and Shafir, respectively (Fig. 2). The most significant changes in soluble protein accumulation were observed between 25 and 35 kDa. These proteins accumulated much faster and to a higher level in the resistant cv. Shafir and are suspected to be PR proteins, whereas some proteins around 23 kD and 90 kDa decreased significantly in concentration both in the resistant and the susceptible cultivars and are suspected to be photosynthetically active proteins present in the plastid ADPG pyrophosphorylase complex and in the photosystem II complex like Rubisco; these proteins are partially degraded in chlorotic and necrotic leaf tissue. To confirm these hypotheses a number of gel slices containing the differentially accumulated or degraded proteins were analysed by mass spectrometry. In total 15 proteins were identified (Table 1). Twelve proteins (gel slices II to IV) originated from wheat and contained for the major part accumulated pathogenesis-related (PR) proteins such as β-1,3-glucanases (PR-2), chitinases (PR-3) and peroxidases (PR-9). This was particularly true for gel slice II and III that contained protein bands in the 25-35 kDa range that had mainly accumulated in the resistant cultivar Shafir at 7dpi and remained at a high concentration until

21 dpi; these proteins also accumulated in the susceptible cultivar Obelisk but much later and to a significantly lower amount (see gel slice IV). Three proteins that were identified in gel slices IV (1) and V (2), originated from *M. graminicola* with two that contained a secretion signal with strong homology to α-L-arabinofuranosidase and a six-hairpin glycosidase from *Pyrenophora tritici-repentis*. The third protein showed strong homology with a methionine synthase of *C. fulvum*.

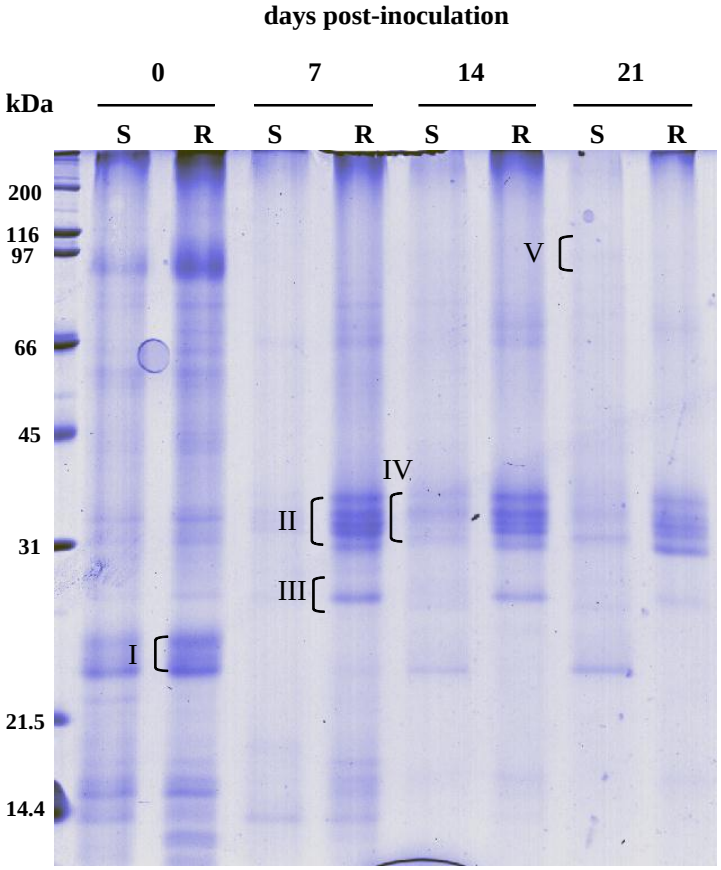

Fig. 2. A SDS-PAGE gel stained with Coomassie blue showing protein profiles present in apoplastic fluids that were isolated from primary leaves of the susceptible (S; Obelisk) and resistant (R; Shafir) wheat cultivars at 0, 7, 14 and 21 days post-inoculation with *Mycosphaerella graminicola* strain IPO323. Molecular masses of marker proteins are indicated on the left (in kDa). The protein bands present in the gel slices I-V were identified by mass spectrometry and are shown in Table 2.

Quantitative analysis of LC-MS^E data by Progenesis. As expected, the two apoplastic fluid samples from cvs Obelisk and Shafir harvested at 0 dpi deviated strongly from all other samples. Consequently, the software was not able to align the 0 dpi samples properly to the reference sample, and therefore the 0 dpi samples were not considered for further analysis. After alignment and warping, a single aggregate map containing all MS peak data from the 7, 14 and 21 dpi was created in which 6,921 features were detected. We performed a principal component analysis (PCA) on the peak intensity data to examine the overall differences between the six samples (Fig. 3). This revealed a clear separation over the vertical axis (PCA2) of the protein samples collected from the AFs of the resistant and susceptible plants. Furthermore, on the x-axis (PCA1) the 21 dpi samples were distinct from the 7 dpi and 14 dpi samples; the latter two were much more proximate to each other.

Table 1. Proteins identified in gel slices excised from an SDS-PAGE gel (indicated in Fig. 1) containing proteins present in apoplastic fluids obtained from the resistant and susceptible wheat cvs Shafir and Obelisk, respectively, at 0, 7, 14 and 21 days post-inoculation with *Mycosphaerella graminicola* strain IPO323.

Gel slice	Protein description	Accession number [a)]	Species [b)]	M_r (kDa) [c)]	# peptide seq. [d)]	Pr. Cov (%) [e)]	Prot. score [f)]
I	ADPG pyrophosphorylase	CK211503: homologue to UniRef100_Q8L686 cluster	*T. aestivum*	23,3	2	15	1934
	Peroxidase 1	TC287158: UniRef100_Q5I3F7	*T. monococcum*	33,3	5	27	83
	Peroxidase 2	TC287852: UniRef100_Q5I3F6	*T. monococcum*	33,6	5	22	152
	Peroxidase 3	TC284704: homologue to UniRef100_Q5I3F5 Cluster	*T. monococcum*	33,2	7	34	161
II	Peroxidase 4	TC280198: homologue to UniRef100_Q5I3F4 Cluster	*T. monococcum*	34,7	3	15	70
	β-1,3-glucanase	TC303277: UniRef100_O82716 Cluster	*T. aestivum*	36,1	10	44.5	403
	β-1,3-glucanase	TC277204 : UniRef100_Q4JH28 Cluster	*T. aestivum*	36,6	10	50	354
	β-1,3-glucanase	TC278817: UniRef100_Q9XEN5 Cluster	*T. aestivum*	35,2	7	39	143
	Glucan endo-1,3-β-D-glucosidase	TC284274: homologue to UniRef100_Q1EMA4 Cluster	*S. cereal*	30,5	7	40.5	161
	β-1,3-glucanase	TC349275: homologue to UniRef100_Q9XEN5 Cluster	*T. aestivum*	35,3	6	29.5	175
	Chitinase 1	TC278023: UniRef100_Q8W429 Cluster	*T. aestivum*	30,8	3	20	393
III	PR17c precursor	TC287586: similar to UniRef100_A7YA60 Cluster	*H. vulgare*	25,4	4	25.5	503
IV	Peroxidase 2	TC287852: UniRef100_Q5I3F6 Cluster	*T. monococcum*	33,6	5	31	95
	Peroxidase 3	TC284704: homologue to UniRef100_Q5I3F5 Cluster	*T. monococcum*	33,2	3	17	117

	Peroxidase 4	TC280198: homologue to UniRef100_Q5I3F4 Cluster	*T. monococcum*	34,7	3	25	80
	Glucan endo-1,3-β-D-glucosidase	TC303277: UniRef100_O82716 Cluster	*S. cereale*	36,1	5	22	146
	β-1,3-glucanase	TC278817: UniRef100_Q9XEN5 Cluster	*T. aestivum*	35,2	4	25	74
	β-1,3-glucanase	TC349275: homologue to UniRef100_Q9XEN5 Cluster	*T. aestivum*	35,3	3	15	56
	BlastP (nr): α-L-arabinofuranosidase (Arabinosidase) ZP_07314546 (*S. griseoflavus*$^{\phi}$ Tu4000]) 2e-120	estExt_Genewise1.C_chr_21868	*M. graminicola*	34,5	4	24	104
V	BlastP (nr): XP_001940715 six-hairpin glycosidase (*P. tritici-repentis**) e=0 GO : Cell adhesion IPR:Coagulation factor 5/8 type, C-terminal	estExt_fgenesh1_pg.C_chr_20902	*M. graminicola*	75,5	6	14	161
	BlastP (nr): AF226997.1 methionine synthase (*C. fulvum*$^{\&}$) e=0	estExt_fgenesh1_kg.C_chr_120169	*M. graminicola*	87,2	3	5.5	84

[a] Accession numbers of identified proteins
[b] Origin of the derived sequence (*Horderum vulgare, Secale cereale, M. graminicola, Triticum aestivum, T. monococcum*)
[c] Relative molecular mass (kDa)
[d] Number of identified peptide sequences
[e] Coverage percentage of amino acid sequence with the matched peptides
[f] Protein score generated by the program Mascot
$^{\phi}$ *Streptomyces griseoflavus, *Pyrenophora tritici-repentis*, $^{\&}$ *Cladosporium fulvum,*

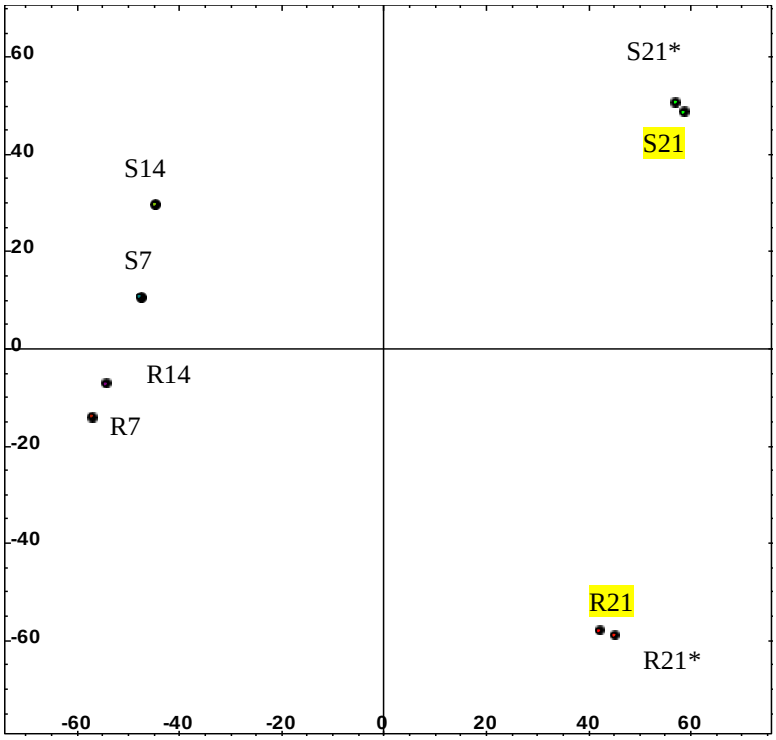

Fig. 3. Principle component analysis on the standardized ^{10}log feature intensity data from LC-MS^{E} analysis comprising peak number (RT-m/z pair), sample name, and ion intensity data of proteins identified in the apoplastic fluids isolated from primary leaves of wheat cvs Shafir (resistant) and Obelisk (susceptible), respectively, at 0, 7, 14 and 21 days post-inoculation with *Mycosphaerella graminicola* strain IPO323 (time point 0 dpi is not included and the samples at 21 dpi were duplicated, indicated by the asterisk and highlighted).

Peptide identification with LC-MS/MS and LC-MS^{E}. LC-MS/MS preferentially identifies the most abundant components in a peptide mixture, as co-eluting low abundant peptides will most likely not be chosen for MS/MS fragmentation. Here, LC-MS/MS analyses of all eight sample runs resulted in 544 unique peptide sequences that matched with 439 wheat peptides and 93 *M. graminicola* peptides (Table 2). In contrast, LC-MS^{E} has no precursor selection before fragmentation and is therefore less biased for identification of predominant peptides resulting in a wider coverage of proteins present in the AFs. A total of 4,735 peptide sequences were identified by MS^{E} from which the majority (4,009) matched to wheat proteins, while 665 peptides matched to *M. graminicola* proteins (Table 2). The percentage of unique peptide sequences identified from the LC-MS^{E} analysis was much higher (~89%) than that obtained with LC-MS/MS analysis, but we also noticed that a substantial part of the peptide sequences resulting from the LC-MS^{E} analysis originated from in source fragmentation of the precursor (tryptic) peptide. Both LC-MS/MS and LC-MS^{E} yielded approximately six times more peptides matching to wheat proteins than to *M. graminicola* proteins.

Table 2. Total number of unique peptide sequences identified with LC-MS/MS and LC-MS^E in the apoplastic fluids obtained from the resistant (Shafir) and susceptible (Obelisk) wheat cvs at four time points after inoculation with *Mycosphaerella graminicola* strain IPO323 (0, 7, 14 and 21 days post-inoculation).

Number of unique peptides sequences	Total	Originated from wheat	Originated from *M. graminicola*
LC-MS/MS [a)]	544	439	93
LC-MS^E [b)]	4735	4009	665
Total	5279	4448	758

[a)] For LC-MS/MS, peptide score ≥50.
[b)] For LC-MS^E, number of unique identified peptides (including in source fragmentation generated from the same source) with peptide score ≥5.

Wheat proteins. Combining the 4,448 matching wheat peptide sequences that were obtained by analyzing the eight samples with LC-MS/MS and LC-MS^E after filtering, revealed in total 2,030 wheat proteins that were identified in AFs isolated from the inoculated resistant and susceptible cultivars of which the majority exhibited either catalytic (1,182 proteins; ~43%) or binding activity (1,122; ~41%). Among these, 1,140 proteins were classified as enzymes and 449 proteins were predicted to have a secretion signal. Blast2Go analysis assigned the host proteins to four major biological processes; cellular process (1,570 sequences; ~30%), metabolic process (1,523 sequences; ~29%), carbon utilization (560 sequences; ~11%) and response to stimulus (535 sequences; ~10%). Further analyses revealed that a diverse group of 151 proteins was involved in defence and included for instance PR proteins, such as PR maize seed protein (PR-1), vacuolar defence proteins (PR-4), thaumatin-like proteins (PR-5), peroxidases (PR-9), germins and several isoforms of β-1,3-glucanase (PR-2) and chitinases (PR-3) that were found in both resistant and susceptible cultivars. As we are mostly interested in fungal proteins that are present during the infection of wheat, the next result section is focussed on identified fungal proteins.

Fungal proteins. Out of the 85 identified fungal proteins, 73 (86%) were exclusively identified in the AFs from the inoculated susceptible plant and mostly from AFs harvested at 14 and 21 dpi (Fig. 4). Finally, we grouped the 85 identified proteins in the *M. graminicola* proteome that were present at different stages of infection in biological processes and functional categories (Fig. 5). In total, 62 of the 85 *M. graminicola* genes were functionally annotated of which 22 were predicted to encode metabolic enzymes. Eleven subgroups of biological processes on the GO level 2 were identified showing that a large portion of the proteins (N=36; ~43%) is involved in metabolic processes, followed by 19 proteins (~23%) involved in cellular processes (Fig. 5A). With respect to the molecular function, the majority

of the identified proteins exhibit either catalytic (N=49; ~62%) or binding activities (N=21; ~27%). A more detailed analysis (GO level 3) revealed that 25 proteins (~52%) with catalytic activity are involved in hydrolase activity and two proteins (~11%) are predicted to bind to nucleic acid (Fig. 5B). A detailed GO description of all identified and annotated *M. graminicola* proteins is included in the Supplementary Information (Table S1). Eleven proteins (~13%) could not be classified, which were either hypothetical proteins or proteins without any BLAST hit. A few fungal proteins were identified at 0 dpi from non-inoculated control plants, but these are considered to originate from fungal contaminations as these plants were placed in the same greenhouse compartment as the inoculated plants. Interestingly, examples of fungal proteins present at 7 dpi were potentially involved in transport and metabolism of amino acids, lipids and coenzymes.

From the 85 identified proteins, 41 (~48%) proteins are predicted to be secreted in the apoplast, which represents the largest fraction, whereas the others are presumably located in the cytoplasm, mitochondria or nucleus and include unnamed proteins, predicted proteins or hypothetical proteins. The fungal secretome appears to be involved in a myriad of biological processes, including general metabolism, cell cycle and DNA processing and response to oxidative stress or pathogenesis. The secreted proteins comprised 12 proteins with unknown function as well as 22 proteins involved in hydrolase or oxidoreductase activities (Table 3) and accumulated in AFs mostly during the necrotrophic phase of pathogenesis (14-21 dpi).They are probably involved in the maceration of outer plant cell-wall components and included xylanases, pectinases, glucanases, arabinases and cutinases that matched predominantly to putative carbohydrate active enzymes implicated in cellulose, hemicelluloses, pectin and cutin degradation (Table 3). In addition to these CWDEs, we also identified six (~14%) secreted extracellular proteases that catalyze the cleavage of peptide bonds of proteins and included both endoproteases - such as metalloprotease, serine protease and aspartic proteases - as well as the exoproteases aminopeptidase and carboxypeptidase. Besides the well-known enzymes, one catalase peroxidase that belongs to the stress response category reported in other fungi, was also identified in the apoplast at 14 and 21dpi. Ten out of the 12 secreted proteins with unknown function are cysteine-rich and are supported by EST data (Kema et al., 2008) and nine are small-secreted protein (SSPs). After examining changes in the individual functional groups, we re-evaluated the LC-MS^E data by analyzing the overall response pattern of several *M. graminicola* proteins for which we had quantitative data (Fig. 6).

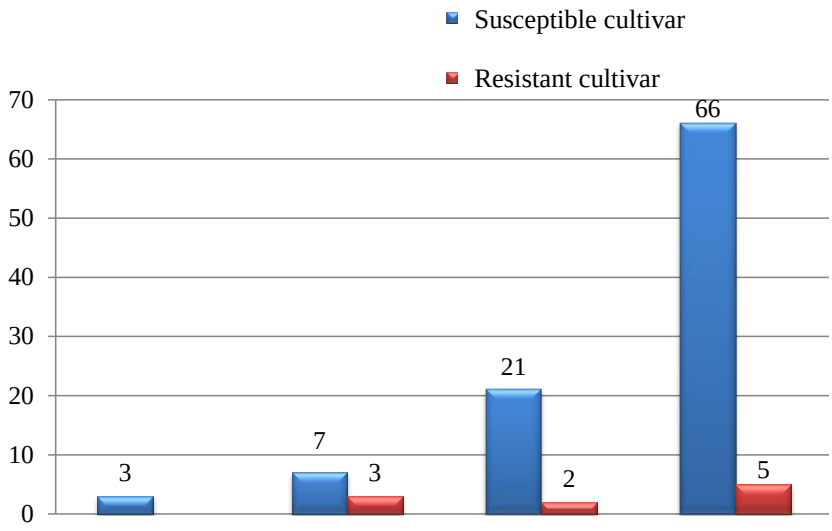

Fig. 4. The total number of *Mycosphaerella graminicola* proteins identified with LC-MS/MS and LC-MS^{E}, present in the apoplastic fluids that were obtained from the primary leaves of the resistant (Shafir) and susceptible (Obelisk) wheat cultivars, respectively, at 0, 7, 14 and 21 days post-inoculation with *M. graminicola* strain IPO323.

A

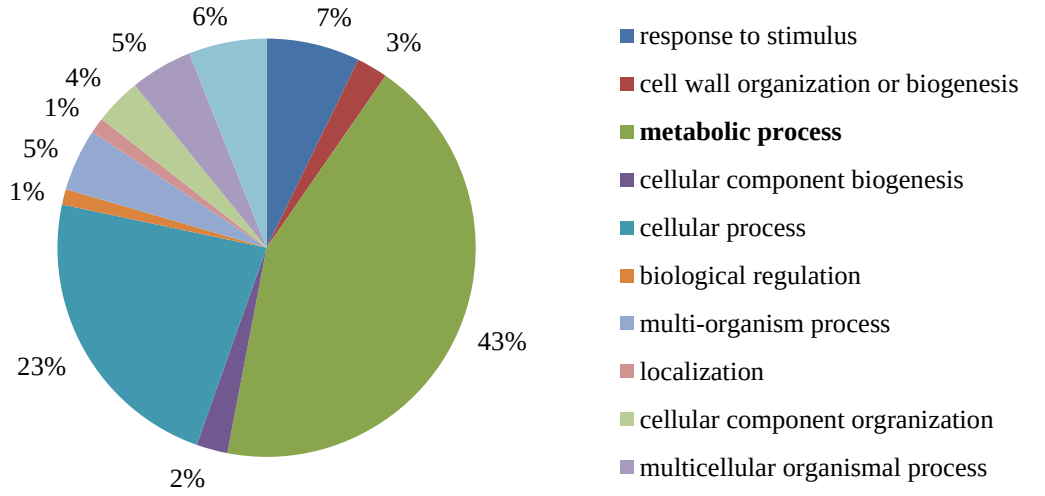

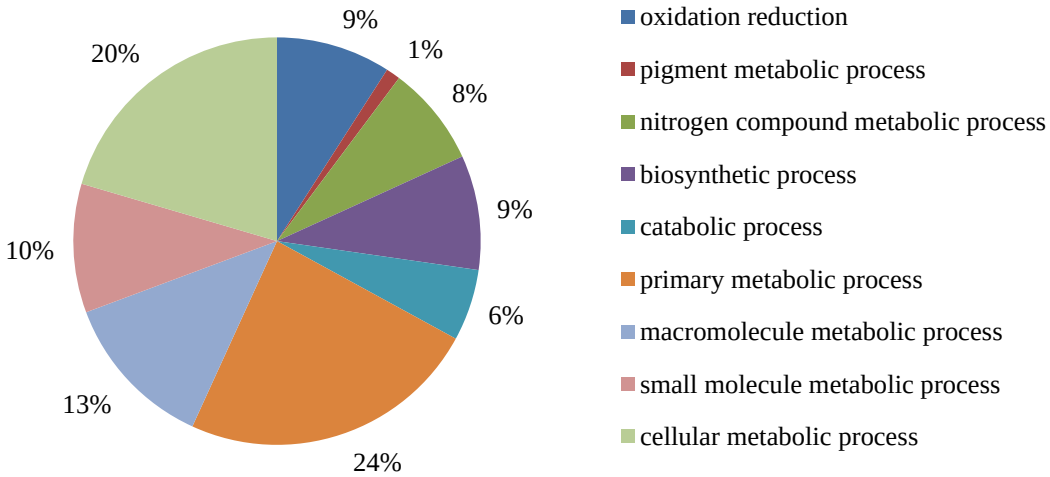

B

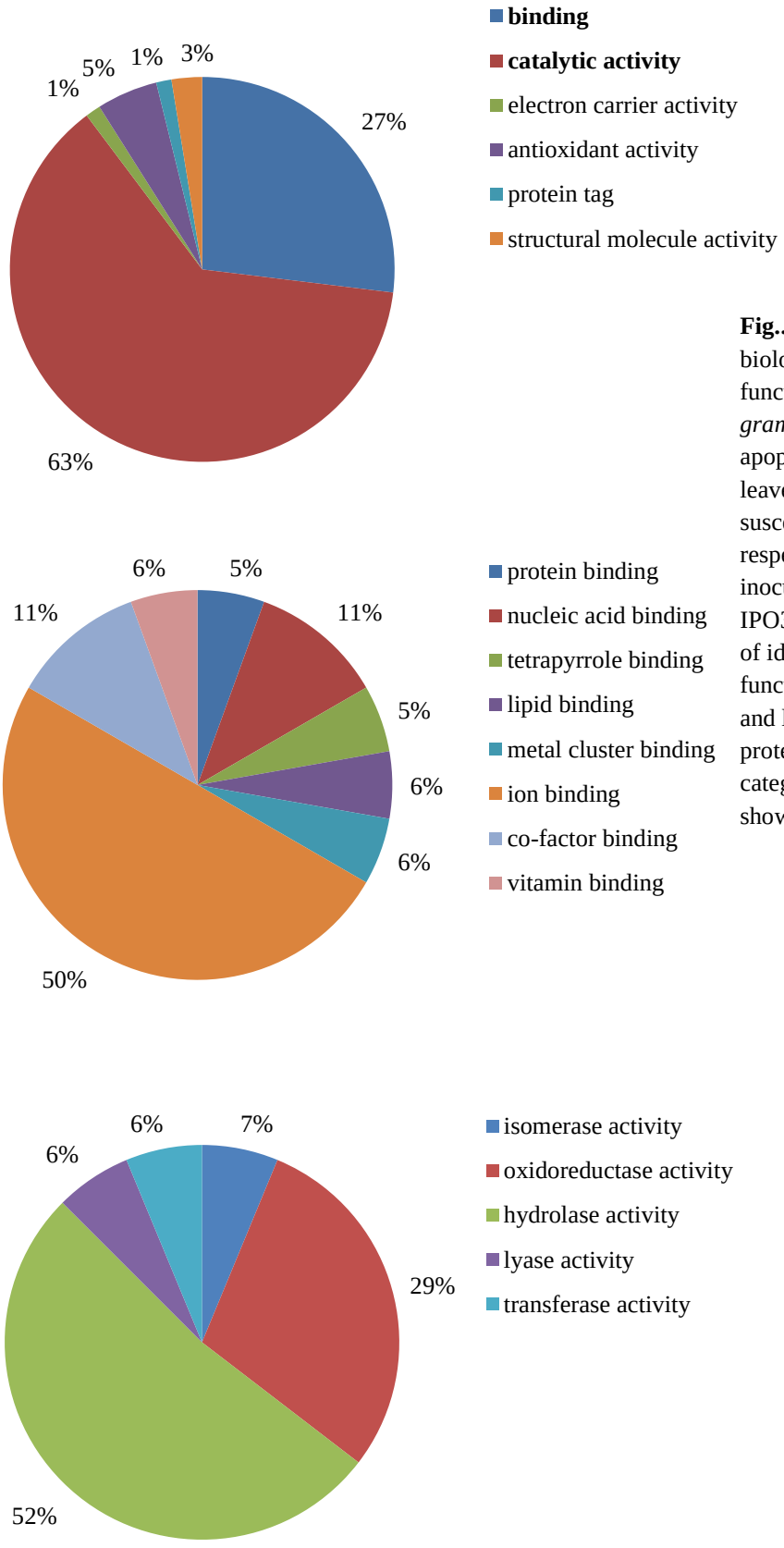

Fig.. 5. Gene ontology analysis, focussed on biological processes (A) or molecular function (B), of 85 *Mycosphaerella graminicola* proteins that were identified in apoplastic fluids obtained from the primary leaves of the resistant (Shafir) and susceptible (Obelisk) wheat cultivars, respectively, at 0, 7, 14 and 21 days post-inoculation with *M. graminicola* strain IPO323. The pie charts show the percentage of identified proteins in the various functional categories (filtered by #Seq=1.0 and level 2) and do not take un-annotated proteins into account. The different categories (level 2, indicated in bold) are shown in more detail (level 3) below

This revealed a consistent accumulation for the hypothetical proteins and the CWDEs from 7 dpi to 21 dpi in the susceptible cv. Obelisk, whereas the same proteins remained at a constant level in the resistant cv. Shafir.

A. Hypothetical proteins

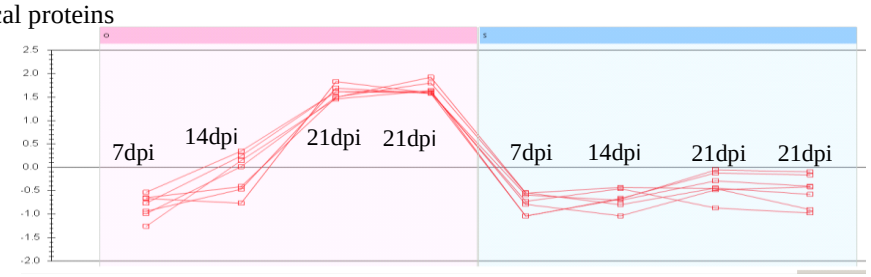

B. Xylanase

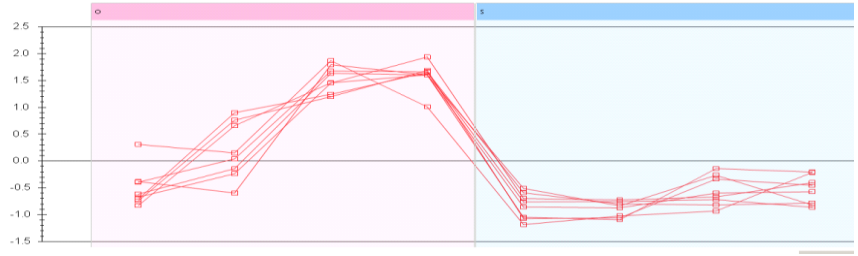

C. Catalase peroxidase

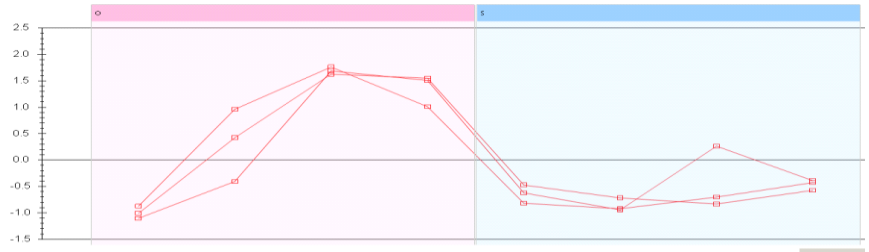

D. Cutinase

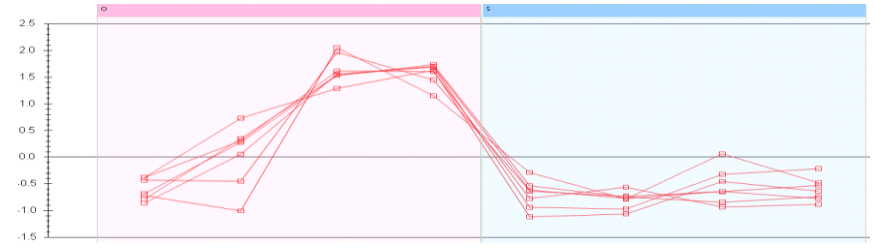

Fig. 6. Quantitative analysis of differentially expressed proteins from *Mycosphaerella graminicola* identified in apoplastic fluids isolated at 7, 14 and 21* (*duplicates) days post-inoculation with *M. graminicola* strain IPO323 from a resistant cultivar (Shafir) and a susceptible cultivar (Obelisk). The Y-axis corresponds to standardized normalized value; red lines correspond to matching peptides assigned to a particular protein or a category of proteins displayed from top to bottom. **A.** Peptides originating from hypothetical secreted proteins corresponding to estExt_fgenesh1_kg.C_chr_30051; estExt_fgenesh1_pg.C_chr_130030 and fgenesh1_pg.C_chr_11000104. **B.** Peptides originating from two xylanases corresponding to gene models estExt_fgenesh1_kg.C_chr_60237 and estExt_fgenesh1_kg.C_chr_70317. **C.** Peptides originating from catalase peroxidase corresponding to gene model estExt_fgenesh1_pg.C_chr_11443. **D.** Peptides originating from cutinase corresponding to gene model estExt_fgenesh1_kg.C_chr_20529.

Table 3. Summary of the secreted *Mycosphaerella graminicola* proteins that were identified in the apoplastic fluids isolated from the resistant (Shafir) and susceptible (Obelisk) wheat cvs at four time points after inoculation with *M. graminicola* strain IPO323 (0, 7, 14 and 21 dpi).

JGI Header [a]	Pep. No [b]	Cov. % [c]	Pep. Score [d]		Mol. Func. [e]	Description	Cult. & time points [f]	Total aa [g]
			Min Score	Max Score				
estExt_fgenesh1_kg.C_chr_20529	21	74	5,4	85,5	hydrolase activity	Cutinase	S, 14&21dpi	224
e_gw1.6.1246.1	14	63	5,1	79,5	hydrolase activity	Cutinase	S, 21dpi	232
estExt_fgenesh1_kg.C_chr_70027	10	23	7,5	80	hydrolase activity	Gpi-anchored cell wall protein; beta –endoglucanase	S, 21dpi	480
estExt_fgenesh1_kg.C_chr_100051	3	23	5,2	6,0	hydrolase activity	Glycoside hydrolase, family 12; endoglucanase a precursor	S, 21dpi	246
estExt_fgenesh1_kg.C_chr_60237	25	73	5,1	94,3	hydrolase activity	Glycoside hydrolase, family 11; endo- -beta-xylanase	S, 21dpi	225
estExt_fgenesh1_kg.C_chr_70317	28	61	5,2	78,1	hydrolase activity	Glycoside hydrolase, family 10; endo- -beta- xylanase	S, 14&21dpi	347
estExt_fgenesh1_pg.C_chr_40433	13	28	6,3	56,6	hydrolase activity	Glycoside hydrolase, family 3; beta-xylosidase	S, 21dpi	769
estExt_fgenesh1_pg.C_chr_40440	2	3	5,0	5,1	hydrolase activity	Glycoside hydrolase, family 3; beta-glucosidase	S, 21dpi	979
estExt_fgenesh1_pg.C_chr_50362	16	40	5,9	79,3	hydrolase activity	Glycoside hydrolase, family 7 ; cellobiohydrolase d	S, 21dpi	444
estExt_fgenesh1_pm.C_chr_30480	7	22	5,2	7,0	hydrolase activity	Glycoside hydrolase, family 62; alpha-L-arabinofuranosidase	S, 14dpi	331
estExt_fgenesh1_pg.C_chr_100384	7	18	6,2	70,9	hydrolase activity	Glycoside hydrolase, family 62; alpha-l-arabinofuranosidase	S, 21dpi	690
estExt_Genewise1.C_chr_21868	22	55	5,5	81,3	hydrolase activity	Glycoside hydrolase, family 62; alpha-n-arabinofuranosidase	S, 14&21dpi	321
estExt_fgenesh1_pg.C_chr_130228	12	29	5,1	84,6	hydrolase activity	Glycoside hydrolase, family 31	S, 14& 21dpi	991

estExt_fgenesh1_kg.C_chr_80005	5	13	5,4	6,7	hydrolase activity	Glycoside hydrolase, family 43; secreted arabinase	S, 21dpi	319
estExt_Genewise1.C_chr_12866	12	52	5,0	6,8	hydrolase activity	Pectinesterase	S, 14&21dpi	330
fgenesh1_pg.C_chr_1001469	34	31	5,0	62,6	hydrolase activity	Glycoside hydrolase, family 3	S, 14&21dpi R, 21dpi	1055
fgenesh1_pg.C_chr_3000807	1	7	52,9	52,9	hydrolase activity	Glycoside hydrolase family, beta –mannanase	S, 14dpi	363
estExt_fgenesh1_kg.C_chr_110051	5	42	5,2	60,8	hydrolase activity	Lipases ; acetyl xylan esterase	S, 14 & 21dpi	301
estExt_fgenesh1_pg.C_chr_70016	3	10	5,5	5,9	Peptidase activity	Peptidase A1, pepsin, aspartyl protease	S, 14dpi	441
fgenesh1_pg.C_chr_4000424	2	10	5,0	5,2	Peptidase activity	Peptidase A1, pepsin, Aspartic Protease	S, 21dpi	460
estExt_fgenesh1_kg.C_chr_70011	5	24	5,2	62,6	Peptidase activity	Peptidase A4, Asparatic protease, scytalidopepsin B	S, 14&21dpi	269
estExt_fgenesh1_pg.C_chr_10314	5	19	5,3	35,5	Peptidase activity	Peptidase; aminopeptidase	S, 21dpi	552
estExt_fgenesh1_pg.C_chr_50636	19	52	5,1	74,0	Peptidase activity	Peptidase S8 and S53, subtilisin, kexin, sedolisin	S, 21dpi	400
estExt_fgenesh1_pg.C_chr_60048	9	27	5,1	6,2	Peptidase activity	Peptidase M14, carboxypeptidase A	S, 21dpi	426
estExt_fgenesh1_pg.C_chr_110083	21	27	7,6	52,9	oxidoreductase activity	FMN-dependent dehydrogenase	S, 14& 21dpi	504
estExt_Genewise1.C_chr_90838	1	3	55,5	55,5	oxidoreductase activity	Glucose-methanol-choline oxidoreductase	S, 21dpi	555
estExt_fgenesh1_pg.C_chr_11443	39	39	7,3	71,9	peroxidase activity	Catalase peroxidase hpi	S, 14 & 21dpi	796
estExt_fgenesh1_pg.C_chr_90237	26	26	5,2	72,0	Transferase activity	TM protein	S, 21dpi	1139
estExt_fgenesh1_pg.C_chr_20902 $^{\infty}$	32	49	5,8	74,5	catalytic activity	No significant hits Six-hairpin glycosidase (*Pyrenophora tritici-repentis* Pt-1C-BFP) XP_001940715.1 e=0.0	S, 21dpi	667
fgenesh1_pm.C_chr_4000019 $^{\Theta}$	1	7	71,4	71,4	---NA---*	Hypothetical protein FG11205.1 (*Gibberella zeae* PH-1)	S, 21dpi	149

						$2e^{-35}$		
estExt_fgenesh1_kg.C_chr_110087 #	1	10	7,6	78,1	---NA---	Unnamed protein product (*Podospora anserina* S mat+) $3e^{-11}$	S, 14 & 21dpi	156
estExt_fgenesh1_kg.C_chr_120103 **	1	6	73,5	73,5	---NA---	Conserved hypothetical protein (*Verticillium albo-atrum* VaMs.102) $4e^{-45}$	S, 21dpi	238
estExt_fgenesh1_pg.C_chr_130030 **	16	31	7,0	80,2469	---NA---	Conserved hypothetical protein (*Pyrenophora tritici-repentis* Pt-1C-BFP) $2e^{-153}$ XP_001930959.1	S, 14& 21dpi	483
fgenesh1_pg.C_chr_11000104 **	9	28	5,6	6,2	---NA---	Conserved hypothetical protein (*Pyrenophora tritici-repentis* Pt-1C-BFP) $1e^{-174}$	S, 21dpi	497
estExt_fgenesh1_kg.C_chr_50387 ϕ	2	28	5,7	8,1	---NA---	Hypothetical protein FG08238.1 (*Gibberella zeae* PH-1) $2e^{-25}$	S, 21dpi	149
estExt_fgenesh1_kg.C_chr_70220 ⊕	1	7	49,3	72	---NA---	Hypothetical protein UREG_02418 (*Uncinocarpus reesii* 1704) $7e^{-11}$ PhiA protein (*Emericella nidulans*) $3e^{-10}$	S, 21dpi	188
estExt_fgenesh1_kg.C_chr_90057	14	25	5,1	82,7	---NA---	Low homology to IgE-binding protein (*Penicillium marneffei*) $3e^{-15}$	S, 21dpi	198
estExt_fgenesh1_pg.C_chr_40369 #	5	39	5,1	79,7	---NA---	No significant hits	S, 14&21dpi	154
estExt_fgenesh1_kg.C_chr_30051 ∅	15	25	5,3	85,6	---NA---	Hypothetical protein SNOG_07926 (*Phaeosphaeria nodorum* SN15) stress response protein Rds1(*Pyrenophora tritici-repentis* Pt-1C-BFP)	S, 14&21dpi	519

estExt_fgenesh1_kg.C_chr_30295 [ϕ]	2	15	5,5	6,2	---NA---	Hypothetical protein MGCH7_ch7g1093 (*Magnaporthe oryzae* $70e^{-15}$)	S, 21dpi	177
estExt_fgenesh1_kg.C_chr_60114 [#]	1	7	87,3	87,3	---NA---	No significant hits	S, 14dpi	154

[a)] JGI headers from http://genomeportal.jgi-psf.org/Mycgr3/Mycgr3.home.html
[b)] Maximum number of identified peptides, including generated in source fragments
[c)] Coverage percentage of amino acid sequence with the matched peptides
[d)] Peptide score (min and max) based on both DDA and MS^E. The score range for significant matches is for $MS^E \geq 5$ and for DDA ≥ 50
[e)] GO term provided for molecular function from Blast2Go functional annotation tool
[f)] S: Susceptible cultivar (Obelisk), R: Resistant cultivar (Shafir)
[g)]Amino acid length
*--NA--: no GO term identified
[#] Unique Small Secreted Protein (SSP)
[**]Conserved SSP
[ϕ] Lowly conserved SSP
[∞] IPR000421: Possible cell adhesion protein
[Θ] IPR010829 Cerato-platinin
[⊕] Essential for phialid development in Aspergillus
[∅] Homology to stress response protein rds1
NB. Proteins identified with only one peptide have lower confidence level that those identified with more than one peptide

DISCUSSION

The apoplastic space is often the niche of a plant that is initially colonized by a microbial pathogen (Bowles, 1990). Hence, this plant-pathogen interface contains a plethora of proteins for mutual molecular communication and its proteomic analysis might provide useful information for unravelling the interaction between a pathogen and its host that will substantially contribute to the understanding of fungal pathogenicity (Bhadauria et al., 2010).

The objective of the current study was to identify *M. graminicola* proteins during wheat infection. Additionally, wheat proteins were also identified and preliminary characterized. Several time points representing distinct phases during both compatible (Obelisk- *M. graminicola* strain IPO323) and incompatible interactions (Shafir- *M. graminicola* strain IPO323) were chosen for isolation of apoplastic fluids (AFs). The major differences in the apoplastic proteins after inoculation of a resistant and a susceptible cultivar were initially analyzed by separating them by one dimensional SDS-PAGE that clearly showed different protein profiles, particularly at early stages of infection of the incompatible interaction. Until 7 dpi, when the fungal proliferation in compatible and incompatible interactions is similar, this resulted in the accumulation of proteins in the molecular mass range of 20-35 kDa that were analysed by mass spectrometry. Most of the differentially accumulating proteins were of wheat origin and comprised primarily PR proteins with antifungal activity such as β-1,3-glucanases (PR-2), chitinases (PR-3) and peroxidases (PR-9). Most of them have previously been described in *M. graminicola*–infected wheat (Muthukrishnan et al., 2001; Shetty et al., 2009). PR proteins are usually seen as markers of incompatibility as reported for many different pathosystems including other plant pathogenic *Dothideomycetes* (Joosten and De Wit, 1989; Wubben et al., 1992). Indeed, Adhikari et al., (2007) showed a rapid response of wheat leaves to the presence of an avirulent *M. graminicola* strain including the activation of *PR* gene expression within 24 hrs after inoculation that was particularly more pronounced during an incompatible interaction. Here it is clearly visible that the resistant cv. Shafir does respond much earlier in the biotrophic phase and to a higher level with the accumulation of the aforementioned defence-related PR proteins. In addition, it also shows that even a susceptible cultivar (Obelisk) initially does not allow much fungal proliferation, likely due to effective basal host defence including both constitutive and active defence mechanisms induced by fungal PAMPs like β-1,3-glucans and chitin fragments released from the fungal cell wall by synergistic activities of plant β-1,3-glucanases and chitinases, and are recognized by yet to be identified host pattern recognition

receptors (PRRs) (Thomma et al., 2011). Fungal PAMPS identified so far include chitin fragments (de Jonge et al., 2010), and β-1,3-glucans (Umemoto et al., 1997; Fliegmann et al., 2004). Shetty et al. (2009) reported that the treatment of wheat leaves with β-1,3-glucans isolated from cell walls of *M. graminicola* triggered a rapid accumulation of β-1,3-glucanases both in resistant and in susceptible cultivars. On top of these, effectors behaving avirulence factors recognized by resistance proteins would induce resistance protein-mediated defence responses leading to a quicker and higher accumulation of PR proteins in resistant cultivars. However, further research needs to be performed to confirm this hypothesis, as no avirulence gene or resistance gene has yet been cloned from the *M. graminicola*-wheat pathosystem.

At 7 dpi and beyond, when the fungus starts to proliferate in the tissue of the susceptible cv. Obelisk that results in necrosis, we expected an increase of soluble proteins of both plant and fungal origins due to leakage of cytoplasmic plant proteins in the apoplast and an increase of secreted fungal proteins resulting from the rapidly increasing fungal biomass and fructification (Kema et al., 1996). By using label–free LC-MS^E and data dependent acquisition LC-MS/MS techniques, all the proteins were blasted to the finished genome sequence of *M. graminicola* strain IPO323, (Goodwin et al., 2011) to identify *M. graminicola* proteins produced during pathogenesis, irrespective of the stages of infection.

Fungal proteins (N=85) were predominantly identified in the susceptible cv. Obelisk particularly during the later phases of infection. Forty-eight per cent (41/85) of the *M. graminicola* proteins were predicted to be secreted but proteins without a classical signal peptides could be secreted by non-classical secretion mechanisms as reported before (Cleves, 1997; Nickel, 2005). Nevertheless, some fungal proteins appeared to be of cytoplasmic origin such as the 40s ribosomal protein S15, 3-isopropylmalate dehydratase and aldehyde dehydrogenase that may result from cell leakage during sample preparation or are leaking out of senescing mycelium during the later stages of infection. The majority of the 41 secreted proteins, however, are associated with pathogenesis and comprised many CWDEs that were identified at the late stages of infection including α-L-arabinofuranosidases, β-glucosidases, β-xylosidases, endoglucanases, endo-β-xylanases and pectinesterases, suggesting active cell wall hydrolysis. CWDEs are of special interest because they are not only implicated in cell wall hydrolysis to release nutrients for the colonizing pathogen (De Lorenzo et al., 1997), but also contribute to virulence (Bateman and Basham, 1976; Kapat et al., 1998; Kang and Buchenauer, 2000; Mary Wanjiru et al., 2002). In addition, it has been reported that some cell wall that break down products such as β-1,3-glucans and oligalacturonides can elicit defence responses in plants (Esquerré-Tugayé et al., 2000; De Lorenzo et al., 1997). In *M.*

graminicola, the involvement of CWDEs in virulence has been suggested in several reports (Cohen and Eyal, 1993; Kema et al., 1996; Duncan and Howard, 2000; Shetty et al., 2003; Shetty et al., 2007; Kema et al., 2008). Recently, a comparative CAZy analysis (carbohydrate-active enzymes) (http://www.cazy.org/Genomes.html) for a range of fungal genomes, including *M. graminicola* and other members of the *Dothideomycetes*, suggested that the switch from biotrophy to necrotrophy might be associated with the production of specific CWDEs that could release toxic cell wall fragments triggering cell-death (Goodwin et al., 2011). In addition, Siah et al. (2010) suggested a correlation between the *in planta* production of endo-β-1,4-xylanase and the transition from biotrophy to necrotrophy during infection of wheat by *M. graminicola.* Our current observations of massive increase in secreted proteins at the necrotrophic stage of infection comply with earlier reports (Kema et al., 1996; Cohen and Eyal, 2007; Rudd et al., 2008).

Two of the five cutinase genes in the genome of *M. graminicola* have been identified in this proteome study. Cutinases have been reported to play roles in cuticular penetration (Li et al., 2003), spore attachment (Deising et al., 1992; Pascholati et al., 1993) and generation of cutin monomers as signaling molecules (Woloshuk and Kolattukudy, 1986; Podila et al., 1988; Francis et al., 1996) and even in protection of the host plant. Indeed, certain cutin monomers released by fungal cutinases can protect tomato against infection by powdery mildew (Wang et al., 2000). More recently, it has been reported that one of the cutinases of *Magnaporthe* (Cut2) is involved in surface sensing, mediating appressorium differentiation and formation of the penetration peg (Skamnioti and Gurr, 2007, 2008). In *M. graminicola* that enters its host via stomata without appressorium formation (Kema et al., 1996) cutinase most likely has another function. The high number of predicted cutinases in the *M. graminicola* genome, more than in *Neurospora crassa* (N=3) and *Aspergillus nidulans* (N=4), but less than in *Botrytis cinerea* (N=11), *Fusarium graminearum* (N=12) and *M. grisea* (N=7) (Skamnioti et al., 2008) of which two appear active in the apoplast calls for alternative roles in pathogenesis. However, it should be noted that cutinases are not always well defined and some could have lipase activities.

Besides CWDEs, our proteome analysis confirms the secretion of a large number of proteases into the apoplast during colonization of the susceptible cultivar Obelisk. Several different classes of proteases were identified including aspartic proteases, aminopeptidases and carboxypeptidases. Secreted proteases are potential virulence factors in fungi (Monod et al., 2002) and can be involved in degradation of cell wall-embedded proteins but can also play regulatory roles in defence as has been shown for cysteine proteinase avrRpt2 that triggers

RPS2-mediated defence that also requires RIN4 (Axtell and Staskawicz, 2003). In addition, proteases might inactivate PR proteins, although many PR proteins are known to be fairly resistant to proteases (Edreva, 2005). Goodwin et al., (2011) recently compared gene families and PFAM domains of *M. graminicola* with several other fungi and reported that peptidases and α-amylases were significantly expanded suggesting alternative modes of nutrition that may include hydrolysis of proteins and starch, respectively, during the biotrophic phase of infection. In addition, the presence of proteins required as coenzymes, amino acid and lipid transport and metabolism in the susceptible plant at 7 dpi might give more insight in the mechanism of nutrient retrieval from the environment during the biotrophic phase.

Furthermore, proteins that are associated with protection against anti-fungal oxidative stress responses of plants were also identified. The generation of reactive oxygen species (ROS) by plants is an early response to invading pathogens. ROS are not only toxic on their own at fairly high concentrations, but they can also serve as signal molecules at lower concentrations that can trigger different plant defence responses, including the production of PR proteins and phytoalexins (Lamb and Dixon, 1997; Mellersh et al., 2002; Torres and Dangl, 2005; Torres et al., 2006). As a consequence, pathogens use antioxidant defence systems or detoxify ROS (Skamnioti et al., 2007). Catalases and peroxidases are among these oxidative stress-related proteins that protect against oxidative stress and are therefore essential for fungal survival during host invasion but even more so during the necrotrophic phase when massive amounts of ROS including H_2O_2 are present (Skamnioti et al., 2007). It has been suggested that *M. graminicola* is able to colonize susceptible wheat plants by avoiding recognition, suppressing or scavenging H_2O_2 (Shetty et al., 2003; Shetty et al., 2007). Indeed, the antioxidant catalases and peroxidases might degrade H_2O_2 accumulation during various phases of infection. Shetty et al. (2007) showed that infiltration of catalase in wheat leaves effectively scavenged early produced H_2O_2, thus fostering increased penetration, mesophyll colonization and proliferation of the fungus resulting in a decreased latency period. This confirms a crucial role of H_2O_2 in the defence of wheat against *M. graminicola*. However, the fungus can apparently cope with increased H_2O_2 accumulation which likely makes it a successful necrotrophic pathogen. We identified only two proteins of the three catalase/peroxidase genes present in the *M. graminicola* genome during infection of the susceptible plant of which only one appears to be secreted. Indeed, in subsequent experiments, we have shown that only a knock-out mutant of this particular catalase/peroxidase was impaired in pathogenicity (Mehrabi et al., unpublished), a finding

that is not always corroborated in other pathosystems (Garre et al., 1998; Schouten et al., 2002; Robbertse et al., 2003).

In proteomic studies often a large number of proteins with unknown function is identified. In this study, we identified 12 secreted cysteine-rich proteins (3-10 cysteine residues) of which nine were small secreted proteins (SSPs). Several SSPs have shown to exhibit effector functions in other pathosystems (Rep, 2005; Houterman et al., 2007; Bolton et al., 2008). One of the identified SSPs at 21 dpi showed homology with the PhiA protein from *A. nidulans*, which was also identified in AFs of *C. fulvum*-infected tomato (Bolton et al., 2008), where it is involved in phialide and conidium formation, a function that is likely very basic in filamentous ascomycetes (Melin et al., 2003). In addition, it also mapped to the quantitative trait locus for pycnidium development in cv. Obelisk on chromosome 5 (Ware, 2006). We therefore hypothesize that it may also function during pycnidium formation and conidiogenesis in *M. graminicola* and, speculate that it plays an important role in the completion of the disease cycle. The remainder of the SSPs did not have any functional domain, were partially unique to *M. graminicola* and appeared to reside mainly in repetitive DNA stretches located in a rich TE region, a phenomenon also observed for SSPs produced by *Leptosphaeria maculans* (Rouxel et al., 2011).

Here, we presented a global overview of the *M. graminicola* proteins secreted in the wheat apoplast during infection. We anticipate to identify more proteins in the future by applying more sensitive proteome analyses. Particularly during the biotrophic phase where fungal proliferation is slow and biomass is low, we hope to identify additional proteins playing a crucial role in the switch to necrotrophy where fungal proliferation is enormous (Kema et al., 1996; Ware, 2006; Rudd et al., 2008). Obviously, absence of protein sequences in the database will preclude their identification, but lowly abundant fungal proteins could also be easily obscured by highly abundant plant proteins, such as photosynthetic enzymes and structural proteins. The use of a 6 frame translation of the *M. graminicola* genome sequence would help in part to solve this problem, as it identifies non annotated genes and/or corrects erroneous gene models.

In summary, this study provides a first global insight into the *in planta* proteome of *M. graminicola* that complements recent genome analyses (Goodwin et al., 2011). The identified plethora of proteins provides a rich resource for detailed analysis of their role(s) in *M. graminicola* pathogenicity.

MATERIALS AND METHODS

The Dutch *M. graminicola* sequenced reference strain IPO323 was used throughout this study to inoculate seedlings of wheat cvs Obelisk (susceptible) and Shafir (resistant) (Kema et al., 1996; Kema et al., 2000; Brading et al., 2002; Goodwin et al., 2011). Experimental procedures for plant and fungal materials and pre/post-inoculation conditions were as described previously (Kema et al., 1996; Ware, 2006). The inoculated primary leaves of both cultivars were collected at 0, 7, 14 and 21 days post-inoculation (dpi). At each time point, AFs was isolated from ~ 160 plants (16 pots with 10 plants/pot) according to de Wit and Spikman (1982), with slight modifications, and subsequently filtered through a 0.22 µm filter (Millipore. Corp., Bedford, MA), frozen, lyophilized and stored at -20°C until further use.

Protein extractions for SDS-PAGE and LC-MS analysis

Protein extractions started with resuspending AFs in 0.2 ml of 8 M urea, 2 M thiourea, 5 mM diothreitol (DTT) (Sigma-Aldrich Chemie, Steinheim, Germany) followed by incubation for 1 hr at 30°C in a shaker (GFL, Burgwedel, Germany), alkylation of proteins with 15 mM iodoacetamide (IAA) (GE Healthcare, UK) for 30 min. at room temperature (in the dark) and centrifugation (15 min, 15,000 g). A fraction of the supernatant (50 µl) was used for sodium dodecyl sulphate polyacrylamide gel electrophoresis (SDS-PAGE) analysis. For this purpose proteins were precipitated by adding nine volumes of cold acetone, after which the air-dried pellet was heated for 5 min at 95°C in SDS sample buffer. SDS-PAGE was performed on 15% Midget gels (Pharmacia, Co. Sweden, Laemmli 1970) and gels were stained with Coomassie Brilliant Blue R-250 (CBB). Subsequently, the gel was sliced, and gel slices containing (stained) proteins of interest were excised from the lanes for in-gel tryptic digestion and peptide sequencing. Each gel slice was first destained in 40% acetonitrile and 200 mM ammonium bicarbonate for two times for 30 min and then air-dried by vacuum centrifugation (Savant Speedvac, USA) after which trypsin (10 ng/µl) (Sequence grade modified, Promega, WI, USA) was added, followed by overnight incubation at 37°C. Tryptic peptides were extracted with 50% acetonitrile containing 0.1% trifluoroacetic acid (TFA) (Fluka, Buchs, Switzerland) and air-dried by vacuum centrifugation (Shevchenko et al., 1996).

For comparative LC-MS analysis protein samples from AF harvested at 0, 7, 14 and 21 dpi were digested in solution by trypsin. The remainder of the supernatant (150 µl; see above) was diluted with three volumes of 0.1 M ammonium bicarbonate and proteolytic digestion was initiated by adding 2 µl of trypsin (0.2 µg/µl). The sample was subsequently incubated overnight at 37°C, after which the tryptic digestion was terminated by adding TFA to a final concentration of 0.5% (v/v). After centrifugation at 15,000 g for 10 min, the supernatant was cleaned by filtering through a SupelClean™ LC-18 1 ml SPE column (Supelco, Bellefonte, USA) equilibrated with 0.1% TFA and peptides were eluted with 84% acetonitrile (ACN) (HPLC Supra-gradient, Biosolve, Valkenswaard, The Netherlands), containing 0.1% formic acid (FA) (Merck, Darmstadt, Germany) and dissolved in 40 µl 0.1% FA prior to LC-MS analysis.

Comparative LC-MS/MS and LC-MS^E

Label-free data-independent acquisition (DIA) LC/MS^E combined with data-dependent acquisition (DDA) LC-MS/MS approaches allowed detailed identification and quantification of complex protein samples (America et al., 2006; America and Cordewener, 2008; Salvatore et al., 2010). For peptide separation a nanoAcquity UPLC system (Waters Corporation, Manchester, UK) was used with a BEH C18 column (75 µm x 25 cm with 1.7 µm particles, Waters, UK) and a 65 min linear gradient from 3 to 40% ACN (in 0.1 % FA) at a flow rate of 200 nl/min. The eluting peptides were on-line injected into a Synapt Q-TOF MS instrument (Waters Corporation, Manchester, UK). MS analyses were performed in positive mode using Electrospray ionization (ESI) with a NanoLockSpray source. As lock mass [Glu^1]fibrinopeptide B (1 pmol/µl, Sigma) was delivered from a syringe pump (Harvard Apparatus, location, USA) to the reference sprayer of the NanoLockSpray source at a flow rate of 0.2 µl/min and the lock mass channel was sampled every 30 s. Accurate LC-MS data were collected with the Synapt Q-TOF MS instrument operating in either the MS/MS or MS^E mode (DDA and DIA) using low (6 eV) and elevated (ramp from 15 to 35 eV) energy spectra every 0.6 s over a 140-1900 m/z range, respectively. LC-MS/MS was performed by peptide fragmentation on the three most intense multiple charged ions that were detected in the MS survey scan within 0.6 s over a 300-1400 m/z range and a dynamic exclusion window of 60 s with an automatically adjusted collision energy based on the observed precursor m/z and charge state.

Data base construction and data analysis

LC-MS/MS and MS^E data were processed using ProteinLynx Global Server software (PLGS version 2.4, Waters Corporation, Manchester, UK) and the resulting list of masses containing all the fragment information was searched for matching proteins using a merged non-redundant database including all gene models of *M. graminicola* IPO323 (Goodwin et al., 2011) and from COGEME (http://cogeme.ex.ac.uk/sequence.html). Sequences from wheat [TaGI v11 071508] were obtained from the Gene Index Databases, Dana-Farber Cancer Institute, Boston, MA 02115 USA (URL: http://compbio.dfci.harvard.edu/tgi) (Pertea et al., 2003; Lee et al., 2005) and sequences of common contaminants, such as trypsin and keratin, were also included. These databases were merged into a single database using an in-house developed FastaFileMerger tool (FFM) that only maintained the longest protein sequence with 100% homology from repeated sequences. This eventually resulted in a non-redundant database for *M. graminicola* and wheat comprising 238,013 sequences.

For MS^E, the search was performed using the following parameters: a minimum of five fragments ions per peptide and a minimum of nine fragments ions per protein, a minimum of one peptide match per protein and a maximum of one missed trypsin cleavage. Furthermore, we used (i) carbamidomethylation as fixed modification, (ii) oxidation as variable modifications, and (iii) a false positive threshold of four percent. For LC-MS/MS analysis the peptide mass tolerance was set to 50 ppm and a fragment mass tolerance of 0.1 Da. Carbamidomethylation was used as fixed modification, and deamidation and oxidation as variable modifications. The AutoMod search was applied as secondary search to the database search results. The AutoMod analysis tool increases protein coverage by taken into account missed trypsin cleavages and non-specific cleavages, post-translational modifications, and amino acid substitutions. In case of in-gel digested samples, the database search was performed with MASCOT on the FFM merged database, but with precursor and fragment mass tolerance at 0.8 Da and carbamidomethylation as fixed modification and deamidation, oxidation and dioxidation as variable modifications. Finally, the LC-MS/MS and MS^E outputs were further merged and wheat proteins that were identified only once across all time points were not considered for further analysis. Since we used all gene models of *M. graminicola,* additional filtering steps were performed for proteins with alternative models (based on additional peptides obtained but not covered by the present gene models of the *M. graminicola* data base at the United States Department of Energy-Joint Genome Institute, DOE-JGI) and eventually only best (revised) models were used. Furthermore, the

identification of *M. graminicola* proteins was certified if a protein was assigned on at least two peptides with a LC-MS/MS score ≥50 and/or MS^E >5. However, for proteins with only one assigned peptide, particularly for the (small secreted proteins (SSPs), these were kept only when the MS^E score was > 6 and/or for LC-MS/MS when the score was ≥50. Single peptides that overlapped with other proteins with the same identified peptide were excluded (for the single hit protein) from further analysis.

Protein quantification using Progenesis

For quantitative analyses, the MS^E data were processed in Progenesis LC-MS V2.6 (Nonlinear Dynamics, Newcastle, UK), which imported high resolution raw profile data (with lock-spray mass-calibration) into custom mzNLD format and extracted peptide intensity features from MS^E data. The MS^E data of cvs Shafir and Obelisk at time points 0, 7, 14 and 21 dpi (duplicates) were used for quantification. The LC-MS^E chromatograms of all acquired datasets were aligned against a chosen reference run (cv. Obelisk at 14 dpi). Retention time alignment by warping allowed the creation of a single aggregate peak map containing all peak data from all samples of which only 2+, 3+ and 4+ charged peptides were included in the comparison. After peak detection on the aggregate map the intensities were determined for each peak per individual run. The peak intensity data were normalized using the average of peak intensity ratios for each run versus the reference, after removing the outliers (majority of differential peaks). The generation of so-called feature tables allowed then quantitative comparisons of peak intensities between samples. Peptide identification results from Proteinlynx database searches of MS^E data were imported into Progenesis for linking identified peptides to their corresponding peak features. In Progenesis subsequent filtering steps were carried out; number of peptide hits ≥2 over all runs and a ProteinLynx Global SERVER (PLGS), peptide score >5. Consequently, a relative expression profile was generated per peak for the different samples and the different time points. The expression profiles, when at least two or more peptides were assigned to a protein of interest, were checked and peptides were filtered when the alignment was not clear. Multivariate principal component analysis (PCA) was performed with GeneMaths (Applied Maths, Belgium).

Functional characterization of proteins and the identification of conserved domains

Functional annotation was performed using the Blast2GO v2 program (Götz et al., 2008), which enables the annotation of each protein with a GO number and categorizes them

to molecular function, biological process or cellular component. Sequences were directly annotated using BLASTp against the NCBI non-redundant protein sequence database using a cut-off E-value of $1e^{-6}$ and functional domains were searched with InterPro Scan, SignalP, PSORT II, and TMHMM-based algorithms and resulted in level 2 and level 3 analyses, illustrating general functional categories. The Multiloc2 program was used for subcellular localization prediction (Torsten et al., 2009). We used the obtained sequence information to search for conserved domains using the InterPro Scan program (http://www.ebi.ac.uk/Tools/InterProScan/) and online software (Marchler-Bauer et al., 2009) (www.ncbi.nlm.nih.gov/Structure/cdd/wrpsb.cgi) to determine the classifications and possible functions of identified hypothetical proteins.

ACKNOWLEDGEMENTS

The authors thank the US Department of Energy Joint Genome Institute (DOE-JGI) for their excellent work on the Mycosphaerella genome sequence and the members of the International Mycosphaerella Genomics Consortium for discussions. We thankfully remember the late Joost de Groot and his kind provision of the FastaFileMerge tool. We gratefully acknowledge Cris Wijnen for helping with the Progenesis analysis. We also thank Els Verstappen for excellent *M. graminicola* maintenance and greenhouse management and Ineke de Vries for technical assistance. Sarrah Ben M'Barek is sponsored by an UNESCO L'Oréal fellowship.

LITERATURE CITED

Ackerveken, G.F.J.M., Kan, J.A.L., and Wit, P.J.G.M. 1992. Molecular analysis of the avirulence gene avr9 of the fungal tomato pathogen *Cladosporium fulvum* fully supports the gene for gene hypothesis. The Plant Journal 2:359-366.

Adhikari, T.B., Balaji, B., Breeden, J., and Goodwin, S.B. 2007. Resistance of wheat to *Mycosphaerella graminicola* involves early and late peaks of gene expression. Physiological and Molecular Plant Pathology 71:55-68.

America, A., and Cordewener, J. 2008. Comparative LC-MS: a landscape of peaks and valleys. Proteomics 8:731-749.

America, A., Cordewener, J., van Geffen, M., Lommen, A., Vissers, J., Bino, R., and Hall, R. 2006. Alignment and statistical difference analysis of complex peptide data sets generated by multidimensional LC-MS. Proteomics 6:641-653.

Axtell, M.J., and Staskawicz, B.J. 2003. Initiation of RPS2-specified disease resistance in Arabidopsis is coupled to the AvrRpt2-directed elimination of RIN4. Cell 112:369-377.

Bateman, D., and Basham, H. 1976. Degradation of plant cell walls and membranes by microbial enzymes. Encyclopedia of plant physiology 4:316-355.

Bearchell, S.J., Fraaije, B.A., Shaw, M.W., and Fitt, B.D.L. 2005. Wheat archive links long-term fungal pathogen population dynamics to air pollution. Proceedings of the National Academy of Sciences of the United States of America 102:5438-5442.

Bhadauria, V., Banniza, S., Wang, L., Wei, Y., and Peng, Y. 2010. Proteomic studies of phytopathogenic fungi, oomycetes and their interactions with hosts. European Journal of Plant Pathology 126:81-95.

Bolton, M.D., Esse, H.P.V., Vossen, J.H., Jonge, R.d., Stergiopoulos, I., Stulemeijer, I.J.E., Berg, G.C.M.V.D., Borrás-Hidalgo, O., Dekker, H.L., Koster, C.G.D., Wit, P.J.G.M.D., Joosten, M.H.A.J., and Thomma,

B.P.H.J. 2008. The novel *Cladosporium fulvum* lysin motif effector Ecp6 is a virulence factor with orthologues in other fungal species. Molecular Microbiology 69:119-136.

Bowles, D.J. 1990. Defense-Related Proteins in Higher Plants. Annual Review of Biochemistry 59:873-907.

Brading, P.A., Verstappen, E.C.P., Kema, G.H.J., and Brown, J.K.M. 2002. A gene-for-gene relationship between wheat and *Mycosphaerella graminicola*, the Septoria tritici blotch pathogen. Phytopathology 92:439-445.

Cleves, A.E. 1997. Protein transport: The nonclassical ins and outs. Current Biology 7:318-320.

Cohen, L., and Eyal, Z. 1993. The histology of processes associated with the infection of resistant and susceptible wheat cultivars with *Septoria tritici*. Plant Pathology 42:737-743.

Cohen, L., and Eyal, Z. 2007. The histology of processes associated with the infection of resistant and susceptible wheat cultivars with *Septoria tritici*. Plant Pathology 42:737-743.

de Jonge, R., Peter van Esse, H., Kombrink, A., Shinya, T., Desaki, Y., Bours, R., van der Krol, S., Shibuya, N., Joosten, M.H.A.J., and Thomma, B.P.H.J. 2010. Conserved Fungal LysM Effector Ecp6 Prevents Chitin-Triggered Immunity in Plants. Science 329:953-955.

De Lorenzo, G., Castoria, R., Bellincampi, D., and Cervone, F. 1997. Fungal invasion enzymes and their inhibition. The Mycota. V. Plant Relationships, Part B, GC Carroll and P. Tudzynski, eds (Berlin: Springer-Verlag):61–83.

Deising, H., Nicholson, R., Haug, M., Howard, R., and Mendgen, K. 1992. Adhesion pad formation and the involvement of cutinase and esterases in the attachment of uredospores to the host cuticle. The Plant Cell:135-156.

De Wit, P.J.G.M., and Spikman, G. 1982. Evidence for the occurrence of race and cultivar-specific elicitors of necrosis in intercellular fluids of compatible interactions of *Cladosporium fulvum* and tomato. Physiological Plant Pathology 21:1-8.

Dodds, P.N., and Rathjen, J.P. 2010. Plant immunity: towards an integrated view of plant–pathogen interactions 11:539-548.

Douaiher, M., Nowak, E., Durand, R., Halama, P., and Reignault, P. 2007. Correlative analysis of *Mycosphaerella graminicola* pathogenicity and cell wall-degrading enzymes produced in vitro: the importance of xylanase and polygalacturonase. Plant Pathology 56:79-86.

Duncan, K., and Howard, R. 2000. Cytological analysis of wheat infection by the leaf blotch pathogen *Mycosphaerella graminicola*. Mycological Research 104:1074-1082.

Edreva, A. 2005. Pathogenesis-related proteins: research progress in the last 15 years. Gen Appl Plant Physiol 31:105-124.

Esquerré-Tugayé, M.-T., Boudart, G., and Dumas, B. 2000. Cell wall degrading enzymes, inhibitory proteins, and oligosaccharides participate in the molecular dialogue between plants and pathogens. Plant Physiology and Biochemistry 38:157-163.

Eyal, Z. 1999. The *Septoria tritici* and *Stagonospora nodorum* blotch diseases of wheat. European Journal of Plant Pathology 105:629-641.

Fliegmann, J., Mithofer, A., Wanner, G., and Ebel, J. 2004. An ancient enzyme domain hidden in the putative beta- glucan elicitor receptor of soybean may play an active part in the perception of pathogen-associated molecular patterns during broad host resistance. J. Biol. Chem. 279:1132-1140.

Francis, S.A., Dewey, F.M., and Gurr, S.J. 1996. The role of cutinase in germling development and infection by *Erysiphe graminis* f.sp. *hordei*. Physiological and Molecular Plant Pathology 49:201-211.

Garre, V., Müller, U., and Tudzynski, P. 1998. Cloning, Characterization, and Targeted Disruption of *cpcat1*, Coding for an in Planta Secreted Catalase of *Claviceps purpurea*. Molecular Plant-Microbe Interactions 11:772-783.

Goodwin, S.B., Ben M'Barek, S., Dhillon, B., Wittenberg, A.H.J., Crane, C.F., Hane, J.K., Foster, A.J., Van der Lee, T.A.J., Grimwood, J., Aerts, A., Antoniw, J., Bailey, A., Bluhm, B., Bowler, J., Bristow, J., van der Burgt, A., Canto-Canché, B., Churchill, A.C.L., Conde-Ferràez, L., Cools, H.J., Coutinho, P.M., Csukai, M., Dehal, P., De Wit, P., Donzelli, B., van de Geest, H.C., van Ham, R.C.H.J., Hammond-Kosack, K.E., Henrissat, B., Kilian, A., Kobayashi, A.K., Koopmann, E., Kourmpetis, Y., Kuzniar, A., Lindquist, E., Lombard, V., Maliepaard, C., Martins, N., Mehrabi, R., Nap, J.P.H., Ponomarenko, A., Rudd, J.J., Salamov, A., Schmutz, J., Schouten, H.J., Shapiro, H., Stergiopoulos, I., Torriani, S.F.F., Tu, H., de Vries, R.P., Waalwijk, C., Ware, S.B., Wiebenga, A., Zwiers, L.-H., Oliver, R.P., Grigoriev, I.V., and Kema, G.H.J. 2011. Finished Genome of the Fungal Wheat Pathogen *Mycosphaerella graminicola* Reveals Dispensome Structure, Chromosome Plasticity, and Stealth Pathogenesis. PLoS Genet 7(6): e1002070.

Götz, S., Garcia-Gomez, J., Terol, J., Williams, T., Nagaraj, S., Nueda, M., Robles, M., Talon, M., Dopazo, J., and Conesa, A. 2008. High-throughput functional annotation and data mining with the Blast 2 GO suite. Nucleic acids research 36:3420-3435.

Greenberg, J.T. 1997. Programmed cell death in plant-pathogen interactions. Annual Review of Plant Biology 48:525-545.

Hammond-Kosack, K.E., and Rudd, J.J. 2008. Plant resistance signalling hijacked by a necrotrophic fungal pathogen. Plant Signaling & Behavior 3:993-995.

Heath, M.C. 2000. Hypersensitive response-related death. Plant Molecular Biology 44:321-334.

Horbach, R., Navarro-Quesada, A., Knogge, W., and Deising, H. 2011. When and how to kill a plant cell: Infection strategies of plant pathogenic fungi. Journal of Plant Physiology 168: 51-62.

Houterman, P., Speijer, D., Dekker, H., De Koster, C., Cornelissen, B., and Rep, M. 2007. The mixed xylem sap proteome of *Fusarium oxysporum*-infected tomato plants. Molecular Plant Pathology 8:215-221.

Jones, J., and Dangl, J. 2006. The plant immune system. Nature 444:323-329.

Joosten, M., and de Wit, P. 1988. Isolation, purification and preliminary characterization of a protein specific for compatible *Cladosporium fulvum* (syn. *Fulvia fulva*)-tomato interactions. Physiological and Molecular Plant Pathology 33:241-253.

Joosten, M.H.A.J., and De Wit, P.J.G.M. 1989. Identification of several pathogenesis-related proteins in tomato leaves inoculated with *Cladosporium fulvum* (syn. *fulvia fulva*) as 1, 3-β-glucanases and chitinases. Plant physiology 89:945-951.

Joosten, M., and de Wit, P. 1999. The tomato *Cladosporium fulvum* interaction: A Versatile Experimental System to Study Plant-Pathogen Interactions. Annual Review of Phytopathology 37:335-367.

Kamoun, S. 2006. A catalogue of the effector secretome of plant pathogenic oomycetes. 44:41-60.

Kang, Z., and Buchenauer, H. 2000. Cytology and ultrastructure of the infection of wheat spikes by *Fusarium culmorum*. Mycological Research 104:1083-1093.

Kapat, A., Jung, J., and Park, Y. 1998. Improvement of extracellular recombinant glucose oxidase production in fed-batch culture of *Saccharomyces cerevisiae*: Effect of different feeding strategies. Biotechnology Letters 20:319-323.

Kema, G.H.J., Verstappen, E.C.P., and Waalwijk, G. 2000. Avirulence in the wheat septoria tritici leaf blotch fungus *Mycosphaerella graminicola* is controlled by a single locus. Molecular Plant-Microbe Interactions 13:1375-1379.

Kema, G.H. J., Yu, D., Rijkenberg Frits, H.J., Shaw Michael, W., and Baayen Robert, P. 1996. Histology of the pathogenesis of *Mycosphaerella graminicola* in wheat. Phytopathology 86:777-786.

Kema, G.H.J, van der Lee, T.A., Mendes, O., Verstappen, E.C., Lankhorst, R.K., Sandbrink, H., van der Burgt, A., Zwiers, L.H., Csukai, M., and Waalwijk, C. 2008. Large-scale gene discovery in the septoria tritici blotch fungus *Mycosphaerella graminicola* with a focus on in planta expression. Mol Plant Microbe Interact 21:1249-1260.

Keon, J., Antoniw, J., Carzaniga, R., Deller, S., Ward, J., Baker, J., Beale, M., Hammond-Kosack, K., and Rudd, J. 2007. Transcriptional adaptation of *Mycosphaerella graminicola* to programmed cell death (PCD) of its susceptible wheat host. Molecular Plant-Microbe Interactions 20:178-193.

Laemmli, U.K. 1970. Cleavage of Structural Proteins during the Assembly of the Head of Bacteriophage T4. Nature 227:680 685.

Lamb, C., and Dixon, R.A. 1997. The oxidative burst in plant disease resistance. Annual Review of Plant Physiology and Plant Molecular Biology 48:251-275.

Laugé, R., Goodwin, P., de Wit, P., and Joosten, M. 2000. Specific HR-associated recognition of secreted proteins from *Cladosporium fulvum* occurs in both host and non-host plants. The Plant Journal 23:735-745.

Lee, Y., Tsai, J., Sunkara, S., Karamycheva, S., Pertea, G., Sultana, R., Antonescu, V., Chan, A., Cheung, F., and Quackenbush, J. 2005. The TIGR Gene Indices: clustering and assembling EST and known genes and integration with eukaryotic genomes. Nucleic acids research 33:71-74.

Li, D., Ashby, A., and Johnstone, K. 2003. Molecular evidence that the extracellular cutinase Pbc1 is required for pathogenicity of *Pyrenopeziza brassicae* on oilseed rape. Molecular Plant-Microbe Interactions 16:545-552.

Lievens, B., Houterman, P.M., and Rep, M. 2009. Effector gene screening allows unambiguous identification of *Fusarium oxysporum* f. sp. *lycopersici* races and discrimination from other formae speciales. FEMS Microbiology Letters 300:201-215.

Marchler-Bauer, A., Anderson, J.B., Chitsaz, F., Derbyshire, M.K., DeWeese-Scott, C., Fong, J.H., Geer, L.Y., Geer, R.C., Gonzales, N.R., Gwadz, M., He, S., Hurwitz, D.I., Jackson, J.D., Ke, Z., Lanczycki, C.J., Liebert, C.A., Liu, C., Lu, F., Lu, S., Marchler, G.H., Mullokandov, M., Song, J.S., Tasneem, A., Thanki, N., Yamashita, R.A., Zhang, D., Zhang, N., and Bryant, S.H. 2009. CDD: specific functional annotation with the Conserved Domain Database. Nucl. Acids Res. 37:205-210.

Mary Wanjiru, W., Zhensheng, K., and Buchenauer, H. 2002. Importance of cell wall degrading enzymes produced by *Fusarium graminearum* during infection of wheat heads. European Journal of Plant Pathology 108:803-810.

McDougall, P. 2003. The cost of new agrochemical product discovery, development and registration in 1995 and 2000. A Consultancy Study for CropLife America and the European Crop Protection Association.

Mehrabi, R. 2006. Signaling pathways involved in pathogenicity and development of the fungal wheat pathogen *Mycosphaerella graminicola.* Wageningen University, The Netherlands: Ph.D. thesis.

Melin, P., Schnürer, J., and Wagner, E. 2003. Characterization of *phiA*, a gene essential for phialide development in *Aspergillus nidulans*. Fungal Genetics and Biology 40:234-241.

Mellersh, D., Foulds, I., Higgins, V., and Heath, M. 2002. H2O2 plays different roles in determining penetration failure in three diverse plant–fungal interactions. The Plant Journal 29:257-268.

Monod, M., Capoccia, S., Léchenne, B., Zaugg, C., Holdom, M., and Jousson, O. 2002. Secreted proteases from pathogenic fungi. International Journal of Medical Microbiology 292:405-419.

Muthukrishnan, S., Liang, G., Trick, H., and Gill, B. 2001. Pathogenesis-related proteins and their genes in cereals. Plant Cell, Tissue and Organ Culture 64:93-114.

Nickel, W. 2005. Unconventional Secretory Routes: Direct Protein Export Across the Plasma Membrane of Mammalian Cells. Traffic 6:607-614.

Pascholati, S., Deising, H., Leiti, B., Anderson, D., and Nicholson, R. 1993. Cutinase and non-specific esterase activities in the conidial mucilage of *Colletotrichum graminicola*. Physiological and Molecular Plant Pathology 42:37-51.

Perrone, G., Logrieco, A., Kema, G.H.J., Ritieni, A., Bottalico, A. 2000. Phytotoxic activity of *Mycosphaerella graminicola* culture filtrates. Developments in Plant Genetics and Breeding 6:195-201.

Pertea, G., Huang, X., Liang, F., Antonescu, V., Sultana, R., Karamycheva, S., Lee, Y., White, J., Cheung, F., and Parvizi, B. 2003. TIGR Gene Indices clustering tools (TGICL): a software system for fast clustering of large EST datasets. Bioinformatics 19:651-652.

Podila, G., Dickman, M., and Kolattukudy, P. 1988. Transcriptional activation of a cutinase gene in isolated fungal nuclei by plant cutin monomers. Science 242:922-925.

Quaedvlieg, W., Kema, G.H.J., Groenewald, J.Z., Verkley, G.J.M., Seifbarghi, S., Razavi, M., Mirzadi Gohari, A., Mehrabi, R., and Crous, P.W., 2011. *Zymoseptoria* gen. nov.: a new genus to accommodate Septoria-like species occurring on graminicolous hosts. Persoonia 26:57-69.

Rep, M. 2005. Small proteins of plant-pathogenic fungi secreted during host colonization. FEMS Microbiology Letters 253:19-27.

Robbertse, B., Yoder, O.C., Nguyen, A., Schoch, C.L., and Turgeon, B.G. 2003. Deletion of all *Cochliobolus heterostrophus* monofunctional catalase-encoding genes reveals a role for one in sensitivity to oxidative stress but None with a role in virulence. Molecular Plant-Microbe Interactions 16:1013-1021.

Rouxel, T., Grandaubert, J., Hane, J.K., Hoede, C., van de Wouw, A.P., Couloux, A., Dominguez, V., Anthouard, V., Bally, P., and Bourras, S. 2011. Effector diversification within compartments of the *Leptosphaeria maculans* genome affected by Repeat-Induced Point mutations. Nature Communications 2:202.

Rudd, J., Keon, J., and Hammond-Kosack, K. 2008. The wheat mitogen-activated protein kinases TaMPK3 and TaMPK6 are differentially regulated at multiple levels during compatible disease interactions with *Mycosphaerella graminicola*. Plant Physiology 147:802-815.

Russell, P. 2005. A century of fungicide evolution. The Journal of Agricultural Science 143:11-25.

Salvatore, C., Paolo, N., Marco, B., Fredrik, L., Piera, V., Aldo, R., Sergio, C., and Linda, P. 2010. Improved Label-Free LC-MS Analysis by Wavelet-Based Noise Rejection. Journal of Biomedicine and Biotechnology 2010.

Schouten, A., Tenberge, K.B., Vermeer, J., Stewart, J., Wagemakers, L., Williamson, B., and Van Kan, J.A.L. 2002. Functional analysis of an extracellular catalase of *Botrytis cinerea*. Molecular Plant Pathology 3:227-238.

Shetty, N., Kristensen, B., Newman, M., Møller, K., Gregersen, P., and Jørgensen, H. 2003. Association of hydrogen peroxide with restriction of *Septoria tritici* in resistant wheat. Physiological and Molecular Plant Pathology 62:333-346.

Shetty, N., Mehrabi, R., Lutken, H., Haldrup, A., Kema, G.H.J, Collinge, D., and Jorgensen, H. 2007. Role of hydrogen peroxide during the interaction between the hemibiotrophic fungal pathogen *Septoria tritici* and wheat. New Phytologist 174:637-647.

Shetty, N.P., Jensen, J.D., Knudsen, A., Finnie, C., Geshi, N., Blennow, A., Collinge, D.B., and Jorgensen, H.J.L. 2009. Effects of β-1,3-glucan from *Septoria tritici* on structural defence responses in wheat. The Journal of Experimental Botany. 60:4287-4300.

Shevchenko, A., Wilm, M., Vorm, O., and Mann, M. 1996. Mass Spectrometric Sequencing of Proteins from Silver-Stained Polyacrylamide Gels. Analytical Chemistry 68:850-858.

Siah, A., Deweer, C., Duyme, F., Sanssené, J., Durand, R., Halama, P., and Reignault, P. 2010. Correlation of in planta endo-beta-1, 4-xylanase activity with the necrotrophic phase of the hemibiotrophic fungus *Mycosphaerella graminicola*. Plant Pathology 59:661–670.

Skamnioti, P., and Gurr, S. 2007. Magnaporthe grisea cutinase2 mediates appressorium differentiation and host penetration and is required for full virulence. The Plant Cell 19:2674.

Skamnioti, P., and Gurr, S. 2008. Cutinase and hydrophobin interplay: A herald for pathogenesis? 3:248-250.

Skamnioti, P., Furlong, R., and Gurr, S. 2008. Evolutionary history of the ancient cutinase family in five filamentous Ascomycetes reveals differential gene duplications and losses and in *Magnaporthe grisea* shows evidence of sub-and neo-functionalization. New Phytologist 180:711-721.

Skamnioti, P., Henderson, C., Zhang, Z., Robinson, Z., and Gurr, S.J. 2007. A Novel Role for Catalase B in the Maintenance of Fungal Cell-Wall Integrity During Host Invasion in the Rice Blast Fungus *Magnaporthe grisea*. Molecular Plant-Microbe Interactions 20:568-580.

Stergiopoulos, I., and de Wit, P. 2009. Fungal effector proteins. Annual Review of Phytopathology 47:233-263.

Takken, F., and Rep, M. 2009. The arms race between tomato and *Fusarium oxysporum*. Molecular plant pathology 11:309-314.

Thomma, B.P.H.J., Esse, H.P.V., Crous, P.W., and Wit, P.J.G.M.D. 2005. *Cladosporium fulvum* (syn. *Passalora fulva*), a highly specialized plant pathogen as a model for functional studies on plant pathogenic Mycosphaerellaceae. Molecular Plant Pathology 6:379-393.

Thomma, B.P.H.J., Nürnberger, T., and Joosten, M.H.A.J. 2011. Of PAMPs and Effectors: The Blurred PTI-ETI Dichotomy. The Plant Cell 23: 4-15.

Torres, M., and Dangl, J. 2005. Functions of the respiratory burst oxidase in biotic interactions, abiotic stress and development. Current opinion in plant biology 8:397-403.

Torres, M., Jones, J., and Dangl, J. 2006. Reactive oxygen species signaling in response to pathogens. Plant physiology 141:373-378.

Torsten, B., Sebastian, B., and Oliver, K. 2009. MultiLoc2: integrating phylogeny and Gene Ontology terms improves subcellular protein localization prediction. Bmc Bioinformatics 10:274.

Umemoto, N., Kakitani, M., Iwamatsu, A., Yoshikawa, M., Yamaoka, N., and Ishida, I. 1997. The structure and function of a soybean beta-glucan-elicitor- binding protein. Proceedings of the National Academy of Sciences of the United States of America 94:1029-1034.

Wang, C., Chin, C.-K., and Gianfagna, T. 2000. Relationship between cutin monomers and tomato resistance to powdery mildew infection. Physiological and Molecular Plant Pathology 57:55-61.

Ware, S.B. 2006. Aspects of sexual reproduction in Mycosphaerella species on wheat and barley: Genetic studies on specificity, mapping, and fungicide resistance: Genetic studies on specificity, mapping and fungicide resistance. Wageningen University, The Netherlands: Ph.D. thesis.

Woloshuk, C., and Kolattukudy, P. 1986. Mechanism by which contact with plant cuticle triggers cutinase gene expression in the spores of *Fusarium solani* f. sp. *pisi*. Proceedings of the National Academy of Sciences of the United States of America 83:1704-1708.

Wubben, J.P., Joosten, M.H.A.J., Van Kan, J.A.L., and De Wit, P.J.G.M. 1992. Subcellular localization of plant chitinases and 1, 3-β-glucanases in *Cladosporium fulvum* (syn. *Fulvia fulva*)-infected tomato leaves. Physiological and molecular plant pathology 41:23-32.

SUPPLEMENTAL DATA

Table S1. Summary of the *Mycosphaerella graminicola* proteins that were identified in the apoplastic fluids isolated from the resistant (Shafir) and susceptible (Obelisk) wheat cvs at four time points after inoculation with *M. graminicola* strain IPO323 (0, 7, 14 and 21 dpi).

ProteinID [a)]	Loc.[b)]	Gen. Pos. [c)]	Cul. & time pt [d)]	Seq. Description [e)]	Seq. Length [f)]	Min. eValue	Mean Sim.	#GOs	GOs [g)]	Enz. Codes	InterProScan
72330	chr_5	1637435-1639659	S, 7 dpi	conserved hypothetical protein [*Pyrenophora tritici-repentis* Pt-1C-BFP]	490	5,3e-84	57,80%	0			no IPS match
101999	chr_1	476075-477568	S, 21 dpi	peptidyl-prolyl cis-trans isomerase	224	3,5 e-70	77.7%	3	P:protein folding; C:cytoplasm; F:peptidyl-prolyl cis-trans isomerase activity	EC:5.2.1.8	IPR002130; IPR015891; IPR020892; PTHR11071 (PANTHER), PTHR11071:SF70 (PANTHER)
102172	chr_1	1618300-1619574	S, 14 & 21 dpi	zinc-binding dehydrogenase	352	1,3e-137	75.15%	3	F:zinc ion binding; P:oxidation reduction; F:oxidoreductase activity	0	IPR002085; IPR011032; IPR013149; IPR016040; PTHR11695:SF5 (PANTHER), SSF51735 (SUPERFAMILY)
103440	chr_2	3139008-3140849	S, 21 dpi	elongation factor 1-gamma	416	4,1 e-153	72.85%	3	F:translation elongation factor activity; C:eukaryotic translation elongation factor 1 complex; P:translational elongation	0	IPR001662; IPR004045; IPR004046; IPR010987; IPR012335; IPR012336; IPR017933; PTHR11260

											(PANTHER), PTHR11260:SF7 (PANTHER)
103485	chr_2	3479067-3479856	S, 14 & 21 dpi	Cutinase	224	6,3 e-28	54.9%	5	F:molecular_function; P:metabolic process; F:hydrolase activity; P:biological_process; C:cellular_component	0	IPR000675; G3DSA:3.40.50.1820 (GENE3D), SignalP (SIGNALP), SSF53474 (SUPERFAMILY)
103564	chr_3	448714-450470	S, 21 dpi	Homology to stress response protein rds1	519	0.0	73.75%	0	0	0	SignalP (SIGNALP)
103591	chr_3	677070-678160	S, 7 & 21 dpi	superoxide dismutase	154	2,4 e-69	88.0%	7	F:copper ion binding; P:oxidation reduction; C:cytoplasm; P:superoxide metabolic process; F:superoxide dismutase activity; F:antioxidant activity; F:zinc ion binding	EC:1.15.1.1	IPR001424; IPR018152; PTHR10003:SF12 (PANTHER)
103790	chr_3	2150116-2150930	S, 21 dpi	hypothetical protein MGCH7_ch7g1093 [*Magnaporthe oryzae* 70-15]	177	2,3 e-40	53,70%	3	F:molecular_function; P:biological_process; C:cellular_component	0	SignalP (SIGNALP)
103891	chr_3	2795134-2796198	S, 21 dpi	glutathione s-transferase	267	7,5 e-98	68.3%	3	F:helicase activity; F:binding; F:transferase activity	0	IPR004045; IPR004046; IPR010987; IPR012335; IPR012336; IPR017933; PTHR11260 (PANTHER), PTHR11260:SF8 (PANTHER)
104376	chr_5	497461-498831	S, 21 dpi	dienelactone hydrolase family protein	249	3,4 e-91	72.6%	1	F:hydrolase activity	0	IPR002925; G3DSA:3.40.50.1820 (GENE3D),

										PTHR17630 (PANTHER), PTHR17630:SF19 (PANTHER), SSF53474 (SUPERFAMILY)
104697	chr_5	2792882-2793612	S, 21 dpi	small secreted protein	149	7,8 e-21	58.35%	3	F:molecular_function; P:biological_process; C:cellular_component	0	SignalP (SIGNALP)
104794	chr_6	962972-963778	S, 14 dpi	---NA---	157	0	0	0	0	0	SignalP (SIGNALP)
104811	chr_6	1057209-1058327	S, 0 dpi	histone h3	136	4,9 e-67	99.25%	7	C:nucleosome; P:mycelium development; F:DNA binding; P:nucleosome assembly; F:protein binding; C:nucleus; P:DNA repair	0	IPR000164; IPR007125; IPR009072
104907	chr_6	1657807-1658690	S. 21 dpi	Glycoside hydrolase, family 11; endo- -beta-xylanase	225	3,9 e-78	75.85%	2	P:xylan catabolic process; F:endo-1,4-beta-xylanase activity	EC:3.2.1.8	IPR001137; IPR008985; IPR013319; IPR018208; SignalP (SIGNALP)
104911	chr_6	1679481-1680212	S, 14 & 21 dpi; R 21 dpi	Ubiquitin	155	1,9 e-60	96.25%	4	C:ribosome; P:protein modification process; F:structural constituent of ribosome; P:translation	EC:3.6.5.3	IPR000626; IPR002906; IPR019954; IPR019955; IPR019956; G3DSA:3.10.20.90 (GENE3D), PTHR10666 (PANTHER), PTHR10666:SF2 (PANTHER), SSF54236

											(SUPERFAMILY)
105029	chr_7	45580-46668	S, 14 dpi	Peptidase A4, Asparatic protease, scytalidopepsin B	269	3,9 e-22	49.9%	4	P:proteolysis; F:hydrolase activity; F:aspartic-type endopeptidase activity; F:peptidase activity	0	IPR008985; PF01828 (PFAM), SignalP (SIGNALP)
105037	chr_7	215048-215885	S, 21 dpi	glutathione s-	224	9,4 e-72	56.85%	1	F:transferase activity	0	IPR004045; IPR004046; IPR010987; IPR012335; IPR012336; IPR017933; PTHR11260 (PANTHER), PTHR11260:SF8 (PANTHER)
105043	chr_7	234265-236055	S, 21 dpi	gpi-anchored cell wall protein; beta –endoglucanase	480	8,2 e-70	65.15%	1	F:hydrolase activity, acting on glycosyl bonds	0	IPR017853; SignalP (SIGNALP)
105223	chr_7	1219399-1220237	S, 21 dpi	essential for phialid development in aspergillus	188	3,2 e-05	48,14%	0	0	0	SignalP (SIGNALP)
105317	chr_7	2500781-2502585	S, 14 & 21 dpi	Glycoside hydrolase, family 10; endo- -beta- xylanase	347	9,6 e-96	65.15%	2	F:hydrolase activity, acting on glycosyl bonds; P:metabolic process	0	IPR001000; IPR013781; IPR017853; SignalP (SIGNALP)
105322	chr_8	140967-142117	S, 21 dpi	Glycoside hydrolase, family 43; secreted arabinase	319	1,6 e-112	70.1%	2	P:carbohydrate metabolic process; F:hydrolase activity, hydrolyzing O-glycosyl compounds	EC:3.2.1.0	IPR006710; G3DSA:2.115.10.20 (GENE3D), PTHR22925:SF7 (PANTHER), SignalP (SIGNALP), SSF75005

										(SUPERFAMILY)
105408	chr_8	922276-924783	S, 21 dpi	bifunctional catalase-peroxidase cat2	751	0.0	80.35%	4	F:heme binding; P:oxidation reduction; F:catalase activity; P:hydrogen peroxide catabolic process	EC:1.11.1.6	IPR000763; IPR002016; IPR010255; IPR019793; IPR019794; G3DSA:1.10.420.10 (GENE3D), G3DSA:1.10.520.10 (GENE3D)
105677	chr_9	577525-578458	S, 21 dpi	Low homology to IgE binding protein	198	1,3 e-08	45.3%	0	0	0	SignalP (SIGNALP)
105791	chr_9	1802461-1804269	S, 21 dpi	aldehyde dehydrogenase	498	0	87,40%	4	F:aldehyde dehydrogenase (NAD) activity; C:cytoplasm; P:oxidation reduction; P:growth or development of symbiont on or near host	EC:1.2.1.3	IPR015590; IPR016160; IPR016161; IPR016162; PTHR11699:SF46 (PANTHER)
105870	chr_10	310310-311338	S, 21 dpi	Glycoside hydrolase, family 12; endoglucanase a precursor	246	2,2e-64	69.85%	2	F:hydrolase activity, hydrolyzing O-glycosyl compounds; P:polysaccharide catabolic process	EC:3.2.1.0	IPR002594; IPR008985; IPR013319; SignalP (SIGNALP)
106075	chr_11	312607-313691	S, 14 & 21 dpi	lipases ; acetyl xylan esterase	301	3,4 e-136	68.35%	3	C:extracellular region; P:interaction with host via protein secreted by type II secretion system; F:hydrolase activity	0	IPR010126; G3DSA:3.40.50.1820 (GENE3D), PF10503 (PFAM), SignalP (SIGNALP), SSF53474 (SUPERFAMILY)
106105	chr_11	645344-646043	S, 14 & 21	hypothetical protein [*Podospora anserina* S mat+]	156	1,5 e-05	46.8%	0	0	0	SignalP (SIGNALP)

			dpi								
106333	chr_12	590841-591839	S, 21 dpi	hypothetical protein FG09841.1 [*Gibberella zeae* PH-1]	238	6,1 e-39	67,20%	1	P:growth or development of symbiont on or near host	0	SignalP (SIGNALP)
106395	chr_12	1121162-1123790	S, 21 dpi	5-methyltetrahydropteroyltriglutamate-homocysteine methyltransferase	771	0.0	88.6%	4	P:mycelium development; P:methionine biosynthetic process; F:zinc ion binding; F:5-methyltetrahydropteroyltriglutamate-homocysteine S-methyltransferase activity	EC:2.1.1.14	IPR002629; IPR006276; IPR013215; G3DSA:3.20.20.210 (GENE3D), SSF51726 (SUPERFAMILY)
106754	chr_1	374948-376599	S, 14 & 21 dpi	mannitol dehydrogenase NADP-dependent mannitol dehydrogenase [*Passalora fulva*] 6e-133	350	5,3 e-132	87.95%	4	P:oxidation reduction; F:mannitol 2-dehydrogenase (NADP+) activity; F:binding; F:carbonyl reductase (NADPH) activity	EC:1.1.1.138; EC:1.1.1.184	IPR002198; IPR002347; IPR016040; PTHR19410:SF62 (PANTHER), SSF51735 (SUPERFAMILY)
106892	chr_1	1278369-1280116	S, 21 dpi	Aminopeptidase	552	3,6 e-119	65.65%	1	F:hydrolase activity	0	IPR001382; IPR003137; IPR007484; G3DSA:3.40.630.10 (GENE3D), G3DSA:3.50.30.30 (GENE3D), PTHR11742:SF8 (PANTHER), SignalP (SIGNALP), SSF52025 (SUPERFAMILY), SSF53187 (SUPERFAMILY)
107208	chr_1	2831206-	S, 21	alpha-galactosidase 5 precursor	521	9,8 e-129	53.55%	3	P:anatomical structure development; F:hydrolase activity, acting on	0	IPR000111; IPR002241;

		2833105	dpi						glycosyl bonds; P:multicellular organismal development		IPR005084; IPR008979; IPR013785; IPR017853; PTHR11452 (PANTHER), SSF51011 (SUPERFAMILY)
107631	chr_1	4895241-4900979	R, 14 dpi	pisatin demethylase	1168	2,1 e-96	63.75%	1	F:copper ion binding	0	IPR001128; IPR002403; IPR007533; IPR011051; IPR017972; PTHR19383:SF11 (PANTHER)
107650	chr_1	5027950-5030585	S, 14 & 21 dpi	catalase peroxidase hpi	796	0.0	71.45%	4	P:metabolic process; F:iron ion binding; F:peroxidase activity; P:response to oxidative stress	EC:1.11.1.7	IPR000763; IPR002016; IPR006162; IPR010255; IPR019793; IPR019794; G3DSA:1.10.420.10 (GENE3D), G3DSA:1.10.520.10 (GENE3D), SignalP (SIGNALP)
107827	chr_2	310334-312233	S, 14 & 21 dpi	Phosphoglucomutase	554	0.0	87.8%	4	P:glucose metabolic process; C:cytoplasm; F:magnesium ion binding; F:phosphoglucomutase activity	EC:5.4.2.2	IPR005841; IPR005843; IPR005844; IPR005845; IPR005846; IPR016055; IPR016066; G3DSA:3.30.310.50 (GENE3D),

											PTHR22573 (PANTHER), PTHR22573:SF5 (PANTHER), SSF55957 (SUPERFAMILY)
108336	chr_2	3406572-3407604	S, 21 dpi	nad dependent epimerase	283	2,3 e-66	56.3%	0	0	0	PTHR10366 (PANTHER), PTHR10366:SF1 (PANTHER)
108346	chr_2	3476222-3478294	S, 21 dpi	Possible cell adhesion protein	667	0.0	56.65%	1	F:catalytic activity	0	IPR000421; IPR008928; SignalP (SIGNALP)
108472	chr_3	724008-727379	S, 7 dpi	mitochondrial precursor	756	5,0 e-165	81.5%	3	F:iron ion binding; F:ferrochelatase activity; P:heme biosynthetic process	EC:4.99.1.1	IPR001015; IPR019772; G3DSA:3.40.50.1400 (GENE3D), SSF53800 (SUPERFAMILY)
108994	chr_4	718979-721632	S, 14 & 21 dpi	Feruloyl	670	2,5 e-102	57.15%	1	P:growth or development of symbiont on or near host	0	IPR011118; SSF53474 (SUPERFAMILY)
109137	chr_4	1636648-1637355	S, 14 & 21 dpi	---NA---	154	0	0	0	0	0	SignalP (SIGNALP)
109175	chr_4	1830528-1833220	S, 21 dpi	Glycoside hydrolase, family 3; beta-xylosidase	769	0.0	67.65%	3	F:hydrolase activity, acting on glycosyl bonds; P:metabolic process; P:growth or development of symbiont on or near host	0	IPR001764; IPR002772; IPR017853; G3DSA:3.40.50.1700 (GENE3D), SignalP (SIGNALP)

109182	chr_4	1857892-1862465	S, 21 dpi	Glycoside hydrolase, family 3; beta-glucosidase	979	0.0	77.95%	2	F:hydrolase activity, hydrolyzing O-glycosyl compounds; P:polysaccharide catabolic process	EC:3.2.1.0	IPR001764; IPR002772; IPR017853; IPR019800; G3DSA:3.40.50.1700 (GENE3D), SignalP (SIGNALP)
109536	chr_5	1490390-1492833	S, 7 dpi	not2 family protein	532	4,9 e-37	53.65%	3	P:regulation of transcription; F:transcription regulator activity; C:nucleus	0	IPR007282; PTHR23326 (PANTHER)
109538	chr_5	1507739-1510169	S, 7 & 21 dpi	3-isopropylmalate dehydratase	775	0.0	83.95%	4	F:3-isopropylmalate dehydratase activity; C:3-isopropylmalate dehydratase complex; F:4 iron, 4 sulfur cluster binding; P:leucine biosynthetic process	EC:4.2.1.33	IPR000573; IPR001030; IPR004430; IPR004431; IPR012235; IPR015928; IPR015931; IPR015932; IPR015936; IPR015937; IPR018136
109543	chr_5	1526256-1527825	S, 21 dpi	Glycoside hydrolase, family 7 ; cellobiohydrolase d	444	2,3 e-128	68.5%	2	P:carbohydrate metabolic process; F:hydrolase activity, acting on glycosyl bonds	0	IPR001722; IPR008985; SignalP (SIGNALP)
109629	chr_5	2107492-2110472	S, 21 dpi	cystathionine beta-lyase	819	1,0 e-172	84.25%	4	F:pyridoxal phosphate binding; P:cellular amino acid metabolic process; F:cystathionine beta-lyase activity; F:cystathionine gamma-lyase activity	EC:4.4.1.8; EC:4.4.1.1	IPR000277; IPR006238; IPR015421; IPR015422; IPR015424; G3DSA:3.40.50.300 (GENE3D), PTHR11808:SF18 (PANTHER),

											SSF52540 (SUPERFAMILY)
109687	chr_5	2690164-2691472	S, 21 dpi	Peptidase S8 and S53, subtilisin, kexin, sedolisin	400	1,2 e-69	65.35%	1	F:peptidase activity	0	IPR000209; IPR009020; IPR015500; IPR022398; PTHR10795:SF32 (PANTHER), SignalP (SIGNALP)
109715	chr_6	252833-254516	S, 21 dpi	Peptidase M14, carboxypeptidase A	426	4,6 e-104	61.65%	3	F:hydrolase activity; P:growth or development of symbiont on or near host; P:developmental maturation	0	IPR000834; IPR009020; G3DSA:3.40.630.10 (GENE3D), PTHR11705 (PANTHER), PTHR11705:SF11 (PANTHER), SignalP (SIGNALP), SSF53187 (SUPERFAMILY)
109722	chr_6	276467-278545	S, 14 & 21 dpi	---NA---	221	0	0	0	0	0	no IPS match
110047	chr_7	62348-64716	S, 14 dpi	aspartyl protease	441	8,9 e-20	40,60%	4	P:proteolysis; F:aspartic-type endopeptidase activity; F:hydrolase activity; F:peptidase activity	0	IPR001461; IPR002052; IPR009007; IPR021109; PTHR13683:SF78 (PANTHER), SignalP (SIGNALP)

110753	chr_9	985335-990401	S, 21 dpi	TM protein	1139	7,3 e-59	56.9%	4	F:hydrolase activity, hydrolyzing O-glycosyl compounds; P:xylan catabolic process; F:transferase activity; P:carbohydrate metabolic process		IPR000073; IPR006710; G3DSA:3.40.50.1820 (GENE3D), SignalP (SIGNALP), SSF53474 (SUPERFAMILY), SSF75005 (SUPERFAMILY)
110869	chr_9	1779151-1780382	S, 21 dpi	translation initiation factor eif-2b alpha	349	2,1 e-106	71.7%	2	F:translation initiation factor activity; P:cellular metabolic process	0	IPR000649; G3DSA:3.40.50.10470 (GENE3D), PTHR10233:SF7 (PANTHER), SSF100950 (SUPERFAMILY)
111130	chr_10	1379647-1381988	S, 21 dpi	Glycoside hydrolase, family 62; alpha-l-arabinofuranosidase	690	0.0	65.25%	3	F:hydrolase activity, acting on glycosyl bonds; P:metabolic process; P:growth or development of symbiont on or near host	0	IPR010720; IPR017853; SignalP (SIGNALP)
111197	chr_11	342361-344373	S, 14 & 21 dpi	FMN-dependent dehydrogenase	504	8,6 e-110	68.1%	5	F:oxidoreductase activity; F:coenzyme binding; P:metabolic process; P:growth or development of symbiont on or near host; P:response to cAMP	0	IPR000262; IPR008259; IPR012133; IPR013785; PTHR10578 (PANTHER), PTHR10578:SF10 (PANTHER), SignalP (SIGNALP), SSF51395 (SUPERFAMILY)
111590	chr_13	165942-	S, 14 & 21	hypothetical protein [*Podospora*	483	1,7 e-148	68.65%	1	P:growth or development of symbiont	0	SignalP

		167518	dpi	*anserina* S mat+]					on or near host		(SIGNALP)
111695	chr_13	846325-849673	S, 14 & 21 dpi	Glycoside hydrolase, family 31	991	0.0	70.85%	2	P:metabolic process; F:hydrolase activity, hydrolyzing O-glycosyl compounds	EC:3.2.1.0	IPR000322; IPR002044; IPR013783; IPR013784; IPR017853; PTHR22762:SF9 (PANTHER), SignalP (SIGNALP)
99716	chr_3	3025946-3027175	S, 14 dpi	Glycoside hydrolase, family 62; alpha-L-arabinofuranosidase	331	1,4 e-122	79.75%	4	F:xylan 1,4-beta-xylosidase activity; F:alpha-N-arabinofuranosidase activity; P:arabinan metabolic process; P:L-arabinose metabolic process	EC:3.2.1.37; EC:3.2.1.55	IPR008985; IPR013320; IPR015289; SignalP (SIGNALP)
99989	chr_4	2009297-2010187	S, 21 dpi	short-chain dehydrogenase reductase sdr	257	3,5 e-46	66.25%	6	P:oxidation reduction; F:binding; P:response to stress; F:oxidoreductase activity; P:metabolic process; F:catalytic activity	0	IPR002198; IPR002347; IPR016040; PTHR19410:SF98 (PANTHER), SSF51735 (SUPERFAMILY)
100378	chr_5	2773357-2775651	S, 21 dpi	glucose-6-phosphate isomerase	537	0.0	87.75%	4	C:cytoplasm; P:gluconeogenesis; F:glucose-6-phosphate isomerase activity; P:glycolysis	EC:5.3.1.9	IPR001672; IPR018189; G3DSA:3.40.50.10490 (GENE3D), SSF53697 (SUPERFAMILY)
53805	chr_1	4254555-4255738	S, 21 dpi	Pectinesterase	330	1,8 e-104	69.7%	3	F:hydrolase activity, acting on ester bonds; P:interaction with host via protein secreted by type II secretion system; P:cell wall organization	0	IPR000070; IPR011050; IPR012334; IPR018040; SignalP

											(SIGNALP)
55830	chr_2	2908495-2909491	S, 14 & 21 dpi	Glycoside hydrolase, family 62; alpha-n-arabinofuranosidase	321	5,9 e-115	81.0%	2	P:L-arabinose metabolic process; F:alpha-N-arabinofuranosidase activity	EC:3.2.1.55	IPR005193; SignalP (SIGNALP)
62222	chr_9	644786-645985	S, 21 dpi	Quinone	367	9,7 e-108	72.15%	3	F:zinc ion binding; P:oxidation reduction; F:oxidoreductase activity	0	IPR002085; IPR002364; IPR011032; IPR013149; IPR013154; IPR016040; PTHR11695:SF31 (PANTHER), SSF51735 (SUPERFAMILY)
62585	chr_9	1548963-1550926	S, 21 dpi	Glucose-methanol-choline oxidoreductase	555	6,6 e-163	55.8%	3	F:oxidoreductase activity, acting on CH-OH group of donors; P:metabolic process; F:binding	0	IPR000172; IPR007867; PR00411 (PRINTS), G3DSA:3.50.50.60 (GENE3D), PTHR11552 (PANTHER), SignalP (SIGNALP), SSF51905 (SUPERFAMILY), SSF54373 (SUPERFAMILY)
82115	chr_9	842624-843298	S, 21 dpi	Thioredoxin	106	3,5 e-30	75.65%	15	P:cellular response to reactive oxygen species; C:cytosol; P:glycerol ether metabolic process; P:sulfate assimilation; C:fungal-type vacuole; P:retrograde vesicle-mediated transport, Golgi to ER; P:cell redox homeostasis; P:DNA-dependent DNA replication;	0	IPR005746; IPR006662; IPR012335; IPR012336; IPR013766; IPR015467; IPR017936;

									F:electron carrier activity; P:vacuole fusion, non-autophagic; P:ER to Golgi vesicle-mediated transport; C:membrane; C:Golgi apparatus; C:nucleus; F:protein disulfide oxidoreductase activity		IPR017937; PTHR10438:SF16 (PANTHER)
82536	chr_11	320804-322900	S, 14 dpi	cell wall glucanase	233	4,0 e-55	64.8%	1	F:hydrolase activity, acting on glycosyl bonds	0	IPR000490; IPR017853
90052	chr_1	5077954-5083290	S, 14 & 21 dpi; R 21 dpi	Glycoside hydrolase, family 3	1055	0.0	64.1%	1	F:hydrolase activity, acting on glycosyl bonds	0	IPR000626; IPR001764; IPR001878; IPR002772; IPR017853; IPR019800; IPR019955; IPR019956; G3DSA:3.10.20.90 (GENE3D), G3DSA:3.40.50.1700 (GENE3D), PTHR10666 (PANTHER), PTHR10666:SF9 (PANTHER), SignalP (SIGNALP), SSF54236 (SUPERFAMILY)
92097	chr_3	3090563-3091754	S, 14 dpi	glycoside hydrolase family, beta – mannanase	363	2,9 e-44	46,80%	7	F:hydrolase activity, hydrolyzing O-glycosyl compounds; F:carbohydrate binding; F:hydrolase activity; P:carbohydrate metabolic process; F:catalytic activity; F:cation binding; C:extracellular region	0	IPR001547; IPR013781; IPR017853; SignalP (SIGNALP)

92644	chr_4	1779848-1781597	S, 21 dpi	Peptidase A1, pepsin, Aspartic Protease	460	1,2 e-49	45.05%	4	P:proteolysis; F:aspartic-type endopeptidase activity; F:hydrolase activity; F:peptidase activity	0	IPR001461; IPR009007; IPR021109; PTHR13683:SF20 (PANTHER), SignalP (SIGNALP)
94878	chr_8	76855-77391	R, 7 dpi	---NA---	178	0	0	0	0	0	no IPS match
94971	chr_8	481257-483623	R, 14 dpi	c6 transcription	602	9,6 e-123	54.75%	1	F:binding	0	IPR007219
96032	chr_10	138043-141936	R, 7 dpi	mfs transporter	921	2,07 e-123	60.0%	0	0	0	IPR010658; IPR016196; PTHR21576 (PANTHER)
96325	chr_10	1097980-1102694	S, 21 dpi	endonuclease exonuclease phosphatase family protein	1156	0.0	69.3%	1	F:nuclease activity	0	IPR000418; IPR001917; IPR005135
96541	chr_11	418281-420033	S, 21 dpi	conserved hypothetical protein [*Pyrenophora tritici-repentis* Pt-1C-BFP]	497	2,3 e-169	67.1%	1	P:growth or development of symbiont on or near host	0	SignalP (SIGNALP)
97222	chr_12	1351082-1351892	S, 0 dpi	disrupter of telomere silencing protein	228	5,7 e-39	72.6%	2	F:oxidoreductase activity; F:antioxidant activity	0	IPR000866; IPR012335; IPR012336; IPR017936; PTHR10681 (PANTHER), PTHR10681:SF5 (PANTHER)
85504	chr_4	189303-189827	S, 21 dpi	epl1 protein (Cerato-platinin)	149	1,5 e-31	70.85%	2	P:interaction with host via protein secreted by type II secretion system; P:pathogenesis	0	IPR010829; SignalP (SIGNALP)

15713	chr_3	2711711-2712379	S, 14 & 21 dpi; R 21 dpi	Ubiquitin	223	1,8 e-116	99.8%	2	P:mycelium development; P:protein modification process	0	IPR000626; IPR019954; IPR019955; IPR019956; G3DSA:3.10.20.90 (GENE3D), PTHR10666 (PANTHER), PTHR10666:SF9 (PANTHER), SSF54236 (SUPERFAMILY)
21200	chr_6	87406-89533	R,21 dpi	c6 transcription factor	672	2,5 e-167	51.0%	1	F:binding	0	no IPS match
38869	chr_3	1962430-1963771	S, 21 dpi	d-xylose reductase	426	5,5 e-123	80.25%	3	P:oxidation reduction; F:D-xylulose reductase activity; P:D-xylose metabolic process	EC:1.1.1.9	IPR001395; IPR018170; IPR020471; PTHR11732:SF34 (PANTHER)
40059	chr_4	2337703-2338646	R, 14 dpi	short-chain dehydrogenase reductase sdr	277	3,1 e-98	55.8%	3	P:metabolic process; F:oxidoreductase activity; F:binding	0	IPR002198; IPR002347; IPR016040; IPR020904; PTHR19410:SF85 (PANTHER), SSF51735 (SUPERFAMILY)
43394	chr_6	1659594-1660595	S, 21 dpi	Cutinase	232	3,4 e-61	68.35%	2	P:carbohydrate metabolic process; F:hydrolase activity	0	IPR000675; G3DSA:3.40.50.1820 (GENE3D), SignalP (SIGNALP), SSF53474 (SUPERFAMILY)

43998	chr_6	2347520-2348298	S, 14 & 21 dpi	metalloprotease 1	239	2,1 e-48	62.3%	1	P:interaction with host via protein secreted by type II secretion system	0	IPR008754; PTHR19325 (PANTHER), PTHR19325:SF53 (PANTHER), SSF55486 (SUPERFAMILY)
44631	chr_7	626639-628143	S, 7 dpi	l-serine	477	6,2 e-88	64.25%	1	F:catalytic activity	0	IPR000634; IPR001926; G3DSA:3.40.50.1100 (GENE3D), PTHR10314 (PANTHER), PTHR10314:SF10 (PANTHER)
49185	chr_10	941292-941590	S, 14 & 21 dpi	Ubiquitin	99	8,3 e-46	97.55%	12	F:binding; F:protein tag; F:oxidoreductase activity; F:structural constituent of ribosome; P:ribosome biogenesis; P:protein ubiquitination; P:oxidation reduction; C:cytosolic large ribosomal subunit; C:nucleus; P:translation; C:mitochondrion; P:DNA repair	EC:3.6.5.3	IPR000626; IPR001975; IPR019954; IPR019955; IPR019956; G3DSA:3.10.20.90 (GENE3D), PTHR10666 (PANTHER), PTHR10666:SF9 (PANTHER), SSF54236 (SUPERFAMILY)
49989	chr_11	140248-141100	S, 7 dpi	acyl-protein thioesterase 1/esterase lipase superfamily	254	2,5 e-47	51.5%	2	F:hydrolase activity; C:intracellular part	0	IPR003140; G3DSA:3.40.50.1820 (GENE3D), PTHR10655 (PANTHER), PTHR10655:SF6 (PANTHER), SSF53474

											(SUPERFAMILY)
51592	chr_14	324822-328051	S, 21 dpi	patatin-like serine	981	4,0 e-133	46.4%	8	P:lipid metabolic process; F:metal ion binding; F:phospholipase A2 activity; P:metabolic process; F:hydrolase activity; F:zinc ion binding; P:lipid catabolic process; F:protein binding	0	IPR002641; IPR016035; IPR017907; PTHR18958 (PANTHER), PTHR18958:SF57 (PANTHER)

[a)] ProteinID from JGI (http://genomeportal.jgi-psf.org/Mycgr3/Mycgr3.home.html)
[b)] Chromosomal location on *Mycosphaerella graminicola* strain IPO323 genome
[c)] Genomic coordinates (bp)
[d)] S: Susceptible cultivar (Obelisk), R: Resistant cultivar (Shafir)
[e)] Sequence description from Blast2Go functional annotation tool
[f)] Amino acid length
[g)] GO term provided for molecular function from Blast2Go functional annotation tool
*--NA--: no GO term identified.

Chapter 5

The septoria tritici blotch pathogen *Mycosphaerella graminicola* secretes proteins in culture media that differentially induce necrosis in wheat

Sarrah Ben M'Barek, Jan H.G. Cordewener, Mahmod Tabib Ghaffary, Theo A.J. van der Lee, Zhaohui Liu, Rahim Mehrabi, Antoine H.P. America, Timothy L. Friesen, Sonia Hamza, Pierre J.G.M. de Wit and Gert H.J. Kema

Manuscript in preparation

ABSTRACT

Culture filtrates (CFs) of the fungal wheat pathogen *Mycosphaerella graminicola* were assayed for necrosis-inducing activity after infiltration in leaves of various wheat cultivars. Fractions with activity were partially purified and characterized. The necrosis-inducing factors in CFs are proteinaceous, heat stable and their necrosis-inducing activity is temperature and light dependent. The *in planta* activity of CFs was tested by a time series of proteinase K co-infiltrations, which was unable to affect activity 30 min after CF infiltrations. This indicates that the necrosis inducing proteins (Nips) are mostly absent from the apoplast within that short time frame and likely actively transported into mesophyll cells. This is reminiscent of the activity of host-selective toxins of other Dothideomycete pathogens such as *Stagonospora nodorum* and *Pyrenophora tritici-repentis*. Further purification and fractionation of the CFs with the highest necrosis-inducing activity involved fast performance liquid chromatography, sodium dodecyl sulphate-polyacrylamide electrophoresis and mass spectrometry. This revealed that most of the proteins present in the fractions have not been described before. The two most prominent MgNip candidates were heterologously expressed in *Pichia pastoris* and subsequent infiltration assays showed their differential activity in a range of wheat cultivars. The genes encoding these proteins reside on chromosomes 11 and 5 of the *M. graminicola* genome and are designated *MgNip1* and *MgNip2*.

INTRODUCTION

Phytopathogenic fungi exhibit different lifestyles and modes of interaction with their host plants (Horbach et al., 2011). Biotrophic fungi have an intimate relationship with their host. They colonize living cells and secrete effectors, whose intrinsic function is to manipulate the host. However, they can also act as avirulence factors or elicitors that directly or indirectly interact with resistance genes often leading to the typical resistance protein-mediated hypersensitive response (HR). This phenomenon is also known as effector- triggered immunity (ETI) and is characteristic for pathosystems that comply with the "gene-for-gene" interaction (GFG) (Flor, 1971; Keen, 1990; Ackerveken et al., 1992; Jones and Dangl, 2006; Dodds et al., 2009; Thomma et al., 2011). Necrotrophic fungal pathogens are assumed to overcome defense responses by producing low-molecular-weight secondary metabolites or proteinaceous toxins that perturbate host cells, causing leakage of cell contents that are used as nutrients by the pathogen (Howlett, 2006). Host-selective toxins (HSTs), either proteins or secondary metabolites, are determinants of pathogenicity or virulence of necrotrophs and are produced by a range of fungal genera, particularly in the *Dothideomycetes.* This class of fungi comprises the largest and ecologically most diverse group of *Ascomycetes* with approximately 20,000 species (Hane et al., 2011), including many plant pathogenic genera such as *Alternaria*, *Cochliobolus*, *Leptosphaeria*, *Venturia*, *Ascochyta* and *Pyrenophora* (Friesen et al., 2008a). Several HSTs, such as PtrToxA, SnToxA, SnTox1, SnTox2, SnTox3 and SnTox4, in the cereal necrotrophs *Pyrenophora tritici-repentis* and *Stagonospora nodorum*, have been identified and characterized. They induce necrosis and promote disease development in toxin-sensitive wheat plants in a light-dependent manner (Liu et al., 2004; Friesen et al., 2008b; Friesen et al., 2009; Manning et al., 2009). In contrast to GFG interactions that mostly involve dominant resistance genes in the host, susceptibility to necrotrophs was found to depend on the presence of dominant sensitivity genes and these interactions are therefore recently considered as inverse GFG (iGFG) (Friesen et al., 2008a; Friesen and Faris, 2010). The underlying mechanism has been named effector-triggered susceptibility (ETS), but irrespective whether systems comply with GFG or iGFG the involved effectors operate in a species- and cultivar-specific manner (Wolpert et al., 2002; Friesen et al., 2008a; De Wit et al., 2009).

Mycosphaerella graminicola (Fuckel) J. Schröt. in *Cohn* (anamorph *Zymoseptoria tritici* (Desm.) Quaedvlieg & Crous) (Quaedvlieg et al., 2011), the causal agent of the septoria tritici blotch (STB) disease of wheat, is a Dothideomycete hemibiotroph that has an initial

biotrophic and subsequent necrotrophic phase. *M. graminicola* enters the host through the stomata without formation of an appressorium (Kema et al., 1996a). The biotrophic phase of hemibiotrophs varies substantially in length, for instance 10 and 30 days for the related *M. graminicola* and the banana black Sigatoka pathogen *M. fijiensis*, respectively (Kema et al., 1996a; Churchill, 2010). During this latent symptomless phase there is hardly any macroscopic symptom and fungal biomass development (Kema et al., 1996a; Ware, 2006; Rudd et al., 2008). Recently, we showed that the genome of *M. graminicola* contains very few cell-wall degrading enzymes suggesting that it avoids host defence during the biotrophic stage of infection by turning on genes encoding proteases possibly amylases to degrade starch from chloroplasts that are released during cell collapse, a mechanism that might have been evolved from endophytic ancestors (Goodwin et al., 2011). The transition from biotrophy to necrotrophy is accompanied by a reduction in photosynthesis, a massive accumulation of H_2O_2, leading to cell death and necrosis (Shetty et al., 2003; Shetty et al., 2007). Finally the fungus produces numerous asexual and - under natural conditions - sexual fructifications, the pycnidia and pseudothecia, respectively (Kema et al., 1996a; Kema et al., 1996b). Very little is known about the mechanism of this switch in lifestyle (Keon et al., 2007; Kema et al., 2008), but several reports suggested that during the biotrophic phase the fungus prepares for the necrotrophic phase by turning on enzymes or pathways for the production of secondary metabolites compounds and proteins (Kema et al., 1996a; Perrone, 2000; Shetty et al., 2003; Shetty et al., 2007; Rudd et al., 2008; Shetty et al., 2009). For instance, early chloroplast condensation in wheat mesophyll cells without proximate *M. graminicola* hyphae suggested that toxic fungal compounds affect cell integrity (Kema et al., 1996a). In many pathogens, necrosis is part of the resistance response that can be very local and restricts the pathogen from further colonization. The classical HR occurring in the incompatible interaction of (obligate) biotrophic fungal pathogens is a good example of that response (Dangl and Jones, 2001; Keon et al., 2007; Rudd et al., 2008). In *M. graminicola* pathogenesis, however, necrosis is associated with compatibility that seems to facilitate fungal proliferation (Keon et al., 2007; Rudd et al., 2008).

Since HSTs are such prominent pathogenicity factors in related Dothideomycete pathogens, we were interested to investigate whether *M. graminicola* does produce similar proteins that might be involved in the above described biotrophy-necrotrophy switch. Here, we report the production, purification and characterization of *M. graminicola* culture filtrates (CFs) by exploiting the fungus' finished genome sequence of strain IPO323 (Goodwin et al., 2011) and identified a range of candidate Nips. Two of them, which we designate as MgNip1

and MgNip2 are encoded by the genes *MgNip1* and *MgNip2* and differentially induce chlorosis and necrosis in different wheat cultivars.

RESULTS

Necrosis-inducing activity and preliminary characterization of *M. graminicola* culture filtrates

The CFs showed necrosis-inducing activity on 20 wheat cultivars, irrespective whether they are susceptible or resistant to *M. graminicola* strain IPO323 despite some slight quantitative differences (Table 2, Fig. 1). Similar results were observed with CFs from other strains such as IPO94269 and IPO95052 that are virulent on bread wheat and durum wheat, respectively (data not shown).

Preliminary characterization of the CFs included determination of the effect of different temperatures, light conditions on necrosis inducing activity and the proteinaceous character of the CFs was tested by sensitivity to *in vitro* digestion with Proteinase K (PK). Necrosis inducing activity appeared sensitive to heat treatment as incubation of CFs at 100°C strongly reduced its necrosis inducing activity (Fig. 2). Furthermore, necrosis inducing activity of CFs was degraded after PK treatment whereas *in planta* PK treatment at different time points after CFs infiltration resulted in a gradual increase of necrosis intensity (%) over time until 2 hrs after infiltrations when necrosis inducing activity was no longer induced by this treatment (Fig. 2). In addition, necrosis inducing activity appeared to be dependent of light. After incubation of CFs for 48 hrs in darkness, no necrosis inducing activity was observed, but after exposure of these, darkness-incubated leaves to light again, necrosis inducing activity became clearly visible (Fig. 2).

Fractionation of culture filtrates

To characterize the protein(s) responsible for necrosis-inducing activity in more detail, dialyzed CFs were applied to a cation-exchange HiTrap column. The bound proteins were eluted with a linear salt gradient and collected in 12 fractions (Fig. 3). All fractions containing proteins, including the flow-through of the HiTrap column, were subsequently tested in necrosis inducing activity assays. The highest necrosis inducing activity was observed in fraction 5 that was recovered from the HiTrap column at approximately at 0.18 M NaCl, with some activity in fractions 6 and 7 (Fig. 3). No significant necrosis inducing activity occurred

Table 2. Percentages necrosis and pycnidia formation on the primary leaves of 20 bread-wheat accessions at 21 days after inoculation with *Mycosphaerella graminicola* strain IPO323.

Cultivar	**Origin**	**Symptom development**	
		Necrosis %	Pycnidia %
Apache	France	100	80
Baguette11	France	50	0
Balance	France	25	0
Bermude	France	100	25
BR34	Brazil	5	0
Cordiale	France	100	80
FD3	France	80	60
FD12	France	100	10
Grandin	USA	5	0
Kulm	USA	0	0
M3	CIMMYT	0	0
Mazurka	Hungary	100	30
Nogal	France	5	0
Nuage	France	5	0
Obelisk	The Netherlands	100	70
Rubigus	France	20	0
SE11	France	5	0
Soissons	France	100	60
Solitär	Germany	5	0
Timber	France	0	0

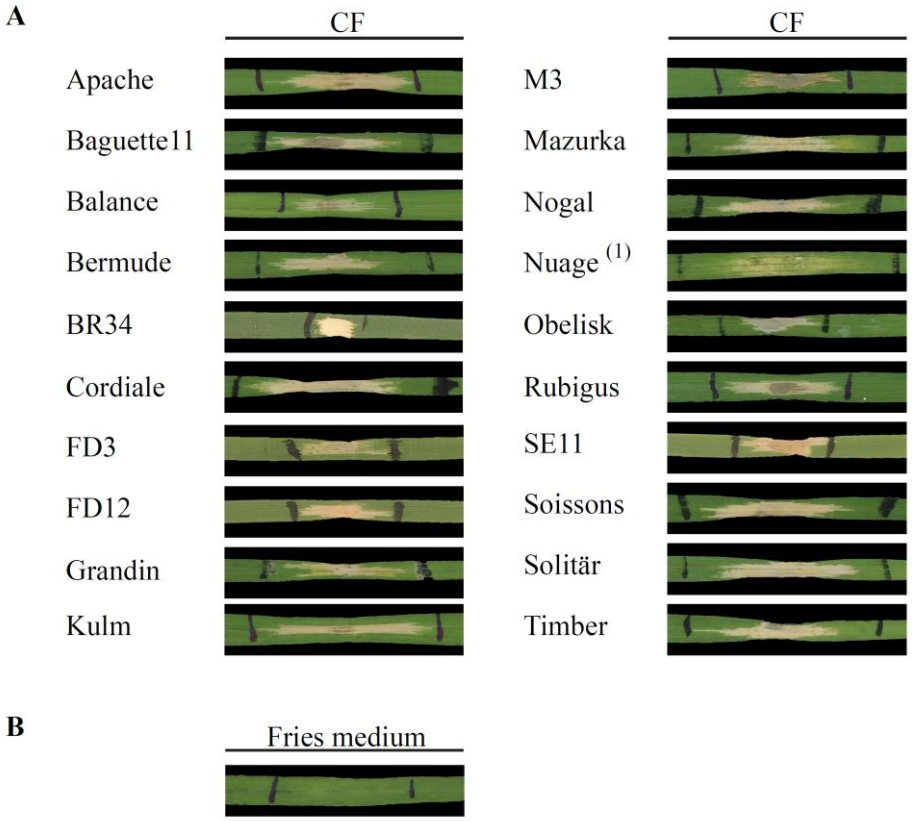

Fig. 1. Necrosis-inducing activity of CFs from *Mycosphaerella graminicola* strain IPO323 in 20 wheat cultivars at four days after-infiltration **(A)** using Fries medium in cv. Obelisk as a control **(B)**.
[1)] Reduced necrosis-inducing activity compared to other cultivars

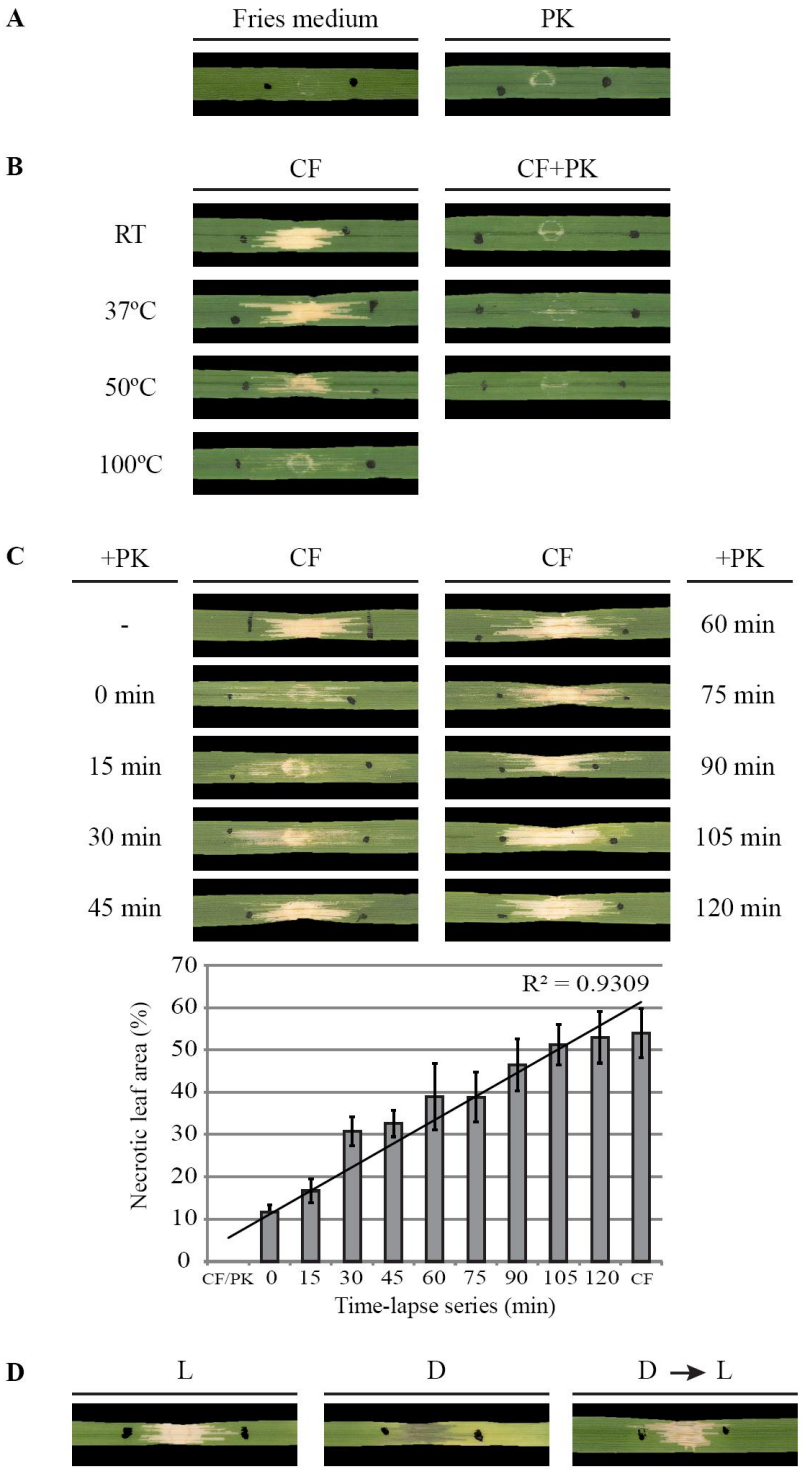

Fig. 2. Necrosis-inducing activity of *Mycosphaerella graminicola* strain IPO323 culture filtrates (CFs) in the sensitive wheat cv. Obelisk after different treatments. **A.** Fries medium and Proteinase K (PK) controls. **B.** The effect of temperature and *in vitro* Proteinase K treatments on necrosis-inducing activity of CFs. **C.** The *in planta* effect of proteinase K treatment (100 µl of 1 mg/ml) at different time points on CF-infiltrated leaves from 0 to 120 min. Below: Chart displaying time-lapse series (min.) of *in planta* PK infiltration of CFs-infiltrated leaves **D.** The effect of light on necrosis inducing activity of CFs. Assays were placed under ambient light conditions (L), in darkness for 72 hrs (D), or exposed to ambient light after 48 hrs of darkness (D->L). Black dots on leaves delimit the infiltrated area.

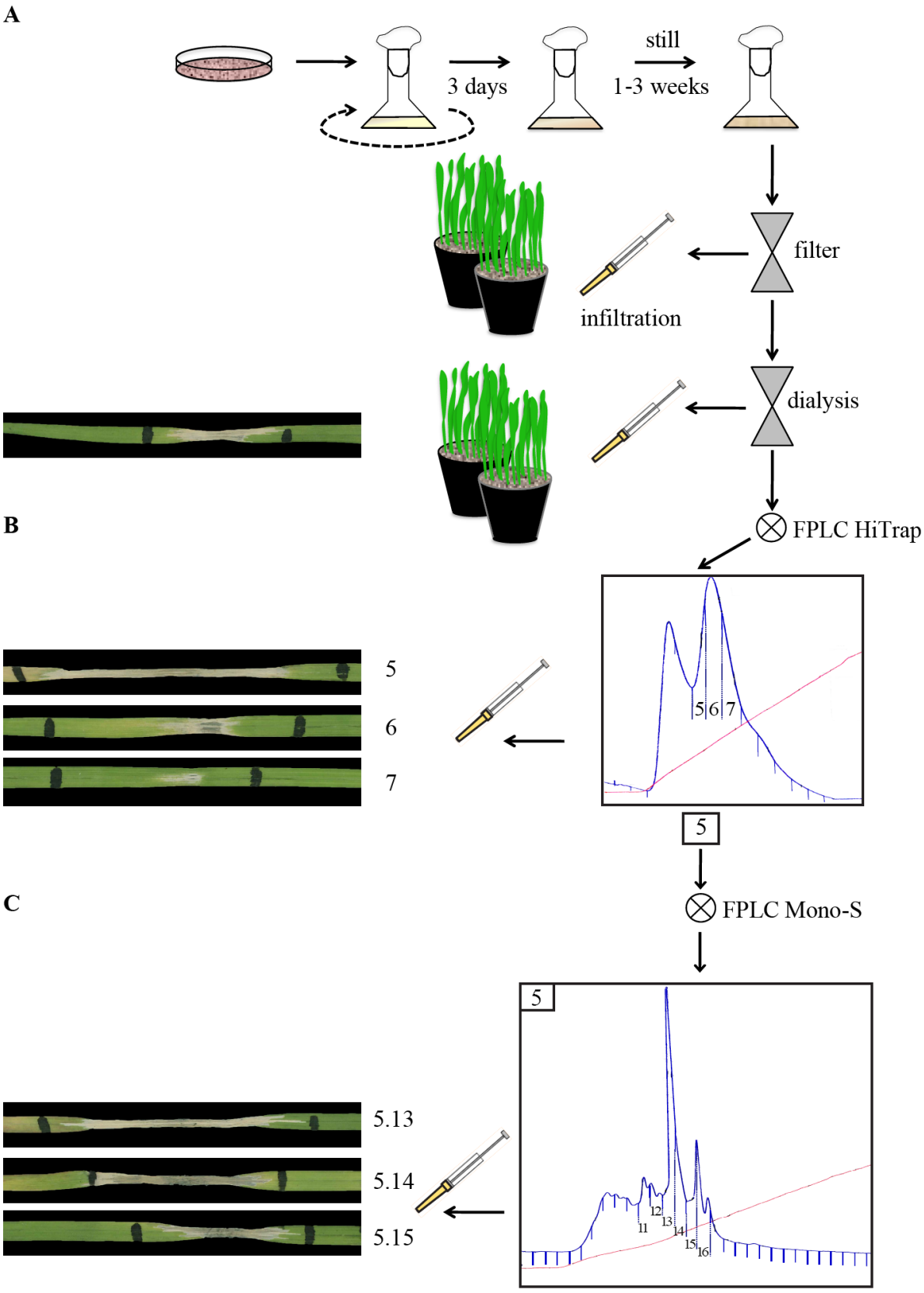

Fig. 3. Schematic representation of the purification procedure of culture filtrates (CFs) of *Mycosphaerella graminicola* strain IPO323 and necrosis inducing activity assays in cv. Obelisk. **A.** *M. graminicola* was grown on V8-PDA agar medium for 5-10 days; spores were collected and transferred to liquid Fries medium. Flasks were incubated in a shaker for three days at 27°C at 100 rpm followed by two to three weeks of stationary growth

at 21°C in the dark. CFs were filtered, dialyzed and infiltrated. **B.** Dialyzed CF was applied to a FPLC HiTrap strong cation-exchange column and the bound proteins were eluted in different fractions and assayed for necrosis inducing activity. **C.** Fraction 5 was further purified using a FPLC Mono-S strong cation-exchange column, the collected fractions were assayed for necrosis inducing activity and fractions 5.13-5.15 were further analyzed by SDS-PAGE. Fraction 5.14 was further analyzed by mass spectrometry for identification of the proteins. The red lines in the chromatograms are NaCl gradients (0-0.5M, blue lines are absorbances at 280 nm. The profile of the effluent containing the non-bound proteins is omitted from the chromatogram.

when seedlings were infiltrated with any of the other eluting fractions or with the unbound proteins present in the flow-through of the HiTrap column. Further purification of fraction 5 on an analytical cation-exchange FPLC column (Mono-S) yielded a more complex absorption pattern at 280 nm (Fig. 3). Fractions 5.13, 5.14, 5.15 that eluted from the Mono-S column between 0.16 and 0.2 M NaCl showed the highest necrosis inducing activity in the infiltration assay. These were subsequently analyzed by SDS-PAGE that revealed that the necrosis-inducing fractions 5.13-5.15 still contained several protein bands over a broad molecular mass range that clearly differed from the band profiles of fractions 5.12 and 5.16 in the neighboring lanes that did not show activity upon infiltration. Fraction 5.14 was subsequently analyzed by mass spectrometry (Fig. 4).

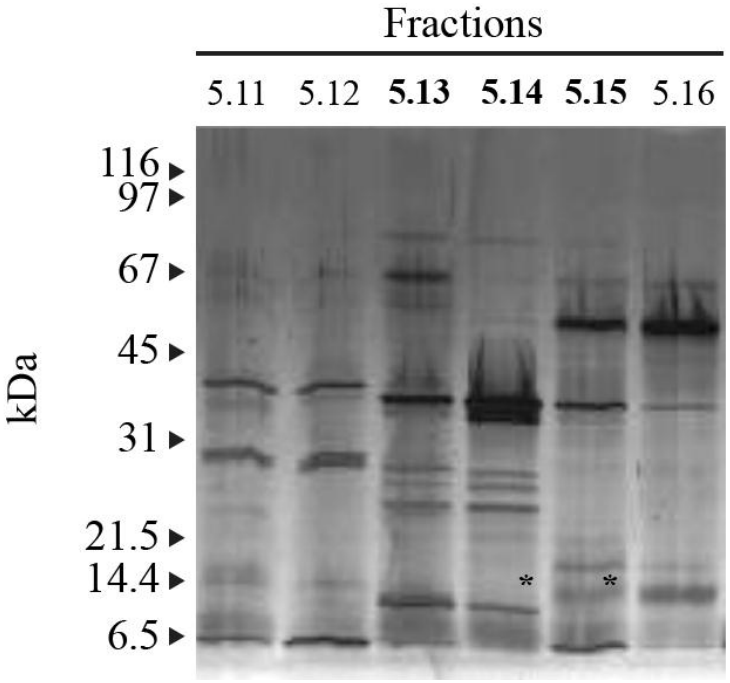

Fig. 4. Silver stained SDS-PAGE gel of protein fractions eluted from the Mono-S HR 5/5 cation exchange column by a 0-0.5 M NaCl gradient. Fraction numbers correspond to those presented in Fig. 3. The fraction numbers shown in bold contained the highest necrosis-inducing activity. Fraction 5.14 was analyzed by mass spectrometry. M: standard molecular weight markers (kDa values are indicated). Asterisk indicates the relative position of the two identified proteins (see text) after removal of the signal peptide, approximately between 15 and 16.9 kDa in 5.14. MgNip1 was also present in 5.15.

Characterization of proteins with necrosis inducing activity by mass spectrometry

LC-MS analysis of the tryptic digests of the partially necrosis inducing fraction 5.14 yielded peptide matches with 13 proteins (Table 3) in the merged database that matched characteristics of secreted hypothetical proteins. Two proteins contained a transmembrane domain and seven proteins contained conserved domains. We identified Nip candidates that also had EST support. The first protein matched with five peptide sequences, representing approximately 34% of the theoretical length of a ~17 kDa protein and in encoded by a gene that is located on chromosome 11 (genomic coordinates 1118374-1119074 bp). It encodes a predicted protein of 162 amino acids (aa) including the predicted 19 aa signal peptide and contains four cysteine residues. . The gene contains a putative TATAAA box 134 bp upstream of the start codon (Fig. 5).

Sequence analyses with PSI-Blast revealed low matches with a hypothetical protein SNOG_04278 of *S. nodorum* (42.4 bits, E-value 0.022) and Ecp2 of *C. fulvum* (0.34 bits, E-value 0.48). Interestingly, peptides did not map to the best predicted model ascribed to this gene, which indicates that this gene was apparently wrongly annotated. We have designated this gene as *MgNip.1.* The second protein matched with two peptide sequences found by LC-MS, representing approximately 17% of the theoretical length of a ~18.7 kDa protein that is encoded by a gene located on chromosome 5 with coordinates 1287999-1288716 bp and contains one intron. The predicted protein is 178 aa in length, including the predicted 18 aa signal peptide and contains four cysteine residues (Fig. 5). Blasting the protein sequence revealed homology with a putative ML (MD-2-related lipid-recognition) domain from *Aspergillus clavatus* (181 bits, E-value $5e^{-44}$) and with a phosphatidylglycerol/phosphatidylinositol transfer protein precursor from *P. tritici-repentis* (178 bits, E-value $3e^{-43}$). We have designated this gene as *MgNip2.*

Table 3. Summary of the most interesting proteins of *Mycosphaerella graminicola* strain IPO323 that were present in the partially purified active fraction 5.14 and identified by mass spectrometry.

JGI Header [a)]	Method	Pep. No [b)]	Pep. Score [c)]	Tot. aa. [d)]	Gen. Pos. [e)]	Domains [f)]	BlastP (nr) [g)]
estExt_Genewise1Plus.C_chr_22216 *	LC-MS/MS –MS^{E}	DIQVSTDHGATWQSGLTR	6,9	215	chr_2:3662482-3663264	IPR012997 Rare lipoprotein A, bacterial IPR018226 Barwin, conserved site	Hypothetical protein [*Leptosphaeria maculans*] (209 bits, E value 2 e^{-52})
		SAGFGVDVVDLK	6,3				
		EGVSANWFSVQAVNASK	5,3				
		EGVSANWFSVQAVN	5,2				
		WFSVQAVNASK	5,1				
		VSTDHGATWQSGLTR	6,3				
		AGFGVDVVDLK	50,8				
		GFGVDVVDLK	66,7				
		MDYNFFQK	73,3				
		SAGFGVDVVDLK	75,4				
estExt_fgenesh1_kg.C_chr_120103	LC-MS/MS –MS^{E}	IAFPNPTIVEGSNIR	7,2	238	chr_12:590841-591839	CHRD domain [&]	Hypothetical protein GLRG_09422 [*Glomerella graminicola* M1.001] (197 bits, E-value 1e^{-48})
		IAFPNPTIVE	5,4				
		GSNIR	6,1				
		EGSNIR	6,4				
		IAFPNPTIVEGSNIR	69				
estExt_fgenesh1_pg.C_chr_50636	LC-MS/MS –MS^{E}	*AAYLIGLEGTR*	68,2	400	chr_5:2690164-2691472	IPR000209 Peptidase S8 and S53, subtilisin, kexin, sedolisin	Hypothetical protein SS1G_12605 [*Sclerotinia sclerotiorum* 1980 UF-70] (289 bits, E-value 6e^{-76})
		ALVSQNPSTWGLSR	7,3				
		ALVSQNPSTWGLSRISSR	5,3				
		VLSSSGSGSLAGIINGIDWAVNDAR	6,4				
estExt_fgenesh1_kg.C_ch	MS^{E}	VDLNPNPPR	5,9	178	chr_5:1287999-	IPR003172 MD-2_lipid-	ML domain protein,

r_50194					1288716	recog	putative [*Aspergillus clavatus* NRRL 1] (181 bits, E-value $5e^{-44}$)
		YGLITIINQSADLCETVK	5,5				
fgenesh1_pg.C_chr_50001 49	MS^{E}	GVAPHTPHTCNIPLTNSPA YIGLDAVR	6,1		chr_5:721092-721741		Hypothetical protein AURANDRAFT_64293 [*Aureococcus anophagefferens*] (35.8 bits, E-value 3.2)
		YVGEHTPSGPPS	6,9	193			
fgenesh1_pg.C_chr_30004 49 *	MS^{E}	GLPQPITSVR	6,1	289	chr_3:1812934-1813906	IPR000490 Glycoside hydrolase, family 17	Hypothetical protein SS1G_12930 [*Sclerotinia sclerotiorum* 1980 UF-70] (273 bits, E-value $2e^{-71}$)
		ALGSNAPVGHVDTWNA WVNPGTDVVTK	5,7				
		GGLDINRLAEQIYDVR	5				
		PQPITSVR	6				
fgenesh1_pg.C_chr_30001 19 #	LC-MS/MS	*FGNPLVQNNR*	66,7	130	chr_3:487068-488324		Predicted protein [*Naegleria gruberi*] (35.8 bits,E-value 2.1)
fgenesh1_pg.C_chr_20009 75	LC-MS/MS –MS^{E}	WSCVSGWNGQFR	7,5	130	chr_2:3780747-3781139		Hypothetical protein ANI_1_1820144 [*Aspergillus niger* CBS 513.88] (38.9 bits, E-value 0.24)
		GWNGQFR	59				
		VSGWNGQFR	72,5				
		WSCVSGWNGQFR	50,7				
fgenesh1_kg.C_chr_10000 105 *	LC-MS/MS –MS^{E}	NAGTEVTGYICPFKEFSFE K	5,7	95	chr_10:647562-648168		-
		NAGTEVTGYICPFK	78				
		LVR	5,3				
		FEK	5,2				
		NAGTEVTGYI	5,4				
		YCT	5,1				
		GTEVTGYICPFK	6,9				
		YCTLV	6				
		YCTLVR	5,6				

		EFSFEK	5,9				
		YCTLVR	54,5				
fgenesh1_kg.C_chr_8000039 # *	LC-MS/MS –MS^{E}	*LLPPPIPCR*	54,9	56	chr_8:444347-444909		-
		LLPPPIPCR	7,1				
		PPPIPCR	7,8				
		PPIPCR	6,9				
		CASLV	5,9				
		SLVLPVCR	6,8				
Ext_fgenesh1_kg.C_chr_100227	LC-MS/MS	*VACPADLVSR*	52,6	240	chr_10:1542406-1543537	IPR001209 Ribosomal protein S14 0008810 cellulase activity IPR000334 Glycoside hydrolase, family 45	Hypothetical protein SS1G_13860 [*Sclerotinia sclerotiorum* 1980 UF-70] (237 bits, E-value 9e^{-61})
estExt_fgenesh1_kg.C_chr_110053 *	LC-MS/MS –MS^{E}	*SAEQVMADFEK*	68,2	382	chr_11:320719-322900	Exo-beta-1,3-glucanase	Hypothetical protein [*Tuber melanosporum* Mel28] (243 bits, E-value 4e^{-62})
		GTAVEAVLAALDTAR	6,2				
		LDTAR	5,2				
fgenesh1_kg.C_chr_11000163 *	LC-MS/MS –MS^{E}	DDIMDLMK	77,8	162	chr_11:1118374-1119074		Hypothetical protein SNOG_04278 [*Phaeosphaeria nodorum* SN15] (42.0 bits, E-value 0.028)
		SWLISGPR	57,8				
		VDVSGTSGWIGR	74,7				
		TVDVSGTSGWIGR	88,4				
		DSLNLWK	51,3				
		NNCDGSTFVPVTGSAGNAPSK	7,8				
		LISGPR	7.2				
		ISGPR	7				
		SGPR	6.8				
		LNLWK	7.6				

NLWK	7.3
SWLI	6.4
MDLMK	7.8
SWLIS	56
IMDLMK	7
DSLNL	5.8
DSLNLW	5.9
SNLWK	7.4
WLISGPR	7.2
DSLNLWK	7.2
DDIMDLMK	5.6
WDCQLLR	7.3
SWLISGPR	7.9
DSLNLWK	8
DDIMDLMK	7.3
WDCQLLR	7.4

[a)] JGI headers from http://genomeportal.jgi-psf.org/Mycgr3/Mycgr3.home.html. Headers in bold represent the two proteins that were selected for further characterization. (fgenesh1_kg.C_chr_11000163 and estExt_fgenesh1_kg.C_chr_50194 have an isoelectric point (pI) of 6.51 and 6.16, respectively and the length of mature proteins after removal of the predicted signal peptides are 15 kDa and 16.9 kDa, respectively).
[b)] Maximum number of identified peptides, including generated in source fragments for MS^E
[c)] Peptide score based on both LC-MS/MS (italic) and MS^E methods. The score range for significant matches is for MS^E >5 and for LC-MS/MS ≥ 50
[d)] Total amino acid length
[e)] Genomic coordinates on the genome of *M. graminicola* strain IPO323
[f)] InterPro terms reflect the presence of conserved functional domains in the protein
[g)] Predicted function with BlastP (nr)
*A better model than the predicted filtered model from JGI v.2
Predicted one transmembrane domain that overlaps with predicted signal peptide
[&] Related to a novel domain identified in chordin, an inhibitor of bone morphogenetic proteins.
- no significant similarity found

A. *Mycosphaerella graminicola Nip1*

```
GAAGGACTGCGAAGAAGTGTATAAAGAGATGCCTTCTCCCCGTCGAAGGACCATTCTTCATCACCAGCAA
CAACAATATCCAACAACCAACAACCAACAACATCCAGCAACCAACAACACTTCCCAACAACATCCACTCA
ACCCACCACCACAATGCTCTTCACTCAAAGCCTCACCCTCGTGGCCCTCCTCACCACCTCCGCCCTCGCC
              M  L  F  T  Q  S  L  T  L  V  A  L  L  T  T  S  A  L  A
                                Signal peptide
TCTCCCCTTGCCCAGAACGGCGGCGGTACGGCCGGCACCACCGGACTCCGCAACAACTGCGACGGCTCCA
 S  P  L  A  Q  N  G  G  G  T  A  G  T  T  G  L  R  N  N  C  D  G  S
CATTCGTCCCCGTGACCGGCAGCGCCGGCAACGCCCCATCCAAGTGGGACTGCCAGCTGCTCCGCGACGG
T  F  V  P  V  T  G  S  A  G  N  A  P  S  K  W  D  C  Q  L  L  R  D  G
CTACATCGCCAAACAGAACAAGTCCTGGCTCATCTCCGGCCCTCGCATCATTGGTACCGTTCGCACTTGC
  Y  I  A  K  Q  N  K  S  W  L  I  S  G  P  R  I  I  G  T  V  R  T  C
CAATTCTCCGCGACGGTGGATGTCTCCGGTACGTCAGGCTGGATCGGACGGGACGACATTATGGATCTAA
 Q  F  S  A  T  V  D  V  S  G  T  S  G  W  I  G  R  D  D  I  M  D  L
TGAAGGACTCGTTGAACTTGTGGAAGGATGGCGAAACGACGCAGGTTCAGGGCGCGATGCAGGTGGGTGA
M  K  D  S  L  N  L  W  K  D  G  E  T  T  Q  V  Q  G  Q  M  Q  V  G  E
GTCGGGCGATGTGAATTGTGTTGCTGGGAAGAATGGAGAGGGGCAGAAGGTTCGTATTGCTTGGACTCTG
  S  G  D  V  N  C  V  A  G  K  N  G  E  G  Q  K  V  R  I  A  W  T  L
GGGCATTCGTAGGTGGGAGGCCGAATAGGGGGGGTGATGAGCAGAGAGGTCGTCGCAGAGGTGGACCGGA
 G  H  S  *
CCAGGAGATCAGTTTCGCCGATATATATATATGCTGATAGAACGGTGTACATCAGTCGGCTTTGATTGTC
CACGGCAGAATTTCATCTGGTCGATCATGTCCAATTGGTTTTTATTTATCTTCTGAGTTGGTTGATACTG
GCCTGTCGTTGTCAAGACAAAGACTGAATGTATAGCCCA
```

B. *Mycosphaerella graminicola Nip2*

```
CATCACCAACGCCGCTTTGTCGACCTACCTACCTATCTTGACCGCAGTACCTCCACATCCTTCAACCATC
ACACCGTTCGACATGAAGCTTCTATCACTCGCAACCTCTGCGCTTCTCGCTACCCACGTCTCTGCGCGCT
              M  K  L  L  S  L  A  T  S  A  L  L  A  T  H  V  S  A  R
                                Signal peptide
CCACCTTCTTCAGCATCTCCGATGCCGCACCGCTAGACGCCAACCTTGCCATCCCAGGCGAGAACCCTCT
S  T  F  F  S  I  S  D  A  A  P  L  D  A  N  L  A  I  P  G  E  N  P  L
CGAGCACTGCGCAGATCCCAAGGATGACATCCTCGCACTGAAGAAGGTTGACCTCAACCCAAACCCACCA
  E  H  C  A  D  P  K  D  D  I  L  A  L  K  K  V  D  L  N  P  N  P  P
CGCGCGTAGGTCGCTCCATGCTCCGACCATTACACCCCGTCACACCGCTAACGTACTCTTCCAACAGCGG
 R  A                                                              G
CACTGAGCTCACCATCACGGCTTCGGGTATACTCAGCGAGGACGTTGGTGAAGGCGCAAAGATCCAACTG
  T  E  L  T  I  T  A  S  G  I  L  S  E  D  V  G  E  G  A  K  I  Q  L
CAAGTCAAATACGGTCTGATTACCATCATCAACCAAAGCGCCGACCTCTGCGAGACCGTCAAGAACGTCG
 Q  V  K  Y  G  L  I  T  I  I  N  Q  S  A  D  L  C  E  T  V  K  N  V
ATCTGGAATGCCCGCTTAAGAAGGGCAAGATGAGCCTCACGAAGGCGGTGAAGCTGCCAGCGCAGATCCC
D  L  E  C  P  L  K  K  G  K  M  S  L  T  K  A  V  K  L  P  A  Q  I  P
GCCAGGCAACTACCATGTATCTGCGGACGTCGTTTCCAAGGATGGGGACAAGGTGACTTGCTTAAAGGCG
  P  G  N  Y  H  V  S  A  D  V  V  S  K  D  G  D  K  V  T  C  L  K  A
AGCGTTGAGTTCAAGCGTGGAGGAGCTGTGGTGTACAAGCAGGGATTGTAGGCGATAGTAATATGGCACA
 S  V  E  F  K  R  G  G  A  V  V  Y  K  Q  G  L  *
TGTATGTATTAGGGACAAGATCACAGATTCGGCGACAGGCGAAACGTGGTCAAGCTGTAGGCGCTGGTCG
ATACCATGTCCTGTAGATATGCTACGAGTATCTGCAAGGGCACTTAATGATTGTGGACTATGCATGGACG
CACCAAGCAGCGCGGCGTTCTTCGGTATACAGTCTGCTGTCCGTGATGGCTCTCCCGTTCGCAAGTCGTG
```

Fig. 5. Nucleotide sequences and the deduced amino acid (aa) sequences of the *Mycosphaerella genes MgNip1* and *MgNip2*. **A.** *MgNip1* has an ORF of 489 bp and encodes a 162 aa protein that contains a 19 aa predicted signal peptide. **B.** *MgNip2* has an ORF of 537 bp and encodes a 178 aa protein that contains a 18 aa predicted signal peptide. The peptide sequences identified by mass spectrometry are underlined. The aa residues highlighted in grey represent the predicted signal peptide; the four cysteine residues present in each of the proteins are highlighted in blue and predicted to form two disulfide bonds in each of the two proteins. The bold DNA sequence indicates the start (ATG) and stop (TAG) codons. DNA sequence in blue is UTR and the yellow highlighted region in *MgNip1* represents a putative TATAAA box.

Heterologous Expression of *MgNip1 and MgNip2* in *Pichia pastoris*

Infiltration with the control *Pichia pastoris* culture filtrates did not show any necrosis-inducing activity other than the physical damage caused by the syringe and occasional slight necrosis limited to the site of infiltration (Fig. 6).

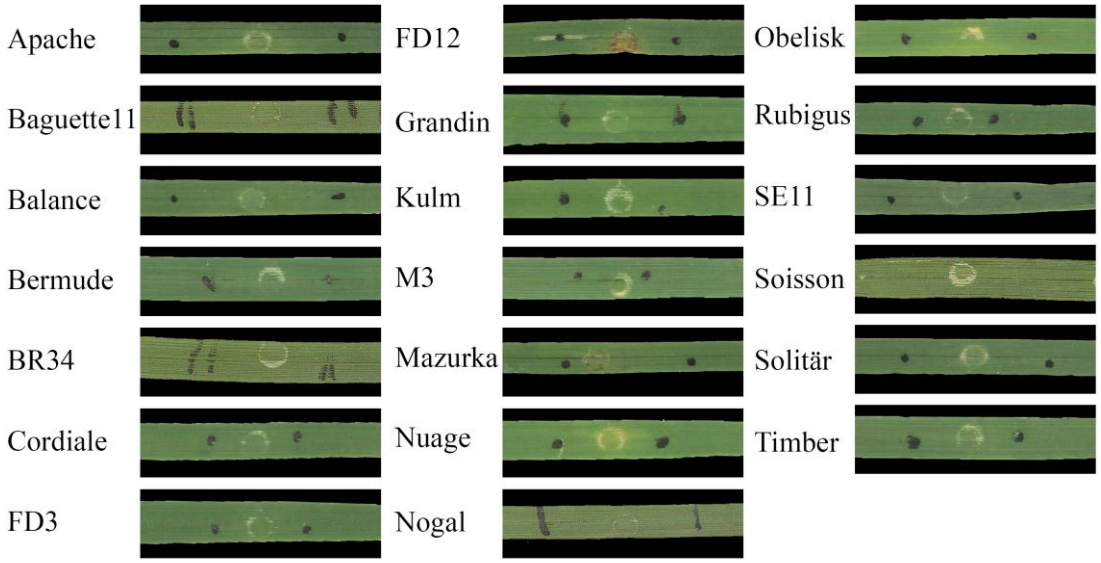

Fig. 6. Necrosis-inducing activity of culture filtrates (CFs) from non-transformed *Pichia pastoris* X33 strain on 20 wheat accessions, including the two parental lines of mapping population. No necrosis-inducing activity was present in CFs from the wild type isolate *P. pastoris.* Black dots on leaves delimit the CF-infiltrated area. Leaves were photographed five days after infiltration.

CF from *P. pastoris*::*MgNip1* showed necrosis-inducing activity in wheat cvs. FD3, FD12, Nuage, Solitär and Kulm albeit of different intensity (Fig. 7). The other wheat accessions including SE11, SE3, Apache, Balance, Cordiale, Soisson, Timber, Bermude, Mazurka, Baguette, Nogal, Grandin, BR34 and M3, did not show any necrosis-inducing activity (Fig. 8) and were comparable to those observed with CF from non-transformed control *P. pastoris*. The CF from *P. pastoris*::*MgNip2* showed strong necrosis-inducing activity in cvs. Nuage, Bermude and FD3, but a weaker response cvs. Kulm and Grandin (Fig. 7). Overall, the two proteins produced in CF of the transformed *P. pastoris* cultures showed differential necrosis inducing activity in a range of wheat cultivars, depending on ambient light and temperature conditions (data not shown).

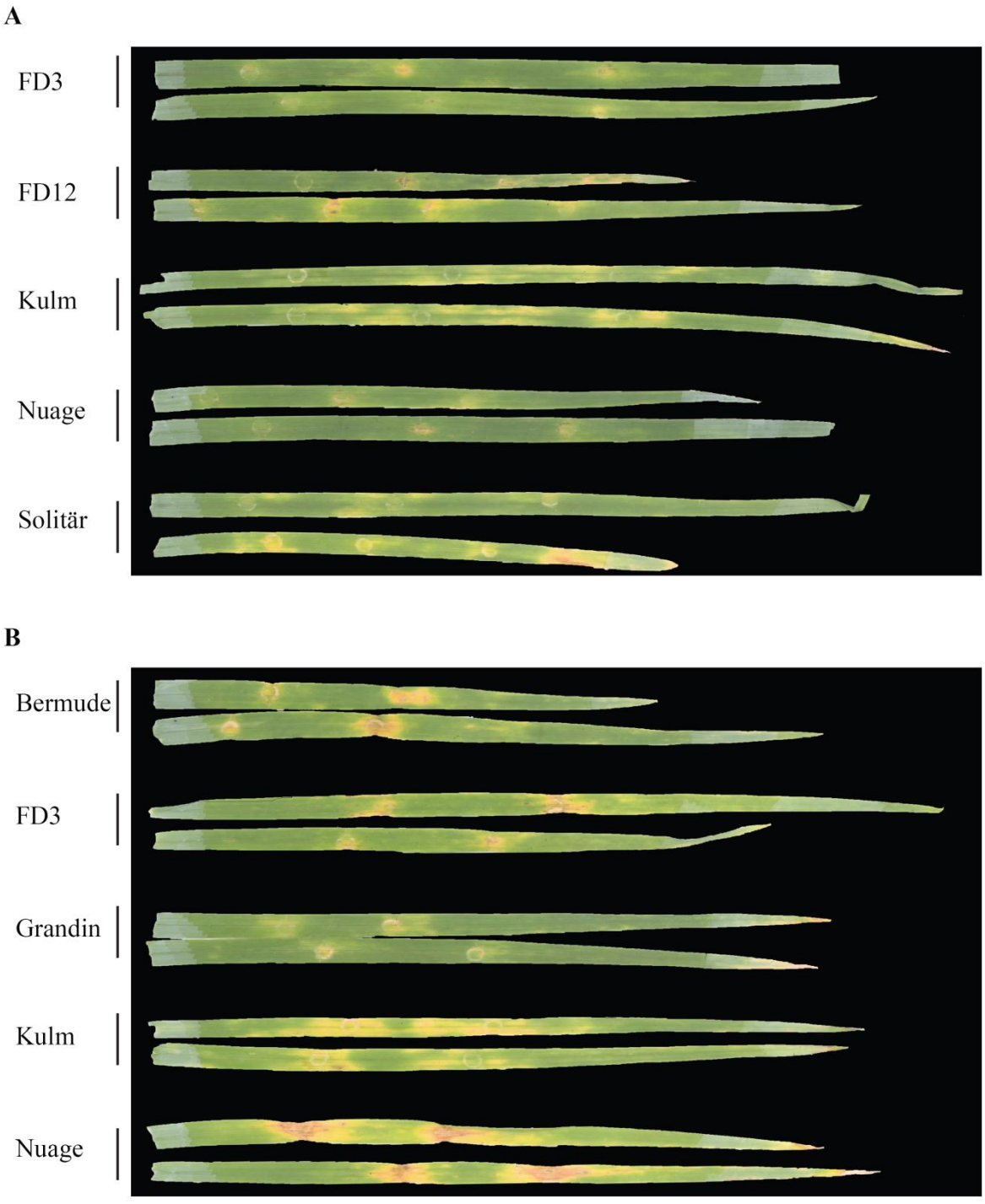

Fig. 7. Necrosis-inducing activity of the MgNip1 **(A)** and MgNip2 **(B)** proteins produced in *Pichia pastoris* cultures on leaves of different wheat cultivars (pictures were taken at five days after infiltration). For MgNip1 and MgNip2, the necrosis-inducing activity of proteins produced by two different *P. pastoris* transformants were assayed (three clones and two clones for each leaf for MgNip1 and MgNip2, respectively are shown).

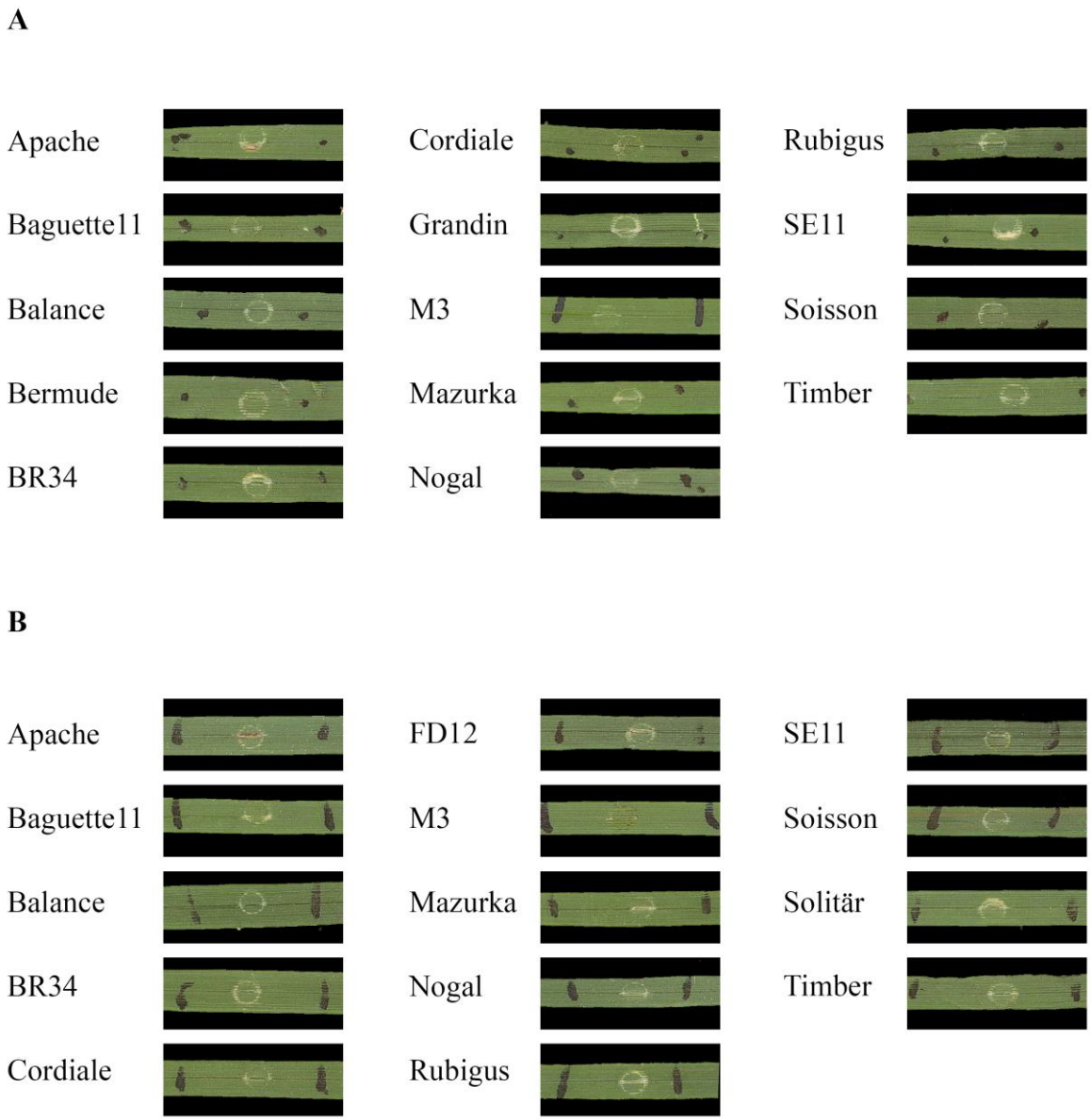

Fig. 8. Absence of necrosis-inducing activity of the MgNip1 **(A)** and MgNip2 **(B)** proteins produced in *Pichia pastoris* cultures on leaves of different wheat cultivars (pictures were taken at five days after infiltration). One clone for each leaf is shown.

In planta **gene expression of** *MgNip1* and *MgNip2*

The expression of *MgNip1* and *MgNip2* was examined during infection in the susceptible wheat cv. Obelisk. *MgNip1* expression correlated with the time point of macroscopical necrotic symptom appearance. Indeed, *MgNip1* expression was up-regulated at 8 days post-inoculation (dpi) and subsequently down-regulated at 12 dpi, coinciding with the transition between the biotrophic and necrotrophic phases of the fungus (Fig. 9). However no

conclusion could be drawn regarding the expression of *MgNip2* as the data between biological replicates were highly variable (Fig. 9).

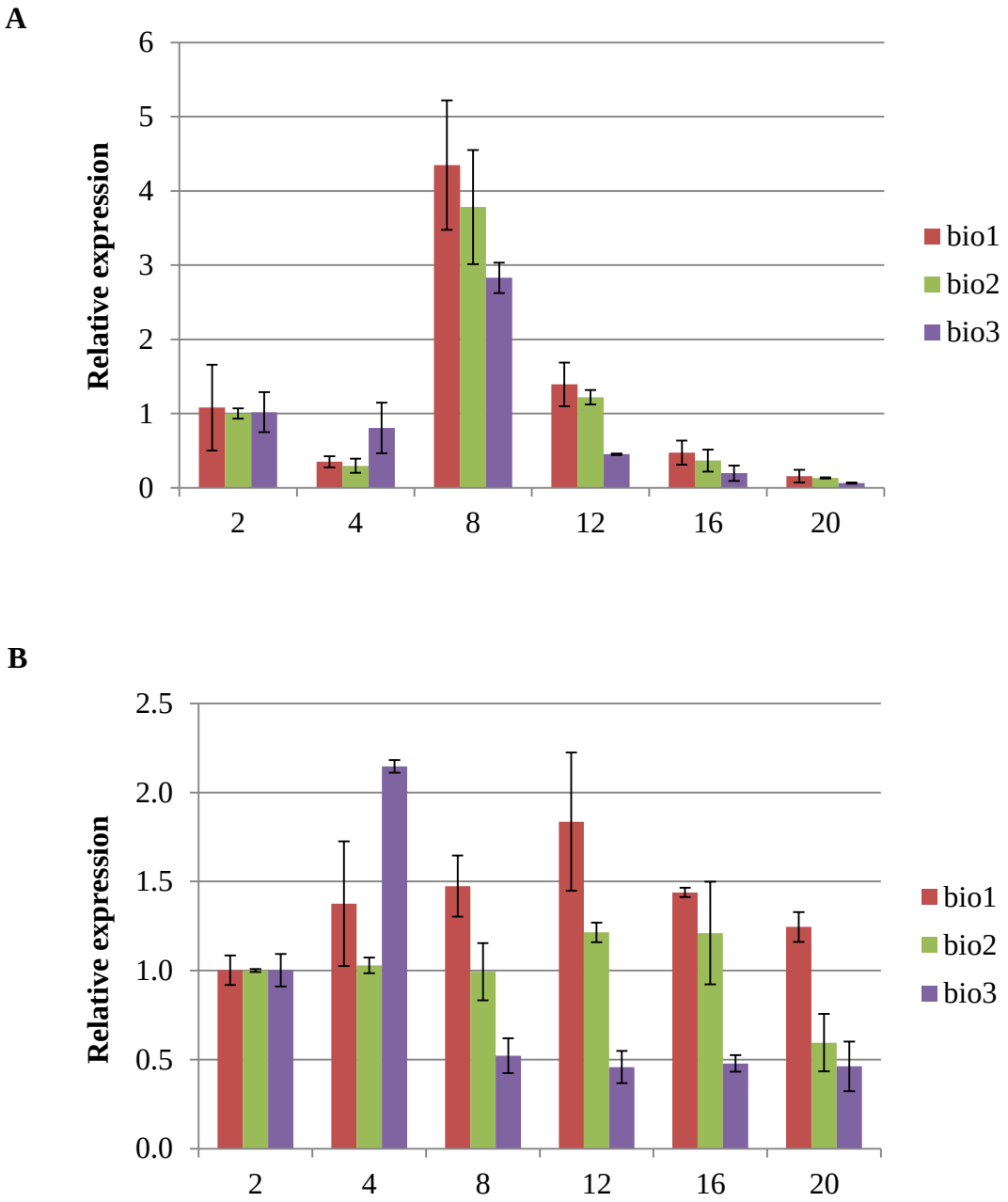

Fig. 9. Real-Time qPCR analysis of *MgNip1***(A)** and *MgNip2* **(B)** in leaves of the susceptible cv. Obelisk that were inoculated with *Mycosphaerella graminicola* strain IPO323 and sampled during the course of infection (2, 4, 8, 12, 16, and 20 days post-inoculation). Bars and numbers indicate the relative expression levels together with the variation. The *M. graminicola beta-tubulin* gene was used for normalization.

DISCUSSION

Plant pathogens have evolved different lifestyles to gain nutrients on their host plants; biotrophs derive their nutrients from living host cells, whereas necrotrophs kill their host

tissue presumably by toxic secondary metabolites or necrogenic proteins before feeding (Horbach et al., 2011).

M. graminicola is a hemibiotroph that has an initial biotrophic phase where it lives in the substomatal cavities and the apoplast between the host plant cells avoiding recognition by the host and feeding on few available nutrients (Goodwin et al., 2011). At this stage the fungal biomass hardly increases and is not much different from the biomass produced on resistant plants. During this phase on a susceptible host, the fungus seems to prepare itself for the necrotrophic phase (Kema et al., 1996a; Ware, 2006; Rudd et al., 2008). It was even suggested that the basic nutrient composition is neither increased nor depleted to any measurable level despite the presence of the fungus during the biotrophic phase (Keon et al., 2007). This is followed by a quick turnover to a destructive phase of pathogenesis where the fungus ramifies the mesophyll, which is accompanied by a reduction in photosynthesis and a massive accumulation of H_2O_2, leading to necrosis. This releases large amounts of nutrients from host cells that facilitates further proliferation of the fungus (Kema et al., 1996a; Shetty et al., 2003; Keon et al., 2007; Shetty et al., 2007; Rudd et al., 2008; Shetty et al., 2009). This seemingly sudden change in pathogenic behavior was considered to be presumably due to the involvement of toxic secondary metabolites or proteins (Kema et al., 1996a; Keon et al., 2007; Hammond-Kosack and Rudd, 2008; Rudd et al., 2008). Indeed, in a recent report, Motteram et al. (2009) identified a single gene from *M. graminicola* encoding a member of the necrosis- and ethylene-inducing peptide 1 (Nep1)-like protein family (NLP) occurring in many eukaryotes that has frequently shown to trigger activation of defence signaling responses in dicotyledonous plants including the hypersensitive response (HR). However, infiltration of the protein into wheat leaves did not cause necrosis-inducing activity and targeted gene-disruption did not compromise virulence of the pathogen.

Here, we report the identification and initial characterization of the first genes in *M. graminicola* that encode necrosis-inducing proteins (Nips), with differential activities in a range of wheat cultivars. We designated these genes *MgNip1* and *MgNip2* and indentified the encoded proteins in culture filtrates of *M. graminicola* IPO323. We therefore employed a proteomic approach in which CFs proteins, produced by *M. graminicola* in a Fries medium were fractionated by FPLC and candidates were subsequently analyzed by mass spectrometry.

Interestingly, the CFs showed necrosis-inducing activity on a wide range of wheat accessions, including the parental lines of mapping population, irrespective of whether these were resistant or susceptible towards strain *M. graminicola* IPO323. This confirmed previous reports that showed no relationship between the toxicity of CFs and virulence of *M.*

graminicola strains (Perrone et al., 2000), which contrasts with findings in related phytopathogenic fungi such as *S. nodorum* and *P. tritici-repentis* (Lamari and Bernier, 1989; Effertz et al., 2002; Liu et al., 2006; Singh and Hughes, 2006; Friesen et al., 2008b; Liu et al., 2009). CFs of the latter two fungi, containing necrogenic proteins, showed necrosis-inducing activity mostly only on susceptible cultivars. For *M. graminicola*, it was suggested that resistance is triggered during the early phases of infection rather than during advanced stages of pathogenesis when the mesophyll tissue is colonized. However, the titer of unknown soluble toxic compounds could increase during the course of infection and eventually kill host cells at a later stage of infection as suggested by Perrone et al. (2000). The current study shows that a range of wheat genotypes was invariably sensitive to crude CFs, but did respond quantitatively differentially to purified proteinaceous fractions. This suggests the involvement of a complex mixture of MgNips with either specific differential or general necrosis inducing activities that may have intrinsic avirulence or virulence functions that may even change during the course of infection. Obviously, differential necrosis inducing activity complies with the GFG of the *M. graminicola*-wheat pathosystem (Brading et al., 2002). At this stage we can only speculate on iGFG since no sensitivity genes in wheat have been mapped.

The temperature sensitivity of the *M. graminicola* CFs was in accord with observations on phytotoxic proteins isolated from other fungal plant pathogens that showed a proportional loss of necrosis-inducing activity after heat treatment between 50-100°C (Ballance et al., 1989; Lamari and Bernier, 1989; Tomas et al., 1990; Sarpeleh et al., 2008). In addition, proteinase K (PK) treatments of *M. graminicola* CFs abolished activity, which confirmed the proteinaceous nature of the active principle present in partially purified fraction. Finally, the necrosis inducing activity of CFs in seedling leaves is light- dependent, which is a property also observed for the the necrogenic proteins in other Dothideomycete-wheat pathosystems (Manning and Ciuffetti, 2005; Friesen et al., 2006; Friesen et al., 2007; Sarpeleh et al., 2008; Abeysekara et al., 2009). We could indirectly confirm this by a time-lapse experiment where crude *M. graminicola* CFs were co-infiltrated with PK in leaves of wheat seedlings. Interestingly, CFs could be inactivated until approximately 30 min after infiltration and were apparently still prone to PK degradation in the apoplast. After 30 min infiltrated necrosis-inducing activity of CFs was no longer sensitive to PK treatment, indicating that the necrogenic proteins would have transversed the cell membrane which presumably could not be transversed by PK. This suggests that the majority of the necrogenic CF components will be taken up subsequently rapidly targeting intracellular targets such as the chloroplasts, which complies with loss of chloroplast integrity observed in histological

studies of colonization of wheat by *M. graminicola* (Kema et al., 1996a). Manning et al. (2007, 2009) demonstrated that host specificity in the *P. tritici-repentis* – wheat interaction relies on the ability of PtrToxA to traverse the cell membrane and to interact with the chloroplast protein ToxABP1. Once it is translocated into the chloroplast, PtrToxA promotes virulence by interfering with photosystem I and II and finally induces reactive oxygen species accumulation in a light-dependent manner (Manning et al., 2009). Our data and previous histological observations suggest that a similar system might be active in the wheat-*M. graminicola* interaction.

We therefore, further fractionated *M. graminicola* CFs by FPLC, SDS-PAGE and subsequently analyzed the partially purified necrosis-inducing activity containing fraction by mass spectrometry, which narrowed down candidate MgNips to almost 1%. This revealed the presence of several unknown hypothetical proteins that were further characterized and resulted in two prominent proteins that we designated MgNip1 and MgNip2. The mature proteins appeared to have a mass of 15 and ~16.9 kDa, respectively and showed differential necrosis-inducing activity in wheat cultivars. The first protein, MgNip1, is a homolog of Ecp2 of *C. fulvum* and is presumably encoded by a fourth paralog of *MgEcp2* (I. Stergiopoulos, personal communication) in addition to the published three others that were previously reported (Stergiopoulos et al., 2010). Interestingly, Ecp2-like effector proteins are also identified in the related Dothideomycete banana pathogen *M. fijiensis* that likely promote virulence by interacting with a putative intracellular host target causing host cell necrosis (Stergiopoulos et al., 2010). Ecp of *C. fulvum* is one of the few effector proteins that can induce necrosis in tomato and tobacco plants irrespective of the presence of the signal peptide indicating that its hosts target is intracellular indeed (Laugé et al., 1997; Laugé et al., 2000; de Kock et al., 2004).

MgNip2 contained a putative ML domain (MD-2-related lipid-recognition). Such proteins are subdivided in four groups depending on the sequence similarity, are mostly secreted and consist of multiple β-strands that create β-sheets and regroup multiple proteins of unknown function in plants, fungi and animals (Inohara and Nunez, 2002). MgNip2 that we identified in our study belongs to the third subgroup that includes the phosphatidylglycerol/phosphatidylinositol transfer protein (PG/PI-TP) of *Aspergillus oryzae.* It has been shown that ML-domain proteins are able to bind lipids and are involved in innate immunity (Kirchhoff et al., 1996; Inohara and Nunez, 2002; Mullen et al., 2003).

Although the activity of *M. graminicola* Nips is reminiscent with HSTs in other pathosystems, in *M. graminicola* necrosis occurs much later and also the type of host response

is different. This variation could be due to dependence of host responses on environmental factors such as temperature and light. Necrosis-inducing activity of these Nips of *M. graminicola* appeared indeed light-dependent. Keon et al. (2007) and also more recently Tabib Ghaffary (2011) reported that light intensity has a marked influence on symptom development in wheat cultivars that were inoculated with *M. graminicola* strains. Higher light intensities result in higher disease severities. However, this depended strongly on the specific resistance genes, such as *Stb2* in cv. Veranopolis that seems to be very sensitive. Reduced light intensities resulted in poor disease development, whereas high intensities resulted in fully sporulating susceptible responses. Also, proteolytic degradation or protein expression and concentration differences could vary from one experiment to the other and influence phenotypic expression. It has been shown that PtrToxA, SnToxA, SnTox1, SnTox2, SnTox3, SnTox4 induce maximal necrosis at three days after-infiltration (Strelkov et al., 1999; Liu et al., 2004; Manning and Ciuffetti, 2005; Friesen et al., 2006; Friesen et al., 2007; Abeysekara et al., 2009; Liu et al., 2009) whereas necrosis-inducing activity with the low-molecular weight ToxC protein was only visible after five days (Effertz et al., 2002). Necrosis-inducing activity of *P. tritici-repentis* toxin ToxB depends strongly on its concentration (Strelkov et al., 1999; Kim and Strelkov, 2007).

We also observed a discrepancy between the appearance of necrosis after infiltration of MgNip1 and MgNip2 and after inoculation with conidia of *M. graminicola.* It is, therefore, still unclear whether the necrosis-inducing activity observed in resistant cultivars is related to a susceptibility or a resistance response as was also reported for other proteins reviewed by Rep et al. (2005). In this respect, *S. nodorum* HSTs induce cell death in susceptible host plants (Friesen et al., 2007; Friesen et al., 2008a) whereas avirulence proteins of *C. fulvum* only induce cell death in tomato plants with the corresponding *Cf* resistance genes (De Wit et al., 2009) and Nip1, a small phytotoxic protein from *R. secalis* that is an avirulence factor that is required for Rrs1- mediated resistance of barley (Rohe et al., 1995), it also stimulates the activity of the barley plasma membrane H+-ATPase in a genotype-unspecific manner as it induces necrotic lesions in leaf tissues of barley and other cereal plant species (Wevelsiep et al., 1991; Wevelsiep et al., 1993; van't Slot et al., 2007). In case of *M. graminicola*, resistant wheat cultivars could be sensitive to a necrosis-inducing protein, but its activity threshold is never reached as fungal proliferation is controlled by effective resistance genes and MgNips produced by the fungus never reach the required concentration in the apoplast. The necrosis-inducing activity observed after infiltration can thus be part of a resistance response that is hardly ever observed in inoculation assays due to the slow build-up of fungal biomass in

resistant wheat cultivars. Another hypothesis would be that one and the same protein induces resistance in resistant plants, but functions as a host-selective toxin in susceptible plants.

Further analysis of the identified MgNips is necessary to elucidate the role of these proteins in *M. graminicola* and their targets need to be identified. Future studies will focus on these aspects and on the distribution of the encoding genes in natural *M. graminicola* populations.

MATERIALS AND METHODS

Fungal and plant materials

The recently sequenced *M. graminicola* bread-wheat strain IPO323 (Goodwin et al., 2011) was used throughout all experiments according to previously described protocols with minor modifications (Kema and van Silfhout, 1997; Mehrabi, 2006). Wheat plants of 20 different cultivars were grown in controlled greenhouse compartments with 16 hours light per day and pre- and post-inoculation temperatures of 18/16°C vs. 22°C at day and night, respectively, and a relative humidity (RH) of ≥85%. Disease symptoms were evaluated 21 days after inoculation as percentages necrosis (N) and pycnidia (P) as described by Tabib Ghaffary et al., (2011). Plants for infiltration assays with CFs or protein fractions were grown at 22°C and a RH of 60%. Necrosis-inducing activity was determined on 20 wheat cultivars that were either susceptible or resistant to *M. graminicola* strain IPO323.

Culture filtrate production and phenotyping assays

CF was generated by growing the fungus on V8-potato dextrose agar medium for 5-10 days until yeast-like colonies were formed. MilliQ water was added and 60 µl of the spore suspension from one plate (Petri dish, 9 cm diameter) was added to 60 ml of liquid Fries medium (Liu et al., 2004). The flasks were subsequently placed in a rotary shaker for three days at 27°C at 100 rpm followed by stationary growth at 21°C in the dark for one to three weeks. CFs were obtained by filtering these cultures through two layers of cheese cloth and Whatman no. 1 filter (Fisher Scientific, Pittsburg, PA, USA) and subsequent vacuum filtration through a 0.45 µm Durapore PVDF pore size filter (Millipore, MA, USA). The CF was either stored at -80°C until use or directly used for determination of necrosis-inducing activity by infiltrating 100 µl in the second leaf of seedlings at growth stage (GS) 13 (Zadoks et al., 1974) with a 1-ml syringe until water-soaking of the tissue was observed (Liu et al., 2004).

The infiltration area was marked with a permanent marker and necrosis-inducing activity was determined three to four days after infiltrations (dai, for protein infiltrations at 5 dai) by collecting and evaluating the leaves after electronic scanning of the symptoms using a photocopier (RICOH Aficio MPC2500). Each infiltrations were repeated at least two times with similar results.

Treatments of culture filtrates

We tested the effect of temperature, proteinase K (PK) and light on the necrosis-inducing activity of the CFs. The effect of temperature on the necrosis-inducing activity was determined by incubating the CFs at room temperature (RT), 37°C, 50°C for four hours and 100°C for 30 min. In addition, the effect of *in vitro* and *in planta* PK treatments (1 mg/ml) (Roche Diagnostics, Almere, Netherlands) on the necrosis-inducing activity of the CFs was tested. CFs were treated with PK and incubated at RT, 37°C and 50°C for four hours. The untreated and treated samples were, along with the controls, infiltrated into the leaves of the sensitive cv. Obelisk. The necrosis-inducing activity was assayed by scoring plants either as sensitive or insensitive as reported previously (Liu et al., 2004). *In planta* PK effects of CF necrosis-inducing activity was tested by co-infiltrations of PK (100 µl of 1 mg/ml) after CFs infiltrations at different time points varying from 0 to 120 min. in three replicates. Necrosis inducing activity was quantified by analysis of electronic images of the symptoms with Assess software (APS, St. Paul, USA). The light effect on necrosis-inducing activity was determined by exposure to normal light conditions or darkness by covering the infiltration zones with aluminum foil for two or three days. All the treated leaves were collected three to four days after treatment and photographed.

Culture filtrate fractionation and SDS-PAGE

CF (~400 ml) harvested after three weeks of stationary growth of *M. graminicola* strain IPO323, was dialyzed at room temperature for 4 hrs against a 20 mM sodium acetate buffer (SAB, pH 5), using SnakeSkin dialysis tubing (Pierce biotechnology, Rockford, IL) with a 7 kDa molecular weight cut off. Fast Protein Liquid Chromatography (FPLC, Pharmacia Biotech, Piscataway, NJ) was performed at room temperature. A 1 ml HiTrap SP Sepharose™ Fast Flow column (GE Healthcare, Piscataway, NJ, USA) was pre-equilibrated with SAB (pH 5) and 60 ml of dialyzed CF was applied at a flow rate of 1 ml/min and washed with SAB until the baseline was stable. Subsequently, a linear gradient to 0.5 M sodium

chloride in SAB was applied at a flow rate of 1 ml/min and 16 fractions of 1 ml were collected. Relative protein concentration was detected by measuring absorbance at 280 nm. All protein-containing fractions were assayed for necrosis-inducing activity. For further protein purification, three successive runs (60 ml) with the HiTrap SP Sepharose column were performed and the fractions with necrosis-inducing activity were pooled. Three pooled fractions were further purified by FPLC using a Mono-S HR 5/5 cation exchange column (GE Healthcare, Piscataway, NJ, USA) equilibrated in SAB (pH 4.5). Samples were diluted twice in SAB buffer before injection onto the Mono-S column and proteins were eluted at 1 ml/min with a 30 ml linear gradient of 0.0-0.5 M sodium chloride in SAB (pH 4.5). One ml fractions were collected and adjusted to pH 5 with sodium acetate (pH 9.4) and assayed for necrosis-inducing activity (Fig. 3). Part of the active fractions was added to Laemmli sample buffer and subjected to sodium dodecyl sulphate-polyacrylamide gel electrophoresis (SDS-PAGE) on 8–18% gradient gels (ExcelGel; Amersham Pharmacia Biotech, Sweden) using SDS buffer strips. Separation was performed on an electrophoretic transfer unit (Multiphor II; Amersham Pharmacia Biotech, Sweden) and the separated proteins were visualized by silver staining (Blum et al., 1987; Rabilloud, 1999) (Fig. 4).

Protein identification by LC-MS analysis

To identify the proteins present in the (partially) purified fractions with necrosis-inducing activity, samples were freeze-dried, dissolved in 50 µl 0.1% (w/v) RapiGest SF Surfactant (Waters, Milford, USA), 5 mM DTT (Sigma) in 0.1 M ammonium bicarbonate and incubated at 50°C for 30 min. Alkylation was performed by incubation with 15 mM iodoacetamide (IAA) (GE Healthcare, UK) for 40 min at room temperature (in the dark). Proteolytic digestion was initiated by adding 2 µl of modified porcine trypsin (0.2 µg/µl; Sequence grade modified; Promega, WI, USA) and incubated overnight at 37°C. After adding trifluoroacetic acid (TFA) (Fluka,-Buchs, GmBH) to a final concentration of 0.5% (v/v), samples were centrifuged at 15,000 g for 10 min. and the supernatant was applied to a SupelClean™ LC-18 1 ml SPE column (Supelco, Bellefonte USA), equilibrated with 0.1% TFA. Bound peptides were eluted with 84% acetonitrile (ACN) (HPLC Supra-gradient, Biosolve, Valkenswaard, NL) containing 0.1% Formic Acid (FA) (Merck, Darmstadt, Germany), dried by vacuum centrifugation, dissolved in 40 µl 0.1% FA and further analyzed by mass spectrometry. The trypsin-digested samples were separated using a nanoAcquity 2D UPLC system (Waters Corporation, Manchester, UK) with orthogonal reversed phase

separation at high and low pH. The mixture of peptides was eluted from the first dimension XBridge C_{18} trap column (in 20 mM ammonium formate, ACN, pH 10) with a discontinuous gradient of 13%, 45% and 65% ACN. For the second dimension an acidic ACN gradient was applied using a BEH C_{18} column (75 µm x 25 cm, Waters, UK) and a 65 min linear gradient from 3 to 40% ACN (in 0.1 % FA) at 200 nl/min. The eluting peptides were on-line injected into a Synapt Q-TOF MS instrument (Waters Corporation, Manchester, UK) using a nanospray device coupled to the second dimension column output. The Synapt MS was operated in positive mode with [Glu^1] fibrinopeptide B (1 pmol/µl; Sigma) as reference (lock mass) and sampled every 30 s. Accurate liquid chromatography-mass spectrometry (LC-MS) data were collected with the Synapt operating in either the MS/MS or MS^E mode for data-dependent acquisition (DDA) or data-independent acquisition (DIA), respectively, using low (6 eV) and elevated (ramp from 15 to 35 eV) energy spectra every 0.6 s over a 140-1900 m/z range, respectively. LC-MS/MS was performed by peptide fragmentation on the three most intense multiple charged ions that were detected in the MS survey scan (0.6 s) over a 300-1400 m/z range and a dynamic exclusion window of 60 s with an automatically adjusted collision energy based on the observed precursor m/z and charge state. LC-MS/MS and MS^E data were processed using ProteinLynx Global Server software (PLGS version 2.4, Waters Corporation, Manchester, UK) and the resulting list of masses, containing all the fragment information was searched for matching proteins using a merged non-redundant database including all gene models of the *M. graminicola* IPO323 database at the United States Department of Energy – Joint Genome Institute (DOE-JGI, http://genome.jgi-psf.org/Mycgr3/Mycgr3.download.ftp.html). Finally, the LC-MS/MS and MS^E outputs were further merged and since we used all gene models of *M. graminicola,* additional filtering steps were performed for proteins with alternative models (based on additional peptides not covered in the DOE-JGI models) and eventually only best models were used. Furthermore, only proteins with a peptide score ≥50 and/or >5 with LC-MS/MS and/or MS^E, respectively, were retained for further analyses.

The resulting proteins were characterized, the molecular mass determined, then searched for the presence of signal peptides (SignalP 3.0, http://www.cbs.dtu.dk/services/SignalP/), and cysteine residues and putative functions were identified. In case no putative function was assigned, online software such as BLASTP against the public NCBI non-redundant (NR) database (http://blast.ncbi.nlm.nih.gov/Blast.cgi) (Marchler-Bauer et al., 2009)

(www.ncbi.nlm.nih.gov/Structure/cdd/wrpsb.cgi) was used to determine the classifications and possible functions of identified hypothetical proteins. For each identified protein the genomic sequence for the encoding gene, along with its 5' and 3' flanking regions were mapped on the *M. graminicola* IPO323 genome sequence (Goodwin et al., 2011) and expression was checked using the EST data base at DOE-JGI. In addition, the molecular masses and isoelectric points of the two most prominent proteins were predicted using the Compute pI/Mw tool at the ExPASy molecular biology server of the Swiss Institute of Bioinformatics (http://www.expasy.org/).

Heterologous expression of cDNA-encoding candidate proteins in *Pichia pastoris*

cDNAs encoding candidate proteins were amplified with primers containing Attb1 and Attb2 sites (Table 1) and amplicons were first gel-purified or directly incubated with donor vector pDONR207 and the Gateway® BP clonase (Invitrogen, Carlsbad, USA) and subsequently sequenced to check the reaction. Luria broth (1% tryptone, 0.5% yeast extract and 1% NaCl) with gentamicin (15-20 μg/ml) was used to culture *Escherichia coli* DH10B transformants at 37°C after the BP reaction. The purified clones were then mixed with a Destination Vector (pMR148, 2.9kb, containing pGAPZ that was slightly modified for application in both *E. coli* and yeast with zeocin as a selectable marker [*Sh ble*] and recombination sites compatible with the Gateway ® system, Mehrabi et al., unpublished) in the Gateway ® Cloning LR reaction (Invitrogen). The resulting expression constructs were sequenced with primers pGAP and 3'AOX1 (Table 1) for sequence confirmation. After the LR reaction, low salt Luria broth (1% tryptone, 0.5% yeast extract, and 0.5% NaCl, pH 7.5) with zeocin (25 μg/ml) was used to culture *E. coli* DH10B transformants at 37°C. The expression vector from positive clones was linearized with *Rca*I and competent *Pichia pastoris* X33 cells (Easy select Pichia Expression system, Invitrogen) were transformed with at least 5 μg of plasmid DNA (Pichia EasyComp Kit manual, Invitrogen). The transformed cells were plated in YPDS agar (1% yeast extract, 2% peptone, 2% sorbitol and 2% dextrose, 2% agar) containing zeocin (100 μg/ml), incubated at 30°C for three to four days and finally three clones were selected to check gene insertions by colony PCR using specific primers. Protein expression in *P. pastoris* X33 was performed in 50 ml YPD liquid medium (1% yeast extract, 2% peptone and 2% dextrose) in 100 ml Erlenmeyer flasks at 29°C for two days. Eventually, cells were centrifuged at 4,000 rpm for four min at 10°C and the supernatant was checked for necrosis-inducing activity.

Table 1. Oligonucleotides used in this study.

Primer pair [1)]	Sequence [2)] 5' to 3'	Predicted size	Application
Attb1-MgNip1F	*GGGGACAAGTTTGTACAAAAAAGCAGG CT*ATGCTCTTCACTCAAAGCCTCAC	547	Amplification of 489-bp full length cDNA for cloning in the Gateway system and yeast expression
Attb2- MgNip1R	*GGGGACCACTTTGTACAAGAAAGCTGG GT*CTACGAATGCCCCAGAGTCCA		
Attb1- MgNip2F	*GGGGACAAGTTTGTACAAAAAAGCAGG CT*ATGAAGCTTCTATCACTCGCAACC	595	Amplification of 537-bp full length cDNA for cloning in the Gateway system and yeast expression
Attb2- MgNip2R	*GGGGACCACTTTGTACAAGAAAGCTGG GT*CTACAATCCCTGCTTGTACACCA		
pGAPF	GTCCCTATTTCAATCAATTGAA		Sequencing yeast expression construct from 5' end
3'AOX1	GCAAATGGCATTCTGACATCC		Sequencing yeast expression construct from 3' end
TubulinF	GCCCAGACAACTTCGTGTTC	103	Partial amplification of *M. graminicola* tubulin gene in Real-Time qPCR analysis
TubulinR	ACGACATCGAGAACCTGGTC		
MgNip1F	GTTCGCACTTGCCAATTCTC	106	Partial amplification of *M. graminicola MgNip1* gene in Real-Time qPCR analysis
MgNip1R	TCCACAAGTTCAACGAGTCC		
MgNip2F	AGAACGTCGATCTGGAATGC	109	Partial amplification of *M. graminicola MgNip2* gene in Real-Time qPCR analysis
MgNip2R	ACGTCCGCAGATACATGGTAG		

[1)] Primer sequences (pGAPF and 3'AOX) for sequencing yeast expression constructs.
[2)] The sequences for other PCR primers were designed using the web-based program primer3.0. All primers were designed with Tm between 58°C-60°C and PCRs were all conducted at an annealing temperature of 60°C. Italics indicate the AttB1and AttB2 sequences that were added to the primers at the N- and C-termini of the genes, respectively.

RT-PCR of *MgNip1* and *MgNip2*

The expression of *MgNip1* and *MgNip2* was analyzed by semi-quantitative reverse transcription-PCR (RT-PCR). The susceptible cv. Obelisk was inoculated with *M. graminicola* strain IPO323 in three biological replicates and infected leaves were collected at 2, 4, 8, 12, 16 and 20 days post-inoculation, flash-frozen in liquid nitrogen and kept at -80°C until use. Total RNA was isolated from ~0,7 ml ground leaf tissue with one ml of TRIzol reagent (Invitrogen, Carlsbad, CA, USA) in 2 ml tubes according to the manufacturer's

instruction. To remove contaminated DNA, total RNA was treated with the RNase-free DNase I (Promega, Madison, USA). First-strand cDNA was generated using Superscript III Reverse Transcriptase (Invitrogen, San Diego, CA, USA) and further diluted (5x) and finally used for SYBR® Green qPCR (Applied Biosystems, Foster City, CA). For each reaction, a 2 µl aliquot of cDNA was used in a 25 µl PCR volume with primers at a final concentration of 0.30 µM at an annealing temperature of 60°C using an ABI 7500 Real-Time PCR System (Applied Biosystems). The expression was normalized with the constitutively expressed *M. graminicola beta-tubulin* gene.

ACKNOWLEDGEMENTS

The authors thank the members of the International Mycosphaerella Genomics Consortium for discussions and suggestions. We thankfully remember the late Joost de Groot and his kind provision of the FastaFileMerge bioinformatics tool. We acknowledge Ioannis Stergiopoulos for helpful discussion about the *Ecp2* paralogs in *M. graminicola*. We also thank Els Verstappen for excellent *M. graminicola* maintenance and greenhouse management and Ineke de Vries for technical assistance. Sarrah Ben M'Barek is sponsored by an UNESCO L'Oréal fellowship.

LITERATURE CITED

Abeysekara, N.S., Friesen, T.L., Keller, B., and Faris, J.D. 2009. Identification and characterization of a novel host–toxin interaction in the wheat–*Stagonospora nodorum* pathosystem. TAG Theoretical and Applied Genetics 120:117-126.

Ackerveken, G.F.J.M., Kan, J.A.L., and Wit, P.J.G.M. 1992. Molecular analysis of the avirulence gene avr9 of the fungal tomato pathogen *Cladosporium fulvum* fully supports the gene for gene hypothesis. The Plant Journal 2:359-366.

Ballance, G., Lamari, L., and Bernier, C. 1989. Purification and characterization of a host-selective necrosis toxin from *Pyrenophora tritici-repentis*. Physiological and Molecular Plant Pathology 35:203-213.

Blum, H., Bier, H., Gross H.J.1987. The best silver stain. Electrophoresis 8:93–99.

Brading, P.A., Verstappen, E.C.P., Kema, G.H.J., and Brown, J.K.M. 2002. A gene-for-gene relationship between wheat and *Mycosphaerella graminicola*, the Septoria tritici blotch pathogen. Phytopathology 92:439-445.

Churchill, A.C.L. 2010. *Mycosphaerella fijiensis*, the black leaf streak pathogen of banana: progress towards understanding pathogen biology and detection, disease development, and the challenges of control. Molecular Plant Pathology 12:307-328.

Dangl, J.L., and Jones, J.D.G. 2001. Plant pathogens and integrated defence responses to infection. Nature 411:826-833.

De Kock, M.J., Iskandar, H.M., Brandwagt, B.F., Laugé, R., de Wit, P.J., and Lindhout, P. 2004. Recognition of *Cladosporium fulvum* Ecp2 elicitor by non-host Nicotiana spp. is mediated by a single dominant gene that is not homologous to known Cf-genes. Molecular plant pathology 5:397-408.

De Wit, P.J.G.M., Mehrabi, R., van Den Burg., H.A., and Stergiopoulos, I. 2009. Fungal effector proteins: past, present and future. Molecular Plant Pathology 10:735-747.

Dodds, P.N., Rafiqi, M., Gan, P.H.P., Hardham, A.R., Jones, D.A., and Ellis, J.G. 2009. Effectors of biotrophic fungi and oomycetes: pathogenicity factors and triggers of host resistance. New Phytologist 183:993-1000.

DOE, JGI. 2011. http://genome.jgi-psf.org/Mycgr3/Mycgr3.home.html

Effertz, R.J., Meinhardt, S.W., Anderson, J.A., Jordahl, J.G., and Francl, L.J. 2002. Identification of a chlorosis-inducing toxin from *Pyrenophora tritici-repentis* and the chromosomal location of an insensitivity locus in wheat. Phytopathology 92:527-533.

Flor, H.H. 1971. Current status of the gene-for-gene concept. Annual Review of Phytopathology 9:275-296.

Friesen, T., Stukenbrock, E., Liu, Z., Meinhardt, S., Ling, H., Faris, J., Rasmussen, J., Solomon, P., McDonald, B., and Oliver, R. 2006. Emergence of a new disease as a result of interspecific virulence gene transfer. Nature Genetics 38:953-956.

Friesen, T., Meinhardt, S., and Faris, J. 2007. The *Stagonospora nodorum*-wheat pathosystem involves multiple proteinaceous host-selective toxins and corresponding host sensitivity genes that interact in an inverse gene-for-gene manner. The Plant Journal 51:681-692.

Friesen, T., Faris, J., Solomon, P., and Oliver, R. 2008a. Host-specific toxins: effectors of necrotrophic pathogenicity. Cellular Microbiology 10:1421-1428.

Friesen, T., Zhang, Z., Solomon, P., Oliver, R., and Faris, J. 2008b. Characterization of the interaction of a novel *Stagonospora nodorum* host-selective toxin with a wheat susceptibility gene. Plant Physiology 146:682.

Friesen, T., Chu, C.G., Liu, Z., Xu, S., Halley, S., and Faris, J. 2009. Host-selective toxins produced by *Stagonospora nodorum* confer disease susceptibility in adult wheat plants under field conditions. TAG Theoretical and Applied Genetics 118:1489-1497.

Friesen, T.L., and Faris, J.D. 2010. Characterization of the wheat-*Stagonospora nodorum* disease system: what is the molecular basis of this quantitative necrotrophic disease interaction?. Canadian Journal of Plant Pathology 32:20-28.

Goodwin, S.B., Ben M'Barek, S., Dhillon, B., Wittenberg, A.H.J., Crane, C.F., Hane, J.K., Foster, A.J., Van der Lee, T.A.J., Grimwood, J., Aerts, A., Antoniw, J., Bailey, A., Bluhm, B., Bowler, J., Bristow, J., van der Burgt, A., Canto-Canché, B., Churchill, A.C.L., Conde-Ferràez, L., Cools, H.J., Coutinho, P.M., Csukai, M., Dehal, P., De Wit, P., Donzelli, B., van de Geest, H.C., van Ham, R.C.H.J., Hammond-Kosack, K.E., Henrissat, B., Kilian, A., Kobayashi, A.K., Koopmann, E., Kourmpetis, Y., Kuzniar, A., Lindquist, E., Lombard, V., Maliepaard, C., Martins, N., Mehrabi, R., Nap, J.P.H., Ponomarenko, A., Rudd, J.J., Salamov, A., Schmutz, J., Schouten, H.J., Shapiro, H., Stergiopoulos, I., Torriani, S.F.F., Tu, H., de Vries, R.P., Waalwijk, C., Ware, S.B., Wiebenga, A., Zwiers, L.H., Oliver, R.P., Grigoriev, I.V., and Kema, G.H.J. 2011. Finished Genome of the Fungal Wheat Pathogen *Mycosphaerella graminicola* Reveals Dispensome Structure, Chromosome Plasticity, and Stealth Pathogenesis. PLoS Genet 7:e1002070.

Hammond-Kosack, K.E., and Rudd, J.J. 2008. Plant resistance signalling hijacked by a necrotrophic fungal pathogen. Plant Signaling & Behavior 3:993-995.

Hane, J.K., Rouxel, T., Howlett, B.J., Kema, G.H.J., Goodwin, S.B., and Oliver, R.P. 2011. A novel mode of chromosomal evolution peculiar to filamentous Ascomycete fungi. Genome Biology 12:R45.

Horbach, R., Navarro-Quesada, A., Knogge, W., and Deising, H. 2011. When and how to kill a plant cell: Infection strategies of plant pathogenic fungi. Journal of Plant Physiology.168: 51-62.

Howlett, B.J. 2006. Secondary metabolite toxins and nutrition of plant pathogenic fungi. Current opinion in plant biology 9:371-375.

Inohara, N., and Nunez, G. 2002. ML-a conserved domain involved in innate immunity and lipid metabolism. Trends in biochemical sciences 27:219-221.

Jones, J., and Dangl, J. 2006. The plant immune system. Nature 444:323-329.

Keen, N. 1990. Gene-for-gene complementarity in plant-pathogen interactions. Annual Review of Genetics 24:447-463.

Kema, G.H.J., and van Silfhout, C. 1997. Genetic variation for virulence and resistance in the wheat-*Mycosphaerella graminicola* pathosystem III. Comparative seedling and adult plant experiments. Phytopathology 87:266-272.

Kema, G.H.J., Yu, D., Rijkenberg Frits, H.J., Shaw Michael, W., and Baayen Robert, P. 1996a. Histology of the pathogenesis of *Mycosphaerella graminicola* in wheat. Phytopathology 86:777-786.

Kema, G.H.J, van der Lee, T.A., Mendes, O., Verstappen, E.C., Lankhorst, R.K., Sandbrink, H., van der Burgt, A., Zwiers, L.H., Csukai, M., and Waalwijk, C. 2008. Large-scale gene discovery in the septoria tritici blotch fungus *Mycosphaerella graminicola* with a focus on *in planta* expression. Mol Plant Microbe Interact 21:1249-1260.

Kema, G.H.J., Verstappen, E.C.P., Todorova, M., and Waalwijk, C. 1996b. Successful crosses and molecular tetrad and progeny analyses demonstrate heterothallism in *Mycosphaerella graminicola*. Current Genetics 30:251-258.

Keon, J., Antoniw, J., Carzaniga, R., Deller, S., Ward, J.L., Baker, J.M., Beale, M.H., Hammond-Kosack, K., and Rudd, J.J. 2007. Transcriptional adaptation of *Mycosphaerella graminicola* to programmed cell death (PCD) of its susceptible wheat host. Mol Plant Microbe Interact 20:178-193.

Kim, Y.M., and Strelkov, S. 2007. Heterologous expression and activity of Ptr ToxB from virulent and avirulent isolates of *Pyrenophora tritici-repentis*. Canadian Journal of Plant Pathology 29:232-242.

Kirchhoff, C., Osterhoff, C., and Young, L. 1996. Molecular cloning and characterization of HE1, a major secretory protein of the human epididymis. Biology of reproduction 54:847-856.

Lamari, L., and Bernier, C. 1989. Toxin of *Pyrenophora tritici-repentis*: Host-specificity, significance in disease, and inheritance of host reaction. Phytopathology 79:740-744.

Laugé, R., Goodwin, P., de Wit, P., and Joosten, M. 2000. Specific HR-associated recognition of secreted proteins from *Cladosporium fulvum* occurs in both host and non-host plants. The Plant Journal 23:735-745.

Laugé, R., Joosten, M.H.A.J., Van den Ackerveken, G.F.J.M., Van den Broek, H.W.J., and De Wit, P.J.G.M. 1997. The *in planta*-produced extracellular proteins ECP1 and ECP2 of *Cladosporium fulvum* are virulence factors. Molecular Plant-Microbe Interactions 10:725-734.

Liu, Z., Faris, J., Meinhardt, S., Ali, S., Rasmussen, J., and Friesen, T. 2004. Genetic and physical mapping of a gene conditioning sensitivity in wheat to a partially purified host-selective toxin produced by *Stagonospora nodorum*. Phytopathology 94:1056-1060.

Liu, Z., Friesen, T., Ling, H., Meinhardt, S., Oliver, R., Rasmussen, J., and Faris, J. 2006. The Tsn1-ToxA interaction in the wheat-*Stagonospora nodorum* pathosystem parallels that of the wheat-tan spot system. Genome 49:1265-1273.

Liu, Z., Faris, J.D., Oliver, R.P., Tan, K.-C., Solomon, P.S., McDonald, M.C., McDonald, B.A., Nunez, A., Lu, S., Rasmussen, J.B., and Friesen, T.L. 2009. SnTox3 Acts in effector triggered-susceptibility to induce disease on wheat carrying the *Snn3* gene. PLoS Pathog 5:e1000581.

Manning, V., Chu, A., Steeves, J., Wolpert, T., and Ciuffetti, L. 2009. A Host-Selective Toxin of P*yrenophora tritici-repentis*, Ptr ToxA, induces photosystem changes and reactive oxygen species accumulation in sensitive wheat. Molecular plant-microbe interactions: MPMI 22:665-676.

Manning, V.A., and Ciuffetti, L.M. 2005. Localization of Ptr ToxA produced by *Pyrenophora tritici-repentis* reveals protein import into wheat mesophyll cells. The Plant Cell Online 17:3203-3212.

Manning, V.A., Hardison, L.K., and Ciuffetti, L.M. 2007. Ptr ToxA interacts with a chloroplast-localized protein. Molecular Plant-Microbe Interactions 20:168-177.

Marchler-Bauer, A., Anderson, J.B., Chitsaz, F., Derbyshire, M.K., DeWeese-Scott, C., Fong, J.H., Geer, L.Y., Geer, R.C., Gonzales, N.R., Gwadz, M., He, S., Hurwitz, D.I., Jackson, J.D., Ke, Z., Lanczycki, C.J., Liebert, C.A., Liu, C., Lu, F., Lu, S., Marchler, G.H., Mullokandov, M., Song, J.S., Tasneem, A., Thanki, N., Yamashita, R.A., Zhang, D., Zhang, N., and Bryant, S.H. 2009. CDD: specific functional annotation with the Conserved Domain Database. Nucl. Acids Res. 37:205-210.

Mehrabi, R. 2006. Signaling pathways involved in pathogenicity and development of the fungal wheat pathogen *Mycosphaerella graminicola*. Wageningen University, The Netherlands: PhD Thesis.

Motteram, J., Küfner, I., Deller, S.N., Brunner, F., Hammond-Kosack, K.E., Nürnberger, T., and Rudd, J.J. 2009. Molecular Characterization and Functional Analysis of *MgNLP*, the Sole NPP1 Domain-Containing Protein, from the Fungal Wheat Leaf Pathogen *Mycosphaerella graminicola*. Molecular Plant-Microbe Interactions 22:790-799.

Mullen, G.E.D., Kennedy, M.N., Visintin, A., Mazzoni, A., Leifer, C.A., Davies, D.R., and Segal, D.M. 2003. The role of disulfide bonds in the assembly and function of MD-2. Proceedings of the National Academy of Sciences of the United States of America 100:3919-3924.

Perrone, G., Logrieco, A., Kema, G.H.J., Ritieni, A., Bottalico, A. 2000. Phytotoxic activity of *Mycosphaerella graminicola* culture filtrates. Developments in Plant Genetics and Breeding 6:195-201.

Quaedvlieg, W., Kema, G.H.J., Groenewald, J.Z., Verkley, G.J.M., Seifbarghi, S., Razavi, M., Mirzadi Gohari, A., Mehrabi, R., and Crous, P.W., 2011. *Zymoseptoria* gen. nov.: a new genus to accommodate Septoria- like species occurring on graminicolous hosts. Persoonia 26:57-69.

Rabilloud, T., and Chevallet, M. 1999. Solubilization of proteins in 2-D electrophoresis, in Proteome Research: Two-Dimensional Gel Electrophoresis, and Identification Methods Rabilloud, T., Ed., Springer-Verlag, Heidelberg, pp. 9–30.

Rohe, M., Gierlich, A., Hermann, H., Hahn, M., Schmidt, B., Rosahl, S., and Knogge, W. 1995. The race-specific elicitor, NIP1, from the barley pathogen, *Rhynchosporium secalis*, determines avirulence on host plants of the Rrs1 resistance genotype. The EMBO Journal 14:4168.

Rudd, J., Keon, J., and Hammond-Kosack, K. 2008. The wheat mitogen-activated protein kinases TaMPK3 and TaMPK6 are differentially regulated at multiple levels during compatible disease interactions with *Mycosphaerella graminicola.* Plant Physiology 147:802-815.

Sarpeleh, A., Wallwork, H., Tate, M.E., Catcheside, D.E.A., and Able, A.J. 2008. Initial characterisation of phytotoxic proteins isolated from *Pyrenophora teres.* Physiological and Molecular Plant Pathology 72:73-79.

Shetty, N., Mehrabi, R., Lutken, H., Haldrup, A., Kema, G., Collinge, D., and Jorgensen, H. 2007. Role of hydrogen peroxide during the interaction between the hemibiotrophic fungal pathogen *Septoria tritici* and wheat. New Phytologist 174:637-647.

Shetty, N.P., Kristensen, B.K., Newman, M.A., Møller, K., Gregersen, P.L., and Jørgensen, H.J.L. 2003. Association of hydrogen peroxide with restriction of *Septoria tritici* in resistant wheat. Physiological and Molecular Plant Pathology 62:333-346.

Shetty, N.P., Jensen, J.D., Knudsen, A., Finnie, C., Geshi, N., Blennow, A., Collinge, D.B., and Jorgensen, H.J.L. 2009. Effects of β-1,3-glucan from *Septoria tritici* on structural defence responses in wheat. The Journal of Experimental Botany. 60:4287-4300.

Singh, P.K., and Hughes, G.R. 2006. Inheritance of insensitivity to culture filtrate of *Pyrenophora tritici-repentis*, race 2, in wheat (*Triticum aestivum* L.). Plant breeding 125:206-210.

Stergiopoulos, I., van den Burg, H.A., Ökmen, B., Beenen, H.G., van Liere, S., Kema, G.H.J., and de Wit, P.J.G.M. 2010. Tomato Cf resistance proteins mediate recognition of cognate homologous effectors from fungi pathogenic on dicots and monocots. Proceedings of the National Academy of Sciences 107:7610-7615.

Strelkov, S.E., Lamari, L., and Ballance, G.M. 1999. Characterization of a host-specific protein toxin (Ptr ToxB) from *Pyrenophora tritici-repentis*. Molecular Plant-Microbe Interactions 12:728-732.

Tabib Ghaffary, S.M., Robert, O., Laurent, V., Lonnet, P., Margalé, E., van der Lee, T.A.J., Visser, R.G.F., and Kema, G.H.J. 2011. Genetic analysis of resistance to septoria tritici blotch in the French winter wheat cultivars Balance and Apache. TAG Theoretical and Applied Genetics:1-14.

Tabib Ghaffary, S.M. 2011. Efficacy and mapping of resistance to *Mycosphaerella graminicola* in wheat. Wageningen University, The Netherlands: PhD Thesis.

Thomma, B.P.H.J., Nürnberger, T., and Joosten, M.H.A.J. 2011. Of PAMPs and Effectors: The Blurred PTI-ETI Dichotomy. The Plant Cell 23:4-15.

Tomas, A., Feng, G., Reeck, G., Bockus, W., and Leach, J. 1990. Purification of a cultivar-specific toxin from *Pyrenophora tritici-repentis*, causal agent of tan spot of wheat. Molecular Plant-Microbe Interactions 3:221-224.

van't Slot, K.A.E., Gierlich, A., and Knogge, W. 2007. A single binding site mediates resistance-and disease-associated activities of the effector protein NIP1 from the barley pathogen *Rhynchosporium secalis.* Plant physiology 144:1654-1666.

Ware, S.B. 2006. Aspects of sexual reproduction in Mycosphaerella species on wheat and barley: genetic studies on specificity, mapping, and fungicide resistance. Wageningen University, The Netherlands: PhD Thesis.

Wevelsiep, L., Kogel, K.H., and Knogge, W. 1991. Purification and characterization of peptides from *Rhynchosporium secalis* inducing necrosis in barley. Physiological and Molecular Plant Pathology 39:471-482.

Wevelsiep, L., Rupping, E., and Knogge, W. 1993. Stimulation of barley plasmalemma H+-ATPase by phytotoxic peptides from the fungal pathogen *Rhynchosporium secalis*. Plant physiology 101:297-301.

Wolpert, T., Dunkle, L., and Ciuffetti, L. 2002. Host-selective toxins and a virulence determinants: What's in a name? Annual Review of Phytopathology 40:251-285.

Zadoks, J.C., Chang, T.T., and Konzak, C.F. 1974. A decimal code for the growth stages of cereals. Weed research 14:415-421.

Chapter 6

General discussion

“Human diversity makes tolerance more than a virtue; it makes it a requirement for survival"
— René Dubos

This thesis, entitled "Genome structure and pathogenicity of the fungal wheat pathogen *Mycosphaerella graminicola*" provides new insights into the organization of the genome of the destructive wheat leaf pathogen *Mycosphaerella graminicola* and about the identification and characterization of new proteinaceous potential pathogenicity factors. In this discussion, I will reflect on the experimental findings described in this thesis. The first part focuses on the genome plasticity with an emphasis on the exploration of the underlying mechanisms such as meiotic recombination and horizontal chromosome transfer in shaping eukaryotic fungal genomes. The second part primarily deals with the identification of necrosis-inducing proteins (NIPs) of *M. graminicola* and the implications of this finding are discussed in the context of its hemi-biotrophic lifestyle and its interaction with wheat. Previously, this pathosystem was shown to comply with the gene-for-gene (GFG) model. Here, I discuss how the obtained results fit into this model or whether it is likely that an additional inverse gene-for-gene (iGFG) model is operating.

Genome plasticity: "the good, the bad and the ugly"

Genomics toolbox in *M. graminicola*

The discovery of the teleomorph of *Zymoseptoria tritici* (Desm.) Quaedvlieg and Crous (Quaedvlieg et al., 2011), *Mycosphaerella graminicola* (Fuckel) J. Schröt, by Sanderson in New Zealand in 1972 emphasized the possible role of airborne inoculum in disease establishment. Indeed, the discovery of its mating system (Kema et al. 1996d) unveiled the very active sexual cycle of *M. graminicola* in disease epidemiology (Kema et al., 1996c; Hunter et al., 1999; Suffert et al., 2010; Ponomarenko et al., 2011). The subsequent isolation of bipolar mating-type genes (Waalwijk et al., 2002), has significantly contributed to an overall understanding of sex in shaping natural populations of this fungus (Zhan et al., 2003) and recently it was shown that, irrespective of whether being inhibited by fungicide treatment or after deposition on a resistant wheat cultivar, *M. graminicola* can still produce viable ascospores (Ware, 2006). This results in high levels of genetic diversity and in virulence of field populations, which contributes to the overall aggressiveness of this fungus on wheat (Chen and McDonald, 1996; Kema et al., 1996a; Kema et al., 1996c; Kema and van Silfhout, 1997; Zhan et al., 2002; Zhan et al., 2003; Ware, 2006).

Since then, the developments of tools for the analysis of genome structures have greatly improved our ability to detect changes in genome organization: chromosome number

and chromosome length polymorphisms (CNPs and CLPs, respectively) and to monitor their dynamics over generations. In this respect, chromosome dynamics was revealed by electrophoretic and cytological karyotyping that mainly showed changes in chromosome length and number among different populations of field isolates (McDonald and Martinez, 1991; Mehrabi et al., 2007) but also chromosomal translocations could be detected (Kema et al., 1996d). However, the resolution of this technique is limited as it only detects larger changes in the chromosomal complement. A detailed analysis of the transmission of genetic information through sexual mechanisms provided the basis for the construction of high-density genetic linkage maps that uncovered translocations and chromosome rearrangements **(Chapter 2)**. Finally, the availability of the *M. graminicola* genome sequence facilitated the construction of genome wide microarrays to analyse chromosome copy number and size variation at an unparalleled resolution that provided a comprehensive view of sexually driven structural genome changes. In **Chapter 3**, we present the finished genome of *M. graminicola* that was completed by the United States Department of Energy-Joint Genome Institute in 2008. This opened new avenues to study of a variety biological processes, such as marker-based analysis of the second meiotic division during ascosporogenesis that was important in the generation of genome plasticity. In this way, several types of genomic changes were frequently observed, including chromosomal rearrangements, CNPs and CLPs. The *M. graminicola* genome has a core set of 13 chromosomes and a variable set of eight dispensable chromosomes that can be lost individually or in combination and is collectively named the dispensome. The dispensome is distinct in structure with small-sized chromosomes, reduced gene density and a higher repeat content compared to the core set of chromosomes.

Several key questions arose from these studies, which must be addressed to enhance our understanding of chromosomal non-disjunction and the meiotic origin of genome plasticity in general. Obvious burning research questions relate to explaining (i) the underlying non-disjunctional mechanisms that generate CNPs, (ii) how the fungus can tolerate genomic rearrangements while staying biologically fit, (iii) the beneficial and deleterious effects of genome plasticity, and finally its contribution to virulence or possibly host-jumping and speciation.

Why chromosomes occasionally undergo nondisjunction is an enigma and requires re-addressing the basic mechanisms behind sexual and asexual reproduction that incidentally may give rise to abnormal chromosome behaviour. Sexual reproduction in *Ascomycetes* comprises two meiotic divisions and a subsequent mitotic cell division that give rise to eight ascospores with many new combinations of alleles depending on the frequency of cross-overs

(COs) that occurred. New genomic variation also occurs during asexual reproduction which usually gives many generations of conidia that accumulate mutations induced by different environmental conditions including UV light (Felsenstein 1974; Barton and Charlesworth 1998; Lamb et al., 2003). For example, during vegetative growth in *Saccharomyces cerevisiae*, the mutation rate typically occurs at a rate of 10^{-6}–10^{-7} per locus per generation whereas during meiosis, this can be as high as 10^{-1}–10^{-2} (Keeney, 2001). How is one and the same process that is responsible for genetic recombination and diversity also driving CNPs? Understanding the individual steps of meiosis in detail is required to understand where and how this can happen.

Meiosis: "the orchestrated symphony"

Although many of meiotic processes are very well understood, many aspects of the process remain obscure (Page and Hawley, 2003). Meiosis (Fig. 1) is a special type of cell division that produces haploid gametes from diploid parental cells. During meiosis, the chromosomes originating from each parent pair and subsequently segregate during which process recombination by CO does occur. Despite the degree of variation in the order and timing of early recombination events in different organisms, the basic components are conserved between species (Lamb et al., 2005). In the current model, during meiosis I, homologues chromosomes initiate a process of meiotic pairing initiated by double strand breaks (DSBs). This is catalysed by the evolutionary conserved protein Spo11 in conjunction with several other proteins, that is present in a large number of organisms, including budding yeast, fission yeast, filamentous fungi, flies, worms, plants, and mammals (Keeney, 2001). Subsequently, rejoining of broken ends takes place. A subset of the broken ends from a chromatid is joined to the corresponding sequence on the homologous chromosome (Allers and Lichten, 2001). Repair results in either a CO, a reciprocal exchange accompanied by a tract subject to gene conversion, or gene conversion without crossover (NCO) and not associated with reciprocal exchange (Whitby, 2005). The CO products form chiasmata, the physical evidence of recombination. Together with chiasmata, the monopolar behaviour of sister kinetochores facilitates the bipolar attachment of homologs to the spindle such that homologs are separated during the first meiotic division. Hence, genetic recombination not only separates allelic combinations along the chromosomes but also and more importantly, it ensures proper segregation of chromosomes (Roeder, 1997; Page and Hawley, 2003; Nishant and Rao, 2006).

Finally, in the second meiotic division, sister chromatids are segregated from each other and cohesins, that function as linkages between sister chromatids separate and segregate (Nasmyth, 2001); in *Ascomycetes* an additional mitotic division takes place.

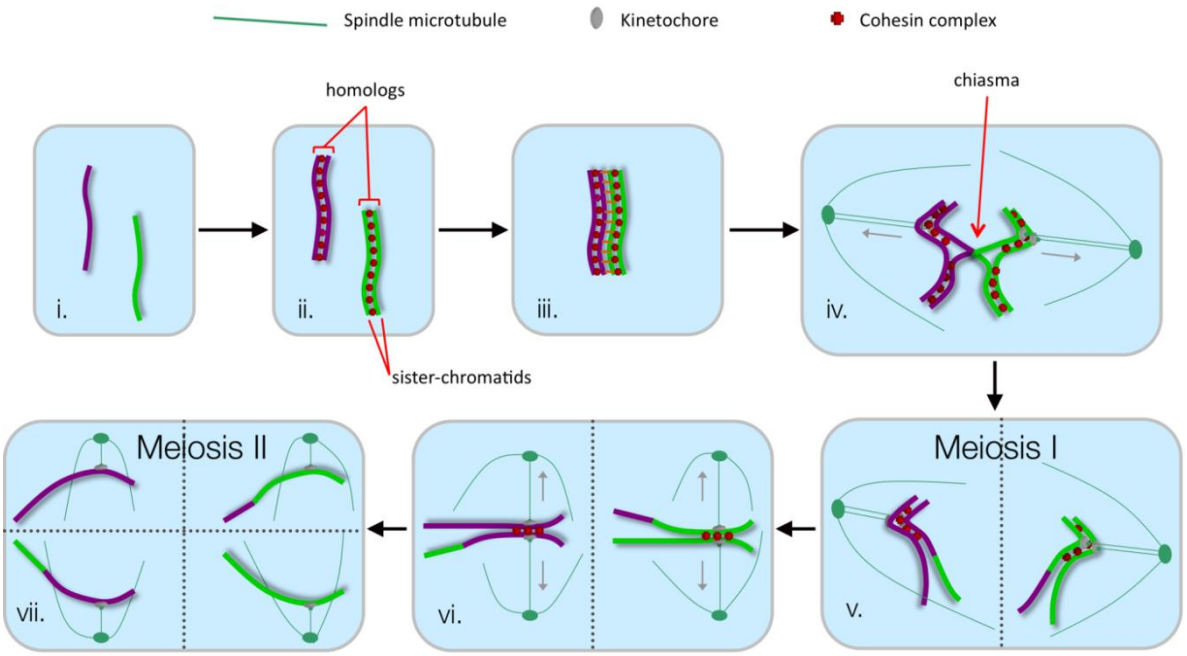

Fig. 1. Schematic representation of the process of meiosis.
(i) Single pair of homologous chromosomes in a diploid cell (purple and green lines). (ii) Chromosomes replicate to give pairs of sister chromatids connected by cohesin. (iii) Homologs pair and become synapsed over their entire length. Crossing-over occurs during this period. (iv) Chiasma link the homologs and thereby facilitates stable bipolar attachment to the meiosis-I spindle. (v) Cohesion between the chromosome arms is lost and homologous chromosomes segregate to opposite poles. (vi) Maintenance of cohesion between centromeres allows bipolar attachment of sister chromatid pairs to the meiosis-II spindle. (vii) The remaining cohesion is lost and sister chromatids subsequently segregate to opposite poles during meiosis II, which results in the formation of nonidentical haploid gametes. Grey arrows indicate directions of the pulling forces generated by microtubules. Dashed lines indicate the planes of cell division (Lao and Hunter, 2010).

In order to have proper chromosome segregation during meiosis, every chromosome requires at least one CO of which the distribution seems to be governed by at least two levels of regulation: the location of DNA double-strand breaks (DSBs) and whether those DSBs are repaired as CO (Blitzblau et al., 2007). It has been shown that meiotic recombination occurs in repetitive regions called hotspots (Page and Hawley, 2003), while it is suppressed in certain locations including areas flanking centromeric regions (Lamb et al., 2005). For example, in *Schizosaccharomyces pombe*, many of the recombination hotspots produce noncoding RNAs (Wahls et al., 2008). In *S. cerevisiae,* mapping meiotic DSBs revealed pericentrometric regions known for low recombination rates, suggesting that centromeric suppression of recombination occurs at the level of DSB break repair rather than DSB formation.

Additionally, most DSBs occur in hotspots such as in promoter regions, but also within a ~100 kb region from the telomeres. Interestingly, concentration of DSBs close to chromosome ends increases the relative DSB density for small chromosomes, suggesting that DSB placement appears to be controlled both by chromatin structure as well as by relative positions towards chromosomal landmarks such as telomeres (Blitzblau et al., 2007; Mancera et al., 2008).

Recently, new roles for centromeres in meiosis I chromosome segregation have been identified. Although there is low level of sequence conservation of centromeres between species, the looped-out structure of centromeric DNA is conserved. The length can vary from a few hundreds of base pairs also called point centromeres such as in *S. cerevisiae* (~120 bp with few repetitive sequences) (Cottarel et al., 1989) to the holocentric centromeres of *Caenorhabditis elegans*, which span the entire length of the chromosome (Ekwall, 2007) or megabases of entirely repeated sequences as found in plants (Tek and Jiang, 2004) or humans (Willard and Rudd, 2006). The specification of centromeres is referred to as being epigenetic, which is defined as an inherited state not based on the DNA sequence (Karpen and Allshire, 1997). Centromeres are required for normal chromosome segregation in mitosis and meiosis by assembling the large protein structures kinetochores, the sites for microtubule attachment. Additionally, centromeres are involved in meiotic homolog pairing. In *S. cerevisiae,* chromosome pairing at the centromeres is independent of chromosome homology and the centromeric interactions depend on the synaptonemal complex component Zip1 (Gladstone et al., 2009) and the transition to homologous coupling depends on the Spo11 protein (Tsubouchi and Roeder, 2005). On the other hand, in polyploid wheat (AABBDD, n=42), it has been shown that the Ph1 locus on chromosome 5B enforces strictly homologous bivalent pairing preventing therefore homeologous pairing. Wheat varieties that lack the Ph1 locus, exhibit a high level of homoeologues pairing (Lukaszewski and Kopecký, 2010), which significantly contributed to the introgression of genes from wild graminaceous relatives.

Furthermore, centromeres play a role in the protection of centromeric cohesion in meiosis I. In fact, during meiosis I, cohesins that are located along the chromosome are lost allowing homologs to move to opposite ends of the spindle. Simultaneously, cohesions around centromeres are retained by a number of kinetochore-localized factors, preventing sister chromatids from premature separation (Michaelis et al., 1997).

Hence, meiotic recombination is a remarkably complex process that involves several highly coordinated events. Having mentioned its importance, it becomes therefore clear that any deviation from this highly regulated process could give rise to chromosome non-disjunction resulting in CNPs in the offspring that may result in lethality on the one hand, but could also have advantages under particular environmental conditions.

In model organisms such as *S. cerevisiae* and *Coprinus cinereus*, but also in humans, disturbances in the recombination pathway have been linked to abnormalities in chromosome segregation. The most obvious ones involve mutations that disturb the recombination process, which increase the frequency of chromosome mal-segregation. In a number of organisms, abolishment of Spo11 function results in the elimination of meiotic recombination and thus chromosome non-disjunction (Keeney, 2001). Aberrant meiosis can also be due to breakdown in centromere/spindle functions and/or in the checkpoints that monitor them (Selmecki et al., 2010). Additionally, the location of the recombination breakpoints also seems to a play a role. When they occur in close or distant proximity of the centromere, they increase the risk of non-disjunction (Lamb et al., 2005). For instance, during meiosis I, misplaced CO in proximity of telomeres resulted in aneuploidy in humans and are the primary cause of trisomy that eventually can result in miscarriage (Lamb et al., 2005; Hassold et al., 2007). Similarly, non-disjunction events at meiosis II in Drosophila (Koehler et al., 1996), humans (Lamb et al., 2005) and budding yeast (Rockmill et al., 2006) are the consequence of centromere-proximal CO that resulted from the disruption of sister chromatid cohesion and premature separation of sister chromatids, which then segregate randomly. When the crossing over occurs within the centromere itself this would lead to attachment of the centromere to both halves of the spindle, resulting in chromosome breakage and loss (Talbert and Henikoff, 2010). In this respective, it has been suggested that aneuploidy in *Candida albicans* may have arisen from centromere instability as their centromeres are very small in size (~3kb) and not flanked by repetitive DNA (Selmecki et al., 2010).

It is therefore obvious that centromeres play an essential role in accurate chromosome segregation and hence genome stability. In case of *M. graminicola*, centromeres have not been determined yet although Wittenberg (2007) showed regions with relatively low recombination rates on each chromosome, speculating that they may represent centromeres. One way to identify centromeres is to use chromatin immunoprecipitation centromere-specific histone H3 isoform CEN (CENH3) that is known to be constitutively found at nearly all eukaryotic centromeres and to interact directly with components of the kinetochore complex (Malik and Henikoff, 2009).

Understanding centromeric sequences would reveal insights into their functional regulation, in addition to providing a more complete understanding of genome structure and organization. In addition, tetrad analysis, can be employed to dissect the different aspects of the meiotic process including mapping of centromeres, detection of cytoplasmic inheritance and gene conversion, measuring recombination frequencies as it was carried out for *S. cerevisiae* for which genome-wide maps are available (Mancera et al., 2008).

Towards the *Mycosphaerella graminicola* "pan genome"

The importance of meiosis for genome plasticity in *M. graminicola*, does not rule out mitosis as a potential driving force for chromosome gain or loss or translocations in field populations. Indeed, mitotic nondisjunction may occur when sister chromatids fail to separate during mitosis. However, the mechanisms that can cause bypassing cell cycle checkpoints, which normally inhibit such events, have not been explored (Selmecki et al., 2010).

In *Cryptococcus neoformans*, which is a dikaryotic fungus that causes meningoencephalitis in human, several cases of disomy were reported, for instance as a result of exposure to high concentration of fluconazole (FLC). When the drug was removed, one of the duplicated copies was lost suggesting that it may have arisen from non-disjunction during mitosis. This would represent a novel mechanism of adaptation that contributes to the failure of FLC therapy for cryptococcosis (Sionov et al., 2010) as well as for candidasis (Selmecki et al., 2006).

In fact, preliminary results of *in vitro* experiments with the sequenced *M. graminicola* strain IPO323 involving several rounds of sub-culturing demonstrated loss of chromosome(s) and in some cases was shown to reduce virulence (unpublished results). In the future, it would be interesting to investigate in more detail the importance of mitosis in genome plasticity and to determine whether the loss of chromosomes can repeatedly affect virulence and or fitness. In addition, we may induce chromosomal loss in *M. graminicola* by artificial evolution experiments as have been carried out in *Aspergillus nidulans* (Schoustra et al., 2007) consisting of step-wise sub-culturing to determine whether it is possible to achieve a viable strain that carries only the core set of chromosomes. Alternatively, this can also be achieved by intercrossing *M. graminicola* strains carrying different markers on different chromosomes of the dispensome. This will enable us to determine the minimal core gene set that is required for survival of the fungus. Moreover, to fully explore gene variability and thus to understand the global complexity and competitiveness of *M. graminicola*, genomes of multiple isolates

with variation in aggressiveness are required to determine the "pan genome". This type of experiment was conducted with the bacterium *Streptococcus agalactiae* (Tettelin et al., 2005) that showed its genome make-up consisting of a core genome containing essential conserved genes and a dispensable genome composed of genes or chromosomes absent from one or more isolates and genes that are unique for particular isolates that are assumed to be involved in specificity, virulence or adaptation to particular environmental niches.

Is horizontal chromosome transfer a powerful weapon to combat changing environments or does it make a fungus vulnerable?

There are some indications that dispensable chromosomes of *M. graminicola* might have been obtained by horizontal transfer (HCT) from (an) unknown donor(s). HCT is a powerful evolutionary force that has accelerated and shaped evolution of microbial species. In bacteria, horizontal gene transfer (HGT) located on mobile genetic elements including insertion sequences, transposons, integrons, bacteriophages, genomic islands can be exchanged between a broad spectrum of bacteria and significantly contribute to bacterial genome plasticity enabling adaptation to various different environments including pathogenicity towards plants and animals. Recent discoveries, partly resulting from whole-genome sequencing, have shown that chromosome and gene transfer also occurs between Eukaryotes such as in plants, fungi and mammals even including humans (Sørensen et al., 2005; Anderson and Seifert, 2011). It has now become clear that entire chromosomes can horizontally travel from one individual fungal strain to another; a mechanism that is totally different from vertical transfer of chromosomes known to occur during sexual and asexual cycles. Indeed, horizontal gene transfer (HGT) and HCT has significantly contributed to new or more aggressive fungal isolates or species towards plants as recently reviewed by Mehrabi et al., (2011). One of the best examples is the transfer of a gene encoding a host selective toxin (ToxA) from the wheat pathogen *S. nodorum* to *P. tritici-repentis* a previously harmless fungus growing on wheat, that transformed the latter fungus into a serious wheat pathogen, a biological event that marked the first outbreak of tan spot on wheat in 1941 (Friesen et al., 2006). Examples of HCT have been described for two different fungal species including *Alte*rnaria *alternata* and *Fusarium oxysporum* species. In laboratory experiments, it was shown that a hybrid strain of *A. alternata* between two different pathotypes harboring the conditionally dispensable chromosomes containing the host-specific toxin biosynthetic genes from both parental strains had an expanded pathogenicity range (Akagi et al., 2005; Akagi et

al., 2009). Another example of HCT involves transfer of two lineage-specific (LS) chromosomes between strains of *F. oxysporum*, that could convert a non-pathogenic strain into a pathogen hereby also explaining the polyphyletic origin of host specificity and the emergence of new pathogenic lineages in *F. oxysporum* (Ma et al., 2010).

Despite the recent development of high-throughput sequencing tools and more sophisticated genomic and proteomic techniques, not much is known about the mechanism of HCT. Several possible mechanisms involving anastomosis that precede HCT and HGT have been reported and recently reviewed (Mehrabi et al., 2011).

Most fungi have lower numbers of dispensable chromosomes than *M. graminicola*; most of the reported dispensable chromosomes have been shown to be involved in host-specificity and pathogenicity (Han et al., 2001; Hatta et al., 2002; Garmaroodi and Taga, 2007; Ma et al., 2010). As mentioned in the previous section, it was shown that effectors of *F. oxysporum* f.sp. *lycopersici* secreted in the xylem sap are encoded by genes located on LS chromosomes (Ma et al., 2010). In many types of fungi, including *S. cerevisiae*, polyploidy or aneuploidy may result as a response to different types of stress (Hilton et al., 1985; Fraser et al., 2005; Schoustra et al., 2007; Rancati et al., 2008; Poláková et al., 2009) and in some cases, aneuploidy provides a selective advantage (Selmecki et al., 2006; Gresham et al., 2008; Rancati et al., 2008; Selmecki et al., 2009). Indeed in *C. albicans*, low carbon source availability (Janbon et al., 1998) or antifungal drug exposure (Selmecki et al., 2009) but also growth in the host, heat shock or transformation of DNA have been shown to confer a selective advantage under these stressful conditions. It has been suggested that malsegregation of whole-chromosome or chromosome segments might be a common response associated with stress (Selmecki et al., 2010).

Interestingly, polyploid organisms with complete genome duplications (as is the case for autopolyploids such as potato), or allopolyploids with a combination of different genomes (as is the case for the genome of wheat) have all arisen from rare mitotic or meiotic non-disjunctions and are common in certain plant and animal taxa, and can be surprisingly stable (Comai, 2005). As an example, angiosperms have remarkably plastic genomes that can tolerate a considerable increase in genomic polyploidy (Leitch and Leitch, 2008).

So far, we have seen no evidence that genome plasticity did affect sexual or pathogenic fitness and recently it was shown that all mapped pathogenicity loci of *M. graminicola* reside on the core set of 13 chromosomes (Ware, 2006). In addition, from our proteomic analysis **(Chapter 4**) none of the identified secreted proteins mapped on the chromosomes of the dispensome. In fact, many of the unique genes that reside on the

dispensome appear to be associated with particular biological processes such as metabolism and transcriptional regulation. We speculate that they could facilitate rapid adaptation to changing environments **(Chapter 2-3)**. This warrants their further characterization. Recently, parental isolates and their progeny that were included in comparative genomic hybridizations **(Chapter 3)** were resequenced. This will provide further insight in the process of meiosis in this fungus by determining overall recombination rates, chromosome homology, recombination breakpoints and overall genome organization, such as generation and maintenance of the dispensome (chromosomes 14-21) as well as activation of transposons and repeat induced point mutations (RIP) after a single meiotic cycle and at base-pair resolution.

« Le savoir-faire » of hemibiotrophic fungi

Phytopathogenic fungi have developed a plethora of strategies to infect their host, both at the morphological level by the formation of diverse infection structures and at the molecular level by a wide range of toxins and/or effectors that vary in their chemical composition and mode of action (Horbach et al., 2011). Their nutritional lifestyle ranges from obligate biotrophs, such as powdery mildew and rust fungi (Schulze-Lefert and Vogel, 2000; Zhang et al., 2005), to necrotrophs such as *Cochliobolus heterostrophus* (Yoder, 1988) and *Botrytis cinerea* (Prins et al., 2000). The distinction between biotrophs and necrotrophs does not hold for all pathogens. Some pathogens have aspects of both life styles such as hemibiotrophs. The bacterium *Pseudomonas syringae* (Abramovitch and Martin, 2004), the fungus *Slerotinia sclerotiorum* (Hegedus and Rimmer, 2005) or the oomycete *Phytophthora infestans* (Judelson and Blanco, 2005), all show both biotrophic and necrotrophic infection strategies to colonize the host. Their early stages of infection are characterized by absence of symptoms and the pathogen seems to suppress programmed cell death (PCD) or avoids host defence responses; this is achieved by the effectors Avr3a of *P. infestans* (Armstrong et al., 2005) and Avr1b of *P. sojae* (Dou et al., 2008). During their later stages of infection they undergo a transition from asymptomatic biotrophic growth to a destructive necrotrophic phase, presumably by the activities of secreted lytic enzymes and necrogenic proteins (Horbach et al., 2011). Fungal and oomycete pathogens likely secrete an arsenal of proteins that are implicated in maintaining a biotrophic lifestyle; however, their modes of action are still poorly understood.

M. graminicola is a hemibiotroph pathogen with a stealth pathogenesis **(Chapter 3)**. It has a relatively long latent phase and apparently avoids recognition by the host while living

from nutrients in the apoplastic space. In addition, recent results suggest that there is little or no nutrient uptake during the biotrophic phase (Keon et al., 2007). Alternatively, the fungus could take up nutrients from degraded starch and proteins without affecting the viability of the colonized host cells **(Chapter 3)**. Fungi secrete numerous extracellular enzymes that hydrolyze polymers, such as cellulose, lignin, proteins and lipids and the resulting breakdown products including monosugars, amino acids, and fatty acids are absorbed by intercellular fungal hyphae by means of plasma membrane-localized transporters. The variety of transporters includes sugar, amino acid and lipid transporters. Alternatively, fungi do also contain many ABC and MFS transporters that enable them to excrete or detoxify antimicrobial host factors and thus to occupy a large number of ecological niches (Talbot, 2010). This also holds true for plants that cope with diseases. It was recently shown that a wheat ABC transporter conferred durable resistance to several fungal wheat pathogens, including leaf rust and powdery mildew (Krattinger et al., 2009). Recent studies in *U. maydis* identified a plasma membrane-localized sucrose transporter (Srt1) that is specifically active during plant infection to compete with plant transporters enabling the uptake of sucrose without prior hydrolysis by invertases (Wahl et al., 2010). This may prevent the activation of plant defence as long as the plant does not sense changes in the apoplastic glucose concentrations (Bolton, 2009). Interestingly, Srt1 was also shown to be required for virulence, which emphasizes the crucial role of this transporter for efficient sugar uptake and modulating apoplastic signals that are potentially recognized by the host (Wahl et al., 2010). Such a system might also occur in *M. graminicola* and certainly needs further investigation.

In *M. graminicola,* the long latent phase is followed by a necrotrophic phase that is characterized by a reduction in photosynthesis and a massive accumulation of H_2O_2 leading to cell-death (Keon et al., 2007; Shetty et al., 2007; Rudd et al., 2008), and finally to symptom appearance (Kema et al., 1996b; Duncan and Howard, 2000). Keon et al. (2007) showed that necrotic responses occurring in the *M. graminicola*-wheat interaction are reminiscent of the hypersensitive-response (HR) which is a characteristic response associated with resistance against biotrophic pathogens. In **Chapters 4** and **5,** I have performed experiments for the initial characterization of the fungal proteome with an emphasis on the secretome. We have employed various advanced protein analyses that resulted in the identification of an array of proteins that need to be functionally validated. This will eventually result in the identification of key determinants of the biotrophic and necrotrophic phases and hence a better understanding how they possibly induce resistance or susceptibility.

Interestingly, it has been shown that *P. infestans* possesses an 'accelerator and brake' strategy that fine-tunes the transition from biotrophy to necrotrophy (Fig. 2). Indeed, the secreted effector protein (Sne1) from *P. infestans* that is specifically expressed during the early biotrophic phase, suppresses the action of secreted necrosis-inducing effectors (Nep1-like proteins) during biotrophic growth, such as PiNPP1.1 and PsojNIP in *P. infestans* and *P. sojae*, respectively, but also suppresses PCD mediated by a broad spectrum of Avr-R protein interactions. This major finding suggests that some effector proteins can act antagonistically during the two distinct phases of hemibiotrophy, a mechanism that might also operate in other eukaryotic plant pathogens (Kelley et al., 2010; Lee and Rose, 2010).

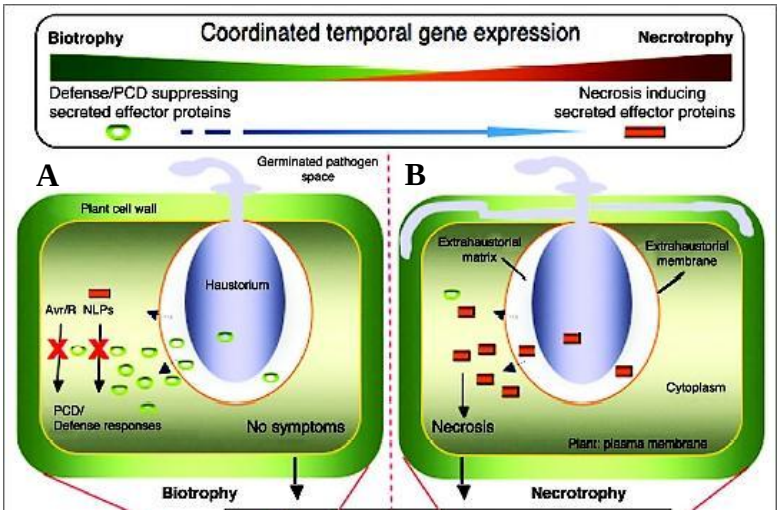

Fig. 2. Hypothetical model explaining the 'accelerator and brake' strategy in *Phytophtora infestans.* **A.** In the biotrophic phase, secreted effector proteins such as SNE1 are expressed and block programmed cell death (PCD) and plant defense responses that would normally be induced by Avr/R protein interactions but also secreted proteins such as Nep1-like proteins (NLPs). **B.** NLP secretion during the later phase of infection induces rapid cell death and tissue necrosis (after Lee and Rose, 2010).

We do not know whether a similar system applies to *M. graminicola* even though there has been significant progress on the molecular characterization of the *M. graminicola*-wheat interaction. We have identified genes that are associated with necrosis development. These findings confirm recent models (Fig. 3) (Hammond-Kosack and Rudd, 2008) and earlier observations (Kema et al., 1996b; Perrone et al., 2000; Shetty et al., 2009) that suggested an active cell destruction pathway operating in this pathosystem. The initial characterization of MgNips in this fungus **(Chapter 5)** "lifts the veil" of a likely complex molecular control of the nutritional requirements of *M. graminicola* and its interaction with wheat. Their temporal expression, mode of action, and targets are research areas that require to be investigated in order to determine whether a GFG and/or an iGFG system operate in this pathosystem. In summary, the role of toxins, either secondary metabolites or proteinaceous toxins in GFG or iGFG is still under debate and further research is required. The finished

genome sequence of *M. graminicola* **(Chapter 3)**, advanced protein and RNAseq technologies will facilitate further exploration of the stealthy world of this hemibiotroph.

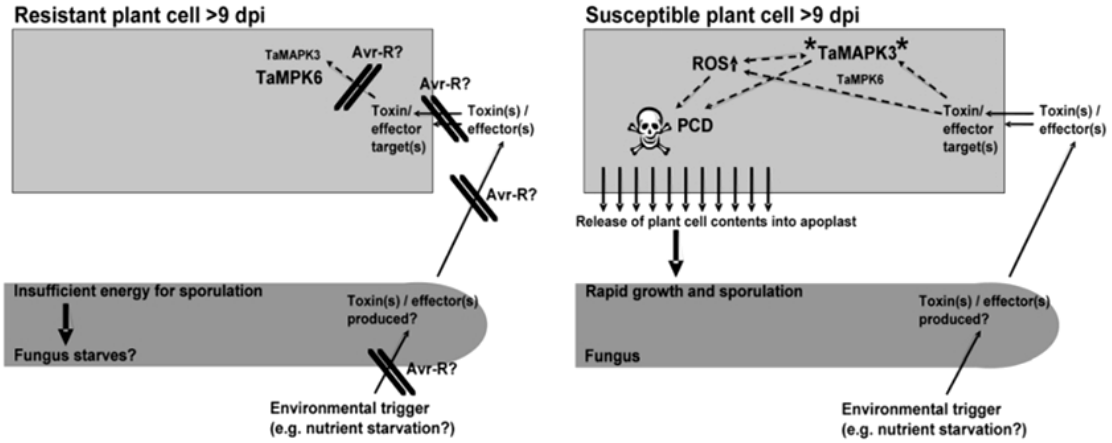

Fig. 3. Models illustrating the events that occur in wheat leaf cells during susceptible and resistant interactions with the fungal pathogen, *Mycosphaerella graminicola*.
In a susceptible disease interaction, around nine days post inoculation (dpi), inverse changes in the relative levels of the two MAPK proteins are observed. At this stage the fungus produces, as yet un-identified, toxin(s) and/or effector(s) that trigger the post-translational activation (**) of TaMPK3. These events occur in parallel with the activation of programmed cell death (PCD) signalling, which may lead to the generation of reactive oxygen species (ROS). They all affect cell permeability resulting in nutrient leakage from dying plant cells that facilitates fungal proliferation in the apoplast. These responses do not occur in the resistant interaction. Parallel crosses lines represent the possible sites for protective function of corresponding Avr-R protein combinations. The lack of plant cell reactions during host resistance is a limitation on the nutrients available to the fungus which prevents its further proliferation (Hammond-Kosack and Rudd, 2008).

Concluding remarks

M. graminicola is a pathogen of major economical importance, and to date its control still heavily relies on chemicals. Selecting resistant plants was one of the earliest practices that growers and breeders used to combat plant pathogens. Biffen (1905) was the first to genetically analyze host resistance to a fungal plant pathogen by studying the inheritance of stripe rust in wheat. Since then hundreds of resistance genes to other cereal diseases have been characterized (McIntosh et al., 2007), but so far only 18 resistance genes (*Stb*) to *M. graminicola* have been identified and mapped, exclusively in bread wheat (Arraiano et al., 2007; Goodwin, 2007; Chartrain et al., 2009; Tabib Ghaffary, 2011) but none have yet been genetically cloned. The first gene was identified only in 1979 (Wilson, 1979) despite the dramatic severity of STB in this crop. However, none have been identified in tetraploid durum wheat despite its importance as a North African staple crop and its extreme susceptibility to STB (Maccaferri, personal communication).

The discovery of genes that play a key role in virulence and avirulence in the *M. graminicola*–wheat interaction will help breeders to identify more germplasm with resistance to STB in both bread and durum wheat. The results of this thesis provide the foundation for the further discovery of key determinants that *M. graminicola* employs to colonize host cells and eventually kill them for massive proliferation and survival under natural condition. With an increasing community and collaborative and ever increasing resources, we can take genomics to the field for practical implementation in the foreseeable future.

LITERATURE CITED

Abramovitch, R.B., and Martin, G.B. 2004. Strategies used by bacterial pathogens to suppress plant defenses. Current opinion in plant biology 7:356-364.

Akagi, Y., Akamatsu, H., Yamamoto, M., Tsuge, T., Otani, H., and Kodama, M. 2005. Characterization of the genomic region, controlling biosynthesis of host-specific AAL-toxins, on the conditionally dispensable chromosome of the tomato pathotype of *Alternaria alternata.* Fungal Genet. Newsl 52:188.

Akagi, Y., Taga, M., Yamamoto, M., Tsuge, T., Fukumasa-Nakai, Y., Otani, H., and Kodama, M. 2009. Chromosome constitution of hybrid strains constructed by protoplast fusion between the tomato and strawberry pathotypes of *Alternaria alternata*. Journal of General Plant Pathology 75:101-109.

Allers, T., and Lichten, M. 2001. Differential Timing and Control of Noncrossover and Crossover Recombination during Meiosis. Cell 106:47-57.

Anderson, M.T., and Seifert, H.S. 2011. Opportunity and Means: Horizontal Gene Transfer from the Human Host to a Bacterial Pathogen. mBio 2(1):e00005-11.

Armstrong, M.R., Whisson, S.C., Pritchard, L., Bos, J.I.B., Venter, E., Avrova, A.O., Rehmany, A.P., Böhme, U., Brooks, K., and Cherevach, I. 2005. An ancestral oomycete locus contains late blight avirulence gene Avr3a, encoding a protein that is recognized in the host cytoplasm. Proceedings of the National Academy of Sciences of the United States of America 102:7766-7771.

Arraiano, L.S., Chartrain, L., Bossolini, E., Slatter, H.N., Keller, B., and Brown, J.K.M. 2007. A gene in European wheat cultivars for resistance to an African isolate of *Mycosphaerella graminicola.* Plant Pathology 56:73-78.

Barton, N., and Charlesworth, B. 1998. Why sex and recombination? Science 281: 1986-1990.

Biffen, R.H. 1905. Mendel's laws of inheritance and wheat breeding. The Journal of Agricultural Science 1:4-48.

Blitzblau, H.G., Bell, G.W., Rodriguez, J., Bell, S.P., and Hochwagen, A. 2007. Mapping of meiotic single-stranded DNA reveals double-strand-break hotspots near centromeres and telomeres. Current Biology 17:2003-2012.

Bolton, M.D. 2009. Primary metabolism and plant defense-fuel for the fire. Molecular Plant-Microbe Interactions 22:487-497.

Brading, P.A., Verstappen, E.C.P., Kema, G.H.J., and Brown, J.K.M. 2002. A gene-for-gene relationship between wheat and *Mycosphaerella graminicola*, the Septoria tritici blotch pathogen. Phytopathology 92:439-445.

Chartrain, L., Sourdille, P., Bernard, M., and Brown, J.K.M. 2009. Identification and location of *Stb9*, a gene for resistance to septoria tritici blotch in wheat cultivars Courtot and Tonic. Plant Pathology 58:547-555.

Chen, R.S., and McDonald, B.A. 1996. Sexual reproduction plays a major role in the genetic structure of populations of the fungus *Mycosphaerella graminicola.* Genetics 142:1119-1127.

Comai, L. 2005. The advantages and disadvantages of being polyploid. Nature Reviews Genetics 6:836-846.

Cottarel, G., Shero, J.H., Hieter, P., and Hegemann, J.H. 1989. A 125-base-pair CEN6 DNA fragment is sufficient for complete meiotic and mitotic centromere functions in *Saccharomyces cerevisiae.* Molecular and Cellular Biology 9:3342-3349.

Dou, D., Kale, S.D., Wang, X., Chen, Y., Wang, Q., Jiang, R.H.Y., Arredondo, F.D., Anderson, R.G., and Thakur, P.B. 2008. Conserved C-terminal motifs required for avirulence and suppression of cell death by *Phytophthora sojae* effector Avr1b. The Plant Cell 20:1118-1133.

Duncan, K., and Howard, R. 2000. Cytological analysis of wheat infection by the leaf blotch pathogen *Mycosphaerella graminicola.* Mycological Research 104:1074-1082.

Ekwall, K. 2007. Epigenetic control of centromere behavior. Annual Revieuw of Genetics. 41:63-81.

Felsenstein, J. 1974. The evolutionary advantage of recombination. Genetics 78: 737-756.

Fraser, J.A., Huang, J.C., Pukkila-Worley, R., Alspaugh, J.A., Mitchell, T.G., and Heitman, J. 2005. Chromosomal translocation and segmental duplication in *Cryptococcus neoformans.* Eukaryot Cell 4:401 - 406.

Friesen, T., Stukenbrock, E., Liu, Z., Meinhardt, S., Ling, H., Faris, J., Rasmussen, J., Solomon, P., McDonald, B., and Oliver, R. 2006. Emergence of a new disease as a result of interspecific virulence gene transfer. Nature Genetics 38:953-956.

Garmaroodi, H., and Taga, M. 2007. Duplication of a conditionally dispensable chromosome carrying pea pathogenicity (PEP) gene clusters in *Nectria haematococca*. Molecular Plant-Microbe Interactions 20:1495-1504.

Gladstone, M.N., Obeso, D., Chuong, H., and Dawson, D.S. 2009. The Synaptonemal Complex Protein Zip1 Promotes Bi-Orientation of Centromeres at Meiosis I. PLoS Genet 5:e1000771.

Goodwin, S.B. 2007. Back to basics and beyond: increasing the level of resistance to Septoria tritici blotch in wheat. Australasian Plant Pathology 36:532-538.

Gresham, D., Desai, M.M., Tucker, C.M., Jenq, H.T., Pai, D.A., Ward, A., DeSevo, C.G., Botstein, D., and Dunham, M.J. 2008. The repertoire and dynamics of evolutionary adaptations to controlled nutrient-limited environments in yeast. PLoS Genetics 4:e1000303.

Hammond-Kosack, K.E., and Rudd, J.J. 2008. Plant resistance signalling hijacked by a necrotrophic fungal pathogen. Plant Signaling & Behavior 3:993-995.

Han, Y.N., Liu, X.G., Benny, U., Kistler, H.C., and VanEtten, H.D. 2001. Genes determining pathogenicity to pea are clustered on a supernumerary chromosome in the fungal plant pathogen *Nectria haematococca*. Plant Journal 25:305-314.

Hassold, T., Hall, H., and Hunt, P. 2007. The origin of human aneuploidy: where we have been, where we are going. Human molecular genetics 16:203-208.

Hatta, R., Ito, K., Hosaki, Y., Tanaka, T., Tanaka, A., Yamamoto, M., Akimitsu, K., and Tsuge, T. 2002. A conditionally dispensable chromosome controls host-specific pathogenicity in the fungal plant pathogen *Alternaria alternata*. Genetics 161:59-70.

Hegedus, D.D., and Rimmer, S.R. 2005. *Sclerotinia sclerotiorum*: When "to be or not to be" a pathogen? FEMS microbiology letters 251:177-184.

Hilton, C., Markie, D., Corner, B., Rikkerink, E., and Poulter, R. 1985. Heat shock induces chromosome loss in the yeast Candida albicans. Molecular and General Genetics MGG 200:162-168.

Horbach, R., Navarro-Quesada, A., Knogge, W., and Deising, H. 2011. When and how to kill a plant cell: Infection strategies of plant pathogenic fungi. Journal of Plant Physiology 168:51-62.

Hunter, T., Coker, R.R., and Royle, D.J. 1999. The teleomorph stage, *Mycosphaerella graminicola*, in epidemics of septoria tritici blotch on winter wheat in the UK. Plant Pathology 48:51-57.

Janbon, G., Sherman, F., and Rustchenko, E. 1998. Monosomy of a specific chromosome determines L-sorbose utilization: a novel regulatory mechanism in *Candida albicans*. Proceedings of the National Academy of Sciences of the United States of America 95:5150-5155.

Judelson, H., and Blanco, F. 2005. The spores of Phytophthora: weapons of the plant destroyer. Nat Rev Microbiol 3:47 - 58.

Karpen, G.H., and Allshire, R.C. 1997. The case for epigenetic effects on centromere identity and function. Trends in Genetics 13:489-496.

Keeney, S. 2001. Mechanism and control of meiotic recombination initiation. Current topics in developmental biology 52:1-53.

Kelley, B.S., Lee, S.-J., Damasceno, C.M.B., Chakravarthy, S., Kim, B.-D., Martin, G.B., and Rose, J.K.C. 2010. A secreted effector protein (SNE1) from *Phytophthora infestans* is a broadly acting suppressor of programmed cell death. The Plant Journal 62:357-366.

Kema, G.H.J., and van Silfhout, C. 1997. Genetic variation for virulence and resistance in the wheat-*Mycosphaerella graminicola* pathosystem III. Comparative seedling and adult plant experiments. Phytopathology 87:266-272.

Kema, G.H.J., Sayoud, R., Annone, J., and Van Silfhout, C. 1996a. Genetic variation for virulence and resistance in the wheat-*Mycosphaerella graminicola* pathosystem. II: Analysis of interactions between pathogen isolates and host cultivars. Phytopathology 86:213-220.

Kema, G.H.J., Yu, D., Rijkenberg Frits, H.J., Shaw Michael, W., and Baayen Robert, P. 1996b. Histology of the pathogenesis of *Mycosphaerella graminicola* in wheat. Phytopathology 86:777-786.

Kema, G.H.J., Annone, J., G, Sayoud, R., Van Silfhout, C.H., Van Ginkel, M., and De Bree, J. 1996c. Genetic variation for virulence and resistance in the wheat-*Mycosphaerella graminicola* pathosystem: I. Interactions between pathogen isolates and host cultivars. Phytopathology 86:200-212.

Kema, G.H.J., Verstappen Els, C.P., Todorova, M., and Waalwijk, C. 1996d. Successful crosses and molecular tetrad and progeny analyses demonstrate heterothallism in *Mycosphaerella graminicola*. Current Genetics 30:251-258.

Keon, J., Antoniw, J., Carzaniga, R., Deller, S., Ward, J., Baker, J., Beale, M., Hammond-Kosack, K., and Rudd, J. 2007. Transcriptional adaptation of *Mycosphaerella graminicola* to programmed cell death (PCD) of its susceptible wheat host. Molecular Plant-Microbe Interactions 20:178-193.

Koehler, K.E., Boulton, C.L., Collins, H.E., French, R.L., Herman, K.C., Lacefield, S.M., Madden, L.D., Schuetz, C.D., and Hawley, R.S. 1996. Spontaneous X chromosome MI and MII nondisjunction events in *Drosophila melanogaster* oocytes have different recombinational histories. Nature genetics 14:406-414.

Krattinger, S.G., Lagudah, E.S., Spielmeyer, W., Singh, R.P., Huerta-Espino, J., McFadden, H., Bossolini, E., Selter, L.L., and Keller, B. 2009. A putative ABC transporter confers durable resistance to multiple fungal pathogens in wheat. Science 323:1360.

Lamb, B., Dilip, K.A., and George, G.K. 2003. Meiotic Recombination in Fungi: Mechanisms and Controls of Crossing-over and Gene Conversion. Applied Mycology and Biotechnology 3:15-41.

Lamb, N., Sherman, S., and Hassold, T. 2005. Effect of meiotic recombination on the production of aneuploid gametes in humans. Cytogenetic and genome research 111:250-255.

Lao, J.P., and Hunter, N. 2010. Trying to Avoid Your Sister. PLoS Biol 8:e1000519.

Lee, S.J., and Rose, J.K.C. 2010. Mediation of the transition from biotrophy to necrotrophy in hemibiotrophic plant pathogens by secreted effector proteins. Plant Signaling & Behavior 5:769.

Leitch, A.R., and Leitch, I.J. 2008. Genomic Plasticity and the Diversity of Polyploid Plants. Science 320:481-483.

Lukaszewski, A., and Kopecký, D. 2010. The Ph1 Locus from Wheat Controls Meiotic Chromosome Pairing in Autotetraploid Rye (*Secale cereale* L.). Cytogenetic and genome research 129:117-123.

Ma, L., van der Does, H., Borkovich, K., Coleman, J., Daboussi, M., Di Pietro, A., Dufresne, M., Freitag, M., Grabherr, M., and Henrissat, B. 2010. Comparative genomics reveals mobile pathogenicity chromosomes in Fusarium. Nature 464:367 - 373.

Malik, H.S., and Henikoff, S. 2009. Major evolutionary transitions in centromere complexity. Cell 138:1067-1082.

Mancera, E., Bourgon, R., Brozzi, A., Huber, W., and Steinmetz, L.M. 2008. High-resolution mapping of meiotic crossovers and non-crossovers in yeast. Nature 454:479-485.

McDonald, B.A., and Martinez, J.P. 1991. Chromosome Length Polymorphisms in a *Septoria tritici* Population. Current Genetics 19:265-272.

McIntosh, R.A., Devos, K.M., Dubcovsky, J., Rogers, W.J., Morris, C.F., Appels, R., Somers, D.J., Anderson, O.A. 2007. Catalogue of gene symbols for wheat: 2007 Supplement.

Mehrabi, R., Taga, M., and Kema, G.H.J. 2007. Electrophoretic and cytological karyotyping of the foliar wheat pathogen *Mycosphaerella graminicola* reveals many chromosomes with a large size range. Mycologia 99:868-876.

Mehrabi, R., Bahkali, A.H., Abd-Elsalam, K.A., Moslem, M., Ben M'Barek, S., Gohari, A.M., Jashni, M.K., Stergiopoulos, I., Kema, G.H.J., and de Wit, P.J.G.M. 2011. Horizontal gene and chromosome transfer in plant pathogenic fungi affecting host range. FEMS Microbiology 35:542-554.

Michaelis, C., Ciosk, R., and Nasmyth, K. 1997. Cohesins: chromosomal proteins that prevent premature separation of sister chromatids. Cell 91:35-45.

Nasmyth, K. 2001. Disseminating the genome: joining, resolving, and separating sister chromatids during mitosis and meiosis. Annual Review of Genetics 35:673-745.

Nishant, K., and Rao, M. 2006. Molecular features of meiotic recombination hot spots. Bioessays 28:45-56.

Page, S.L., and Hawley, R.S. 2003. Chromosome Choreography: The Meiotic Ballet. Science 301:785-789.

Perrone, G., Logrieco, A., Kema, G.H.J., Ritieni, A., Bottalico, A. 2000. Phytotoxic activity of *Mycosphaerella graminicola* culture filtrates. Developments in Plant Genetics and Breeding 6:195-201.

Poláková, S., Blume, C., Zárate, J.Á., Mentel, M., Jørck-Ramberg, D., Stenderup, J., and Piškur, J. 2009. Formation of new chromosomes as a virulence mechanism in yeast Candida glabrata. Proceedings of the National Academy of Sciences 106:2688.

Ponomarenko, A., Goodwin, S.B., and Kema, G.H.J. 2011. Septoria tritici blotch (STB) of wheat. Plant Health Instructor.

Prins, T.W., Tudzynski, P., Von Tiedemann, A., Tudzynski, B., Ten Have, A., Hansen, M., Tenberge, K., and Van Kan, J. 2000. Infection strategies of *Botrytis cinerea* and related necrotrophic pathogens. Fungal pathology 8:33-64.

Quaedvlieg, W., Kema, G.H.J., Groenewald, J.Z., Verkley, G.J.M., Seifbarghi, S., Razavi, M., Mirzadi Gohari, A., Mehrabi, R., and Crous, P.W., 2011. *Zymoseptoria* gen. nov.: a new genus to accommodate Septoria-like species occurring on graminicolous hosts. Persoonia 26:57-69.

Rancati, G., Pavelka, N., Fleharty, B., Noll, A., Trimble, R., Walton, K., Perera, A., Staehling-Hampton, K., Seidel, C.W., and Li, R. 2008. Aneuploidy underlies rapid adaptive evolution of yeast cells deprived of a conserved cytokinesis motor. Cell 135:879-893.

Rockmill, B., Voelkel-Meiman, K., and Roeder, G.S. 2006. Centromere-proximal crossovers are associated with precocious separation of sister chromatids during meiosis in *Saccharomyces cerevisiae*. Genetics 174:1745.

Roeder, G.S. 1997. Meiotic chromosomes: it takes two to tango. Genes & Development 11:2600-2621.

Rudd, J., Keon, J., and Hammond-Kosack, K. 2008. The wheat mitogen-activated protein kinases TaMPK3 and TaMPK6 are differentially regulated at multiple levels during compatible disease interactions with *Mycosphaerella graminicola*. Plant Physiology 147:802-815.

Schoustra, S.E., Debets, A.J.M., Slakhorst, M., and Hoekstra, R.F. 2007. Mitotic recombination accelerates adaptation in the fungus *Aspergillus nidulans*. PLoS Genetics 3:e68.

Schulze-Lefert, P., and Vogel, J. 2000. Closing the ranks to attack by powdery mildew. Trends in plant science 5:343-348.

Selmecki, A., Forche, A., and Berman, J. 2006. Aneuploidy and isochromosome formation in drug-resistant *Candida albicans*. Science 313:367 - 370.

Selmecki, A., Forche, A., and Berman, J. 2010. Genomic Plasticity of the Human Fungal Pathogen *Candida albicans.* Eukaryotic Cell 9:991-1008.

Selmecki, A.M., Dulmage, K., Cowen, L.E., Anderson, J.B., and Berman, J. 2009. Acquisition of aneuploidy provides increased fitness during the evolution of antifungal drug resistance. PLoS Genet 5:e1000705.

Shetty, N., Mehrabi, R., Lutken, H., Haldrup, A., Kema, G., Collinge, D., and Jorgensen, H. 2007. Role of hydrogen peroxide during the interaction between the hemibiotrophic fungal pathogen *Septoria tritici* and wheat. New Phytologist 174:637-647.

Shetty, N.P., Jensen, J.D., Knudsen, A., Finnie, C., Geshi, N., Blennow, A., Collinge, D.B., and Jorgensen, H.J.L. 2009. Effects of b-1,3-glucan from *Septoria tritici* on structural defence responses in wheat. The Journal of Experimental Botany 60:4287-4300.

Sionov, E., Lee, H., Chang, Y.C., and Kwon-Chung, K.J. 2010. *Cryptococcus neoformans* Overcomes Stress of Azole Drugs by Formation of Disomy in Specific Multiple Chromosomes. PLoS Pathog 6:e1000848.

Sørensen, S.J., Bailey, M., Hansen, L.H., Kroer, N., and Wuertz, S. 2005. Studying plasmid horizontal transfer in situ: a critical review. Nature Reviews Microbiology 3:700-710.

Suffert, F., Sache, I., and Lannou, C. 2010. Early stages of septoria tritici blotch epidemics of winter wheat: build-up, overseasoning, and release of primary inoculum. Plant Pathology: 60:166–177.

Tabib Ghaffary, S.M., Robert, O., Laurent, V., Lonnet, P., Margalé, E., van der Lee, T.A.J., Visser, R.G.F., and Kema, G.H.J. 2011. Genetic analysis of resistance to septoria tritici blotch in the French winter wheat cultivars Balance and Apache. TAG Theoretical and Applied Genetics:1-14.

Tabib Ghaffary, S.M. 2011. Efficacy and mapping of resistance to *Mycosphaerella graminicola* in wheat. PhD Thesis, Wageningen University, The Netherlands.

Talbert, P.B., and Henikoff, S. 2010. Centromeres convert but don't cross. PLoS Biology 8 (3):e1000326.

Talbot, N.J. 2010. Living the Sweet Life: How Does a Plant Pathogenic Fungus Acquire Sugar from Plants? PLoS Biol 8:e1000308.

Tek, A.L., and Jiang, J. 2004. The centromeric regions of potato chromosomes contain megabase-sized tandem arrays of telomere-similar sequence. Chromosoma 113:77-83.

Tettelin, H., Masignani, V., Cieslewicz, M.J., Donati, C., Medini, D., Ward, N.L., Angiuoli, S.V., Crabtree, J., Jones, A.L., Durkin, A.S., DeBoy, R.T., Davidsen, T.M., Mora, M., Scarselli, M., Margarit y Ros, I., Peterson, J.D., Hauser, C.R., Sundaram, J.P., Nelson, W.C., Madupu, R., Brinkac, L.M., Dodson, R.J., Rosovitz, M.J., Sullivan, S.A., Daugherty, S.C., Haft, D.H., Selengut, J., Gwinn, M.L., Zhou, L., Zafar, N., Khouri, H., Radune, D., Dimitrov, G., Watkins, K., O'Connor, K.J.B., Smith, S., Utterback, T.R., White, O., Rubens, C.E., Grandi, G., Madoff, L.C., Kasper, D.L., Telford, J.L., Wessels, M.R., Rappuoli, R., and Fraser, C.M. 2005. Genome analysis of multiple pathogenic isolates of *Streptococcus agalactiae*: Implications for the microbial "pan-genome". Proceedings of the National Academy of Sciences of the United States of America 102:13950-13955.

Tsubouchi, T., and Roeder, G.S. 2005. A synaptonemal complex protein promotes homology-independent centromere coupling. Science 308:870.

Waalwijk, C., Mendes, O., Verstappen E.C.P., De Waard M.A., and Kema G.H.J. 2002. Isolation and characterization of the mating-type idiomorphs from the wheat septoria leaf blotch fungus *Mycosphaerella graminicola*. Fungal Genetics and Biology 35:277-286.

Wahl, R., Wippel, K., Goos, S., Kämper, J., and Sauer, N. 2010. A Novel High-Affinity Sucrose Transporter Is Required for Virulence of the Plant Pathogen *Ustilago maydi*s. PLoS Biol 8:e1000303.

Wahls, W.P., Siegel, E.R., and Davidson, M.K. 2008. Meiotic Recombination Hotspots of Fission Yeast Are Directed to Loci that Express Non-Coding RNA. PLoS One 3:e2887.

Ware, S.B. 2006. Aspects of sexual reproduction in Mycosphaerella species on wheat and barley : genetic studies on specificity, mapping, and fungicide resistance. PhD Thesis, Wageningen University, The Netherlands.

Whitby, M. 2005. Making crossovers during meiosis. Biochemical Society Transactions 33:1451-1455.

Willard, H.F., and Rudd, M.K. 2006. Genomic organization and function of human centromeres. *Genomic Disorders:* 115-129.

Wilson, R. 1979. Resistance to *Septoria tritici* in two wheat cultivars, determined by independent, single dominant genes. Australasian Plant Pathology 8:16-18.

Wittenberg, A.H.J. 2007. Genetic mapping using the Diversity Arrays Technology (DArT): application and validation using the whole-genome sequences of Arabidopsis thaliana and the fungal wheat pathogen *Mycosphaerella graminicola.* PhD Thesis, Wageningen University, The Netherlands.

Yoder, O. 1988. Cochliobolus heterostrophus, cause of southern corn leaf blight. Adv. Plant Pathol 6:93-112.

Zhan, J., Pettway, R., and McDonald, B. 2003. The global genetic structure of the wheat pathogen *Mycosphaerella graminicola* is characterized by high nuclear diversity, low mitochondrial diversity, regular recombination, and gene flow. Fungal Genetics and Biology 38:286-297.

Zhan, J., Kema, G.H.J., Waalwijk, C., and McDonald, B.A. 2002. Distribution of mating type alleles in the wheat pathogen *Mycosphaerella graminicola* over spatial scales from lesions to continents. Fungal Genetics and Biology. 2002; 36:128-136.

Zhang, Z., Henderson, C., Perfect, E., Carver, T.L.W., Thomas, B.J., Skamnioti, P., and Gurr, S. 2005. Of genes and genomes, needles and haystacks: *Blumeria graminis* and functionality. Molecular Plant Pathology 6:561-575.

Summary

The phytopathogenic fungus *Mycosphaerella graminicola* (Fuckel) J. Schröt. in Cohn (asexual stage: *Zymoseptoria tritici* (Desm.) Quaedvlieg & Crous) causes septoria tritici leaf blotch (STB) in wheat and is one of the most important diseases of this crop worldwide. However, STB control, mainly based on the use of resistant cultivars and fungicides, is significantly hampered by the limited understanding of the genetic and biochemical bases of pathogenicity, and mechanisms of infection and resistance in the host. *M. graminicola* has a very active sexual cycle under field conditions, which is an important driver of STB epidemics. Moreover, it results in high genetic diversity of field populations that causes a major challenge for the development and sustainable management of resistant cultivars and the discovery of new antifungal compounds. Understanding the role of the sexual and asexual life cycles on genome composition of this versatile pathogen and its infection strategy is crucial in order to develop novel control methods.

Chapter 1 is an introduction to the biology and pathogenicity of *M. graminicola.* In addition, it shortly describes the impact of improved and novel technologies on the speed, scope and scale of comparative genomics research.

Chapter 2 provides detailed genetic analyses of two *M. graminicola* mapping populations, using mainly DArT markers, and the analysis of the meiotic transmission of unequal chromosome numbers. Polymorphisms in chromosome length and number were frequently observed in progeny isolates, of which 15–20% lacked one or more chromosomes despite their presence in one or both parents, but these had no apparent effect on sexual and pathogenic fitness. *M. graminicola* has up to eight so called dispensable chromosomes that can be easily lost - collectively called the dispensome - which is, so far, the highest number of dispensable chromosomes reported in filamentous fungi. They represent small-sized chromosomes and make up 38% of the chromosome complement of this pathogen. Much of the observed genome plasticity is generated during meiosis and could explain the high adaptability of *M. graminicola* in the field. The generated linkage map was crucial for finishing the *M. graminicola* genome sequence.

Chapter 3 describes the *M. graminicola* genome sequence with highlights on genome structure and organization including the eight dispensable chromosomes. The genome comprises a core set of 13 chromosomes and a dispensome, consisting of eight chromosomes that are distinct from the core chromosomes in structure, gene and repeat content. The

dispensome contains a higher frequency of transposons and the genes have a different codon use. Most of the genes present one the dispensome are also present on the core chromosomes but little synteny is observed neither between the *M. graminicola* dispensome and the core chromosomes nor with the chromosomes of other related *Dothideomycetes*. The dispensome likely originates from ancient horizontal transfer(s) from (an) unknown donor(s).

Chapter 4 shows a global analysis of proteins secreted by *M. graminicola* in apoplastic fluids during infection. It focuses mainly on fungal proteins secreted in a compatible interaction. The study showed that many of the annotated secreted proteins have putative functions in fungal pathogenicity, such as cell wall degrading enzymes and proteases, but the function of a substantial number of the identified proteins is unknown. During compatible interactions proteins are primarily secreted during the later stages. However, many pathogenesis-related host proteins, such as PR-2, PR-3 and PR-9, accumulated earlier and at higher concentrations during incompatible interactions, indicating that fungal effectors are recognized by resistant plants and trigger resistant gene-mediated defence responses, though without a visible hypersensitive response.

Chapter 5 further details the initial identification and characterization of necrosis-inducing proteins that are produced in culture filtrates (CFs) of *M. graminicola*. The necrosis-inducing activity of CFs is light dependent and inactivated by proteinase K and heat treatment (100°C). This is reminiscent of the necrosis-inducing properties of host selective toxins of other Dothideomycete pathogens such as *Stagonospora nodorum* and *Pyrenophora tritici-repentis.* Subsequent purifications of CFs and *mass spectrometry* identified several candidate proteins with necrosis-inducing activity. Heterologous expression of the two most prominent proteins in *Pichia pastoris* produced sufficient quantities for infiltration assays in a panel of wheat cultivars that showed differential responses, suggesting specific recognition.

Chapter 6 provides a general discussion of the thesis and puts the results obtained in a broader perspective with a focus on the genome structure of *M. graminicola* and its function. In addition, aspects of the hemi-biotrophic lifestyle, the relevance of secreted proteins for the wheat-*M. graminicola* pathosystem in relation to gene-for-gene models and the potential implications for resistance breeding strategies are discussed.

Samenvatting

De plantpathogene schimmel (Fuckel) J. Schröt. in Cohn (asexual stage: *Zymoseptoria tritici* (Desm.) Quaedvlieg & Crous) veroorzaakt septoria tritici bladvlekkenziekte in tarwe en is wereldwijd één van de belangrijkste ziekten in dit gewas. De beheersing van deze ziekte, vooral door het gebruik van resistente rassen en fungiciden, wordt echter bemoeilijkt door het beperkte inzicht in de genetische en biochemische basis van pathogeniteit, en de mechanismen voor infectie en waardplantresistentie. *M. graminicola* heeft een zeer actieve seksuele cyclus in het veld die de ontwikkeling van epidemieën aanjaagt. Bovendien resulteert dit in een grote genetische diversiteit van natuurlijke populaties die een uitdaging vormt voor de ontwikkeling en het duurzaam management van nieuwe resistente tarwerassen en van nieuwe en effectieve gewasbemingsmiddelen. Het doorgronden van de (a)seksuele voortplanting en de infectiestrategie van dit veranderlijke pathogeen is cruciaal voor het ontwerpen van nieuwe beheersingsmethoden.

Hoofdstuk 1 is een introductie in de biologie en pathogeniteit van *M. graminicola*. Daarnaast wordt in het kort beschreven hoe verbeterde en nieuwe technologieën de snelheid, omvang en schaal van vergelijkend genoomonderzoek beïnvloeden.

Hoofdstuk 2 geeft een gedetailleerde koppelingsanalyse van twee *M. graminicola* kruisingspopulaties waarin vooral DArT merkers zijn gebruikt evenals de analyse van de meiotische transmissie van ongelijke chromosoomaantallen in de ouderisolaten. Polymorfismen in chromosoomlengte en aantallen werden frequent waargenomen in de gegenereerde nakomelingen, waarvan 15-20% één of meer chromosomen miste ondanks hun aanwezigheid in één of beide ouderisolaten, maar hadden geen duidelijk effect op seksuele of pathogene fitheid. *M. graminicola* heeft maximaal acht niet noodzakelijke chromosomen die gezamenlijk het dispensoom worden genoemd. Dit betreft het grootste aantal geïdentificeerde niet noodzakelijke chromosomen in filamenteuze schimmels, die relatief klein zijn en in *M. graminicola* 38% omvatten van het totale aantal chromosomen. Deze zogenaamde genoomplasticiteit, die het aanpassingsvermogen van de schimmel in het veld mede kan verklaren, wordt voornamelijk gegenereerd tijdens de meiose. De in deze studie gemaakte koppelingskaarten zijn ook cruciaal gebleken bij de afronding en completering van het *M. graminicola* genoomsequentie programma.

Hoofdstuk 3 beschrijft de sequentieanalyse van *M. graminicola* met nadruk op de genoomstrucuur en –organisatie, inclusief de acht niet noodzakelijke chromosomen. Het

genoom bevat 13 chromosomen en het dispensoom dat acht chromosomen omvat die sterk van de andere chromosomen afwijken in structuur en inhoud. Het dispensoom bevat meer tranposons en de genen hebben een ander codongebruik. De meeste genen in het dispensoom komen ook voor op de 13 andere chromosomen en er is niet veel overeenkomst tussen het *M. graminicola* dispensoom en de andere chromosomen of met chromosomen in andere gerelateerde Dothideomyceten. Hierom wordt verondersteld dat deze chromosomen via een onbekend proces zijn overgedragen door één of meerdere onbekende donoren.

Hoofdstuk 4 geeft een totaaloverzicht en analyse van de eiwitten die *M. graminicola* gedurende het infectieproces in het apoplast uitscheidt, vooral tijdens de compatibele interactie met tarwe. Veel van de geannoteerde uitgescheiden eiwitten hebben veronderstelde functies in pathogeniteit zoals celwandafbrekende enzymen en proteasen, maar de functie van een aanzienlijk aantal van de geïdentificeerde eiwitten is onbekend. De eiwitten werden voornamelijk tijdens vergevorderde infectie uitgescheiden. Veel pathogenese gerelateerde planteiwitten, zoals PR-2, PR-3 en PR-9, daarentegen, accumuleerden eerder en meer tijdens de incompatibele interactie. Dit geeft aan dat effectoren van *M. graminicola* in resistente tarweplanten herkend worden en daarmee verdedigingsprocessen in gang zetten die tot resistentie leiden, overigens zonder de karakteristieke overgevoeligheidsreactie.

Hoofdstuk 5 gaat verder in op de initiële identificatie en karakterisering van necrose inducerende eiwitten die in cultuurfiltraten (CFs) van *M. graminicola* voorkomen. Hun activiteit is afhankelijk van licht en zij worden geïnactiveerd door proteinase K en temperatuurbehandelingen boven 100°C. Dit vertoont analogie met de necrose inducerende eigenschappen van waardplant specifieke toxinen die worden geproduceerd door andere Dothideomyceten zoals *Stagonospora nodorum* en *Pyrenophora tritici-repentis*. Opeenvolgende zuiveringstappen en massa-spectrometrie van de CFs resulteerde in meerdere necrose inducerende kandidaat eiwitten. Heterologe expressie van de twee beste kandidaat eiwitten in *Pichia pastoris* resulteerde in een voldoende hoeveelheid eiwit voor infiltratieproeven in een reeks tarwerassen die daarop een differentiële reactie vertoonden hetgeen wijst op specifieke herkenning.

Hoofdstuk 6 is een algemene discussie van dit proefschrift en plaatst de verkregen resultaten in een breder perspectief met een focus op de genoomstructuur van *M. graminicola* en haar functie. Daarnaast worden aspecten van de hemibiotrofe levenswijze en de relevantie

van de uitgescheiden eiwitten voor het tarwe-*M. graminicola* pathosysteem in relatie tot gen-om-gen modellen en de potentiële implicaties voor de resistentieveredeling besproken.

Résumé

Le champignon *Mycosphaerella graminicola* (Fuckel) J. Schröt, in Cohn (forme asexuée : *Zymoseptoria tritici* (Desm.) Quaedvlieg & Crous) est l'agent causal de la septoriose du blé (STB) qui est la principale maladie biotique foliaire dans le monde. Cependant, le contrôle de la STB qui repose sur l'utilisation des variétés résistantes et des fongicides, est fortement gênée par le manque de compréhension des bases génétiques et biochimiques de la pathogénicité, et notamment des mécanismes d'infection et de résistance dans la plante hôte.

M. graminicola ayant un cycle sexuel actif dans les conditions en plein champ, qui représente la plus importante source de progression de l'épidémie, induit une grande diversité génétique de populations et reste un défi pour la mise en place d'une stratégie de lutte durable basée sur la découverte de nouvelles variétés de blé résistantes et des composés antifongiques. En effet, la compréhension du mécanisme d'infection de ce champignon versatile et le rôle des cycles sexuel et asexuel sur la composition génomique, est cruciale pour développer de nouvelles stratégies de contrôle.

Chapitre 1 est consacré à l'introduction de la biologie et de la pathogénicité de *M. graminicola*. Il décrit également et brièvement l'impact des nouvelles technologies et celui des anciennes améliorées sur la vitesse, l'envergure et l'échelle de la recherche dans les génomiques comparatives.

Chapitre 2 présente deux cartes génétiques des populations de *M. graminicola*, à partir de marqueurs DArT et l'analyse par la suite de l'inégalité en nombre dans la transmission méiotique des chromosomes. Des polymorphismes en nombre et en longueur de chromosomes sont en effet, fréquemment observés dans les descendants et ce dans une proportion de 15-20% où ils leur manquent un ou plusieurs chromosomes et ceci malgré leur présence chez les deux parents et sans avoir pour autant, un effet apparent sur la sexualité ou sur le fitness. Nous avons pu ainsi démontrer que *M. graminicola* possède huit chromosomes non essentiels, appelés -dispensome-. Ceux-ci sont de petites tailles, constituent 38% du génome de ce champignon et représentent ainsi à ce jour le plus grand nombre de chromosomes non essentiels chez les champignons filamenteux. Cette plasticité génomique est immanquablement générée durant la méiose et pourrait expliquer la grande adaptabilité de *M. graminicola* en plein champ. La carte génétique ainsi établie dans cette étude, était cruciale

pour achever la séquence génomique de *M. graminicola*. Cette dernière est décrite dans le chapitre suivant.

Chapitre 3 met en relief la structure et l'organisation génomique incluant les huit chromosomes non essentiels. La séquence du génome est composée de 13 chromosomes et du dispensome, qui est distinct des chromosomes essentiels de part sa structure et son contenu en gènes et en éléments répétitifs. En effet, il contient une fréquence élevée de transposons et de gènes avec des usages de codes différents. La plupart des gènes ainsi présents sur le dispensome sont aussi présents sur les chromosomes essentiels. Par ailleurs, un très faible niveau de synténie est observé entre le dispensome de *M. graminicola* et les chromosomes des autres dothidéomycètes. Leur origine provient sans doute du mécanisme de transfert horizontal par un donneur inconnu.

Chapitre 4 présente une analyse globale des protéines de *M. graminicola* secrétées dans le fluide apoplastique durant les différents stades d'infection, et particulièrement les protéines fongiques secrétées durant l'interaction compatible. L'étude montre qu'un nombre important de protéines secrétées ont des fonctions possibles dans la pathogénicité, à l'instar des enzymes capables de dégrader les parois végétales et les protéases. Néanmoins, la fonction d'un grand nombre de protéines reste encore méconnue. Les protéines secrétées durant l'interaction compatible sont dans la majeure partie présentes dans les stades d'infection tardifs alors que beaucoup de protéines PR sont secrétées plus tôt avec une concentration plus élevée dans l'interaction incompatible, prouvant ainsi que les effecteurs sont reconnus par les plantes résistantes engendrant de ce fait des réponses de défense, sans être accompagnées par une réaction hypersensible.

Le Chapiter 5 décrit l'identification et la caractérisation initiale des protéines à activité nécrotique qui sont présentes dans les filtrats de culture (FCs) de *M. graminicola*. Cette activité nécrotique est fortement dépendante de l'action de la lumière et est inactivée après traitement à la protéinase K et à une élévation de la température (100°C). En outre, ces constatations évoquent une similitude avec l'activité toxique des toxines spécifiques des autres pathogènes dothidéomycètes comme *Stagonospora nodorum* et *Pyrenophora tritici-repentis*. Les purifications ultérieures des FCs suivies de spectrométrie de masses ont identifié plusieurs protéines candidates à l'activité toxique. L'expression hétérologue des deux plus importantes protéines dans *Pichia pastoris* a montré, une fois infiltrées dans les feuilles de blé, qu'elles induisent des nécroses dans un ensemble de cultivars.

Chapitre 6 : Ce dernier présente une discussion générale et intègre les résultats obtenus dans un contexte plus large en mettant en exergue les nouvelles découvertes concernant la structure et la fonction du génome. En outre, cette discussion générale s'intéresse au mode de vie hémibiotrophique, à l'importance des protéines secrétées durant l'interaction blé-*M. graminicola* en relation avec les modèles gène pour gène et gène-pour-gène inverse et à leur implication dans les stratégies de sélection pour la résistance.

Acknowledgements

In a warm and sunny day from a post-revolution Tunisia, I am writing the last part of my thesis …..as we all know 'all good things come to an end"…

Undertaking this PhD has been a truly life-changing experience for me and it would not have been possible without the guidance and support that I received from many people.

First of all, I would like to express my deepest gratitude to my supervisor Dr. Gert Kema for his guidance, wisdom and to have offered me the opportunity to work on this exciting area of research that without him would not have been achievable. Gert, you encouraged me to successfully apply for the UNESCO-L'Oréal fellowship so that I could stay longer in the lab. During this period, you gave me the freedom to pursue various projects without objection and I highly appreciated the many discussions that we had but also your continuous scientific and moral support. In addition to your undeniable qualities as a man of science, you gave the example of humility, understanding, tolerance and listening to the most multinational and diverse research members that worked in your laboratory.

I would like to say a very big thank you to my daily supervisor Dr Theo van der Lee, for his guidance, advices and prompt availability whenever needed during these years.
Theo, I sincerely appreciated your constant motivation, I enjoyed and learned a lot from the long evening discussions about the project. You expected and encouraged me to think more independently about the experiments and results. Nonetheless, I could always knock on your door for questions and whenever I was doubting or was insecure about my work, you always saw the positive side which truly raised my self-confidence and strengthen my personality. You are such an energetic and enthusiastic advisor with a great sense of humor!

Gert and Theo you both have been my mentors not just in science but in several aspects of life and I feel like you assisted me in tapping into potentials that I did not know I had. My deepest respect to you. Ik wacht nog steeds op jullie komst in Tunis!

I would like to thank my promoter Prof. dr. Pierre de Wit for his valuable input that has helped me to successfully complete this thesis. Pierre, I appreciated very much your advices and pertinent comments especially in the last steps of my thesis. I truly valued your quick-proofreading even when you were supposed to be on holidays… zoals je het zegt, "maar zo gaat het vaak in het leven van een hoogleraar"!

Je voudrais également remercier le professeur Moncel El Harrabi de l'université de l'INAT pour m'avoir vivement conseillé d'intégrer l'équipe de recherche de Dr. Kema et établir ainsi les premiers contacts.

Quant aux professeurs Fehti Lebdi, Sonia Hamza et Elies hamza de l'université de l'INAT qui ont guidé mes premiers pas dans la recherche, je ne saurais trop vous remercier pour le suivi régulier de toutes les étapes de mes recherches et d'avoir facilité mon intégration dans l'équipe enseignante de l'INAT. Je compte réellement sur vous pour consolider et affermir les liens déjà établis entre l'INAT et Wageningen University.

I also acknowledge the UNESCO-l'Oréal for the award given to carry out my PhD research and 'le ministère de l'Enseignement Supérieur et de la Recherche Scientifique, Tunisie' and the "Fonds de Soutien à l'Obtention Végétale (FSOV)" for their partial Ph.D scholarships.

Furthermore, the work presented herein has truly been a collaborative effort involving many research groups.

My special thanks go out to the support I received from our long-term collaborative work with Dr. Steve Goodwin and his lab from the Botany and Plant Pathology department at Purdue University that I had the chance to visit. I am especially grateful to Dr. Charles Crane, Dr. Braham Dhillon and Jessica Cavaletto. It has been a fruitful learning experience, particularly when it came to bioinformatics. I have enjoyed working with you!

I also would like to thank the people at the Joint Genome Institute (JGI) for all the support related to the genome sequences of *M. graminicola* and other dothideomycetes.

I am very grateful to Dr. Chris Maliepaard from the Department of Plant Breeding at PRI; for his help in data handling and analysis regarding the CGH experiment that is partly presented in this thesis.

I also greatly appreciated the collaborative work undertaken with Dr. Timothy Friesen and Dr. Zhaohui Liu from USDA-ARS Cereal Crop Research Unit at North Dakota. Many thanks for your insightful suggestions. It was an excellent opportunity for me to work with such great experts in toxins! I gained so much valuable experience. I sincerely hope that our collaboration continues in the future.

During this project, we also had nice collaborations with the proteomics lab. I sincerely appreciated the support received from Dr. Twan America and Dr. Jan Cordewener. I had the chance to work in your lab for several months and I am very grateful that you took the time to introduce me to the fascinating world of proteins. It was a rich learning experience. Twan, as a genuine expert of proteomics, you taught me how spectrometry works and the most important things about LC-MS. We spent so much time analyzing the complex data, so complex that I had to knock on your door many times particularly during writing of the manuscript; but you always had the time to explain. Jan, I am very thankful that you assisted me in the lab and even later whenever I had questions or problems with my experiments, you were always reachable, willing to help and give advices. You were a great teacher and your enthusiasm and refreshing approach for science really inspired me!

I would like to express my gratitude to all the present members of the Molecular Phytopathology Cluster group as well as the Biointeractions and Plant Health business Unit at Plant Research International for always being so helpful and friendly and particularly for being the most famous brides and grooms! ☺ I am glad to have interacted with many members. A special thanks to Dr. Jan Bergervoet for his general expert help in flow cytometry and Dr. Cees Waalwijk regarding all GMO regulations and his valuable suggestions for this work. I also would like to thank Els Verstappen, Ineke de Vries and

Odette Mendes for their excellent technical assistance, for providing insightful suggestions and help with instrumentation, general greenhouse and lab questions. I know that I could always ask you for advices and opinions on lab related issues. Additionally, thank you for having made this lab a nice place to work. In the last years, we became friends and I will always remember you.

I would like to thank people from the laboratory of phytopathology, particularly from the cladosporium group and from the CBS institute (Centraalbureau voor Schimmelcultures) especially my external supervisor, Lute-Harm Zwiers for all the discussions that we had during my PhD research.

My deep appreciation goes out to the diverse team members that were at some point part of the Mycosphaerella group, for sharing their scientific experience and knowledge and all the good times spent together in the lab over the past couple of years.

I have had the chance to work and interact with many great scientists and I particularly would like to express my greatest gratitude to Mahmod Tabib Ghaffary, Rahim Mehrabi, Ioannis Stergiopoulos and Thierry Marcel. I also would like to thank Alexander Wittenberg and Sarah Ware, who generated the genetic linkage maps and initiated the work on the dispensome that became one of my major projects of my PhD thesis. Additionally, I would like to thank Amir Mirzadi Gohari, Zhao Chunzhao, Reza Talebi, Leila Khodhaei, Pablo Chong Aguirre, Tristan de Jong, Viviane Cordovez Da Cunha and Lamia Aouini and all the "Brazilian members" Ulisses Nunes da Rocha, Suzanna Garcia and the Embrapa staffs, Claudia Fortes Ferreira, Adilson Kobayashi, Miguel Dita Rodriguez, Gilvan Ferreira da Silva (your sentence "working from sunday to sunday but at the end what do you get?.....nothinnnng" ☺ became a very famous quote in the lab), Joao Nunes Maciel and Manoel de Souza.

I hope we can keep these connections alive. I wish you the very best in your personal life and future career!

To Rafael and Esperanza Arango, this sentence will forever stick in my mind "life is complicated, difficult and sad"…….. but it was such a great time in the office. It is a real pity that you will not be present for my defence but I am sure as you told me you will watch it live from Colombia… and you will feel sorry for the "dear candidate" ☺. I hope that one day our paths will cross again!

Inge Kaaijk-Wijdogen and Inge Oudenaarde van de l'Oréal, leuk om jullie ontmoet te hebben en we houden zeker contact! I also would like to thank Radi (I still have very good memories of our lunch breaks!), Ying and Gisella for their friendship and wish them all the best for their future.

To my "preciosa amiga", Caucasella Diaz Trujillo: we had so much fun during these years! You are a wonderful and generous friend and above all a proud Mexican! I admire your perseverance and positive outlook. I wish you lots of success in completing your thesis. …Pela los dientes… Viva México!

A “ma pote” Emilie Fradin, you were always there when I needed you. You helped me in numerous ways during various stages of my life. You are a caring, supportive friend and always with great sense of humor and creativity! We shared so many laughs together! I wish you all the best as you embark on the next phase of your life! Et que notre amitié dure jusqu’à l’âge de madame Sarfati!

A tous mes ami(e)s au pays de Carthage, merci infiniment pour votre soutien !

Mes vifs remerciements à la famille Ben M’Barek; vous avez toujours témoigné un grand intérêt à mes travaux de recherche avec beaucoup de générosité et de fierté comme l’histoire tri-millénaire de “Vaga” me l’a toujours enseignée !.....Un bon lablabi “mrabreb” nous attend!

Aan de familie Oudijk; jullie hebben mij altijd heel goed geholpen. Ik wil graag iedereen ontzettend bedanken voor jullie aanwezigheid en gezelligheid. Ik zal het nooit vergeten! You are the “Oudijk’s sensation”!

Finally, I am very grateful to my beloved family who provided unconditional love, care and support. In particular, I would like to thank my father who has taught me the value of commitment, hard work and to be ambitious. You've always been behind me and pushed me to be the best that I can be. You gave me such good advices and support! Papa, merci du fond du coeur! My heartfelt thanks to “mijn allerliefste mutti” for the value of family, devotion and humility. You have always put your family first and you were always there for us. Je n’aurais pas pu y arriver sans vous. I also thank my loving elder sister, Lilia. As a very hard-working person, you’ve been my inspiration model ever since we were kids. I wish you lot of happiness with Oualid and with my lovely niece and nephew, Nour and Amine that filled my life with so much joy. Un grand merci pour tout ce que vous avez fait pour moi !

I also would like to thank my family in law. I am truly blessed to have them. They have always welcomed me into their home, cared for me as if I am one of their own. Thank you for your great generosity, warmth and kindness and particularly for giving me the most amazing man in the world, my best friend, soul-mate, and husband. Slim, you have been a true and great supporter and you always believed in me. We came across difficult and wonderful times but we both learned a lot during these years that surely strengthened our commitment and determination to each other,“*You are the best thing that ever happened to me*”. Merci infiniment pour ton amour et ta patience!

Aan het eind gekomen van mijn proefschrift, kijk ik terug op een geweldige en leerzame ervaring in mijn vlakke land….

Sarrah ❁ سارة

Curriculum vitae

Sarrah Ben M'Barek-Ben Romdhane was born on January 6, 1979 in Tunis, Tunisia. After completing her academic high school in 1997, she joined the National Agronomic Institute of Tunisia (INAT) where she studied agronomic engineering and obtained her BSc in 2002. Subsequently, at Wageningen University (the Netherlands), Sarrah followed an MSc degree in plant biotechnology with specialization in Plant breeding. The MSc thesis was realized at the department of Biointeractions and Plant Health, Plant Research International & Wageningen Research Center (PRI) under the supervisions of Dr. Gert Kema and Dr. Rients Niks. The work presented in her master thesis concerned the aspects of fungicide resistance, genetics and detection of *Mycosphaerella graminicola*, wheat Septoria tritici leaf blotch. After that, she performed an internship at the University of Orsay, Paris in the group of Dr. Marie-José Daboussi and Dr. Marie Dufresne in which she participated in the development of a novel gene tagging system using MITES in Fusaria pathogenic to cereals. From 2005 until present, Sarrah is partly working as an assistant in INAT and taught practicum courses in plant biology, physiology and molecular biology and tutorial classes in genetics of micro-organisms. In 2006, Sarrah was awarded by the UNESCO-L'Oréal fellowship for Women in Science to carry out her PhD research at PRI under the supervisions of Dr. Gert Kema and Prof. dr. Pierre de Wit. This thesis summarizes the research results of her PhD program in exploring the genome structure and pathogenicity factors of the cereal pathogen *M. graminicola*. She will continue her career in wheat pathology while keeping strong connections to Wageningen University and encouraging cooperation between INAT and Wageningen University in various fields.

List of publications

Ben M'Barek, S., Cordewener, J.H.G., van der Lee, T.A.J., America, A.H.P., Hamza, S., de Wit, P.J.G.M., Kema, G.H.J. A global *in planta* proteome analysis of the fungal wheat pathogen *Mycosphaerella graminicola*. Submitted for publication.

Ben M'Barek, S., Cordewener, J.H.G.,Tabib Ghaffary, M., van der Lee, T.A.J., Liu, Z., Mehrabi, R., America, A.H.P., Timothy L. Friesen, T.L., Hamza, S., Pierre JGM de Wit, P.J.G.M. and Kema, G.H.J. The septoria tritici blotch pathogen *Mycosphaerella graminicola* secretes proteins in culture media that differentially induce necrosis in wheat. Manuscript in preparation.

Mehrabi, R., **Ben M'Barek, S.,** Saidi, A., Abrinbana, M., Aghaee, M., de Wit, P.J.G.M., and Kema, G.H.J. 2012. MAP kinase phosphorylation and cAMP assessment in fungi in Plant Fungal Pathogens.: Methods and protocols 835: 769pp.

Goodwin, S.B., **Ben M'Barek, S.,** Dhillon, B., Wittenberg, A.H.J., Crane, C.F., van der Lee, T.A.J., Grimwood, J., Aerts, A., Antoniw, J., Bailey, A., Bluhm, B., Bowler, J., Bristow, J., van der Burgt, I.A., Canto-Canche, B., Churchill, A., Conde-Ferràez, L., Cools, H., Coutinho, P.M., Csukai, M., Dehal, P., Donzelli, B., Foster, A.J., van de Geest, H.C., van Ham, R.C.H.J., Hammond-Kosack, K., Hane, J., Henrissat, B., Kobayashi, A.K., Kilian, A., Koopmann, E., Kourmpetis, Y., Kuzniar, A., Lindquist, E., Lombard, V., Maliepaard, C., Martins, N., Mehrabi, R., Nap, J.P.H., Oliver, R., Ponomarenko, A., Rudd, J., Salamov, A., Schmutz, J., Schouten, H.J., Shapiro, H., Stergiopoulos, I., Torriani, S.F.F., Tu, H., de Vries, R.P., Waalwijk, C., Ware, S.B., Wiebenga, A., de Wit, P.J.G.M., Zwiers, L-H., Grigoriev, I.V., Kema, G.H.J. 2011. Finished Genome of the Fungal Wheat Pathogen *Mycosphaerella graminicola* Reveals Dispensome Structure, Chromosome Plasticity and Stealth Pathogenesis. PLoS Genetics 7 (6): e10020170.

Mehrabi, R., Abd-Elsalam, K.A., Bahkali, A., Moslem, M., **Ben M'Barek, S.,** Mirzadi Gohari, A., Karimi Jashni, M., Stergiopoulos, I., Kema, G.H.J and de Wit, P.J.G.M. 2011. Horizontal gene and chromosome transfer in plant pathogenic fungi. FEMS Microbiology 35:542-554.

Ware, S.B., Van den Bosch, F., Diaz-Trujillo, C., **Ben M'Barek, S.,** van der Lee, T.A.G., de Waard M.A., de Wit, P.J.G.M., Kema, G.H.J. 2011. Plant pathogen dodges disease management through sex. Manuscript in preparation.

Mehrabi, R*****., **Ben M'Barek, S*.,** van der Lee, T.A.J., de Wit, P.J.G.M., Kema, G.H.J. 2009. Gα and Gβ proteins regulate the cAMP pathway required for development and pathogenicity of the fungal pathogen *Mycosphaerella graminicola*. Eukaryotic Cell 8 (7): 1001-1013.

Wittenberg, A.H.J*****., van der Lee, T.A.J*****., **Ben M'Barek, S*.,** Ware, S.B., Goodwin, S.B., Killian, A., Visser, R.G.F., Kema, G.H.J., Schouten, H.J. 2009. Meiosis Drives Extraordinary Genome Plasticity in the Haploid Fungal Plant Pathogen *Mycosphaerella graminicola*. PLoS ONE 4(6): e5863.

Dufresne, M., van der Lee, T.A.J., **Ben M'Barek, S.,** Vasnier, C., Xu, X., Zhang, X., Liu, T., Waalwijk, C., Zhang, W., Kema, G.H.J and Daboussi, M.J. 2008. Transposon-tagging identifies novel pathogenicity genes in *Fusarium graminiearum.* Fungal genetics and Biology 45(12):1552-1561.

Bergemann, M., Lespinet, O., **Ben M'Barek, S.,** Daboussi, M.J., and Dufresne, M. 2008. Genome-wide analysis of the *Fusarium oxysporum* mimp family of MITEs and mobilization of both native and de novo created mimps. Molecular Evolution. 67(6):631-642.

Dufresne, M., Hua-Van, A., El Wahab, A.H., **Ben M'Barek, S.**, Vasnier, C., Teysset, L., Kema, G.H.J. and Daboussi, M.J. 2007. Transposition of a fungal miniature inverted-repeat transposable element through the action of a Tc1-like transposase. Genetics 175:441-452.

*****Equal contribution

Education Statement of the Graduate School
Experimental Plant Sciences

The Graduate School EXPERIMENTAL PLANT SCIENCES

Issued to: Sarrah Ben M'Barek
Date: 17 October 2011
Group: Laboratory of Phytopathology, Wageningen University & Research Centre

1) Start-up phase	date
► **First presentation of your project**	
Progress in cloning the avirulence gene in *Mycosphaerella graminicola*	Dec, 2006
► **Writing or rewriting a project proposal**	
Cloning and functional analysis of avirulence genes of the pathogen *Mycosphaerella graminicola,* causal agent of septoria tritici leaf	14 Sep 2006
► **Writing a review or book chapter**	
► **MSc courses**	
► **Laboratory use of isotopes**	
Safe handling with radioactive materials and sources	03-05 Oct 2006
Subtotal Start-up Phase	*9,0 credits**

2) Scientific Exposure	date
► **EPS PhD student days**	
EPS PhD student day, Wageningen University	19 Sep 2006
The SVD_PhD Student day, Paris, France	24-25 May 2007
► **EPS theme symposia**	
EPS Theme 4 symposium 'Genome Plasticity', University of Amsterdam	08 Dec 2006
EPS Theme 2 symposium 'Interactions between Plants and Biotic Agents', University of Amsterdam	02 Feb 2007
EPS Theme 2 symposium & Willie Commelin Scholten day 'Interactions between Plants and Biotic Agents', Utrecht University	22 Jan 2009
► **NWO Lunteren days and other National Platforms**	
► **Seminars (series), workshops and symposia**	
CBS/PRI/Wageningen Phytopathology Symposium	22 Jun 2007
Microarray workshop, Leiden university	21 Sep 2007
Embrapa-PRI-CBS, Symposium, Wageningen	16 Oct 2007
Seminar Dr Richard Oliver "Genomics of *Stagonospora nodorum* ; genes, genomes and growers"	16 Oct 2008
Workshop in Tunisia: Les applications des biotechnologies pour l'amelioration génétique du blé, Tunis, Tunisia	17 Apr 2009
KNPV-Werkgroep Graanziekten	6 Apr 2010
Tunisia Workshops on conservation Agriculture & Septoria, Tunis, Tunisia	26-30 Apr 2010
Seminar Paul Birch 'Trying to understand susceptibility and exploit resistance in potato-*Phytophthora infestans* interactions'	20 May 2010
Seminar Prof. Richard Michelmore at Keygene, Wageningen	03 Jun 2010
Seminar Brande Wulff 'Isolation of novel resistance genes for stem rust race Ug99 from diploid wheat relatives'	09 Jun 2010
First workshop INRA/WUR on Septoria diseases, Versailles, France	16-17 Sep 2010
Joint MPI-Marburg Phytopathology meeting, Wageningen	28-29 Oct.2010
Seminar Prof. Regine Kahmann "Effectors of the plant-pathogen fungus Ustilago maydis"	29 Oct 2010
Joint workshop INRA/WUR on Septoria, Wageningen	07-08 Jun 2011
Seminar series 'Phytopathology' (estimated 3x/year)	2006-2011
► **Seminar plus**	
► **International symposia and congresses**	
9th European Conference on Fungal genetics, Edinburgh, Scotland	05-08 Apr 2008
7th European Symposium on Septoria and Stagonospora Diseases of cereals, Ascona, Switzerland	18-22 Aug 2008
Dothideomycete Comparative Genomics Jamboree at DOE Joint Genome Institute, Walnut Creek,CA , USA	10-12 Nov 2008
25th Fungal genetics Conference, Asilomar, USA	17-22 Mar 2009
JGI User Meeting Genomics of Energy & Environment, CA, USA	25-27 Mar 2009
WG1 MEETING: Technical aspects inherent to Plant Proteomics "Classical and novel approaches in Plant Proteomics" Viterbo, Italy	05-06 May 2009
KNPV, Fast Forward Spring meeting, Wageningen, The Netherlands	25 May 2009
10th European Conference on Fungal genetics, Leiden, The Netherlands	29-01 Apr 2010
► **Presentations**	
Poster: 5th PhD Summerschool on Environmental signaling: Arabidopsis as a model, Utrecht University, Utrecht, The Netherlands	27-29 Aug 2007
Oral: Microarray workhop, Leiden, The Netherlands	21 Sep 2007
Oral: Summerschool:"On the evolution of plant-pathogen interactions:from Principles to Practice", The Netherlands	18-20 Jun 2008
Oral: 7th European Symposium on Septoria and Stagonospora Disease cereals, Ascona, Switzerland	18-22 Aug 2008
Oral (2x): Dothideomycete Comparative Genomics Jamboree at DOE Joint Genome Institute, Walnut Creek,CA , USA	10-12 Nov 2008
Oral: 25th fungal genetics conference, Asilomar, California, USA	17-22 Mar 2009
Poster: 25th Fungal genetics Conference, Asilomar, USA	25-27 Mar 2009
Oral: COST FA0603-WG1, Technical aspects inherent to plant Proteomics meeting, Viterbo, Italy	05-06 May 2009
Oral: KNPV, Fast Forward Spring meeting, Wageningen, The Netherlands	25 May 2009
Oral: Dothideomycete Comparative Genomics satellite meeting, 10th European Fungal Genetics Conference, Leiden, The Netherlands	29-01 Apr 2010
Poster: 10th European Conference on Fungal genetics, Leiden, The Netherlands	29-01 Apr 2010
Oral: Tunisia Workshops on conservation Agriculture & Septoria, Tunis, Tunisia	26-30 Apr 2010
Oral: Workshop INRA/WUR on Septoria diseases, Versailles, France	16-17 Sep 2010
Oral: FSOV Serasem, Bioplante, France	11 Oct 2010
Oral: Joint MPI-Marburg Phytopathology meeting, Wageningen	28-29 Oct 2010
Oral: 2nd Workshop INRA/WUR/Bioplante om Septoria diseases, Wageningen	07 June 2011
► **IAB interview**	05 Dec 2008
► **Excursions**	
Bioplante Field visit, breeding for resistance to Septoria and Fusarium, Florimond Desprez Capelle-en-Pévèlle, Lille, France	12 Jul 2006
Bioplante Field visit, breeding for resistance to Septoria and Fusarium, Florimond Desprez Capelle-en-Pévèlle, Lille, France	30 Jun 2009
Subtotal Scientific Exposure	*33,5 credits**

3) In-Depth Studies	date
► **EPS courses or other PhD courses**	
Systems Biology: Statistic Analysis of ~Omics Data	11-14 Dec 2006
5th PhD Summerschool on Environmental signaling: Arabidopsis as a model, Utrecht University, the Netherlands	27-29 Aug 2007
PhD Summerschool: "On the evolution of plant-pathogen interactions: from Principles to Practice", The Netherlands	18-20 Jun 2008
Confocol Light Microscopy, fundamentals and Biological applications, UvA	02-06 Jun 2008
► **Journal club**	
Literature discussion Myco-Clado, PRI	2006-2010
► **Individual research training**	
Subtotal In-Depth Studies	*7,8 credits**

4) Personal development	*date*
► **Skill training courses**	
51st Bayer AG student course, Cologne, Germany	29-03 Jul 2008
► **Organisation of PhD students day, course or conference**	
Teaching Practicum courses of Molecular Biology in INAT (National Agronomic Institute of Tunisia), Tunis, Tunisia	2006-2011
► **Membership of Board, Committee or PhD council**	
Subtotal Personal Development	*4,5 credits**

TOTAL NUMBER OF CREDIT POINTS*	**54,8**

Herewith the Graduate School declares that the PhD candidate has complied with the educational requirements set by the Educational Committee of EPS which comprises of a minimum total of 30 ECTS credits

** A credit represents a normative study load of 28 hours of study.*

Printing of this thesis was partially financed by the J.E. Jurriaanse Stichting.

Design cover page: Sarrah Ben M'Barek and Haythem Ben Romdhane

Fromt cover: A mosaic composition displaying from top to bottom the core set of chromosomes arranged in a half-circle surrounded by eight dispensable chromosomes. Petals representing splashed pycnidiopores followed by a wheat head. Ascopores emerging from a pseudothecium and finally the differentes phases of symptom development of wheat leaves infected with *M. graminicola* are shown.

Printed at Wöhrmann Print service, Zutphen